

**INVESTIGATING BREAST CANCER METASTASIS TO BRAIN IN
PRE-CLINICAL MOUSE MODELS OF METASTASIS**

Soo-Hyun Kim

Submitted in total fulfilment of the requirements
of the degree of Doctor of Philosophy

DECEMBER 2015

Peter MacCallum Cancer Centre

&

Department of Pathology

The University of Melbourne

Produced on archival quality paper

Abstract

An increasing number of advanced breast cancer patients develop overt brain metastases. This is partly due to recent advances in therapies for visceral metastases that extend life of patients but remain largely ineffective against late stage brain metastases. Among the subtypes of breast cancer, triple negative breast cancer (TNBC) is particularly aggressive and has a strong propensity to metastasise to the brain. Although TNBC are initially sensitive to chemotherapy (Keam et al., 2007), response to treatment is usually limited by the development of resistance. Moreover, current endocrine or human epidermal growth factor receptor 2 (HER2)-targeting therapies are not effective against TNBC due to the absence of estrogen receptor (ER), progesterone receptor (PR) or HER2 receptor in this tumour subtype.

Unfortunately, the limited availability of mouse models that closely recapitulate the entire metastatic process from the mammary gland to the brain remains a major barrier to identifying relevant prognostic/therapeutic target genes or testing novel therapies against TNBC brain metastases under clinically relevant settings. Thus, the first aim of this project was to develop a clinically relevant and robust mouse model of breast cancer brain metastasis (4T1Br4) that gives rise to a high incidence of spontaneous brain metastases in syngeneic/immune competent animals. Phenotypic, functional and transcriptomic characterisation showed that the 4T1Br4 model is phenotypically, functionally and genetically relevant to human brain-metastatic TNBC. In particular, we found that 4T1Br4 cells are highly migratory, are more adhesive to brain-derived endothelial cells and have increased ability to transmigrate endothelial cells and invade in response to brain-derived factors compared to the parental 4T1 cells from which they are derived.

We identified a cell adhesion molecule, limitrin, whose high expression is associated with the increased brain metastatic abilities of 4T1Br4 tumours. Prognostic analysis of limitrin using BreastMark analysis tool revealed that limitrin is associated with metastasis and poor clinical outcome in basal-like but not other subtypes of breast cancer. In addition, we found that limitrin promotes trans-endothelial migration *in vitro*, a function likely to be critical for the crossing of tumour cells through the blood-brain barrier (BBB).

Lastly, we tested the efficacy of novel histone deacetylase inhibitors (HDACi) namely SB939 and 1179.4b, against mouse (4T1Br4) and human (MDA-MB-231Br) brain metastatic breast cancer cell lines. SB939 and 1179.4b potently inhibited proliferation and survival of both cell lines *in vitro* and inhibited 4T1Br4 tumour growth and spontaneous metastasis to bone and brain *in vivo*. Moreover, we observed that both HDACi have radiosensitising properties against both cell lines *in vitro*.

In summary, we developed a clinically relevant mouse model of spontaneous TNBC brain metastasis amenable to identifying therapeutic/prognostic target genes and evaluating novel therapies against this incurable disease.

Declaration

This is to certify that:

1. The thesis comprises only my original work towards the PhD except where indicated in the Preface,
2. Due acknowledgement has been made in the text to all other material used, and
3. The thesis is fewer than 100,000 words in length, exclusive of tables, maps, bibliographies and appendices.

.....

Soo-Hyun Kim

Preface

I would like to acknowledge everyone for their contribution to this project.

1. Figure 3.6. Dr. Richard Redvers (Peter MacCallum Cancer Centre, Melbourne), for performing gene array profiling and analysing differential gene expression data.
2. Dr. Normand Pouliot for performing gene array profiling and analysing differential gene expression data for limitrin in Chapter 4.
3. Dr. Bruce Kemp (St Vincent's Hospital, Melbourne), for generating limitrin antibodies for Chapter 4.
4. Dr. David P. Fairlie (The University of Queensland, Brisbane), for providing SB939 and 1179.4b for Chapter 5.

Acknowledgements

I really thank God for providing me with everything that I needed in my PhD so that I could focus on my work. I strongly believe that my tuition fees and living costs in the last four years were covered by His grace. Without His help, I would not have been able to finish my PhD. He also kept providing me with comfort and relief so that I could walk my way by Him even when I was complaining about or was frustrated by my work. Doing a PhD in a second language was even more challenging. Yet I praise God for watching and protecting me and helping me grow all the way through.

My special gratitude goes to my principal supervisor Dr. Normand Pouliot for supervising me for the past four years doing my brain metastasis project, which I really loved, for putting up with my broken English (I know you must have been painful), for your consistent insistence (it was tough, but without that, my project could not have made progress this much) and for being my friend (I am sure I will miss your jokes 😊).

Also I would like to thank my co-supervisor Dr. Delphine Denoyer for supervising me with Norm, supporting me and answering my questions. Your co-supervision showed me an array of ideas and insights. I really appreciate that.

And I am grateful to Dr. Nathan Godde as my mentor for giving me support and advice, being a great listener and a role model and treating me so well all the time.

My heartfelt thanks go to Prof. Robin Anderson for her support and affectionate advice and accepting me to the lab that has abundant resources, comfortable environments and great people (Rick, Kara, Cameron, Rebeka, Bill, Allan, Yuan, Judy, Kathryn, Selda, Kellie, Gen, Ash, Lara, Phoebe). I am indebted to every single one of them who taught me English and showed me consistent love and support that really helped me stand and keep doing my PhD.

I cannot be thankful enough to my family in Korea. I thank my parents for supporting me with their prayer and never-ending love and my sister for thinking of me all the time and supporting me in many ways. It means a lot to me.

Most importantly, I would love to thank my husband Daniel for his self-sacrificing spirit (I know that it was a hard decision to give up on your career in Korea and move to Australia for my study) and supporting me financially, mentally (your endless love means a lot to me) and physically (no one likes doing the household chores but you are always willing to do them for me). Without your help and consistent support, I could not have got through my PhD journey. I appreciate it.

Finally, I deeply appreciate the generous scholarship support from the University of Melbourne and the Cancer Council Victoria.

Table of contents

Abstract	ii
Declaration	iv
Preface	v
Acknowledgements	vi
Table of contents	
1. LITERATURE REVIEW	1
1.1 OVERVIEW OF THESIS STRUCTURE AND OBJECTIVES	1
1.2 BREAST CANCER – INCIDENCE, MORTALITY AND SUBTYPES	1
1.3 BREAST CANCER METASTASIS	3
1.4 BREAST CANCER BRAIN METASTASIS	7
1.4.1 INCIDENCE AND SURVIVAL OF PATIENTS WITH BRAIN METASTASES	7
1.4.2 TUMOUR SUBTYPES THAT HAVE A HIGH PROPENSITY TO DEVELOP BRAIN METASTASES	8
1.4.3 DIAGNOSIS OF BRAIN METASTASES	8
1.5 THE NORMAL BLOOD-BRAIN BARRIER (BBB)	10
1.5.1 STRUCTURE AND FUNCTION OF THE NORMAL BBB	10
1.5.1.1 The paracellular pathway	12
1.5.1.2 The transcellular pathway	14
1.5.2 THE BBB IN BRAIN METASTASES	17
1.5.2.1 Trans-endothelial migration mechanisms	17
1.5.2.2 Protection of brain metastases by the BBB	18
1.6 CLINICAL TREATMENT OF BREAST CANCER AND BRAIN METASTASES	19
1.6.1 CURRENT TREATMENTS FOR BREAST CANCER	19
1.6.2 CURRENT TREATMENTS FOR BRAIN METASTATIC DISEASE	25
1.7 HISTONE DEACETYLASE (HDAC) INHIBITORS: EMERGING COMPOUNDS FOR THE TREATMENT OF BREAST CANCER BRAIN METASTASIS	33
1.8 PRECLINICAL MOUSE MODELS OF BREAST CANCER BRAIN METASTASIS	37
1.9 NOVEL BREAST CANCER BRAIN METASTASIS GENES	42
1.9.1 PROGNOSTIC BRAIN METASTASIS GENE SIGNATURES	47
1.10 HYPOTHESES AND SPECIFIC AIMS	48
2. MATERIALS AND METHODS	50
2.1 MATERIALS	50
2.1.1 GENERAL CHEMICALS AND REAGENTS	50
2.1.2 ANTIBODIES	52
2.1.3 OLIGONUCLEOTIDES	54
2.1.4 SIRNA AND SHRNA	55
2.2 CELL CULTURE METHODOLOGY	58
2.2.1 CELLS	58
2.2.2 PREPARATION OF BRAIN CONDITIONED MEDIUM (BCM)	59
2.2.3 PURIFICATION OF LM-511 FROM CONDITIONED MEDIUM	59
2.3 PROTEIN TECHNIQUES	60

2.3.1	PROTEIN ISOLATION	60
2.3.2	WESTERN BLOT ANALYSIS	61
2.4	IN VITRO FUNCTIONAL ASSAYS	62
2.4.1	PROLIFERATION ASSAYS.....	62
2.4.2	COLONY FORMATION ASSAYS.....	63
2.4.3	TUMOUR-ENDOTHELIAL CELL ADHESION ASSAYS.....	64
2.4.4	MIGRATION AND INVASION ASSAYS.....	64
2.4.5	TRANS-ENDOTHELIAL MIGRATION ASSAYS.....	65
2.5	IN VIVO ASSAYS	65
2.5.1	MOUSE HUSBANDRY AND ANIMAL ETHICS APPROVAL	66
2.5.2	METASTASIS ASSAYS	66
2.5.2.1	Spontaneous metastasis.....	66
2.5.2.2	Experimental metastasis.....	67
2.6	HISTOLOGY AND IMMUNOSTAINING METHODS	67
2.6.1	TISSUE FIXATION METHOD	67
2.6.2	HAEMATOXYLIN AND EOSIN (H&E) STAINING.....	68
2.6.3	IMMUNOHISTOCHEMISTRY (IHC).....	68
2.6.4	IMMUNOFLUORESCENCE (IF)	69
2.7	MOLECULAR TECHNIQUES.....	69
2.7.1	ISOLATION OF GENOMIC DNA	70
2.7.2	QUANTITATION OF METASTATIC BURDEN USING A MULTIPLEX TAQMAN® ASSAY.....	70
2.7.3	ISOLATION OF TOTAL RNA.....	71
2.7.4	SYNTHESIS OF CDNA.....	71
2.7.5	ASSESSMENT OF LIMITRIN MRNA EXPRESSION LEVELS UTILISING SYBR GREEN I TECHNOLOGY	72
2.7.6	TRANSIENT KNOCKDOWN OF LIMITRIN USING SMALL INTERFERING RNA (SIRNA).....	72
2.7.7	STABLE KNOCKDOWN OF LIMITRIN USING SHORT HAIRPIN RNA (SHRNA)	73
2.7.7.1	Isolation of plasmid DNA containing human limitrin shRNA	73
2.7.7.2	Transduction of shRNA to limitrin in the human MDA-MB-231Br tumour line	73
2.8	STATISTICAL ANALYSIS AND DIGITAL IMAGING	74
2.8.1	STATISTICAL METHODS.....	74
2.8.2	DIGITAL IMAGING.....	74
3.	<u>DEVELOPMENT AND CHARACTERISATION OF A NOVEL SYNGENEIC MOUSE MODEL OF SPONTANEOUS BREAST CANCER BRAIN METASTASIS ...</u>	<u>76</u>
3.1	INTRODUCTION	76
3.2	RESULTS.....	78
3.2.1	ISOLATION OF A BRAIN METASTATIC BREAST CANCER CELL LINE	78
3.2.2	IN VIVO FUNCTIONAL CHARACTERISATION OF THE 4T1BR4 MODEL	80
3.2.3	PHENOTYPIC ANALYSIS OF 4T1BR4 PRIMARY TUMOURS AND BRAIN METASTASES.....	82
3.2.4	FUNCTIONAL CHARACTERISTICS OF THE 4T1 AND 4T1BR4 CELL LINES IN VITRO	83
3.2.5	GENETIC VALIDATION OF THE 4T1BR4 MODEL AND RELEVANCE TO HUMAN BRAIN METASTATIC TNBC.....	86
3.3	DISCUSSION	89
4.	<u>EVALUATION OF LIMITRIN AS A PROGNOSTIC MARKER AND THERAPEUTIC TARGET FOR BREAST CANCER BRAIN METASTASIS.....</u>	<u>94</u>
4.1	INTRODUCTION	94
4.2	RESULTS.....	96
4.2.1	PROGNOSTIC SIGNIFICANCE OF LIMITRIN EXPRESSION IN BRAIN-METASTATIC BREAST CANCER ..	96
4.2.1.1	Analysis of the prognostic potential of limitrin in different subtypes of breast cancer	96
4.2.1.2	Limitrin expression in various breast cancer cell lines and tumours.....	97
4.2.1.3	Subcellular localisation of limitrin	104

4.2.1.4	<i>Detection of limitrin by immunohistochemistry (IHC)</i>	105
4.2.1.4.1	Optimisation of IHC protocol for anti-limitrin antibodies	105
4.2.1.4.2	Limitrin expression by IHC in mouse and xenograft tissues	109
4.2.1.4.3	Prognostic marker analysis of limitrin in patient tissues	112
4.2.2	<i>FUNCTION OF LIMITRIN IN BRAIN-METASTATIC BREAST CANCER</i>	114
4.2.2.1	<i>Function of limitrin in vitro</i>	114
4.2.2.2	<i>Function of limitrin in vivo</i>	115
4.3	DISCUSSION	122
5.	<u>NOVEL HISTONE DEACETYLASE INHIBITORS (HDACI) TO TREAT BREAST CANCER BRAIN METASTASIS</u>	127
5.1	INTRODUCTION	127
5.2	RESULTS	130
5.2.1	<i>EVALUATION OF THE EFFICACY OF SB939 AND 1179.4B IN VITRO</i>	130
5.2.2	<i>IDENTIFICATION OF BIOMARKER FOR THE EFFICACY OF HDACI IN VITRO</i>	133
5.2.3	<i>IMPACTS OF HDACI ON 4T1BR4 PRIMARY TUMOUR GROWTH AND BRAIN METASTASIS IN VIVO</i>	136
5.2.4	<i>ANALYSIS OF THE RADIOSENSITISING PROPERTIES OF HDACI IN VITRO</i>	140
5.3	DISCUSSION	147
6.	<u>SUMMARY AND CONCLUSION</u>	151

List of tables and figures	x
Abbreviations	xiv
Bibliography	154

List of tables and figures

Tables

Table 1-1. Five-year survival of breast cancer patients.	2
Table 1-2. Histological classification of breast cancer subtypes.	3
Table 1-3. Substrates for drug efflux transporters.	16
Table 1-4. Clinical trials of WBRT plus either focal treatments or chemotherapies.	27
Table 1-5. Outcome of inhibitors of drug transporters.	29
Table 1-6. Levels of drug concentration in normal brain tissues versus brain metastases in mouse models and in patients.	31
Table 1-7. Summary of the median overall survival of HER2 positive patients with CNS metastatic disease who received Trastuzumab treatments.	32
Table 1-8. Various actions of HDACi in cancer.	35
Table 1-9. Preclinical animal models of brain metastasis.	39
Table 1-10. Genes associated with the formation of brain metastases from breast cancer.	42
Table 2-1. List of antibodies used in this study.	52
Table 2-2. Sequences of primers and probes used for amplification of genomic DNA by TaqMan real time PCR.	54
Table 2-3. Sequences of primers used for real time RT-PCR with SYBR Green.	54
Table 2-4. Sequences of siRNAs used in this study.	55
Table 2-5. Sequences of limitrin and scramble shRNAs.	56
Table 3-1. Incidence of mice developing spontaneous brain metastases.	78
Table 3-2. Gene set enrichment analysis of 4T1Br4 versus brain-metastatic human breast tumours.	87
Table 4-1. Mouse limitrin protein coding sequences.	98
Table 4-2. Human limitrin protein coding sequences.	99
Table 4-3 IHC protocol optimisation for limitrin antibodies.	105
Table 5-1. IC ₅₀ of SB939, 1179.4b and SAHA in 4T1Br4 and MDA-MB-231Br cells.	131

Figures

Figure 1.1 The metastatic cascade	6
Figure 1.2 MRI scan of brains	9
Figure 1.3 Structure of the brain	9
Figure 1.4 Endothelial microvasculature in different organs	11
Figure 1.5 Schematic of tight junction and adherens junction.....	12
Figure 1.6 Schematic of the transcellular pathway in brain capillary endothelial cells..	15
Figure 1.7 Efflux pumps of the BBB	15
Figure 1.8 Schematic of treatment options for breast cancer	20
Figure 1.9 Synthetic lethality	25
Figure 1.10 Brain metastases induce breakdown of the BBB.....	31
Figure 1.11 Chromatin structure regulates transcriptional activity	34
Figure 1.12 Genes involved in brain metastases.....	45
Figure 2.1 Schematic diagram of subcellular fractionation adapted from QIAGEN.....	60
Figure 2.2 Schematic diagram of plasmid DNA extraction	72
Figure 3.1 Schematic representation of the development of the 4T1Br4 brain metastatic model.....	78
Figure 3.2 Comparison of 4T1 and 4T1Br4 tumour growth and metastatic burden in distant organs	80
Figure 3.3 Fluorescence and histological examination of 4T1Br4 brain metastases....	80
Figure 3.4 Confirmation of the TNBC phenotype in 4T1Br4 primary tumours and brain metastases	82
Figure 3.5 In vitro functional characterisation of the 4T1 and 4T1Br4 cell lines	84
Figure 3.6 Genetic relevance of 4T1Br4 to breast cancer patients with brain metastases	86
Figure 4.1 Association between limitrin expression in different subtypes of breast cancer and clinical outcomes	96
Figure 4.2 Limitrin mRNA expression in mouse and human breast cancer cell lines and mouse primary tumours	97
Figure 4.3 Anti-limitrin antibodies validation by western blotting in mouse and human breast cancer cell lines	101
Figure 4.4 Limitrin expression by western blotting in mouse mammary cancer cell lines.....	102
Figure 4.5 Limitrin expression by western blotting in human breast cancer cell lines	103
Figure 4.6 Differential subcellular localisation of limitrin in 66cl4 and 4T1Br4 cells....	104

Figure 4.7 Detection of limitrin in normal mammary glands and in 4T1Br4 primary tumours by IHC.....	106
Figure 4.8 Limitrin IHC staining in 4T1Br4 primary tumour tissues with the four generated antibodies from 3rd bleed.....	107
Figure 4.9 Limitrin IHC staining in MDA-MB-231Br xenograft tissues with the four generated antibodies from 3rd bleed.....	107
Figure 4.10 Immunohistochemical detection of limitrin in formalin-fixed paraffin embedded mouse tumours	109
Figure 4.11 Immunohistochemical detection of limitrin in formalin-fixed paraffin embedded human xenograft tumours	110
Figure 4.12 Quantification of limitrin IHC staining in a tissue microarray of 33 breast cancer patient samples	112
Figure 4.13 Suppression of limitrin expression by siRNA in 4T1Br4 cells.....	113
Figure 4.14 Downregulation of limitrin expression inhibits 4T1Br4 trans-endothelial migration.....	114
Figure 4.15 Suppression of limitrin expression by shRNA in MDA-MB-231Br cells ...	115
Figure 4.16 Growth curves of MDA-MB-231Br cells transfected with a control non-targeting shRNA and limitrin-targeting shRNA construct #1 or #4	116
Figure 4.17 Bioluminescence images of brains of mice injected with limitrin knockdown MDA-MB-231Br cells	117
Figure 4.18 Incidence liver and lung metastases in mice	118
Figure 4.19 Overall survival curves of mice injected with limitrin knockdown MDA-MB-231Br cells	118
Figure 4.20 Comparison of metastatic burden in mice injected with control or limitrin knockdown MDA-MB-231Br cells.....	119
Figure 5.1 Chemical structure of SB939 and 1179.4b.....	127
Figure 5.2 SB939 and 1179.4b inhibit survival of 4T1Br4 cells.....	129
Figure 5.3 SB939 and 1179.4b inhibit proliferation of 4T1Br4 and MDA-MB-231Br cells	130
Figure 5.4 IC ₅₀ of SAHA, SB939 and 1179.4b inhibits size of colonies of 4T1Br4 cells	131
Figure 5.5 SB939 and 1179.4b induce dose-dependent hyperacetylation of histone H3 in 4T1Br4 and MDA-MB-231Br cells.....	133
Figure 5.6 SB939 and 1179.4b induce time-dependent hyperacetylation of histone H3 in 4T1Br4 and MDA-MB-231Br cells.....	134
Figure 5.7 SB939 and 1179.4b-induced hyperacetylation of histone H3 is reversible	135
Figure 5.8 Effect of SB939 or 1179.4b on BALB/C mouse weight.....	136

Figure 5.9 SB939 and 1179.4b inhibit 4T1Br4 primary tumour growth and metastatic burden in spines	137
Figure 5.10 SB939 and 1179.4b increase acetylation of histone H3 in 4T1Br4 primary tumours	138
Figure 5.11 Tumour weight after resection	138
Figure 5.12 SB939 and 1179.4b inhibit 4T1Br4 spontaneous brain metastases.....	139
Figure 5.13 SB939 and 1179.4b radiosensitise 4T1Br4 cells	140
Figure 5.14 Radiosensitising effect of SB939 (colony size)	141
Figure 5.15 Radiosensitising effect of 1179.4b (colony size)	142
Figure 5.16 SB939 radiosensitises MDA-MB-231Br cells.....	143
Figure 5.17 1179.4b radiosensitises MDA-MB-231Br cells	145

Abbreviations

ABCB	ATP binding cassette sub-family B
AML	acute myeloid leukemia
ASP3	adipocyte-specific protein 3
BBB	blood-brain barrier
BCM	brain conditioned medium
BMP-2	bone morphogenetic protein 2
BSA	bovine serum albumin
CaCl ₂	calcium chloride
CK	cytokeratin
CNS	central nervous system
COX2	cyclooxygenase-2
CT	computed tomography
CT	cycle threshold
CTRL	control
DAB	3,3' Diaminobenzidine
DAPI	4',6-diamidino-2-phenylindole
DDFS	distant disease free survival
DEF	dose enhancement factor
DICAM	dual immunoglobulin domain containing cell adhesion molecule
DMEM	Dulbecco's modified eagle medium
DMSO	dimethylsulfoxide
DNA-PK	DNA-dependent protein kinase
DSB	double-strand break
E2F1	E2F transcription factor 1
EBRT	external beam radiation therapy
ECL	chemiluminescence
EDTA	ethylenediamine tetra-acetic acid
EGFP	enhanced green fluorescent protein
EGFR	epidermal growth factor receptor
EMT	epithelial-mesenchymal transition
ER	estrogen receptor
esiRNA	endonuclease-prepared siRNA
EST	Express Sequence Tag

FACS	fluorescence activated cell sorting
FBS	fetal bovine serum
FDA	The Food and Drug Administration
FFPE	formalin-fixed paraffin embedded tissues
H&E	haematoxylin and eosin
HA	hyaluronic nanoconjugate
HAT	histone acetyltransferase
HDAC	histone deacetylase
HDACi	histone deacetylase inhibitors
HER1	human epidermal growth factor receptor 1
HER2	human epidermal growth factor receptor 2
HSP90	heat-shock protein 90
IC ₅₀	the half-maximal inhibitory concentration
IDT	Integrated DNA Technologies
IF	immunofluorescence
IgSF	immunoglobulin superfamily
IHC	immunohistochemistry
ISO	isotype-matched antibody
JAM	junctional adhesion molecule
KM	Kaplan Meier
LB-agar	Luria broth-agar
MDR	multidrug resistance gene
MET	mesenchymal to epithelial transition
MgCl ₂	magnesium chloride
MMP	matrix metalloproteinase
MMTV	mouse mammary tumour virus
MMTV-PyMT	mouse mammary tumour virus-polyoma middle T
MRI	magnetic resonance imaging
MRP	multidrug resistance protein
MXRA8	matrix-remodelling-associated protein 8
NaCl	sodium chloride
NBF	neutral buffered formalin
NES	normalised enrichment score
NFF	neonatal foreskin fibroblasts
NF-κB	nuclear factor-κB
NHDF	normal human dermal fibroblasts

NSG	NOD scid gamma
OS	overall survival
P/S	penicillin-streptomycin
PARP	poly-adenosine diphosphate ribose polymerases
PBS	phosphate buffered saline
PBS-TT	PBS containing 0.5% Tween-20 and 0.1% Triton X-100
PEG	poly(ethylene glycol)
PEI	polyethylenimine
PET	positron emission tomography
PFA	paraformaldehyde
P-gp	p-glycoprotein
PR	progesterone receptor
qPCR	real-time quantitative PCR
rhLM-511	recombinant human LM-511
RT	room temperature
RTA	relative transcript abundance
RTB	relative tumour burden
SAHA	suberanilohydroxamic acid
SD	standard deviation
SDS	sodium dodecyl sulfate
SFM	serum free medium
shRNA	short hairpin RNA
siRNA	small interfering RNA
SRB	sulforhodamine B
SRS	stereotactic surgery
SSB	single-strand breaks
TBS	tris-buffered saline
TCA	trichloroacetic acid
TEER	transendothelial electrical resistance
TEMED	N,N,N',N'-Tetramethylethylenediamine
TMA	tissue microarray
TN	triple negative
TNBC	triple negative breast cancer
VEGF	vascular endothelial growth factor
VPA	valproic acid
WBRT	whole brain radiation therapy

α -MEM	α -minimal essential medium
Csf3	Colony-stimulating factor 3
Lama4	laminin subunit alpha 4
B4galt6	beta-1,4-galactosyltransferase 6
Angptl4	angiopoietin-like 4
Peli1	pellino E3 ubiquitin protein ligase 1
Hbegf	heparin-binding EGF-like growth factor
Ltbp1	latent-transforming growth factor beta-binding protein 1

1. Literature Review

1.1 Overview of thesis structure and objectives

Breast cancer metastasises primarily to the lung, liver, bone and brain. Patients with advanced breast cancer die of metastases rather than the primary tumour itself. Despite recent clinical advances in the treatment of metastatic breast cancer, brain metastasis remain incurable and its incidence is increasing (Steeg et al., 2011, Eichler et al., 2011). Patients are not routinely screened for the presence of brain metastases and therefore are often diagnosed when symptoms are already apparent and treatment options are limited. Hence, there is a need for better therapies and/or biomarkers to prospectively identify patients at risk of brain metastasis. However, our understanding of the genes and mechanisms regulating brain metastasis is fragmented, in part due to the lack of clinically relevant models of breast cancer brain metastasis. Accordingly, the overall objective of my PhD project was to characterise a new syngeneic mouse model of spontaneous breast cancer brain metastasis in which to investigate the prognostic significance and function of a novel brain metastasis gene and to test new therapies against brain metastasis.

Chapter 1 below presents a review of current literature and summarises our understanding of breast cancer metastasis to the brain. The chapter highlights some of the issues in the field and areas of clinical needs and, where relevant, draws a parallel between the work presented in the results chapters and how they address some of these issues/needs. The methodology used during my PhD project is described in detail in Chapter 2. Aims 1, 2 and 3 of my project are addressed specifically in the results Chapters 3, 4 and 5 respectively. This is followed by a short Discussion (Chapter 6) that summarises the results from my investigation and the relevance of my findings to the field. In this chapter, I also propose future areas of investigation.

1.2 Breast cancer – incidence, mortality and subtypes

In Australia, approximately 12,000 patients are diagnosed with breast cancer every year. Women's lifetime risk of being diagnosed with breast cancer is 12.5% (1 in 8). Breast cancer is the second most common cause of mortality in women among all types of cancer. Mortality from breast cancer is due primarily to metastatic spread, not

primary tumour. Five-year survival for women with localised disease or lymph node involvement is close to 100% whereas it drops dramatically when they have distant metastases (Table 1-1). Breast cancer metastasis to distant organs such as the lung, liver, bone and brain (Lu and Kang, 2007) is responsible for nearly 3,000 deaths each year in Australia (Australian Institute of Health and Welfare, 2014). In the United States, in 2015 alone, it is estimated that 234,190 women will be diagnosed with breast cancer and 40,730 women will die of it (Siegel et al., 2015).

Table 1-1. Five-year survival of breast cancer patients.

Stages of breast cancer	5-year survival (%)
Localised	98.6
Regional	84.4
Distant	24.3

Table modified from (Howlader N, 2013).

Breast tumours are heterogeneous (Polyak, 2011, Rivenbark et al., 2013) and can be classified into several molecular subtypes based on gene expression profiling of thousands of genes using RNAseq or cDNA microarrays that provide a distinctive “molecular portrait” of each tumour (Perou et al., 2000, Sorlie et al., 2001). The aim of molecular subtyping of tumours is to guide clinical decisions towards personalised therapy. However, how to best implement this new molecular classification of breast cancer patients into routine pathology for diagnostic purposes and the relationships between molecular classification and clinical parameters is still debated.

Clinical classification of breast cancer patients relies primarily on histological examination of primary tumour tissues for the expression of cell surface markers allowing classification into four main histological subtypes (Table 1-2): luminal A (estrogen receptor (ER) positive, progesterone receptor (PR) positive and human epidermal growth factor receptor 2 (HER2) negative), luminal B (positive for ER, PR and HER2), HER2 positive (HER2 amplification) and basal-like (or triple-negative, negative for ER, PR and HER2) (Allison, 2012). The proportions of these histological subtypes of breast cancer are: luminal A, 40%; luminal B, 20%; HER2 positive, 15%; and basal-like, 15-20% (Voduc et al., 2010). The specific breast cancer subtype is a key determinant of the patient’s local and regional recurrences. The luminal A subtype is associated with a low risk of local or regional recurrence, whereas the HER2 positive and basal-like subtypes are associated with a high risk of regional recurrence (Voduc

et al., 2010). The specific molecular/intrinsic subtype is also relevant to the patient's prognosis: while luminal A and B confer good and intermediate prognosis respectively, HER2 positive and basal-like breast cancer patients do worse (Sorlie et al., 2001, van 't Veer et al., 2002). The five-year overall survival rates for luminal A and B breast cancers are 90.3% and 88.7% respectively, whereas that of HER2 positive and basal-like are inferior (78.8% and 79.0% respectively) (Onitilo et al., 2009). The median overall survival is 6.1, 9.2 and 3.4 years for the luminal A/B, HER2 and basal-like subtypes, respectively (Adamo et al., 2011). Of note, the terms triple-negative (TN) and basal-like are sometimes used interchangeably but these two classifications are not perfectly overlapping (Bertucci et al., 2008). Breast tumours categorised as "basal-like" are characterised by the expression of certain basal cytokeratins (CKs) such as CK 5/6 or expression of the epidermal growth factor receptor (EGFR) (Gusterson et al., 2005, Kanapathy Pillai et al., 2012, Gazinska et al., 2013). Although a majority (50-80%) of TN tumours are identified as basal-like, not all basal-like tumours are TN (Bertucci et al., 2008) and recent evidence has revealed that the TN breast cancer (TNBC) is in fact a heterogeneous disease that encompasses many subtypes. For example, Chen et al. identified by meta-analysis of gene expression profiles six TNBC subtypes including two basal-like subtypes (Chen et al., 2012). Therefore caution should be exercised when using "basal-like" to refer to the TN subtype in general.

Table 1-2. Histological classification of breast cancer subtypes.

Molecular subtype	Surrogate markers
Luminal A	Strong ER+, PR+/-, HER2-, weak Ki-67
Luminal B	Weak ER+, PR+/-, HER2+/-, strong Ki-67
HER2	Strong HER2+, ER/PR+/-
Basal-like	ER/PR/HER2-, CK5/6+/-, EGFR+/-

The histological classification of breast cancer subtypes can be distinguished based on immunohistochemistry assay. Ki-67 is a marker of cell proliferation. CK5/6, cytokeratin 5/6; EGFR, epidermal growth factor receptor. +, positive; -, negative. Table modified from (Allison, 2012).

1.3 Breast cancer metastasis

Metastasis refers to a process through which cancer cells spread to distant organs. Intriguingly, different tumours manifest distinct organ selectivity depending on the types of cancer. The disproportionate, non-random distribution of target organs for different types of tumours is termed organotropism. For example, breast cancer patients often suffer from metastases to the lung, liver, bone and brain. Colorectal cancer commonly metastasises to the liver but not to the bone and brain. Ninety per cent of advanced prostate cancer patients develop bone metastases (Lu and Kang, 2007, Hess et al., 2006). Such organ-selectivity of tumours could be attributed to mechanical factors, i.e., the anatomical structure of the vascular system. This concept was first proposed by James Ewing in 1922 and termed the “vascular flow hypothesis” or “theory of embolism” (Ewing, 1922). For example, the high incidence of liver metastases in colorectal cancer patients can be explained by the fact that the first capillary bed encountered by disseminating colorectal cancer cells is the hepatic portal system to the liver (Roth et al., 2009, Chambers et al., 2002). Similarly, in experimental animal models, the route of tumour cell injection substantially influences the anatomical sites that will be colonised, for example different metastatic patterns between intravenous injection (via the tail vein) showing lung and liver metastases and intracardiac (via the left ventricle of the heart) injection showing bone and brain metastases of MDA-MB-231 cells in mice respectively (Lu and Kang, 2007).

However a body of evidence suggests that factors other than blood flow influence metastatic organotropism, and this is in line with the “seed and soil” hypothesis suggested by Stephen Paget (Paget, 1989). From his analysis of 735 autopsy records, Paget observed that certain tumour cells had affinity for specific organs and postulated that the propensity of tumours to metastasise to other organs depended on the compatibility between the cancer cells (the “seed”) and the target organs (the “soil”). Classical experimental data directly supporting this hypothesis came from studies on organ-specific metastasis of melanoma led by Isaiah J. Fidler in the 1970s (Fidler and Nicolson, 1976, Fidler and Nicolson, 1977, Nicolson et al., 1978). When highly metastatic B16-F10 melanoma cells were injected into syngeneic C57BL/6 mice via intravenous (i.v.) injection (experimental model), tumours developed in the lungs and grafted pulmonary tissues in thigh muscle (Hart and Fidler, 1980). Yet, the use of radioactively labelled tumour cells revealed that tumour cells reached the vasculature of all organs. This observation led the authors to conclude that the outcome of metastasis was dependent on both tumour cell properties and host factors. Another piece of evidence was derived from studies by Tarin et al (Tarin et al., 1984). In these studies, patients with incurable abdominal cancers were fitted with peritoneovenous

shunts to relieve their sufferings from ascites. Although the patients had millions of metastatic tumour cells continuously introduced into the circulation for months or even years, no apparent increase in lung metastases was observed. After all, Paget's century-old hypothesis that metastasis is not a random manifestation remains the conceptual foundation for modern tumour metastasis studies.

Metastasis requires the completion of multiple steps including cell proliferation and invasion at the primary site, intravasation, adhesion to the endothelium, extravasation from the circulation and colonisation of a secondary site. These steps are well described in works by the Massagué and Kerbel groups (Nguyen et al., 2009, Francia et al., 2011) (Figure 1.1). This multistep event is an innately inefficient process with each step being potentially rate-limiting, and this provides opportunities to design effective anti-metastatic therapies (Stoletov et al., 2014, Eckhardt et al., 2012). *In vivo* imaging and cell fate analysis have suggested that the most important in these rate-limiting steps is the ability to survive and grow in secondary sites. A seminal study by Luzzi et al. illustrated the fate of b16F1 murine melanoma cells injected through the mesenteric vein of mice to target the liver (Luzzi et al., 1998). In their study, 87% of the injected cells were arrested and present in the liver at 90 min and 83% remained there on day 3, but only 2% formed micrometastases and 0.02% progressed to form macrometastases on day 10 (Luzzi et al., 1998). Similar observations have been reported (Koop et al., 1996, Cameron et al., 2000, Varghese et al., 2002), suggesting that early steps of the metastatic cascade are completed efficiently and the major obstacle to metastatic progression is the regulation of cancer cell growth in the secondary site.

In secondary organs, the vast majority of metastatic cells fail to form macrometastases and perish and a tiny subset proceeds to grow, but some cells remain inactive for an unpredictable period of time until they respond to signals that trigger tumourigenic growth (Luzzi et al., 1998, Cameron et al., 2000). In clinical observations, it has been reported that metastases can occur even decades after primary treatment (Meltzer, 1990, Karrison et al., 1999). What makes tumour cells 'dormant' – neither in proliferation nor apoptosis – is not clearly understood but might be associated with p38-mediated stress signals released by the host organ, which restrains tumour cell proliferation without inducing apoptosis (Sosa et al., 2011). Another source of tumour dormancy might be pre-angiogenic micrometastases, where tumour cells proliferation is balanced by apoptosis (Holmgren et al., 1995). Likewise, little is known about how dormant tumour cells regain tumourigenic properties. This hidden state of dormancy

poses a major challenge in controlling metastasis, as dormant cells are likely to be insensitive to therapies that target actively dividing cancer cells.

Many studies have identified genes that play a role in regulating specific steps of breast cancer metastasis. Genes that appear particularly relevant to brain metastasis are discussed in more detail in section 1.9 of this chapter.

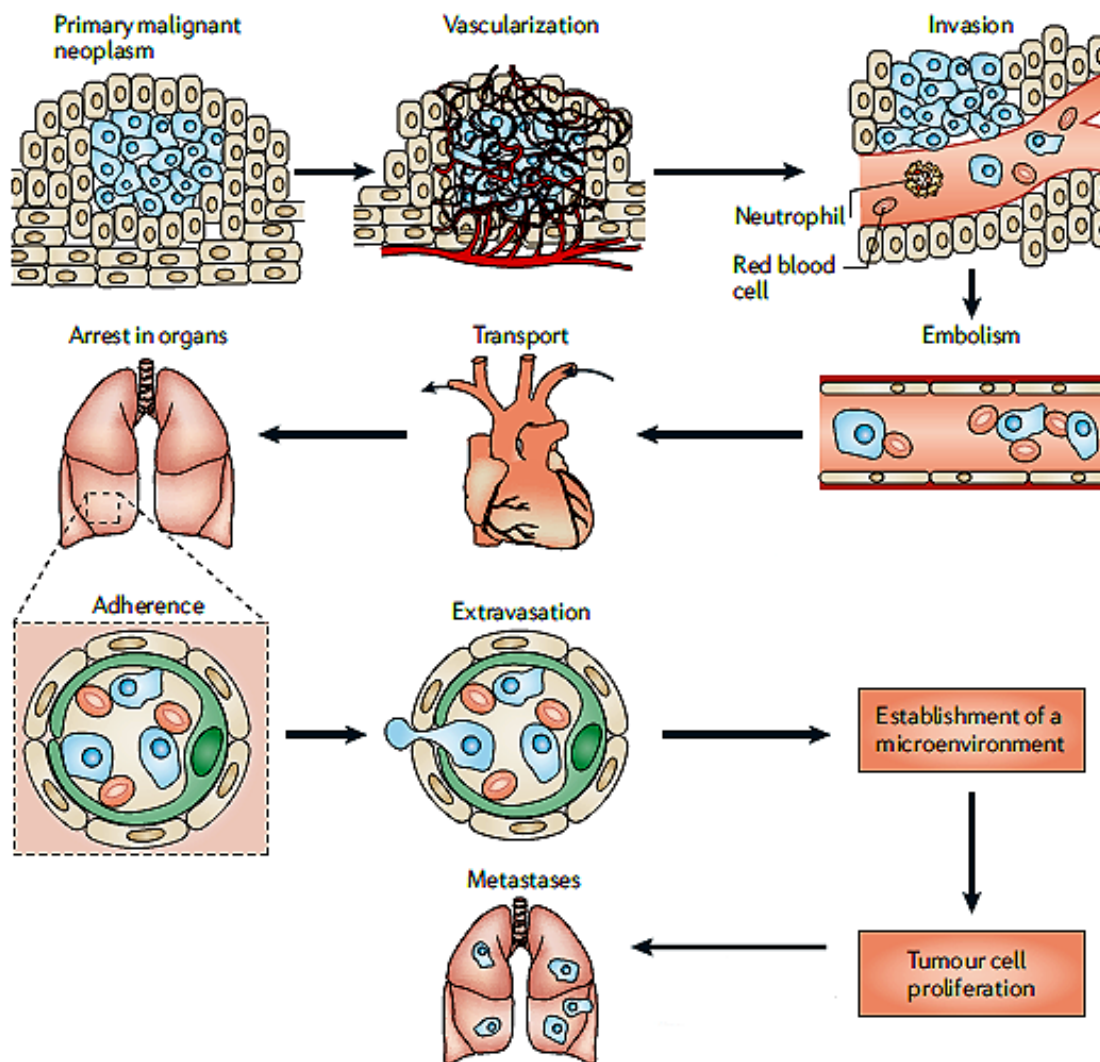


Figure 1.1 The metastatic cascade

Metastasis is a complex process in which each step of dissemination from the primary site via the circulation to a secondary organ must be completed. The primary tumour develops, proliferates, and recruits new blood vessels. Pro-angiogenic cytokines secreted by tumour cells and surrounding stromal cells are thought to play an important role in vascularisation (Folkman and Klagsbrun, 1987). Escaping from the primary site,

tumour cells intravastate into the circulation and are disseminated throughout the body. Circulating tumour cells must survive hostile environments such as hemodynamic shear forces, lack of substratum, and immune cell attack. It is suggested that tumour cells cling to platelets to protect themselves from these harsh environments (Ho-Tin-Noe et al., 2009). Then tumour cells arrest in the vasculature of a secondary site mainly by size restriction, attach to endothelium and cross the vessels to enter the secondary organ. Once extravasated, tumour cells must survive the foreign microenvironment, proliferate, and vascularise to form macrometastases. Overall, these metastatic steps are rate-limiting and inefficient and the most critical and rate-limiting step is the regulation of tumour growth in the host organ (Luzzi et al., 1998, Koop et al., 1996). Image modified from (Francia et al., 2011).

1.4 Breast cancer brain metastasis

1.4.1 Incidence and survival of patients with brain metastases

Historically, 15-20% of patients with metastatic breast cancer develop brain metastases (Liu et al., 2012). However, retrospective studies from autopsies indicate that the incidence of brain metastases in advanced breast cancer patients is as high as 30% (Cheng and Hung, 2007, Steeg et al., 2011). Moreover, the incidence of brain metastases is increasing as a result of improvement in brain imaging modalities and systemic treatments that control extracranial metastases and prolong patient survival but are not curative against brain metastases (Steeg et al., 2011, Eichler et al., 2011).

Prognosis for patients with brain metastases is very poor, with a median survival of approximately 1 month if left untreated, 2 months after symptomatic treatment with steroids and 3-6 months if treated with radiotherapy after diagnosis (Wadasadawala et al., 2007). Strong favourable prognostic factors in patients with metastases in the central nervous system (CNS) include the presence of a single metastasis in the brain, no other site of or controlled metastasis, controlled primary tumour, a long interval from primary diagnosis to brain relapse, positive steroid receptor status, age <60 years and good performance status (Wadasadawala et al., 2007, Eichler et al., 2011). Patients with CNS metastases achieved a median survival of 25.3 months if they had a favourable prognostic factor (Sperduto et al., 2012).

The increasing incidence of brain metastases from breast cancer and the ineffectiveness of the current therapies underpin the urgent need to more thoroughly study this disease.

1.4.2 Tumour subtypes that have a high propensity to develop brain metastases

The TNBC and HER2 positive subtypes of breast cancer have a high affinity for the brain and develop brain metastases early (2-3 years after initial diagnosis of breast cancer) (Heitz et al., 2009, Gaedcke et al., 2007, Hicks et al., 2006). Indeed, the percentage of patients who progress to brain metastasis among breast cancer subtypes is 37.3% in TNBC, 29.4% in HER2 positive, 18.3% in luminal A and 15.1% in luminal B. Moreover, the TNBC subtype confers a shorter median survival after brain recurrence than other subtypes (3.4 months in TNBC, 5.0 months in HER2 positive, 4.0 months in luminal A and 9.2 months in luminal B) (Nam et al., 2008).

1.4.3 Diagnosis of brain metastases

The diagnosis of brain metastasis can be confirmed by contrast-enhanced computed tomography (CT) or magnetic resonance imaging (MRI) (Figure 1.2). The distribution of brain metastases is correlated with blood flow and tissue volume, rather than the specific origin of the primary tumour. Hence, brain metastases are most commonly found in the cerebral hemispheres (80%), cerebellum (10-15%), brain stem (2-3%), spinal cord, dura mater, leptomeninges, pituitary, and choroid plexus (Delattre et al., 1988, Patnayak et al., 2013) (Figure 1.3). However, breast cancer is one of the most common tumours to metastasise to the leptomeninges (Le Rhun et al., 2013), which accounts for 2-6% of brain metastases from breast cancer as evidenced from autopsy (Chang and Lo, 2003).

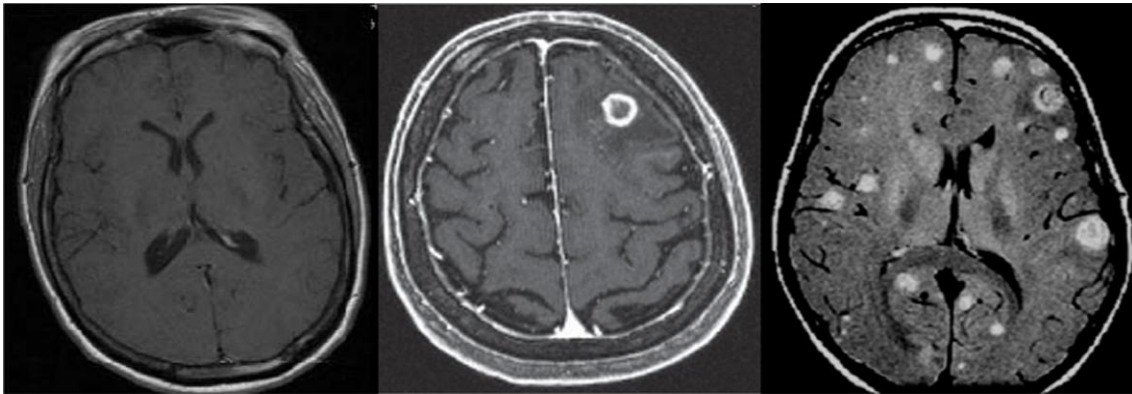


Figure 1.2 MRI scan of brains

Left panel, normal brain. Middle panel, solitary brain metastasis. Right panel, multiple brain metastases. Image modified from (Coutinho et al., 2011, Vallow, 2009, Alsidawi et al., 2014).

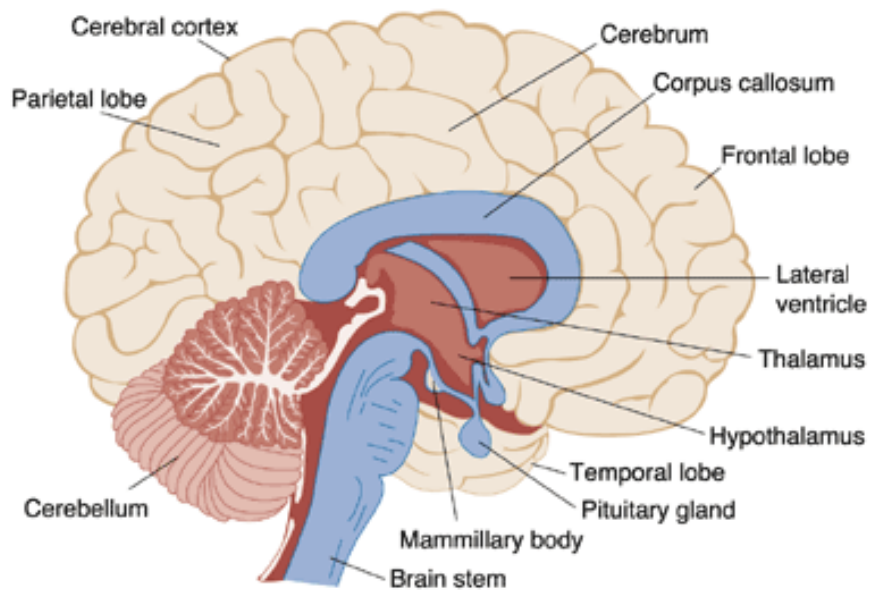


Figure 1.3 Structure of the brain

The brain is composed of three main structural divisions: the cerebrum, the cerebellum, and the brainstem. The cerebrum, cerebellum and brainstem make up 85%, 11% and 4% of the brain by weight, respectively. Image reproduced from (Oscar-Berman et al., 1997).

Brain metastasis is usually a late manifestation of cancer (Chen et al., 2011, Bartelt et al., 2004, Graesslin et al., 2010, Lorgier and Felding-Habermann, 2010). Brain metastasis is asymptomatic in up to 60-85% of patients (Soffiatti et al., 2006, Seaman et al., 1995). This and the prohibitive costs of brain imaging often deter them from undergoing routine screening. For this reason, patients are often diagnosed when symptoms are apparent and treatment options and response are limited. The symptoms of brain metastasis include gait disturbances, seizures, headaches, cognitive dysfunction, nausea, vomiting, cranial nerve dysfunction, cerebellar symptoms (imbalance and nystagmus) and speech disturbances (Chang and Lo, 2003). Therefore, it is absolutely imperative that we find and develop new biomarkers or gene signatures that can predict patients at risk of developing brain metastasis. In this regard, Chapter 4 focuses on characterising a potentially new biomarker/therapeutic target called limitrin.

1.5 The normal blood-brain barrier (BBB)

1.5.1 Structure and function of the normal BBB

The CNS is considered a sanctuary site in the human body due to the presence of the BBB that protects the brain by preventing foreign substances such as toxins and drugs from entering the brain parenchyma (Deeken and Loscher, 2007). The BBB has unique characteristics and is different from capillaries in other organs, such as liver, bone marrow or spleen capillaries that are composed of discontinuous endothelial cells and kidney or gastrointestinal capillaries that are composed of fenestrated endothelial cells (Pries and Kuebler, 2006) (Figure 1.4).

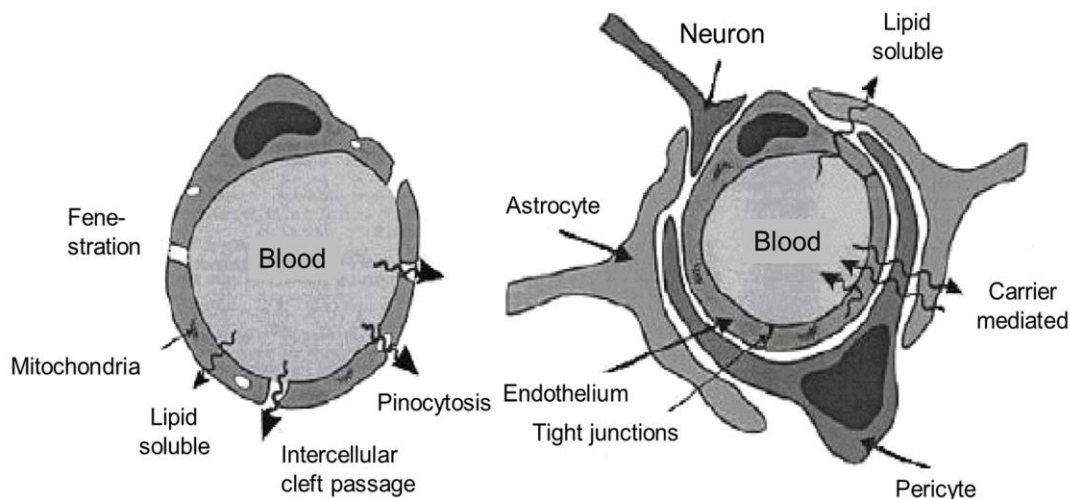


Figure 1.4 Endothelial microvasculature in different organs

Capillaries of the BBB are structurally distinct from capillaries in other organs such as liver or kidney capillaries that are discontinuous or fenestrated (left). Brain capillaries are tightly held together by the presence of tight junctions and surrounding basal membrane, pericytes and astrocyte end-feet (right). Image modified from (Misra et al., 2003).

Continuous capillaries are loose as they have intercellular clefts of 6-7 nm in size between endothelial cells (Figure 1.4, left). Plasma and substrates can be transported from the cell surface to the opposite side of the cell through pinocytotic vesicles. Fenestrae allow diffusion or transport of substrates across endothelial cells. In contrast, brain capillaries are tightly closed by abundant tight junctions and have no fenestrations and low pinocytosis (Figure 1.4, right). They are surrounded by the basement membrane composed of extracellular matrix, including type IV collagen, fibronectin, laminin, tenascin and proteoglycans, as well as pericytes and astrocyte end-feet (Wilhelm et al., 2013). Pericytes regulate blood flow, endothelial proliferation, angiogenesis and inflammatory processes (Wilhelm et al., 2013). Astrocyte end-feet ensheath over 90% of the endothelial cell surface and further contribute to restricting the permeability of the BBB.

In addition to the structural tightness of the BBB, brain capillaries have a high transendothelial electrical resistance (TEER) that prevents the entry of polar and ionic substances into the brain. Brain capillaries' TEER is measured between 1000-2000 Ω

cm^2 compared to $10 \Omega \text{ cm}^2$ in aortic capillaries (Butt et al., 1990). Thus, due to the astonishing level of physiological tightness of the BBB, other substances such as drugs and toxins can enter the brain only via two mechanisms; the paracellular (through cell-cell junctions of endothelial cells) or transcellular (through endothelial cells) pathway (Deeken and Loscher, 2007).

1.5.1.1 The paracellular pathway

The paracellular pathway is mainly regulated by the tight junction proteins between endothelial cells (Figure 1.5). The best characterised among these are occludins, claudins and junctional adhesion molecules (JAMs).

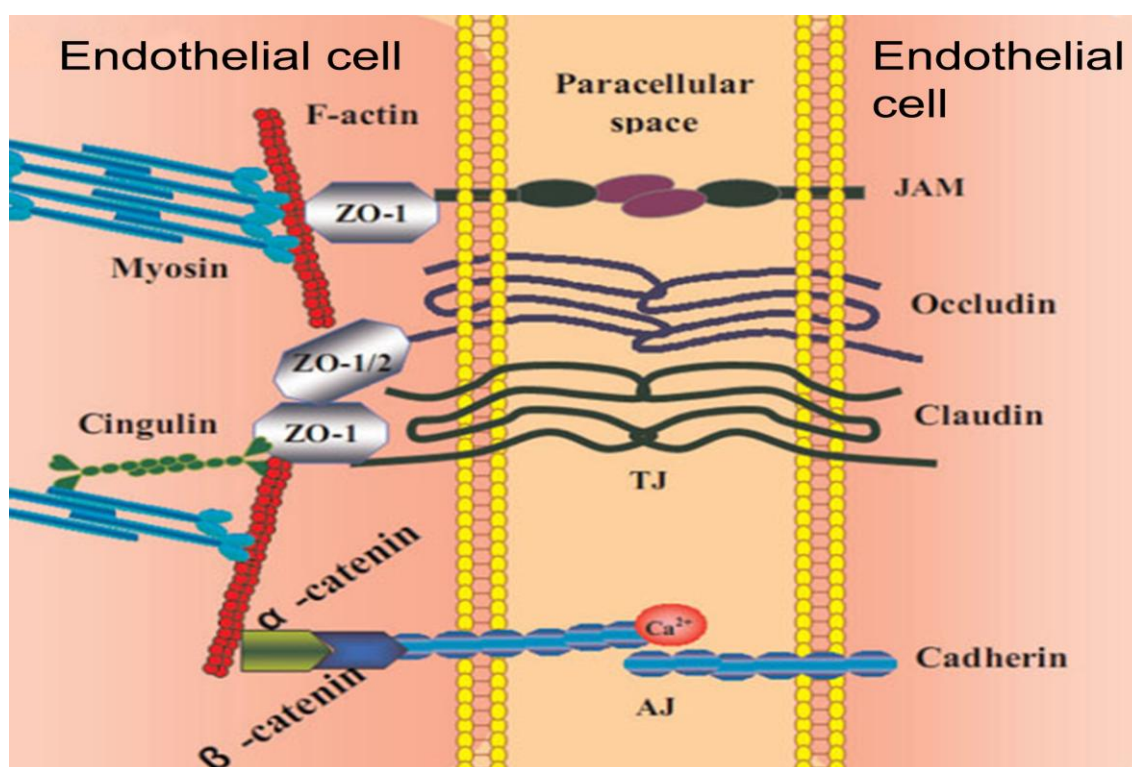


Figure 1.5 Schematic of tight junction and adherens junction

Best characterised tight junction proteins include junctional adhesion molecules (JAMs), occludins and claudins. Adherens junction is cadherin-based. TJ. tight junction; AJ, adherens junction. Image modified from (Huang et al., 2014).

Occludins were the first tight junction proteins identified in both epithelial and endothelial cells in 1933 (Furuse et al., 1993). Occludins have two extracellular loops

with a shorter N-terminal and a longer C-terminal cytoplasmic domain. Claudins have a similar structure to occludins, with two extracellular loops, a shorter N-terminal and a longer C-terminal domain (Ruffer and Gerke, 2004). Among the claudin family, claudins-1, -3, -5 and -12 have been shown to play a role in the formation of tight junction at the BBB *in vivo* (Liebner et al., 2000, Morita et al., 1999, Nitta et al., 2003, Wolburg et al., 2003, Schrade et al., 2012). Claudin-5, for example, is highly expressed in vascular endothelial cells (Hewitt et al., 2006). Consistent with a role in maintaining the BBB functional integrity, claudin-5 deficient mice show selective penetration of small molecules (<800 Da) across the BBB (Nitta et al., 2003, Zhang et al., 2010). Thus, claudins can be used to confirm the histologic identity of certain types of cancer and to predict patients' prognosis (Ouban and Ahmed, 2010).

JAMs belong to the immunoglobulin superfamily and are characterised by homophilic binding and two extracellular loops (Martin-Padura et al., 1998). JAM-A (JAM-1), JAM-B (JAM-2) and JAM-C (JAM-3) are primarily expressed in the brain endothelial cells and are involved in the extravasation of leukocytes (Wilhelm et al., 2013, Ludwig et al., 2005, Johnson-Leger et al., 2002, Chavakis et al., 2004, Ostermann et al., 2002, Santoso et al., 2002). Studies using a blocking antibody to JAM-A showed reduction in leukocyte extravasation *in vitro* and *in vivo* (Del Maschio et al., 1999, Martin-Padura et al., 1998, Ostermann et al., 2002). JAM-A has been described as a homophilic adhesion receptor of tight junctions on epithelial and endothelial cells (Petri and Bixel, 2006, Martin-Padura et al., 1998, Bazzoni et al., 2000, McSherry et al., 2011) but it can bind to LFA-1 (CD11a/CD8 integrin) on leukocytes during inflammation (Ostermann et al., 2002). JAM-B also binds to VLA-4 ($\alpha 4\beta 1$ integrin) (Ludwig et al., 2009) and JAM-C binds to Mac-1 ($\alpha M\beta 2$ integrin) (Santoso et al., 2002) expressed on leukocytes. The function or expression of JAM-A is still a controversial topic. Naik et al. reported that JAM-A is a negative regulator of breast cancer cell invasion and metastasis by showing that T47D and MCF-7 cells, which are less migratory, showed high levels of JAM-A whereas more migratory MDA-MB-468 and MDA-MB-231 cells showed low levels of JAM-A (Naik et al., 2008). On the contrary, McSherry et al. reported that JAM-A mediates migration of breast cancer by interacting with $\beta 1$ integrin (McSherry et al., 2011) and is highly expressed in HER2 positive breast tumour (Brennan et al., 2013) and TNBC breast cancer patients (McSherry et al., 2009). Consistent with McSherry's observations, Murakami and colleagues demonstrated that high expression of JAM-A is related to poor prognosis in breast cancer patients by analysing 444 patients' samples (Murakami et al., 2011). This is a more convincing argument than that of Naik et al., whose study was based on *in vitro* experiments using four human cell lines (Naik et al.,

2008). Choi and colleagues also showed that the expression of JAM-B and JAM-C is increased in brain metastases compared to TNBC primary tumours (Choi et al., 2013). In our analysis, we identified limitrin, a new member of the immunoglobulin superfamily of proteins whose expression is elevated in brain-metastatic breast tumours and that has a similar structure to JAM-A (Yonezawa et al., 2003). The function of limitrin in breast cancer brain metastasis is investigated in detail in Chapter 4.

In addition to tight junction molecules, cadherin-based adherens junctions play an important role in BBB permeability in endothelial cells at the BBB (On et al., 2014, Pal et al., 1997). Cadherins are transmembrane proteins and over 80 types of cadherins have been identified in humans (Tepass et al., 2000). Cadherins play a role in maintaining the structure of cells and tissues and in cellular movement such as cell migration (Tepass et al., 2000). Among cadherins, E-cadherin is expressed in epithelial (Shimoyama et al., 1989) and endothelial cells (Abbruscato and Davis, 1999). It is regulated by calcium and binds to F-actin through α - and β -catenins in cerebral microvessel endothelial cells (Brown and Davis, 2002). Of particular relevance, loss of E-cadherin is associated with tumour metastasis (Beavon, 2000) and could be a predictive marker of brain metastasis in lung cancer patients (Yoo et al., 2012). Cadherin-10 has a pivotal role in the development and maintenance of the BBB in human and mouse (Williams et al., 2005). N-cadherin is commonly found in cancer cells and plays a role in transendothelial migration which is regulated by β -catenins signalling (Ramis-Conde et al., 2009, Qi et al., 2005, Qi et al., 2006).

1.5.1.2 The transcellular pathway

The transcellular pathway (Eichler et al., 2011, Blecharz et al., 2015) consists of passive transcellular diffusion of lipid-soluble agents (Ballabh et al., 2004, Abbott et al., 2010), cell surface transporters for the uptake of glucose, amino acids and nucleosides (Abbott et al., 2010, Tamai and Tsuji, 2000), receptor-mediated transcytosis of hormones or high molecular mass molecules such as insulin and transferrin (Duffy and Pardridge, 1987, Holly and Perks, 2006) and adsorptive-mediated transcytosis of cationic molecules such as albumin and plasma proteins (Pardridge, 1994, Kang and Pardridge, 1994) (Figure 1.6).

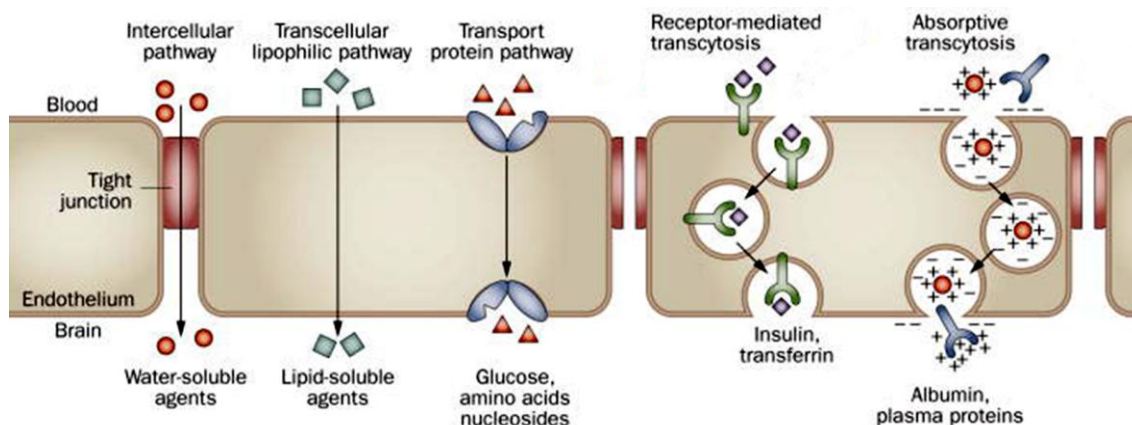


Figure 1.6 Schematic of the transcellular pathway in brain capillary endothelial cells

The transcellular pathway in brain endothelial cells consists of passive transcellular diffusion, transport protein systems, receptor-mediated transcytosis and adsorptive transcytosis. Image modified from (Eichler et al., 2011).

In particular, endothelial cells of the BBB express high levels of drug efflux transporters/pumps that actively prevent many chemicals, including chemotherapeutic drugs and toxic substances, from entering the brain (Loscher and Potschka, 2005, Deeken and Loscher, 2007) (Figure 1.7).

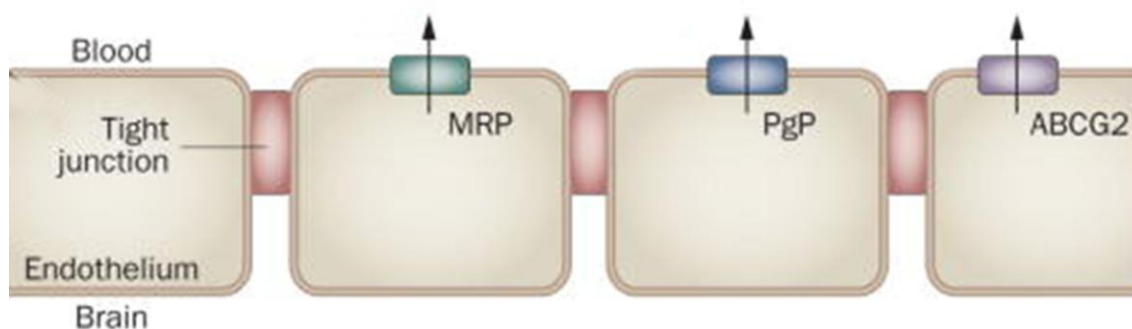


Figure 1.7 Efflux pumps of the BBB

The most extensively studied among the efflux transporters of the BBB are p-glycoprotein (p-gp), multidrug resistance proteins (MRPs) and breast cancer resistance protein (ABCG2). Image modified from (Eichler et al., 2011).

P-glycoprotein (p-gp) is also known as multidrug resistance gene (MDR1) or ATP binding cassette sub-family B member 1 (ABCB1). Multidrug resistance proteins (MRPs) consist of nine members named MRP1 to MRP9. The expression of MRPs varies in the BBB. Studies have confirmed that the concentration of substrates in the brain, including etoposide, is increased in MRP1 knock-out mice compared with wild-type mice (Borst et al., 2000, Wijnholds et al., 2000). Breast cancer resistance protein (ABCG2) was first discovered in a study of the chemotherapy resistant MCF-7 breast cancer cell line (Doyle et al., 1998), where the authors observed higher mRNA expression of ABCG2 compared to that of p-gp and MRP1 in the BBB (Eisenblatter et al., 2003). Substrates for efflux transporters are shown in Table 1-3. Unfortunately, anti-cancer compounds that are substrates for these efflux transporters are actively extruded from the brain endothelium back into the circulation. This is a major issue that limits the efficacy of therapies against brain metastases and is discussed in more detail in section 1.6.2.

Table 1-3. Substrates for drug efflux transporters.

Transporter	Substrates
P-glycoprotein (p-gp)	Doxorubicin, daunorubicin, docetaxel, paclitaxel, epirubicin, idarubicin, vinblastine, vincristine, etoposide
MRP1	Etoposide, teniposide, daunorubicin, doxorubicin, epirubicin, melphalan, vincristine, vinblastine
MRP2	Similar to MRP1
MRP3	Similar to MRP1
MRP4	Methotrexate, 6-mercaptopurine, thioguanine
MRP5	6-mercaptopurine, thioguanine
MRP6	Actinomycin D, cisplatin, daunorubicin, doxorubicin, etoposide
MRP7	Docetaxel, paclitaxel, Ara-C
MRP8	5-FU, cisplatin, methotrexate
Breast cancer resistance protein (ABCG2)	Mitoxantrone, methotrexate, SN-38, topotecan, imatinib, erlotinib, gefitinib

MRP, multidrug resistance protein; Ara-C, arabinofuranosyl cytidine; 5-FU, 5-fluorouracil; ABCG2, ATP-binding cassette sub-family G member 2; SN-38, 7-ethyl-10-hydroxycamptothecin (an active metabolite of irinotecan). Substrate of MRP9 is currently unknown. Table modified from (Deeken and Loscher, 2007).

The permeability of drugs across the BBB is dictated by a number of physical and chemical properties. These include low molecular weight (<500 Da), fewer hydrogen bond donors, fewer positive charges, greater lipophilicity, lower polar surfaces and reduced flexibility. Typically, brain permeable compounds that are small (<450 Da), nonpolar (polar surface area <60-70 Å²), lipophilic (logP 1.5-2.7) with less than eight hydrogen bonds, can cross the BBB by passive transcellular diffusion (transcellular pathway) (Pajouhesh and Lenz, 2005). Polar and/or hydrophilic compounds can penetrate into the brain only by active transport systems (transcellular pathway). Lipophilic drugs show lower permeability if they are substrates for drug efflux transporters (Deeken and Loscher, 2007).

1.5.2 The BBB in brain metastases

1.5.2.1 Trans-endothelial migration mechanisms

Many studies have documented the mechanisms by which leukocytes cross brain endothelial cells (Dejana, 2006, Mamdouh et al., 2009, Engelhardt and Wolburg, 2004). Unfortunately, the genes and mechanisms regulating breast cancer metastasis to the brain are still poorly understood. In 2010, Kienast and colleagues documented the process of melanoma and lung cancer cells metastasising to the brain by using multiphoton laser-scanning microscopy imaging in experimental models (Kienast et al., 2010). The authors showed that cancer cells arrested in vascular branch points by size restriction, rather than by vascular wall adhesion. After extravasating, the cells remained in close contact with the vasculature and proliferated in the brain by vessel co-option or angiogenesis to grow as macrometastases. This study has significance in that how tumour cells colonise the brain to form metastases was observed in a picturesque manner. In the same year, Lorger and Felding-Habermann described that breast cancer cells showed elongated shape to fit into the narrow capillaries in brain after cell injection, stayed close to the vessel walls at the parenchymal side after extravasation before initiating proliferation/growth in the brain into macrometastases (Lorger and Felding-Habermann, 2010). Carbonell and colleagues demonstrated that breast cancer cells formed vasculature using vessel co-option after extravasation in brain (Carbonell et al., 2009). Taken together, these studies suggest that melanoma, lung and breast cancer cells that have a high propensity to metastasise to the brain may undergo similar physical processes to metastasise to the brain.

Breast cancer cells secrete several molecules that may enhance their transmigration through the brain endothelium. For example, MDA-MB-231 breast cancer cells secrete vascular endothelial growth factor (VEGF) that increases the BBB permeability by disrupting endothelial F-actin and VE-cadherin (an adherent junction molecule) through the activation of calcium signalling, thereby facilitating tumour cell adhesion to, and transmigration through the endothelium (Lee et al., 2003). VEGF-induced disruption of ZO-1 (a tight junction molecule) and VE-cadherin in endothelial cells promotes adhesion of HER2 positive breast cancer cells to endothelial cells (Fan et al., 2011). Similarly, proinflammatory neuropeptide substance P facilitates adhesion and transmigration of MDA-MB-231 cells through endothelial cells. Substance P increases BBB permeability by disrupting or redistributing ZO-1 and claudin-5 and decreasing TEER in endothelial cells (Rodriguez et al., 2014). The same was observed in melanoma disrupting tight junction molecules in endothelial cells at the BBB. For instance, when melanoma cells contacted endothelial cells, ZO-1 and claudin-5 were disrupted and TEER was reduced via serine protease-dependent mechanisms (Fazakas et al., 2011).

In addition to the paracellular pathway, breast cancer cells can use the transcellular pathway. Myosin contraction is induced by myosin light chain kinase in endothelial cells when MDA-MB-231 cells contact endothelial cells, and this in turn facilitates transcellular migration of the breast cancer cells (Khuon et al., 2010).

A body of evidence indicates that matrix metalloproteinase (MMP)-2 and MMP-9 are crucial for leukocytes penetration of the basement membrane by cleavage of dystroglycan, a transmembrane receptor located in endfeet of astrocytes that interacts with laminin 111 and 211 (Agrawal et al., 2006), or degradation of claudin-5 (Chiu and Lai, 2013). Similarly, MMP-2 promotes transmigration of breast cancer cells (MDA-MB-231 and MCF-7) (Lee et al., 2011). These observations imply that breast cancer cells may share some mechanisms with leukocytes for trans-endothelial migration in the BBB. In this regard and as mentioned earlier in section 1.5.1.1, JAMs proteins are involved in transendothelial migration of leukocytes and may play a similar role in tumour cell transendothelial migration.

1.5.2.2 Protection of brain metastases by the BBB

While the BBB serves as an effective barrier against foreign substances, ironically tumour cells can benefit from the protection of the BBB against immune cells and anti-

cancer agents once they have entered the brain parenchyma (Wilhelm et al., 2013). Astrocytes help maintain the BBB integrity, provide nutrition to and repair for not only nerve cells but also for brain metastases (Fidler, 2011, Langley and Fidler, 2011). Astrocytes induce up-regulation of survival genes (GSTA5, BCL2L1 and TWIST1) or cytokines (interleukin-6 and -8), resulting in increased protection for MDA-MB-231 cells from chemotherapeutic agents (Kim et al., 2011, Kim et al., 2014). MDA-MB-231Br (a brain metastatic subline of MDA-MB-231) secretes bone morphogenetic protein 2 (BMP-2) in the brain that induces the differentiation of neural progenitor cells (NPCs) into astrocytes and the promotion of tumour cell growth (Neman et al., 2013).

Cancer cells establish blood vessels that provide essential nutrients for tumour growth in the brain. Vascular co-option is one of the mechanisms by which cancer cells recruit blood vessels. After trans-endothelial migration, cancer cells proliferate in the BBB in close contact with existing blood vessels. Other mechanisms of vessel formation including angiogenesis, vasculogenesis and intussusception in the brain are described in detail in (di Tomaso et al., 2011, Jain et al., 2007, Ricci-Vitiani et al., 2010, Soda et al., 2011, Wang et al., 2010).

1.6 Clinical treatment of breast cancer and brain metastases

1.6.1 Current treatments for breast cancer

Five main approaches are used to treat breast cancer patients in practice: surgery, radiation therapy, hormonal therapy, targeted therapy and chemotherapy (Senkus et al., 2015) (Figure 1.8).

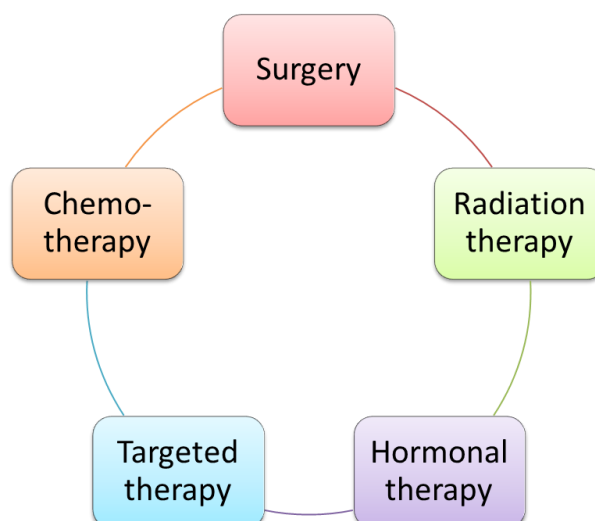


Figure 1.8 Schematic of treatment options for breast cancer

Five options are available to treat breast cancer in the clinic: surgery, radiation therapy, hormonal therapy, targeted therapy and chemotherapy.

Surgery: Surgical removal of the tumour mass from the breast is usually the first treatment for breast cancer patients. Some of the lymph nodes under the armpit may also be removed if cancer cells are found. There are two basic types of surgery to remove breast cancer. Mastectomy is a surgery where the entire breast is removed, and lumpectomy (also known as breast-conserving surgery or partial mastectomy) is a surgical removal of the tumour and a discreet portion of healthy tissues around it without removing the entire breast. Some breast cancer patients may receive chemotherapy prior to surgery, known as neoadjuvant chemotherapy, to shrink the tumour. Surgery improves the survival of breast cancer patients. Since mammography can often detect breast cancer at an early stage, five-year survival for stage 0 breast cancer patients is 99%, and patients with regional lymph node involvement (stage I-III) do well (five-year survival 84%) (Table 1-1). Although surgery is not advised for patients with metastatic breast cancer (stage IV) at diagnosis because the disease is considered incurable, some studies have demonstrated that surgery improves the survival of patients with metastatic breast cancer. In a study by Shien et al., surgery significantly prolonged the overall survival of metastatic breast cancer patients (27 months versus 22 months without surgery) (Shien et al., 2009). They also reported surgery conferred improved overall survival in young patients (<50 years old) compared to old patients (>50 years old) with metastatic disease and recommended it should be considered if the patient is younger than 50 (Shien et al., 2009). The complete surgical

excision of the primary tumour in patients with metastatic disease (especially those with bone metastases only) significantly reduces the risk of death by up to 40% compared with women who do not have surgery (Rapiti et al., 2006). Blanchard and colleagues reported a 27.1 months median survival in patients who had surgery versus 16.8 months without surgery in stage IV breast cancer (Blanchard et al., 2008). In contrast to the study by Rapiti et al. (Rapiti et al., 2006), the effect of surgery on prolonged survival was not evident in patients with bone metastasis only. A potential explanation for these discrepancies was provided by Olson and Marcom (Olson and Marcom, 2008), who pointed out that patients who underwent surgery had more favourable disease characteristics (e.g., small and hormone receptor positive primary tumour and fewer sites of metastases) than patients who did not have surgery. Thus, whether surgery improves the survival of metastatic breast cancer patients still remains controversial.

Radiation therapy: Radiotherapy uses high-energy rays or particles to destroy cancer cells. While sometimes it is given before surgery (neoadjuvant) to shrink the tumour size, in most cases radiation is applied after surgery (adjuvant) to reduce the risk of local and regional recurrence on the basis of the results of studies suggesting that post-operative radiotherapy can reduce the recurrence by at least 60% in patients (Fisher et al., 2002). The most commonly used modality is external beam radiation therapy (EBRT, also known as traditional or whole breast radiation therapy) (Zhang et al., 2015a). EBRT delivers a beam that is highly focused and targets the area affected by the cancer for minutes from outside the body. Typically, it involves several daily treatments over 5 to 7 weeks. Another modality is internal radiation therapy (also known as brachytherapy), which is less common. Instead of directing radiation beams at the breast, brachytherapy involves a radioactive source being inserted inside or adjacent to the tumour area post-resection to kill any remaining cancer cells (Zhou et al., 2015).

Hormonal therapy: Identifying breast cancer subtypes can inform on the best treatment approach for patients. Generally, endocrine therapies are applicable to patients with luminal A and B subtypes as these subtypes express ER. Tamoxifen is an antagonist of the estrogen receptor in the breast tissue and was approved by the Food and Drug Administration (FDA) for adjuvant (after surgery) hormone treatment of pre- and post-menopausal women (or men) with ER positive breast cancer (Jordan, 1993). Tamoxifen reduces breast cancer recurrence and mortality. ER positive breast cancer patients treated with tamoxifen for 5 years show a significant reduction (31%) in the

annual breast cancer death rate (Early Breast Cancer Trialists' Collaborative, 2005). Similarly, women who received tamoxifen showed a 40% reduction in recurrence compared to those who received placebo (Dignam et al., 2003).

Other treatments available for ER positive patients include aromatase inhibitors (anastrozole, letrozole, and exemestane) and selective estrogen receptor downregulators (fulvestrant and ICI 164,384) (Criscitiello et al., 2011). Fulvestrant is used for postmenopausal women with ER positive metastatic breast cancer who have progressed on prior endocrine therapy such as tamoxifen (Bundred, 2005, Johnston and Cheung, 2010, Croxtall and McKeage, 2011) and downregulates ER expression in breast cancer (Jones, 2003, Howell et al., 2004). However, the majority of patients treated with aromatase inhibitors or fulvestrant develop drug resistance. Garcia-Becerra et al. described several mechanisms of hormone resistance including loss or modification in the ER- α expression, regulation of signal transduction pathways, altered expression of specific microRNAs, balance of co-regulatory proteins, and genetic polymorphisms. They also suggested new strategies to overcome such resistance (Garcia-Becerra et al., 2012).

HER2-targeted therapy: Treatment options for patients with HER2 gene amplification include HER2 targeted therapies such as Trastuzumab and Lapatinib. Trastuzumab (Herceptin), a monoclonal antibody against HER2 receptor, is approved by the FDA for patients with metastatic breast cancers that overexpress HER2. Introduction of Trastuzumab into the clinic has significantly improved the prognosis of patients with HER2 positive breast cancer (Piccart-Gebhart et al., 2005, Viani et al., 2007). Piccart-Gebhart et al. analysed data from HER2 positive breast cancer patients randomly assigned to one-year Trastuzumab treatment (n = 1694) or observation (n = 1693) groups (Piccart-Gebhart et al., 2005). In their study, primary recurrence, second metastasis or death was observed in 7.5% of the Trastuzumab treated group versus 13% in the observation group. Viani et al. compiled and analysed 5 clinical studies where HER2 positive early breast cancer patients received one-year Trastuzumab treatment and demonstrated that overall mortality rate was 6% in the Trastuzumab treated group compared to 8.5% in the non-Trastuzumab treated group (Viani et al., 2007). Trastuzumab showed not only significant reduction of mortality but also of recurrence and metastasis rates. Whereas the recurrence and metastasis rates in the non-Trastuzumab treated group were 15.3% and 10.8%, that of the Trastuzumab treated group were 8.2% and 6%, respectively (Viani et al., 2007).

It is noteworthy that although Trastuzumab significantly improves treatment outcome for HER2 positive breast cancer patients, 70% of patients with HER2 positive breast cancers do not respond to the treatment because of *de novo* or acquired resistance to Trastuzumab (Pohlmann et al., 2009). For this reason, several combinations of Trastuzumab with various therapies have been developed to enhance the effect of Trastuzumab and to reduce drug resistance (Lavaud and Andre, 2014, Incurvati et al., 2013, Kumler et al., 2014). The combination of Trastuzumab with chemotherapy has been shown to improve recurrence-free survival in patients with HER2 positive breast cancer (Joensuu et al., 2006, Slamon et al., 2011). The use of Trastuzumab in patients with pre-existing heart disease is limited due to the drug's cardiotoxicity with a range of severity (Piccart-Gebhart et al., 2005, Viani et al., 2007).

Lapatinib, a dual tyrosine kinase inhibitor that targets HER2 and epidermal growth factor receptor (EGFR), is used in combination therapy for HER2 positive breast cancer patients who have progressed after previous treatments with Trastuzumab or chemotherapy (Blackwell et al., 2012). The combination of Trastuzumab and Lapatinib has been shown to lead to a significant increase in the pathological complete response rate in HER2 positive breast cancer patients compared to Trastuzumab alone or the combination of Trastuzumab with chemotherapeutic agents such as taxanes, anthracyclines, cyclophosphamide or fluorouracil (Baselga et al., 2012, Hicks et al., 2015).

TNBC and chemotherapy: As mentioned above, TNBC patients, lacking the three commonly targeted receptors in human breast cancer, i.e., ER, PR, and HER2, do not benefit from hormonal or anti-HER2-targeted monotherapies (Allison, 2012) and have a poorer prognosis than patients with other breast cancer subtypes. However, TNBC has been shown to be more sensitive to chemotherapeutic agents such as anthracyclines, taxanes or platinum agents than other subtypes (Anders and Carey, 2009). It is well known that TNBC patients often carry breast cancer 1 (BRCA1) mutations (Seong et al., 2014, Greenup et al., 2013, Tung et al., 2012). BRCA1 plays a critical role in DNA double-strand breaks (DSBs) repair by homologous recombination and BRCA dysfunctions result in a defective DSB repair system in cancer cells (Turner et al., 2004). This may partly explain why the TNBC subtype is sensitive to DNA-damaging platinum-containing chemotherapeutic agents (i.e., cisplatin and carboplatin) (Telli, 2014, Anders and Carey, 2009). Nevertheless, the majority of patients with TNBC have a high risk of relapse. This is attributable in part to residual disease at the time of surgery that resulted in high risk of relapse and death in the first 3-5 years after surgery

and the development of chemoresistance (Anders and Carey, 2009, Cheang et al., 2008, Dent et al., 2007, Dent et al., 2009, Andre and Zielinski, 2012). Therefore, there is a need for more effective and defined neoadjuvant and adjuvant therapies, surgery protocols and monitoring blood after surgery in TNBC patients.

Novel targeted and combination therapies for TNBC: Although TNBC lacks effective therapeutic targets, i.e., ER, PR, and HER2, the fact that this subtype is a heterogeneous disease encompassing many different phenotypes (Lehmann et al., 2015, Bernardi and Gianni, 2014, Criscitiello et al., 2012, Millis et al., 2015, Metzger-Filho et al., 2012) may bring the possibility of identifying new targets for the treatment of subgroups of TNBC patients. For example, EGFR, also known as human epidermal growth factor receptor 1 (HER1), is expressed significantly more in TNBC patients (approximately 60%) than in breast cancer patients overall (less than 30%) (Irvin and Carey, 2008, Tsutsui et al., 2002). This has led to the suggestion that EGFR may be an attractive therapeutic target for the treatment of advanced TNBC, especially in combination with chemotherapy. For instance, cetuximab, a monoclonal antibody that targets EGFR, showed a higher response rate (17%) in combination with carboplatin than cetuximab alone (6%) in stage IV TNBC (Carey et al., 2012). Also, cetuximab plus paclitaxel achieved a major reduction of skin metastases in a TNBC patient (Gholam et al., 2007). While Lapatinib is used primarily for the treatment of patients with HER2 positive breast cancer, this dual kinase inhibitor also targets EGFR (Kim et al., 2009, McNeil, 2006), which suggests therapeutic potential for TNBC patients. However, there are few ongoing clinical studies using Lapatinib for the treatment of TNBC. One clinical trial is currently recruiting participants (ClinicalTrials.gov identifier #NCT02158507). Another clinical study used Lapatinib in combination with everolimus (inhibitor of mammalian target of rapamycin (mTOR) gene) for the treatment of advanced TNBC patients but this study was stopped and no results were reported (ClinicalTrials.gov identifier #NCT01272141).

Poly-adenosine diphosphate ribose polymerases (PARPs), like BRCA1, play a vital role in DNA repair. In particular, PARP1 is essential for sensing DNA single-strand breaks (SSBs) and recruiting base excision repair proteins at damaged sites, thereby repairing DNA damages (De Vos et al., 2012, Gibson and Kraus, 2012, Riffell et al., 2012). PARP inhibitors block the repair of SSBs, causing some SSBs to become DSBs. BRCA can repair these breaks by homologous recombination. However, due to the common BRCA mutations in TNBC, cancer cells are unable to repair these damages, leading to

cell death, a mechanism called “synthetic lethality” (Cressey, 2010, Polyak and Garber, 2011) (Figure 1.9).

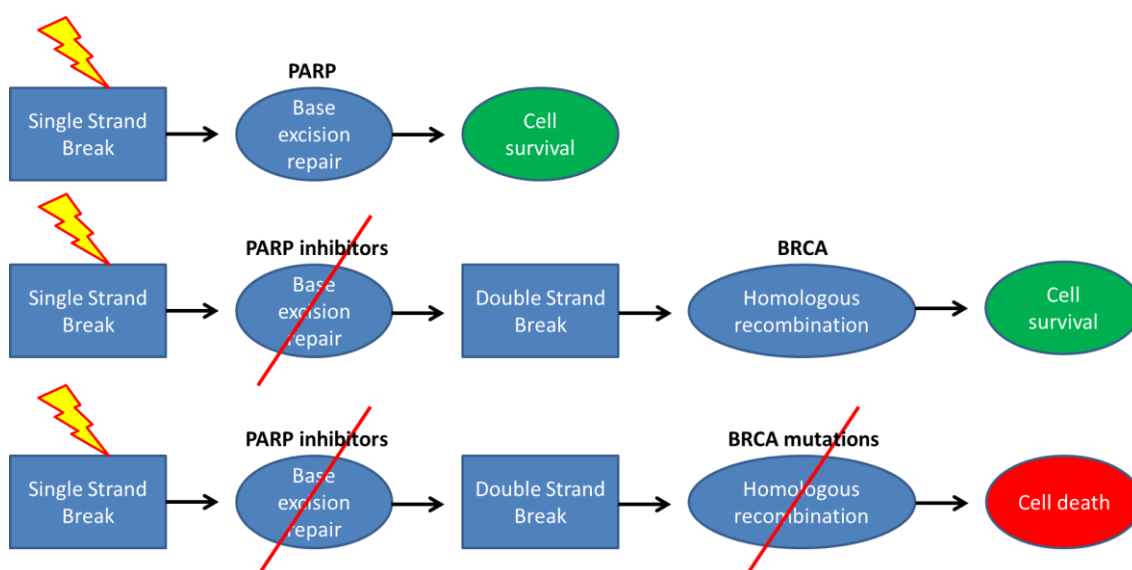


Figure 1.9 Synthetic lethality

DNA repair pathways are categorised into single- and double-strand break mechanisms. PARP inhibitors block the repair of single-strand breaks (SSBs) that results in conversion of SSBs to double-strand breaks (DSBs). Since TNBC often have BRCA mutations, DSBs cannot be efficiently repaired, leading to cancer cell death.

A number of clinical trials of PARP inhibitor combination therapy in breast cancer patients are currently underway. For example a phase 3 randomised trial of carboplatin and paclitaxel with or without veliparib in HER2-negative or BRCA-associated breast cancer patients (ClinicalTrials.gov identifier # NCT02163694). A phase 2 randomised trial combining the PARP inhibitor veliparib (ABT-888) and carboplatin plus paclitaxel in TNBC patients showed a pathologic complete response of 52% compared to 26% in patients that received paclitaxel only (ClinicalTrials.gov identifier # NCT01042379) (Printz, 2014).

1.6.2 Current treatments for brain metastatic disease

Standard treatments for brain metastases are primarily palliative and include corticosteroids, surgery, whole brain radiation therapy (WBRT), chemotherapy and HER2-targeted therapy.

Corticosteroids are used as an adjuvant treatment to reduce cerebral oedema and intracranial pressure. In general, dexamethasone is preferred to other steroids because of its minimal mineralocorticoid effect and long half-life. It is recommended to use 4-8 mg/day for patients who are symptomatic (Ryken et al., 2010).

Surgical resection improves the overall median survival in the range of 14-16 months (Wronski et al., 1997, Pieper et al., 1997). However, surgery is not feasible for patients with multiple or large brain metastases. Accordingly, surgery is usually reserved for patients who have a single brain metastasis (Chargari et al., 2010). As an alternative to surgery, stereotactic surgery (SRS, e.g., Gamma Knife and CyberKnife), using multiple radiation beams with high power energy on target tumour, extends the median survival of patients to 8-13 months (Aoyama et al., 2006, Kocher et al., 2011) (Jaboin et al., 2013, Bashir et al., 2014, Smith et al., 2014) and is recommended for patients who have 3 or fewer brain metastases (<4 cm) (Chargari et al., 2010).

WBRT is the most common treatment for patients with multiple (>3) brain metastases in combination with other modalities. Radiation reduces brain relapses in combination with surgery, SRS or radiosensitisers, but such combinations do not significantly improve the survival of patients compared to WBRT alone (Table 1-4) (Chargari et al., 2010, Rades et al., 2014). Since randomised studies have shown no overall survival benefit and decline in neurocognitive function (e.g., learning, memory and spatial information processing) (Chang et al., 2009, Tsao, 2015) from the combination of WBRT and SRS, the American Society for Radiation Oncology (ASTRO) in 2014 recommended “not to routinely add adjuvant whole brain radiation therapy to stereotactic radiosurgery for limited brain metastases” (Gemici and Yaprak, 2015).

Table 1-4. Clinical trials of WBRT plus either focal treatments or chemotherapies.

Study	Total number of patients/patients with breast cancer	Brain relapse (%), WBRT alone vs. combined treatment	Median overall survival (months)	
			WBRT alone	Combined treatment
(Patchell et al., 1990)	48/3 (6.3%)	52 vs. 20	3.5	9.2 (surgery)
(Kondziolka et al., 1999)	27/4 (14.8%)	100 vs. 8	7.5	11 (SRS)
(Andrews et al., 2004)	333/34 (10.2%)	29 vs. 18	6.5	5.7 (SRS)
(Verger et al., 2005)	82/13 (15.9%)		3.1	4.5 (temozolomide)
(Suh et al., 2006)	515/106 (20.5%)		4.4	6.0 (efaproxiral)
(Scott et al., 2007)	106/106 (100%)		4.5	9.0 (efaproxiral)
(Kim et al., 2012)	400/400 (100%)		5.0	12.8 (chemotherapy*)

*WBRT, whole brain radiation therapy; SRS, stereotactic surgery. Temozolomide is an oral alkylating agent used as a treatment of gliomas (Kast et al., 2015). Efaproxiral is an allosteric effector of haemoglobin that increases the oxygenation of hypoxic tumours (Suh, 2004). *Patients were treated with at least one modality, e.g., taxane-, capecitabine- or anthracycline-containing regimen.*

For breast cancer patients, low-dose (2-3 Gy) radiation (total 30 Gy in 10 fractions) is the standard. However, as WBRT causes cognitive dysfunctions that usually manifest weeks or months after WBRT (Chargari et al., 2010, Welzel et al., 2008), the dose and fractionation schedule must be tailored to each patient to reduce WBRT toxicity in long-term breast cancer survivors (Chang and Lo, 2003).

Multiple classes of radiosensitisers have been developed and tested *in vitro* and *in vivo* in combination with radiotherapy (Russo et al., 2009, Morgan et al., 2010, Gerster et al., 2010, Chung et al., 2009). The rationale for the use of radiosensitisers is to improve the

efficacy of radiation therapy while reducing cognitive losses in patients (Russo et al., 2009, Morgan et al., 2010, Gerster et al., 2010, Chung et al., 2009). However, radiosensitisers have not demonstrated the same benefits in patients (Wadasadawala et al., 2007, Chargari et al., 2010) (Viani et al., 2009, Tsao et al., 2012). Viani et al. analysed eight randomised clinical trial studies (n = 2317 patients in total) and concluded the combination of WBRT and radiosensitisers (e.g., ionidamine, metronidazole, misonodazole, motexafin gadolinium, BUdr, efaproxiral, thalidomide) did not increase the overall survival and tumour response in patients with brain metastases compared to WBRT alone (Viani et al., 2009). However, the combination of WBRT and efaproxiral significantly increased the survival of breast cancer brain metastases patients up to 9 months compared to WBRT alone (4.5 months) (Scott et al., 2007). This study also reported that the quality of life in patients treated with the combination was improved compared to the WBRT alone treated group. A phase 3 randomised trial combining WBRT and efaproxiral to treat brain metastases from breast cancer was completed in 2013, but the results are not available yet (ClinicalTrials.gov identifier #NCT00083304). A phase 2 clinical trial of motexafin gadolinium with WBRT followed by SRS to treat brain metastases patients was completed in 2014 and is awaiting results (ClinicalTrials.gov identifier #NCT00121420).

Chemotherapy alone is unlikely to provide significant benefits as reported in many clinical studies (Boogerd et al., 1992, Postmus and Smit, 1999, Abrey et al., 2001, Barlesi et al., 2011, D'Antonio et al., 2014). There are at least two potential explanations for the controversial efficacy of chemotherapy. First, the BBB in the CNS prevents most chemotherapeutic drugs from entering the brain parenchyma as discussed in section 1.5.2 (Loscher and Potschka, 2005, Deeken and Loscher, 2007). Second, brain metastases could develop resistance to chemotherapy since brain metastasis is generally a late stage event in the course of the disease and is often diagnosed when patients already would have been heavily pretreated with multiple chemotherapeutic agents to treat extracranial metastases (Cheng and Hung, 2007, Steeg et al., 2011, Chargari et al., 2010).

Since 98% of small molecule drugs do not cross the BBB (Pardridge, 2007), numerous strategies have been developed to improve drug delivery into the CNS. Generally, delivery of paclitaxel is limited to approximately 10% of the brain, even though it has been used as an anti-cancer agent with great cytotoxic effect in various types of cancer. This has resulted in the emergence of a strategy to modify the structure of this drug to increase its permeability to the brain. For example, ANG1005 (a paclitaxel-brain

delivery vector angiopep 2 conjugate) shows 4 to 54-fold higher drug uptake in brain metastases of breast cancer than free paclitaxel (Thomas et al., 2009). Another example is paclitaxel-hyaluronic nanoconjugate (HA-paclitaxel). In preclinical studies, HA-paclitaxel increased the survival of mice with brain metastases from breast cancer (MDA-MB-231Br model) by inducing endocytosis in the BBB (Mittapalli et al., 2013).

Another strategy to improve delivery of anti-cancer drugs to the brain is the use of inhibitors of efflux pumps. Drug efflux pumps and properties required for drugs to penetrate the BBB were discussed earlier in section 1.5.2. Inhibitors are used to increase the concentration of substrates in the brain (Table 1-5).

Table 1-5. Outcome of inhibitors of drug transporters.

Transporter	Substrate	Inhibitor	Outcome*	Reference
P-gp	Colchicine and vinblastine	PSC 833, GF 120918 and verapamil	1.8-3 fold	(Cisternino et al., 2001)
	Colchicine and vinblastine	PSC 833 and verapamil	8.4-9 fold	(Drion et al., 1996)
	Paclitaxel	Cyclosporin A, GF120918 and PSC833	3-6.5 fold	(Kemper et al., 2003)
MRP1/2	Cryptotanshinone	Probenecid and MK-571	21.4 fold	(Yu et al., 2007)
ABCG2	Imatinib	Pantoprazole and elacridar	1.8-4.2 fold	(Breedveld et al., 2005)

*Fold increase of brain uptake. P-gp, p-glycoprotein; MRP, multidrug resistance proteins; ABCG2, breast cancer resistance protein. Table modified from (Deeken and Loscher, 2007).

In addition to the combination of transporter inhibitors with chemotherapy, other agents are used to increase drug penetration into the CNS. Mannitol, a hyperosmolar agent, was shown to increase intracerebral methotrexate levels 4-5-fold compared to the non-mannitol infused side (Cosolo et al., 1989). RMP-7, an analogue of bradykinin, increases the permeability of lanthanum in brain endothelial cells by disrupting tight junctions (Sanovich et al., 1995) and significantly increases the uptake of carboplatin in the brain (Emerich et al., 1999, Gregor et al., 1999, Matsukado et al., 1996).

Alternatively, drugs can be delivered into the brain via receptor-mediated transcytosis. For this purpose, therapeutic agents are conjugated to antibodies or peptides that bind to transferrin receptor, insulin receptor, or low density lipoprotein receptor-related protein 1 or 2 (Jones and Shusta, 2007).

The BBB can also be disrupted physically. Radiation, a standard therapy for patients with brain metastases, has been suggested to disrupt the BBB thereby resulting in enhanced drug delivery into the brain. Rats, irradiated at 60 Gy, showed disruption of the BBB at two weeks post-irradiation (Rubin et al., 1994). This may explain in part the improvement in survival for patients with brain metastases who received Trastuzumab in addition to radiation, compared to those treated with radiation alone (see Table 1-4). Likewise, ultrasound has been shown to disrupt the BBB (McDannold et al., 2006, Alkins et al., 2013) and to increase the concentration of Trastuzumab in the brain (Kinoshita 2006).

HER2-targeted therapy: Significantly higher concentrations of drugs, including HER-2 targeting inhibitors such as Trastuzumab and Lapatinib, are often observed in brain metastases compared to that seen in the normal brain tissues (Lockman et al., 2010) (Table 1-6). Increased drug permeability in brain metastases is thought to result from the breakdown of the BBB induced by developing metastatic lesions (Fidler, 2011, Langley and Fidler, 2011) (Figure 1.10). For example, despite the limited permeability of Trastuzumab across the intact BBB due to its high molecular weight (145,531 Da), increased accumulation of Trastuzumab was observed in brain metastases (Dijkers et al., 2010). Indeed, clinical data show that patients treated with Trastuzumab achieved a considerable increase in overall survival (Table 1-7).

Table 1-6. Levels of drug concentration in normal brain tissues versus brain metastases in mouse models and in patients.

Drug	Normal brain tissue level*	Brain tumour level (viable lesion)	Fold increase	Reference
Etoposide	0.1 µg/g	3.9 µg/g	39.0	(Stewart et al., 1984)
Cisplatin	0.25-0.65 µg/g	1.29 µg/g	2.0-5.2	(Stewart et al., 1982)
Vinorelbine	6 ng/g	68 ng/g	11.3	(Stewart et al., 1983)
Paclitaxel ⁺	14 ng/g	22-1,328 ng/g	1.5-94.8	(Lockman et al., 2010)
Doxorubicin ⁺	8 ng/g	15-688 ng/g	1.9-86.0	(Lockman et al., 2010)
Trastuzumab [#]	0.2 [^]	3.5 [^]	17.5	(Dijkers et al., 2010)
Lapatinib ^{#+}	149 ng/g	672 ng/g	4.5	(Taskar et al., 2012)

*Drug levels were measured at resection, autopsy or imaging. *Locations of normal brain tissues were approx. 2-5 cm from tumour lesions. ^Relative uptake value in positron emission tomography (PET) imaging from metastatic breast cancer patients. #Trastuzumab and Lapatinib are HER2-targeted therapy. +Mouse models, patients if not indicated.*

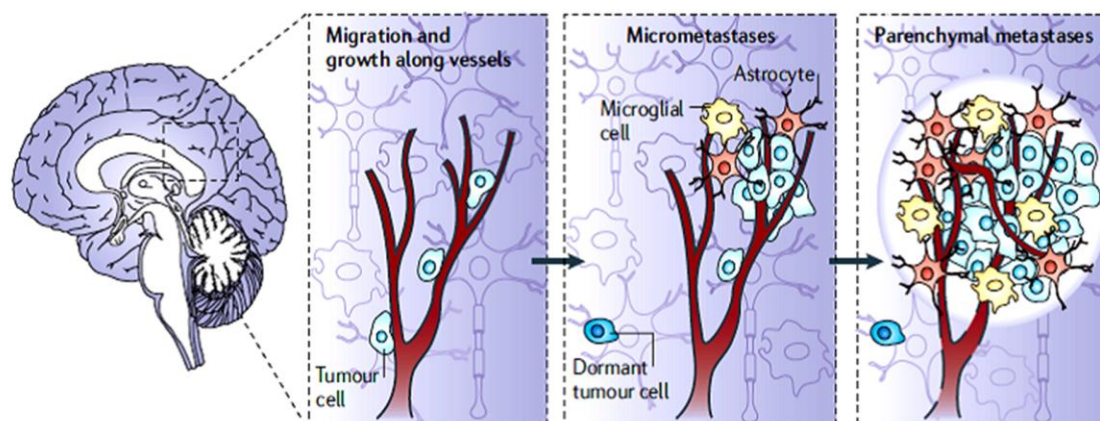


Figure 1.10 Brain metastases induce breakdown of the BBB

Brain metastatic cancer cells migrate and grow along the vessels. After crossing the BBB, tumour cells interact with astrocytes which provide survival signalling to tumour cells (Kim et al., 2011, Kim et al., 2014). Tumour cells survive and grow in the brain parenchyma and form brain macrometastases. As the tumour expands, the vasculature of the brain changes and the BBB is compromised (dashed black lines of the vasculature in the right panel). Image reproduced from (Steeg et al., 2011).

Table 1-7. Summary of the median overall survival of HER2 positive patients with CNS metastatic disease who received Trastuzumab treatments.

Study	No. of patients	Median overall survival (months)	
		With Trastuzumab	Without Trastuzumab
(Kirsch et al., 2005)	47	~ 26	~ 9
(Bartsch et al., 2007)	53	21.0	9.0 ^a and 3.0 ^b
(Brufsky et al., 2011)	377	17.5	16.4 ^a and 3.7 ^b
(Park et al., 2009a)	78	13.6	5.5
(Nam et al., 2008)	56	12.8	4.0
(Church et al., 2008)	26	11.9	3.0
(Dawood et al., 2008)	280	11.6	6.1

The overall survival was from the brain metastasis diagnosis. ^aPatients received chemotherapy only. ^bPatients received no chemotherapy. Table modified from (Pienkowski and Zielinski, 2010).

However, whilst the introduction of Trastuzumab into the clinic has undoubtedly improved outcome in HER2-positive patients, controversies still remain regarding its efficacy as a monotherapy against brain metastases and whether it could actually contribute to the increase in the incidence of brain metastasis. For example, a meta-analysis of adjuvant Trastuzumab for early stage HER2 positive breast cancer showed that despite improvement in disease-free survival, distant disease-free survival and overall survival in the Trastuzumab group than the other chemotherapy-treated group, patients who received Trastuzumab had a significantly higher incidence of brain metastases (Bria et al., 2008). Similar findings have been reported by other groups (Romond et al., 2005, Park et al., 2009b). Taken together, these observations are consistent with the contention that Trastuzumab prolongs survival of HER2 positive patients primarily through better control of systemic disease and may delay the development of CNS metastases but has limited direct efficacy against established brain metastases. Further evidence that Trastuzumab may have “preventive” effect rather than “therapeutic” effect on brain metastases comes from a study by Yap and colleagues who demonstrated that HER2 positive breast cancer patients who received Trastuzumab before the diagnosis of brain metastases had significantly longer time to occurrence of brain metastases (33.2 months) than those who did not (19.1 months) (Yap et al., 2012).

T-DM1 is a Trastuzumab monoclonal antibody conjugated with cytotoxic agent DM1 (derivative of maytansine) and was approved by the FDA in 2013 for HER2-positive patients. T-DM1 alone showed significantly increased progression free (9.6 months) and overall survival (30.9 months) with less toxicity compared to the combination of Lapatinib and capecitabine (progression free survival 6.4 months and overall survival 25.1 months) in HER2 positive patients with advanced breast cancer previously treated with Trastuzumab and a taxane (Verma et al., 2012). A phase 1 clinical study on the effect of T-DM1 on brain metastasis from HER2 positive breast cancer is ongoing (ClinicalTrials.gov identifier # NCT02135159).

Lapatinib also has shown efficacy in animal models of breast cancer brain metastasis and in HER2 positive breast cancer patients with brain metastases. Consistent with the increased permeability of the BBB in brain lesions, the average concentration of Lapatinib was found to be 7-9 fold higher in brain metastases than in normal brain tissues in a HER2 overexpressing experimental mouse model (Table 1-6) (Taskar et al., 2012). In HER2-positive breast cancer patients with brain metastases, Lapatinib increased overall survival (12.8 months), compared to chemotherapy alone and non-treated groups (10.2 months and 2.2 months, respectively) (Kim et al., 2012). Several trials have also shown that combination of Lapatinib with chemotherapy or WBRT increases CNS responses and survival of HER2 breast cancer patients with brain metastases compared to chemotherapy or WBRT alone (Lin et al., 2009, Lin et al., 2013, Bachelot et al., 2013).

In summary, multiple mono- or combination therapies have been developed and shown to efficacy in breast cancer patients with brain metastases. These approaches however extend life only by a few months or years and none are curative. Therefore, studies on novel targeted therapies for curative treatment of brain metastasis are urgently needed, especially for TNBC patients.

1.7 Histone deacetylase (HDAC) inhibitors: Emerging compounds for the treatment of breast cancer brain metastasis

Chromatin structure regulates gene expression and can be remodelled by DNA methyltransferases, histone acetyltransferases (HATs) and histone deacetylases

(HDACs) (Marks et al., 2001, Johnstone, 2002, Hadnagy et al., 2008, Falkenberg and Johnstone, 2014). HATs are responsible for the acetylation of histones that leads to chromatin opening and transcriptional activation, whereas HDACs deacetylate histones, thereby resulting in the condensation of chromatin and transcriptional repression (Figure 1.11). HDAC inhibitors (HDACi) induce hyperacetylation of histones in both normal and cancer cells, which leads to the activation of tumour suppressor genes and/or of transcription factors such as p53, E2F transcription factor 1 (E2F1), nuclear factor- κ B (NF- κ B), α -tubulin and heat-shock protein 90 (Hsp90). This results in the inhibition of tumour growth and survival through various actions in cancer (Table 1-8) (Johnstone, 2002, Bolden et al., 2006, Falkenberg and Johnstone, 2014). Changes in the level of HDAC expression commonly observed in cancer cells have led to the suggestion that HDACs could be potential targets for anti-cancer therapy. Indeed, tumour cells generally show increased sensitivity to HDAC inhibition compared to normal cells. While the precise mechanism by which HDACi exhibit selective cytotoxicity against cancer cells while having no or low toxicity against normal cells remains incompletely understood (Lindemann et al., 2004), the expression levels of class I HDACs are generally higher in various cancers than in normal tissues and could account in part for the selectivity of HDACi towards cancer cells (Krusche et al., 2005, Nakagawa et al., 2007, Weichert, 2009). Several small molecular weight HDACi have been developed and demonstrated to be brain permeable *in vivo* including SAHA, sodium butyrate, phenyl butyrate, MS275 and valporic acid (Steffan et al., 2001, Hockly et al., 2003, Ren et al., 2004, Faraco et al., 2006, Hess-Stumpff et al., 2007).

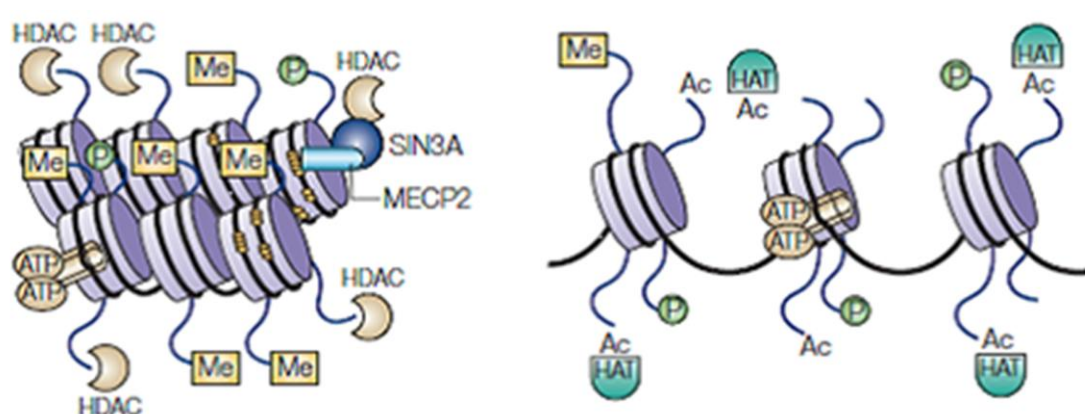


Figure 1.11 Chromatin structure regulates transcriptional activity

Left, histone deacetylation and DNA methylation cause the condensation of DNA around histones. This prevents transcription factors from binding to DNAs, thereby

leading to gene repression. Right, histone acetylation and DNA demethylation induce the relaxation of condensed chromatin. The resulting DNA opening leads to gene activation. DNAs are shown with black lines and histone octamers are in purple. Image reproduced from (Johnstone, 2002).

Table 1-8. Various actions of HDACi in cancer.

Role	Effect	Reference
Apoptosis	Intrinsic pathway (mitochondrial mediated)	(Ruefli et al., 2001)
	Extrinsic pathway (death receptor mediated)	(Insinga et al., 2005)
	DNA damage	(Chen et al., 2007)
Cell cycle arrest	G ₁ /S phase arrest	(Noh et al., 2011)
	G ₂ /M phase arrest	(Du et al., 2014)
Inhibition of angiogenesis	Suppression of pro- angiogenic genes	(Deroanne et al., 2002)
Immune modulation	Activation of NK cells	(Ning et al., 2012)
	Activation of cytotoxic T cells	(Murakami et al., 2008)

HDACi, histone deacetylases inhibitors; NK cells, natural killer cells. Table modified from (Falkenberg and Johnstone, 2014).

SAHA (suberanilohydroxamic acid, also known as Vorinostat) was the first FDA-approved HDACi for the treatment of advanced cutaneous T cell lymphoma in 2006. SAHA mediates potent anti-tumour effects including inhibition of tumour growth, induction of apoptosis and DNA damage response in various cancer cell lines, including breast cancer (Bolden et al., 2006). SAHA also enhances radiosensitivity, as evidenced by induction of γ -H2AX foci (a marker for DNA double strands breaks) in treated cells, and decreases the expression of the DNA repair gene, Rad51 and DNA-dependent protein kinase (DNA-PK), resulting in suppression of lung metastasis in the highly metastatic murine 4T1 breast cancer model (Chiu et al., 2013).

Interestingly, another study reported that the uptake of SAHA was 2-3 fold higher in experimental models of MDA-MB-231Br brain metastases than in normal brain and that the drug distributed evenly throughout brain metastases, in contrast to the heterogeneous distribution of paclitaxel or doxorubicin in brain metastases (Palmieri et

al., 2009b, Steeg et al., 2011). Consistent with the demonstrated efficacy of SAHA against lung metastases and the increased uptake and uniform distribution of SAHA in brain metastases, Palmieri et al. showed that SAHA induces apoptosis *in vitro* and decreases brain metastases partially in the MDA-MB-231Br intracardiac experimental brain metastasis model *in vivo*. This response was accompanied by the induction of γ -H2AX foci and reduced expression of the DNA repair gene, Rad52 (Palmieri et al., 2009b). Further, Baschnagel et al. reported that SAHA sensitises MDA-MB-231Br cells to radiation *in vitro* and *in vivo*, that resulted in a significantly increased survival of mice compared to SAHA or radiation alone. However, this did not produce complete remission and the maximum survival of mice was only up to 30 days (Baschnagel et al., 2009). The combination of SAHA (200, 300 or 400 mg orally once daily) and WBRT for the treatment of brain metastases is being tested in a phase 1 clinical trial (ClinicalTrials.gov identifier # NCT00838929). More recently, several HDACi with increased potency, selective cytotoxicity towards cancer cells and limited toxicity against normal cells have been developed (Batova et al., 2002, Insinga et al., 2005, Nebbioso et al., 2005, Yao et al., 2015, Novotny-Diermayr et al., 2010, Kahnberg et al., 2006). Chapter 5 of this thesis investigates two of these compounds (SB939 and 1179.4b) in brain metastatic breast cancer cell lines *in vitro* and *in vivo*.

TNBC is associated with an aggressive mesenchymal-like phenotype (Guarino et al., 2007, Lehmann et al., 2011, Lindner et al., 2013) that does not respond to anti-estrogens since this molecular subtype does not express hormone receptors. However, recent studies suggest that treatment with HDACi has the potential to convert TNBC to a more epithelial-like phenotype amenable to endocrine therapy. For example, panobinostat (LBH589), a pan-HDAC inhibitor (Khan et al., 2008), significantly reduces MDA-MB-231 lung and brain metastasis presumably by inhibiting the expression of pro-mesenchymal transcription factors ZEB1 and ZEB2 (Rhodes et al., 2014). In another study, panobinostat was shown to upregulate the expression of the epithelial marker, E-cadherin, in MDA-MB-231 cells *in vitro* and *in vivo* (Tate et al., 2012). Epithelial-mesenchymal transition (EMT) is a process whereby stationary epithelial cells are converted to motile mesenchymal cells and plays an important role in tumour cell invasion, migration and metastasis (Thiery, 2002, Yang and Weinberg, 2008). Loss of E-cadherin expression is often considered a common indicator of EMT (Thiery, 2002, Ye et al., 2012). Mesenchymal to epithelial transition (MET) is the reverse process of EMT and the re-expression of E-cadherin is a hallmark of MET (Wells et al., 2008, Tiraby et al., 2011). The expression of E-cadherin is regulated by ER (Ye et al., 2010, Cardamone et al., 2009, Wik et al., 2013, Bouris et al., 2015) and ER promotes MET

(Tiraby et al., 2011). Consistent with the abovementioned results, other studies have reported that HDACi induce the expression of ER- α in ER negative breast cancer cell lines (Keen et al., 2003, Fan et al., 2008) and sensitise tumour cells to endocrine therapy (Sabnis et al., 2011). Taken together, these studies suggest a mechanism by which HDACi could promote a mesenchymal to epithelial transition leading to increases in ER- α expression and response to anti-estrogens. Whether this strategy could be effective against TNBC brain metastases, however, remains to be demonstrated.

The HDAC family is subdivided into 4 classes based on their homology to yeast, subcellular localisation and enzymatic activities (Thiagalingam et al., 2003, Gregoretti et al., 2004). Class I HDACs (HDAC1, HDAC2, HDAC3 and HDAC8) are generally detected in the nucleus. Class IIa HDACs (HDAC4, HDAC5, HDAC7 and HDAC9) are expressed in the nucleus and the cytoplasm. Class IIb HDACs (HDAC6 and HDAC10) are found in the cytoplasm. HDAC11 is a single member of Class IV HDAC and is localised in the cytoplasm (Gregoretti et al., 2004, Bolden et al., 2006, New et al., 2012, West and Johnstone, 2014). HDAC isoforms regulate various biological functions in cancer, including cell survival, proliferation and metastasis (Kim and Bae, 2011, West and Johnstone, 2014). Several potent pan-HDAC inhibitors have been developed to interfere with these biological responses in cancer cells. However, most have shown cardiac toxicity in clinical trials which has prompted the development of isoform-selective HDAC inhibitors (Gryder et al., 2012, Butler and Kozikowski, 2008, Shultz et al., 2011). Nevertheless, whether pan-HDAC inhibitors or selective HDAC inhibitors are most beneficial as anti-cancer drugs is still debated. The fact that most inhibitors in clinical trials are pan-HDACi, suggests that inhibition of multiple HDACs may be necessary to achieve sufficient anti-tumour activity *in vivo*.

1.8 Preclinical mouse models of breast cancer brain metastasis

Metastasis cannot be fully replicated *in vitro* and therefore animal models are required to better investigate this process. While several mouse models of breast cancer metastasis have been developed (Eckhardt et al., 2012, Daphu et al., 2013), few spontaneously metastasise to the brain. For this reason, most studies have employed experimental models of breast cancer brain metastasis that involve injection of a large bolus of tumour cells into the vasculature via the left ventricle of the heart or via the internal carotid artery or injection directly into the brain (Palmieri et al., 2007b, Kodack et al., 2012). While useful to investigate late stage progression, these models lack

clinical relevance since they bypass the formation of a primary tumour, do not mimic the spontaneous escape of metastatic cells from the mammary gland, and often gives rise to numerous brain metastases (>100) that are not usually seen in patients (Gril et al., 2008, Fitzgerald et al., 2008). Moreover, the majority of these models are human-rodent xenografts that require the use of immune deficient mice to prevent rejection of human tumour cells by the murine host (Bos et al., 2009, Palmieri et al., 2007a, Gupta et al., 2013). Therefore, xenograft models do not take into account the important regulatory role of the immune system in metastasis, including metastasis to the brain (Kitamura et al., 2015, Fitzgerald et al., 2008, He et al., 2006, Lorger and Felding-Habermann, 2010).

To the best of our knowledge, the highest incidence of spontaneous brain metastasis observed in a human-mouse xenograft model (42%, 5 out of 12 mice), was reported in a study by Bos et al. (Bos et al., 2009) who used the CN34-BrM2 human breast cancer cell line derived from the parental CN34 line through repeated intracardiac injection. However this model still suffers from the lack of fully functional immune system.

In this context, syngeneic models of spontaneous breast cancer brain metastasis in which mouse mammary tumour cells spontaneously spread from a primary tumour in the mammary fat pad to the brain in immune competent mice provide greater clinical relevance for the functional characterisation of metastasis genes and/or testing of new therapies (Eckhardt et al., 2005, Kusuma et al., 2012, Johnstone et al., 2015). However, few syngeneic models of spontaneous breast cancer brain metastasis have been described to date.

Syngeneic luminal-like or HER2 positive models such as the mouse mammary tumour virus-polyoma middle T (MMTV-PyMT), MMTV-neu or Kunming models (Lin et al., 2003, Herschkowitz et al., 2007, Zheng et al., 2014) circumvent the need for immunocompromised mice but are only weakly metastatic to the lung or the liver and not to the brain. Recently, Erin and colleagues described the generation of the 4TBM brain metastatic cell line (Erin et al., 2013) derived from the 4T1 syngeneic mouse model of spontaneous TNBC metastasis (Aslakson and Miller, 1992, Johnstone et al., 2015). However, the authors did not report on the incidence of brain metastasis in the 4T1BM model, an important practical consideration if the model is to be used to demonstrate the efficacy of novel therapies against brain metastasis. Moreover, the genetic, phenotypic and functional relevance of this model to brain-metastatic human TNBC remains to be validated.

Table 1-9 summarises the major advantages and disadvantages of preclinical mouse models to investigate brain metastasis. The development and characterisation of a new 4T1-derived spontaneous brain-metastatic TNBC model (4T1Br4) is described in detail in Chapter 3.

Table 1-9. Preclinical animal models of brain metastasis.

Model	Method	Advantages	Disadvantages
<u>Syngeneic mouse model</u>			
Immunocompetent mice	Orthotopic or ectopic injection of murine derived cell lines	Compatible tumour-stroma interactions Immune competent More metastatic than xenografts	No human component
<u>Human-rodent xenograft model</u>			
Immunodeficient mice	Primarily intracardiac/carotid injection of patient derived cell lines	Use of human tumour cells Good correlation between responses to drugs in models and patients	Requires immune compromised mice Lack of tumour-host compatibility Provides a less realistic tumour microenvironment Expensive Less metastatic than syngeneic models
<u>Spontaneous metastasis model</u>			
Tumour transplantation in mice	Orthotopic injection in the mammary fat pad	Recapitulates complete steps of spontaneous metastasis Simple procedure Amenable to primary tumour resection/therapeutic setting	Longer duration Requires multiple <i>in vitro</i> or <i>in vivo</i> preselection Limited metastasis to the brain
Transgenic mice	Spontaneous primary tumour formation	Useful for study of tumour initiation Simple procedure	Long tumour latency or metastasis onset Limited spontaneous metastatic

distribution (no bone or brain)			
<u>Hematogeneous metastasis model (experimental)</u>			
Intracardiac injection	Injection of tumour cells into the left ventricle	Good metastatic seeding at secondary site Relatively simple procedure	Bypass early metastasis steps Bolus of cells implanted into circulation No primary tumour
Intracarotid artery injection	Injection of tumour cells into the internal carotid artery	Produces predominately cerebral tumours with minimal noncerebral metastases	Bypass early metastasis steps Complex Time-consuming Significant microsurgical skills required
<u>Direct implantation model (experimental)</u>			
Intraparenchymal implantation	Inoculation of tumour cells directly into the brain parenchyma by hand or stereotactic guidance	Useful to study metastatic tumour growth in the brain	Bypass early metastasis steps Complex Time-consuming Significant microsurgical skills required
Leptomeningeal metastasis	Inoculation of tumour cells directly into the subarachnoid space, or subarachnoid catheter for delivery to the cerebrospinal fluid space	Convenient for longitudinal imaging study with molecular or intravital microscopic imaging	Bypass early metastasis steps Does not models of cerebral brain metastases

1.9 Novel breast cancer brain metastasis genes

Given the lack of efficacy of current therapies against brain metastasis, particularly for TNBC, there has been a significant interest in identifying novel brain metastasis genes that could be used as therapeutic targets in patients as summarised in Table 1-10 and reviewed in (Steeg et al., 2011, Eichler et al., 2011, Eckhardt et al., 2012, Daphu et al., 2013). However, due to the limited availability of fresh matched primary tumour and brain metastases for these analyses, many studies have had to rely on cell cultures or animal models of metastasis.

Table 1-10. Genes associated with the formation of brain metastases from breast cancer.

Gene	Function	Models	Action	References
ST6GALNAC5	Sialyltransferases catalyse the addition of sialic acid to gangliosides and glycoproteins. Cell-surface sialylation has been implicated in cell-cell interactions	Breast cancer patient (CN34) and MDA-MB-231Br	Inhibition suppresses penetration of an artificial BBB and enhances brain-metastasis-free survival	(Bos et al., 2009)
COX2	Important in prostaglandin production, possibly leading to increased permeability of the BBB			
HBEGF	Heparin-binding EGF-like growth factor, a ligand of EGFR, promotes cell growth, motility, and invasiveness			
HER2	Receptor tyrosine kinase of the EGFR family	Breast cancer patients and MDA-MB-231Br	Overexpression increases the incidence of brain metastasis or large brain metastases (>50 μm^2)	(Palmieri et al., 2007a)
HER3	Receptor tyrosine kinase of the EGFR family	Breast cancer patients	HER3 and downstream pathways are involved in cell colonisation	(Da Silva et al., 2010)
Serpins	Serine proteinase inhibitors	MDA-MB-231Br	Counteract plasmins and results in cell survival and vascular co-option	(Valiente et al., 2014)

HK2	Hexokinase 2 important in glucose metabolism, oxidative phosphorylation, and antiapoptosis	MDA-MB-231Br	High HK2 expression is associated with poor patient survival after craniotomy	(Palmieri et al., 2009a)
VEGF-A	Angiogenic growth factor	MDA-MB-231Br	Increased in brain-metastatic clones, and VEGFR inhibition decreases brain tumour burden via a reduced number of blood vessels, decreases proliferation and increases apoptosis	(Kim et al., 2004)
FOXC1	Transcription factor essential for mesoderm development; involved in brain development and brain tumourigenesis	Breast cancer patients	Predicts poor overall survival in basal-like breast cancer, a higher incidence of brain metastasis and a shorter brain-metastasis-free survival in lymph-node-negative patients	(Ray et al., 2010)
NT-3	Neurotrophic factor in nerve growth factor	MDA-MB-361, BCM2, BrainG2	Induces MET and reduces cytotoxic response of microglia that results in increased growth of metastatic breast cancer cells in the brain	(Louie et al., 2013)
Heparanase	Enzyme that degrades polymeric heparan sulfate molecules	MDA-MB-231Br	Inhibition of heparanase by microRNA-1258 decreased cell	(Zhang et al., 2011)

Cathepsin S	Human lysosomal cysteine proteinase	MDA-MB-231Br	invasion <i>in vitro</i> and brain metastases in an <i>in vivo</i> experimental model Cathepsin S mediates transmigration of the BBB in breast cancer cells and inhibition of cathepsin S decreased brain metastasis in an experimental model	(Sevenich et al., 2014)
MMP-2, MMP-3 and MMP-9	Degradation extracellular matrix proteins and cell surface receptors	ENU1564 (Rat)	PD 166793 MMP inhibitor shown to decrease the development breast cancer brain metastases	(Mendes et al., 2005)
$\alpha\beta 3$	Important for sprouting endothelial cells, contributes to angiogenesis, supports invasion and metastasis	MDA-MB-435	Activated $\alpha\beta 3$ enhances brain metastatic tumour cells arrest in the blood flow and tumour growth through continuous upregulation of VEGF, leading to increased angiogenesis and decreased hypoxia	(Felding-Habermann et al., 2001, Loriger et al., 2009)

BBB, blood-brain barrier; EMT, epithelial-mesenchymal transition; MET, mesenchymal-epithelial transition. ENU1564 is an N-ethyl-N-nitrosourea-induced mammary adenocarcinoma cell line.

Surprisingly, there is little or no overlap among metastasis genes identified through these studies (Figure 1.12) (Daphu et al., 2013). The reasons for these discrepancies are not clear but could be due to differences in methodology, differences in tumour models/subtypes interrogated and/or the lack of clinical relevance of some of these models as discussed above. Four genes whose high expression is associated with brain metastasis in both xenograft models and patients' tissues are discussed in more detail below.

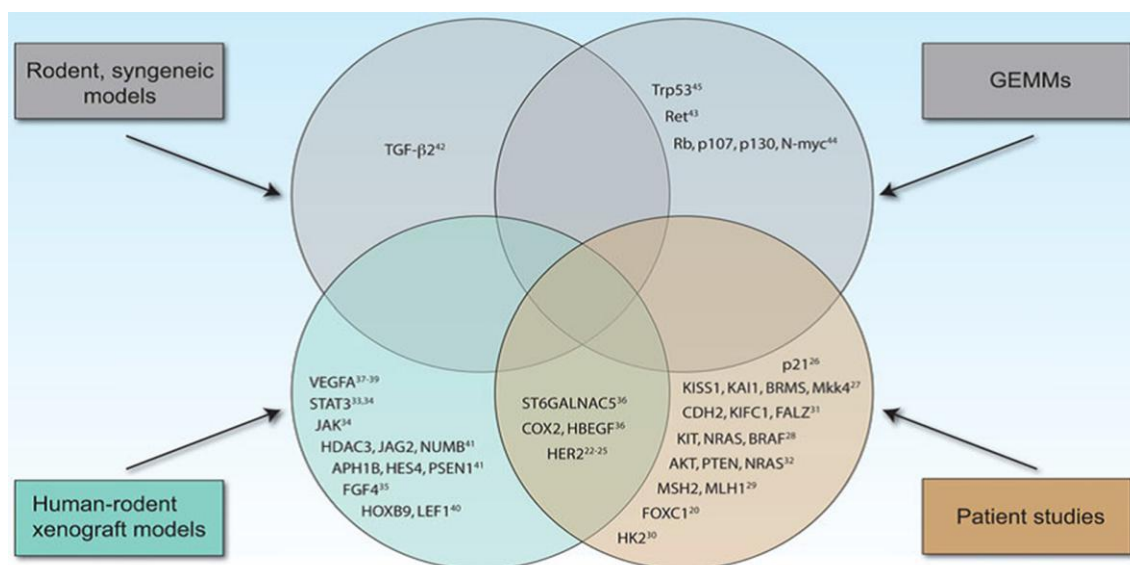


Figure 1.12 Genes involved in brain metastases

Brain metastasis genes identified in animal models and in patients' tissues show little or no overlap. However, there are four overlapping genes observed in both xenograft models and patient studies. Image reproduced from (Daphu et al., 2013).

Of particular interest, Bos and colleagues identified, through gene array analysis (Affymetrix), α 2,6-sialyltransferase (ST6GALNAC5), cyclooxygenase-2 (COX2) and the EGFR ligand heparin-binding EGF (HBEGF) highly expressed in both a brain metastatic breast cancer cell line isolated from a breast cancer patient (CN34) and the MDA-MB-231Br cell line (Bos et al., 2009). They provided *in vitro* evidence that these gene products facilitate trans-endothelial migration through the BBB and showed that suppression of each gene by RNA interference is associated with reduced survival in a human xenograft model *in vivo*, suggesting that COX2 and HBEGF in primary tumour enhance extravasation of cancer cells through the non-fenestrated capillaries of the brain and that ST6GALNAC5 acts a mediator of cancer cell infiltration through the BBB.

Palmieri et al. (Palmieri et al., 2007a) provided experimental evidence that HER2 directly contributes to brain colonisation. Specifically, they showed that exogenous expression of HER2 in MDA-MB-231Br cells increases the incidence of large brain metastases ($>50 \mu\text{m}^2$), suggesting that HER2 overexpression promotes the outgrowth of micrometastases into macrometastases in the brain (Palmieri et al., 2007a). High cathepsin S expression in primary tumour is associated with increased brain metastases in breast cancer patients and cathepsin S mediates the transmigration of the BBB by degrading junctional adhesion molecule B (JAM-B) in MDA-MB-231Br cells (Sevenich et al., 2014).

1.9.1 Prognostic brain metastasis gene signatures

While some risk factors have been identified for brain metastasis, it is still not possible to accurately predict breast cancer patients who will progress to develop brain metastases and those who will not. Prognostic brain metastasis gene signatures have been developed by various research groups to address our inability to predict patients at high risk of developing brain metastasis from breast cancer.

Bos et al. (Bos et al., 2009) analysed genes associated with brain metastasis by comparing CN34 cells (obtained from a breast cancer patient) versus CN34-BrM2 cells (brain-seeking subline of CN34) and MDA-MB-231 cells versus MDA-MB-231Br cells. Comparative genome-wide expression analysis revealed 243 genes are overexpressed or underexpressed in the brain metastatic cells of both cell lines. To prioritise brain metastasis genes, they used univariate analysis using human breast tumour microarray datasets (368 combined cohort from MSK-82 and EMC-286 sets) and defined a 17-gene signature correlated with brain relapse ($P < 0.05$), but not associated with relapse to the bones, liver or lymph nodes. However, it should be noted that 6 genes of the brain metastasis signature overlapped with the lung metastasis gene signature suggesting a potential association or shared mechanisms between lung and brain metastasis.

Klein et al. (Klein et al., 2009) identified two sets of 73 genes that are respectively expressed in brain or bone metastases from breast cancer. Brain metastasis genes were analysed using microarray data sets comparing 10 breast cancers relapsing to the brain and 29 normal human brains. However, a limitation of their study is that the authors did not analyse genes associated with metastasis to other organs such as the lung, liver or lymph nodes so as to differentiate them from the brain metastasis gene

signature. Thus, to unequivocally demonstrate that this signature is specific for the brain rather than a “general” metastasis signature, these genes should be further validated by analysing their expression in non-brain metastatic primary tumour versus brain metastatic primary tumour or in normal brain versus brain metastases, or matched primary tumours and brain metastases.

Mehrotra et al. (Mehrotra et al., 2004) reported a high frequency of five hypermethylated genes (Cyclin D2, RAR-beta, Twist, RASSF1A, and HIN-1) in brain metastasis compared to primary breast tumours. The prognostic utility of these hypermethylated genes is difficult to determine since the study compared unpaired primary tumours and brain metastases. Therefore it is unclear whether hypermethylation of these genes is simply induced by the microenvironment of the brain or represents a set of genes that are hypermethylated in a subpopulation of cells of the primary tumours and their inactivation promotes their spread to the brain. In another study, Woditschka et al. (Woditschka et al., 2014) identified two DNA double-strand break repair genes (BARD1 and RAD51) significantly overexpressed in human brain metastases compared to matched primary tumours. They demonstrated that these genes functionally contribute to brain metastasis *in vivo*. However, the use of a large number of patient samples is warranted to confirm this study, since these genes were identified from only 23 matched primary breast cancer and brain metastases.

While many research groups are eagerly trying to define brain-specific metastasis gene signatures, it is important that brain metastasis genes be identified or validated by using large cohort datasets or a sizable number of matched primary breast tumours and brain metastasis tissues/cell lines.

1.10 Hypotheses and specific aims

The incidence of breast cancer patients developing brain metastases is increasing. Unfortunately, current therapies for brain metastases are not curative and the genes and mechanisms regulating breast cancer metastasis to the brain remain poorly understood. Metastasis requires complex interactions between tumour cells and the stromal microenvironment that can only be fully replicated *in vivo*. However, clinically relevant animal models of spontaneous breast cancer metastasis that recapitulate the complete metastatic cascade from the mammary gland to the brain in immune competent mice are lacking. I hypothesise that such models would provide greater clinical relevance for the identification/characterisation of brain metastasis genes

and/or to test the efficacy of novel therapies against this incurable disease. Accordingly, the first goal of my PhD project was to develop and characterise a new syngeneic mouse model of spontaneous breast cancer brain metastasis (4T1Br4) in which to investigate the function of novel brain metastasis genes and to test novel therapies.

Initial characterisation of 4T1Br4 cells and tumours by gene array profiling uncovered an association between high expression of a novel member of the JAM family proteins, limitrin (DICAM), and brain metastatic potential. The prognostic and functional links between limitrin and breast cancer brain metastasis have not been reported previously and are investigated herein. Lastly, the project made use of the 4T1Br4 model to test the efficacy of two novel HDACi against breast cancer brain metastasis.

The specific aims of my project are as follows:

1. To develop and characterise a novel syngeneic mouse model of spontaneous breast cancer brain metastasis;
2. To determine the prognostic value of limitrin for the identification of breast cancer patients at risk of developing brain metastases and to investigate the functional contribution of limitrin to the spread of breast cancer to the brain; and
3. To test the efficacy of novel HDACi (SB939 and 1179.4b) against brain metastases in a clinically relevant syngeneic mouse model of spontaneous breast cancer metastasis to the brain.

The methodology and results from my PhD project are presented in the following chapters together with a summary of my findings and a discussion of their potential implications for the treatment of breast cancer patients with brain metastases and for future research avenues.

2. Materials and Methods

2.1 Materials

2.1.1 General chemicals and reagents

Reagents	Supplier
α -minimal essential medium (α -MEM)	GibcoBRL
ABC reagent	Vector
Acetic acid	BDH
Acrylamide/bisacrylamide	Amresco
Ampicillin	CSL
β -mercaptoethanol	Sigma
BCA protein assay kit	Biorad
Bovine serum albumin (BSA)	Sigma
Calcein AM	ENZO Life Sciences
Calcium chloride (CaCl_2)	Sigma
Cell scraper	Greiner bio-one
Chemiluminescence (ECL)	Amersham
Chloroform	BDH
Crystal violet	Sigma
3,3' Diaminobenzidine (DAB) substrate	DAKO
4',6-diamidino-2-phenylindole (DAPI)	Vector
Dulbecco's Modified Eagle Medium (DMEM)	GibcoBRL
Dimethylsulfoxide (DMSO)	Sigma
dNTPs mix	Promega
Ethanol	BDH
Ethylenediamine tetra-acetic acid (EDTA)	Boehringer Mannheim
Fetal bovine serum (FBS)	CSL
Ficoll-Paque Plus gradient	GE Healthcare
Filter (0.22 μm)	Millipore
Filter (0.45 μm)	Sigma
Fluconazole	Sandoz
Formaldehyde	BDH
Formalin (10% buffered)	Orion
Glycine	BDH

Reagents	Supplier
Glycerol	BDH
Heparin	Pfizer
HEPES	Sigma
Isoamyl alcohol	Sigma
Isopropanol	BDH
Isoflurane	Abbott
Ketamine hydrochloride	TrygLaboratories
L-glutamine	Trace
Lipofectamine 2000	Invitrogen
Luciferin	Gold Biotechnology
Magnesium chloride (MgCl ₂)	Amresco
Matrigel	BD Biosciences
Methanol	BDH
Microcentrifuge tube	Scientific Specialties
MISSION® esiRNA	Sigma
M-MLV Reverse Transcriptase, RNase H Minus	Promega
N,N,N',N'-Tetramethylethylenediamine (TEMED)	Biorad
Neutral buffered formalin (NBF)	Australian biostain
Opti-MEM	Gibco
Paraformaldehyde (PFA)	Sigma
Penicillin-streptomycin	GibcoBRL
Phenol	Sigma
Poly(ethylene glycol) (PEG) 300	Sigma
Polyethylenimine (PEI)	Polyscience
Polybrene	Santa Cruz
Protease cocktail inhibitors (EDTA free)	Roche
Proteinase K	Promega
Puromycin	Sigma
PVDF membrane	Milipore
Qproteome Cell Compartment Kit	Qiagen
RNase A	Promega
SB939, 10 mM stock solution prepared in DMSO and stored at -80°C until used.	Prof. David P. Fairlie (The University of Queensland,

Reagents	Supplier
Molecular weight is 358 Da.	Australia)
Scalpel blade	Swann-Morton
Skim milk powder	Diploma
Sodium chloride (NaCl)	Sigma
Sodium Dodecyl Sulfate (SDS)	Promega
Sodium pyruvate	Sigma
Sulforhodamine B (SRB)	Sigma
Super RX film	Fujifilm
Sterile water for injection	Sterisafe
SYBR Green I	Applied Biosystems
Syringe	Terumo
Taqman chemistry	Applied Biosystems
Tissue culture plastic ware	BD Biosciences
Transwell polycarbonate membrane inserts	Corning
Trichloroacetic acid (TCA)	BDH
Tris(hydroxymethyl)aminomethane (Tris base)	BDH
Trizol reagent	GibcoBRL
Triton X-100	Sigma
Trypan blue	Gibco
Trypsin	Sigma
Trypsin-EDTA	Gibco BRL
Tween-20	Biorad
Ultra clean water	Invitrogen
Vectastain ABC kit	Vector
Vectashield containing DAPI	Vector
Vivaspin20 ultrafiltration spin columns	Sartorius
Xylene	BDH
1179.4b, 10 mM stock solution prepared in DMSO and stored at -80°C until used.	Dr. David P. Fairlie (The University of Queensland, Australia)
Molecular weight is 473 Da.	Australia)
5X M-MLV RT (H-) buffer	Promega

2.1.2 Antibodies

Table 2-1. List of antibodies used in this study.

Antibodies	Applications	Dilution	Supplier
Anti-ER α (Mouse, monoclonal)	Immunohistochemistry	1:50	DAKO
Anti-PR (Rabbit, polyclonal)	Immunohistochemistry	1:4,000	Santa Cruz Biotech
Anti-HER2 (Mouse, monoclonal)	Immunohistochemistry	1:400	Calbiochem
Anti- pan- cytokeratin (pan- CK) (Mouse, monoclonal)	Immunohistochemistry	1:400	Sigma
Anti-Ki-67 (Rabbit, polyclonal)	Immunohistochemistry	1:250	Millipore
*Anti-limnitrin (Rabbit, polyclonal)	Western blot, immunohistochemistry	Western blot 1:10,000, immunohistochemistry 1:1,000	Prof. Bruce Kemp (St. Vincent's hospital, Victoria, Australia)
Anti-acetylated histone H3 (Rabbit, polyclonal)	Western blot	1:10,000	Millipore
Anti-GAPDH (Mouse, monoclonal)	Western blot	1:10,000	Abcam
Anti-Na ⁺ /K ⁺ ATPase (Rabbit, polyclonal)	Western blot	1:1,000	Cell signalling technology

Antibodies	Applications	Dilution	Supplier
Anti- γ -H2AX (Rabbit, polyclonal)	Immunofluorescence	1:500	Abcam
Goat anti-rabbit IgG (H+L) HRP conjugated	Western blot	1:3,000	BioRad
Goat anti-mouse IgG (H+L) HRP conjugated	Western blot	1:3,000	BioRad
Goat anti-rabbit IgG biotin conjugated	Immunohistochemistry	1:250	Vector
Goat anti-mouse IgG biotin conjugated	Immunohistochemistry	1:250	Vector
Goat anti-rabbit IgG (H+L) Alexa fluor 488	Immunofluorescence	1:500	Molecular probes

**Four limitrin antibodies (R161, R184, R5553 and R6921) were generated in collaboration with Prof. Bruce Kemp (St-Vincent Institute, Melbourne). Rabbit polyclonal anti-limitrin antibodies were raised against a human C-terminal peptide sequence of human limitrin (ELAHSPLPAKYIDLKGFRENCK), as described in (Yonezawa et al., 2003).*

2.1.3 Oligonucleotides

Genomic DNA was detected by TaqMan real time PCR. Primers and probes against mouse Cherry/Vimentin were designed using Primer Express version 2.0 program and manufactured by Applied Biosystems (California, US). Primers and probes against human TurboGFP were designed using NCBI database (www.ncbi.nlm.nih.gov) and manufactured by Integrated DNA Technologies (IDT) (Iowa, US). The sequences of these primers and probes are shown in Table 2-2.

Table 2-2. Sequences of primers and probes used for amplification of genomic DNA by TaqMan real time PCR.

Primers	Sequence	
Mouse Cherry	Forward	5'-GACCACCTACAAGGCCAAGAAG-3'
	Reverse	5'-AGGTGATGTCCAACCTTGATGTTGA-3'
	Probe	6FAM-CAGCTGCCCGGCGCCTACA-TAMRA
Mouse Vimentin	Forward	5'-AGCTGCTAACTACCAGGACACTATTG-3'
	Reverse	5'-CGAAGGTGACGAGCCATCTC-3'
	Probe	VIC-CCTTCATGTTTTGGATCTCATCCTGCAGG-TAMRA
Human TurboGFP	Forward	CAGCGGCTACGAGAACCCCT
	Reverse	GGCCTCGTAGCGGTAGCTGA
	Probe	FAM-AGGACGGCGGCGTGCTGCACGTGAGCT-NFQ

The expression of limitrin mRNA was detected by SYBR Green real time RT-PCR. Primers were designed using NCBI database. Mouse primers were purchased from IDT and human primers from GeneWorks. Sequences of these primers are shown in Table 2-3.

Table 2-3. Sequences of primers used for real time RT-PCR with SYBR Green.

Primers	Sequence	
Mouse limitrin	Forward	5'-AACAGCGCGTGTACGAGCCG-3'
	Reverse	5'-CTGTCCACAGCGCGAATGAGCA-3'
Human limitrin	Forward	5'-TTAACTTGGCGGAGTTCGCT-3'
	Reverse	5'-TCCTTCCGGAACCCTTTGTC-3'

2.1.4 siRNA and shRNA

For *in vitro* studies of limitrin gene knockdown, endonuclease-prepared siRNAs (esiRNAs) against limitrin or EGFP (enhanced green fluorescent protein, control) were obtained from Sigma. The sequences of esiRNAs are shown in Table 2-4.

Table 2-4. Sequences of siRNAs used in this study.

siRNA	Sequence
Limitrin esiRNA cDNA	ACAAGGGATCAGGCTCCATATAGGACTGAGGACATCCAGCTAGATTACA AAAACAACATCCTGAAGGAGAGGGCTGAGCTGGCCCATAGTCCTCTGCC TGCCAAGGATGTGGATCTGGATAAAGAGTTCAGGAAGGAGTACTGCAA TAAATGGACCCTGAGCTTCTGGCTGGGCCAGCAGCTCTGTATCAAAGGA CATCTCCCTGACCCTCCTGCGGTATTCTGGCTCTTCTCAGCGGCTGGT CCGACTTACCTAGAACTTGGCCTAACTTGGCAGAGCAGCTGCCTGTA CTTTGCCCTTCTAGAACTCGCCACCCCTCATCTTGGTGAGCAACTGTGG GTTCCCTAGAGACTCTGGTATAGTACGATTGCTGCCCTTCAGTCACCTGT GCCCACTGATGGTCGTACCCCAACTTAAACACAACAAAGATCCCTTGTT AATATCCACCAAATGCAAAGTCC
EGFP esiRNA cDNA	GTGAGCAAGGGCGAGGAGCTGTTACCGGGGTGGTGCCCATCCTGGTC GAGCTGGACGGCGACGTAAACGGCCACAAGTTCAGCGTGTCCGGCGAG GGCGAGGGCGATGCCACCTACGGCAAGCTGACCCTGAAGTTCATCTGC ACCACCGGCAAGCTGCCCGTGCCCTGGCCCACCCTCGTGACCACCCTG ACCTACGGCGTGACGTGCTTCAGCCGCTACCCCGACCACATGAAGCAGC ACGACTTCTTCAAGTCCGCCATGCCCGAAGGCTACGTCCAGGAGCGCAC CATCTTCTTCAAGGACGACGGCAACTACAAGACCCGCGCCGAGGTGAAG TTCGAGGGCGACACCCTGGTGAACCGCATCGAGCTGAAGGGCATCGAC TTCAAGGAGGACGGCAACATCCTGGGGCACAAGCTGGAGTACAACACTACA ACAGCCACAACGTCTATATCATGGCCGACAAGCAGAAGAACGGCATCAA GGTGAAGTTCAGATCCGCCACAACATCGAGGACGGCAGCGTGCAGCTC GCCGACCACTACCAGCAGAACACCCCATCGGCGACGGCCCCGTGCTG CTGCCCGACAACCACTACCTGAGCACCCAGTCCGCCCTGAGCAAAGACC CCAACGAGAAGCGCGATCACATGGTCCTGCTGGAGTTCGTGACCGCCG CCGGGATCACTCTCGGCATGGACGAGCTGTA

For *in vivo* experiments, pGIPz, pCMV R8.2 and pVSV-G vectors were used. Bacteria transduced with 5 distinct limitrin shRNA integrated in the mir30 lentiviral vector (pGIPz) were provided by Dr. Kaylene Simpson (the Victorian Centre for Functional Genomics (VCFG), Peter MacCallum Cancer Centre, Melbourne, Australia). The sequences of limitrin shRNA and scramble shRNA are shown in Table 2-5. The pGIPz construct has the CMV promoter, the TurboGFP reporter, puromycin resistant markers and a hairpin sequence (Thomas et al., 2014). pCMV R8.2 and pVSV-G were a kind

gift from Dr. Didier Trono (École polytechnique fédérale de Lausanne (EPFL), Switzerland).

Table 2-5. Sequences of limitrin and scramble shRNAs.

shRNA	Sequence
Limitrin shRNA #1	CCAGCTAGATTACAAAAAC
Limitrin shRNA #2	CAGCTAGATTACAAAAACA
Limitrin shRNA #3	AGTACATCGACCTAGACAA
Limitrin shRNA #4	CCAGAAGTCGGGAAAGTCA
Limitrin shRNA #5	CAGAAGTCGGGAAAGTCAA
Scramble/non- silencing control shRNA integrated in the pGIPz vector	<p>NNNNNNNNGACCCGNNGCCCGGTGCCTGAGTTTGTGTTGAATGAGG CTTCAGTACTTTACAGAATCGTTGCCTGCACATCTTGAAACACTTG CTGGGATTACTTCTTCAGGTTAACCCAACAGAAGGCTCGAGAAGGT ATATTGCTGTTGACAGTGAGCGATCTCGCTTGGGCGAGAGTAAGTA GTGAAGCCACAGATGTACTTACTCTCGCCCAAGCGAGAGTGCCTAC TGCCTCGGAATTCAAGGGGCTACTTTAGGAGCAATTATCTTGTGTTAC TAAACTGAATACCTTGCTATCTCTTTGATACATTTTTACAAAGCTGA ATTAATGATAAATTAATCACTTTTTTCAATTGGAAGACTAATG CGGCCGGCCATTACTCCGTCTCGTGTCTTGTGTCATATGTCTGCTG GTTTGTGTTGATGTTGTTTGCGGGCGGGCCCTATAGTGAGTCGTATT ACCTAGGACGCGTCTGGAACAATCAACCTCTGGATTACAAAATTTG TGAAAGATTGACTGGTATTCTTAACTATGTTGCTCCTTTTACGCTAT GTGGATACGCTGCTTTAATGCCTTTGTATCATGCTATTGCTTCCCCT ATGGCTTTCATTTTCTCCTCCTTGTATAAATCCTGGTTGCTGTCTCTT TATGAGGAGTTGTGGCCCGTTGTCAGGCAACGTGGCGTGGTGTGC ACTGTGTTTCTGACGCAACCCCACTGGTTGGGGCATTGCCACC ACCTGTCAGCTCCTTTCCGGGACTTTTCGCTTTCCCCTCCCTATTG CCACGGCGGAATCATCGCCGCTGCCTTGCCCGCTGCTGGACA GGGGCTCGGCTGTTGGGCACTGACAATTCCGTGGTGTGTCGGG GAAGCTGACGTCCTTTCCATGGCTGCTCGCCTGTGTTGCCACCTG</p>

```
GATTCTGCGCGGGACGTCCTTCTGCTACGTCCCTTCGGCCCTCAA
TCCAGCGNANCTTCCTTCCCGCGGNCNGCTGNCNGNTCTGCGGC
NTCTTCCGCGNNTTCNCCTTCNCCNCANANNAN
```

Blue: hairpin flanking regions, yellow: sense sequence, green: loop sequence, red: antisense sequence and white: vector sequence.

2.2 Cell culture methodology

2.2.1 Cells

The mouse mammary tumour cell lines 67NR, 66cl4 and 4T1 were provided by Dr. Fred Miller (Karmanos Cancer Institute, Detroit, US). These lines are clonal populations of cells derived from a spontaneous mammary carcinoma arising in a BALB/C mouse (Dexter et al., 1978). The 4T1 line was further sub-cloned in our laboratory to isolate two bone-seeking cell lines, 4T1.2 (Lelekakis et al., 1999) and 4T1BM2 (Kusuma et al., 2012) and one brain-seeking cell line, mCherry-expressing 4T1Br4 (the generation of these cells is described in Chapter 3). Mouse mammary tumour cell lines were maintained in α -minimal essential medium (α -MEM) supplemented with 5% fetal bovine serum (FBS) and 1% penicillin-streptomycin (P/S).

The human non-metastatic breast cancer cell line MCF-7 was obtained from the American Type Culture Collection (Manassas, VA, US) and human metastatic breast cancer cell lines, luciferase-expressing MDA-MB-231 (lung-metastatic cell line) and MDA-MB-231Br (brain-seeking cell line derived from MDA-MB-231), were obtained from Dr. Joan Massagué (Memorial Sloan Kettering Cancer Center, New York, US). Human breast cancer cell lines were cultured in Dulbecco's Modified Eagles Medium (DMEM) supplemented with 10% FBS and 1% P/S.

The bEnd.3 immortalised murine brain microvascular endothelial cell line was a generous gift from Dr. R. Hallmann (Münster University, Münster, Germany). These cells were maintained in DMEM supplemented with 10% FBS, 2 mM L-glutamine, 1 mM sodium pyruvate and 1% P/S.

All cell lines were maintained in a humidified incubator at 37°C under 5% CO₂. Cells were passaged when sub-confluent. Mouse mammary tumour cells were detached

using 0.01% EDTA in Dulbecco's phosphate buffered saline (PBS) and human breast cancer cells and bEnd.3 cells were detached using 0.05% Trypsin-EDTA in PBS. All cell lines were kept in culture for a maximum of four weeks. Prior to experimentation, cell viability was assessed by trypan blue exclusion and was higher than 90% in all experiments. For long-term storage, cells were frozen at -80°C and kept in liquid nitrogen in a 10% DMSO/90% FBS solution.

2.2.2 Preparation of brain conditioned medium (BCM)

New born pups from BALB/C mice were washed quickly with 70% alcohol and whole brains were removed under sterile conditions. Whole brains were rinsed twice quickly with 20 ml PBS containing 2% P/S and fluconazole (6 mg/L), minced with a scalpel blade and cultured in DMEM supplemented with 20% FBS, 1 mM sodium pyruvate, fluconazole (6 mg/L) and 2% P/S at 37°C under 5% CO_2 . The medium was changed every 2-3 days until cells reached sub-confluence after which brain cells were serum starved overnight in 15 ml of α -MEM serum free medium (SFM) supplemented with 0.05% bovine serum albumin (BSA), 2 mM L-glutamine, 1 mM sodium pyruvate and 1% P/S. The medium was then replaced with 10 ml of fresh SFM which was collected after 48 hrs and centrifuged at 1,200 rpm for 5 min at 4°C (BCM). BCM was kept at -80°C until ready to use and was stable for at least 3 months at -80°C .

2.2.3 Purification of LM-511 from conditioned medium

Recombinant human LM-511 (rhLM-511) was produced by HEK293T cells transfected with plasmids containing full-length cDNAs encoding LMa5, $\gamma 1$ and $\beta 1$ chains (kindly provided by BioStratum Inc, Durham, NC, US). rhLM-511 was purified from serum-free culture supernatant by affinity chromatography as previously described (Doi et al., 2002) with some modifications. HEK293T cells were grown in T175 cm^2 flasks and maintained in DMEM supplemented with 10% FBS, 0.5 mg/ml G418 and 1% P/S. Cells were grown to approximately 60-70% confluence. To produce conditioned medium for the purification of rhLM-511, the cells were washed twice with PBS and serum-starved in 25 ml of DMEM containing 0.5 mg/ml G418, 1 mM sodium pyruvate and insulin-transferrin-selenium supplement per flask for up to 6 days. The medium containing rhLM-511 was harvested, centrifuged at 1,200 rpm for 5 min at 4°C , filtered through a 0.22 μm filter-unit and stored at -20°C until required.

rhLM-511 was purified by gel filtration chromatography (SMART column Superdex 200). Batches of 250 ml of conditioned medium containing rhLM-511 from 10 flasks were filtered and concentrated using Vivaspın20 ultrafiltration spin columns with a 100 kDa cut-off. Columns were centrifuged at 3,000 rpm at 4°C and the concentrated medium was buffered exchange in PBS to a final volume of 500 µl. The concentrated medium was then purified by gel filtration on a Superdex 200 size exclusion column with 1% (w/v) NH₄CO₃. Samples (100 µl each) were run at 40 µl/min and 80 µl fractions were collected. Each fraction was analysed on 4% SDS-PAGE to detect the presence of LM-511 chains. Fractions containing LM-511 were pooled and tested for activity. This work was performed by Selda Onturk (PhD candidate, Peter MacCallum Cancer Centre, Melbourne, Australia).

2.3 Protein techniques

2.3.1 Protein isolation

Sub-confluent cells cultured in T75 cm² flasks were placed on ice and washed twice with ice-cold PBS. Adherent cells were scrapped off in 1 ml of ice-cold lysis buffer containing 30 mM HEPES, 0.5 M EDTA, 5 M NaCl, 1% (v/v) Triton X-100 and protease cocktail inhibitors per 1 X 10⁶ cells. The cell lysate was then gently transferred into a microcentrifuge tube and rotated for 30 min at 4°C before being spun at 13,000 x g for 15 min at 4°C. The supernatant containing the proteins was collected in a fresh microcentrifuge tube and stored at -20°C.

For the detection of acetylated histone H3 protein by western blot, 1 X 10⁶ cells or 50 mg of crushed frozen tissues were lysed in 1 ml of RIPA buffer containing 10 mM PO₄ (pH 7.4), 500 mM EDTA (pH 8), 1% (v/v) Nonidet P-40, 0.5% (v/v) sodium deoxycholate, 0.1% (v/v) SDS and protease inhibitor cocktail. The lysate was sonicated four times for 30 sec and spun at 13,000 x g for 15 min at 4°C. The supernatant was collected and stored at -20°C.

To investigate the differential localisation of limitrin in 66cl4 and 4T1Br4 cells, the Qproteome Cell Compartment Kit was used for subcellular fractionation according to the manufacturer's instructions. Briefly, cell compartments can be selectively isolated by applying different extraction buffers to a cell pellet (Figure 2.1). The Lysis Buffer

disrupts the plasma membrane to isolate cytosolic proteins only. The Extraction Buffer CE2 solubilises the plasma membrane but not the nuclear membrane and the Extraction Buffer CE3 extracts nuclear proteins.

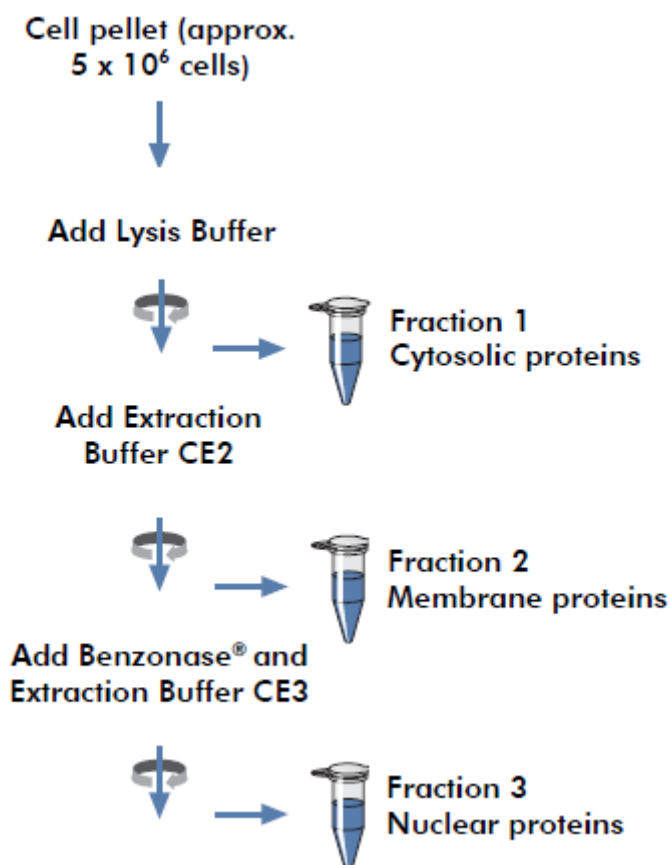


Figure 2.1 Schematic diagram of subcellular fractionation adapted from QIAGEN

The protein concentration of each sample was determined using the Pierce BCA protein assay kit. Briefly, 200 μ l of BCA working solution (50 parts of solution A: 1 part of solution B ratio) was added to each well of a 96-well plate containing 20 μ l of each standard or unknown sample. The plate was incubated for 30 min at 37°C and the optical density of the wells was measured at 562 nm using a microplate reader (VersaMax ELISA plate reader, Molecular Devices). Protein concentrations in the samples were read against a standard curve generated by diluting the 2,000 μ g/ml BSA stock solution in lysis buffer at the following concentrations: 0, 31.25, 62.5, 125, 250, 500, 1,000, 2,000 μ g/ml of BSA.

2.3.2 Western blot analysis

Western blotting was performed using standard methodology (Sambrook et al., 1989). Briefly, forty micrograms of proteins were separated on SDS-PAGE gel (8% acrylamide for limitrin or 15% acrylamide for acetylated histone H3) and transferred to a PVDF membrane in protein transfer buffer (0.19 M glycine, 0.25 M Tris base, 20% methanol) at 100 volt for 1 hr. The membrane was blocked with 10% (w/v) non-fat dried milk in PBS containing 0.05% Tween-20 for 1 hr at room temperature (RT) and incubated with rabbit polyclonal anti-limitrin (1:10,000 dilution) or anti-acetylated histone H3 (1:10,000 dilution) antibody overnight at 4°C. After 3 washes with wash buffer (0.025% Tween-20 and 0.1% BSA in PBS) for 10 min, the membrane was incubated for 1 hr at RT with an appropriate HRP-conjugated secondary antibody diluted at 1:3,000 in wash buffer. The membrane was washed three times as above followed by protein detection using enhanced ECL reagents and Super RX film or ChemiDoc™ MP System (Biorad). An anti-GAPDH antibody was used as a loading control for immunoblotting of whole cell lysates and cytosolic fractions whereas an anti-Na⁺/K⁺ ATPase antibody was used for membrane fractions and an anti-histone H3 antibody for nuclear fractions. The membrane was incubated with either anti-GAPDH (1:10,000 dilution), anti-Na⁺/K⁺ ATPase (1:1,000 dilution) or anti-histone H3 (1:10,000 dilution) antibodies for 1 hr at RT. The incubation with the secondary antibody, washes and ECL development were performed as described above. Densitometric analysis with Image J software (National Institutes of Health) was used to quantitate protein levels.

2.4 *In vitro* functional assays

All *in vitro* functional experiments were repeated three times.

2.4.1 Proliferation assays

Proliferation rate of 4T1 and 4T1Br4 cells was measured using the Sulforhodamine B (SRB) colorimetric assay in the presence or absence of 50% v/v BCM, 1% FBS, 50% v/v BCM + 1% FBS or 5% FBS over 5 days. Five hundred cells in 200 µl of growth medium/well of 96-well plates were seeded in six replicate wells per time point. Three wells containing only medium were used to measure the non-specific binding of the dye to the plastic plates. After 1, 2, 3, 4 and 5 days, tumour cells were fixed in 50 µl of ice-cold 50% trichloroacetic acid and incubated at least for 1 hr at 4°C. Tumour cells were then washed three times with tap water and stained with 100 µl of 0.4% SRB in 1%

acetic acid (SRB dye) for 30 min at RT. Unbound dye was washed 3 times with tap water and once with 1% acetic acid. The SRB dye was solubilised by adding 100 μ l of 10 mM Tris (pH.10.5) to each well. Plates were shaken gently for 5 min on a plate shaker before the optical density was measured at 550 nm using a microplate reader (VersaMax ELISA plate reader, Molecular Devices). Results were expressed as means \pm standard deviation (SD) of six replicate wells per time point.

To investigate the effect of limitrin-targeting shRNA on cell proliferation, MDA-MB-231Br cells transfected with a control non-targeting shRNA or a limitrin-targeting shRNA (1,000 cells per well of 96-well plates in 200 μ l of growth medium) were seeded in six replicate wells. The proliferation rate was measured over 6 days using the SRB assay as described above.

To assess the effect of histone deacetylase inhibitors (SB939 and 1179.4b) on cell proliferation, 1,000 4T1Br4 cells or 4,000 MDA-MB-231Br cells were seeded in six replicate wells of a 96-well plate in 200 μ l of growth medium and incubated overnight at 37°C. The next day, the medium was replaced by 200 μ l of fresh medium containing SB939 (18, 39, 78, 156, 312, 625, 1,250, 2,500 or 5,000 nM) or 1179.4b (3.9, 7.8, 15.6, 31.25, 62.5, 125, 250, 500 or 1,000 nM). Cells incubated with 1% DMSO were used as controls. Proliferation rate was measured by SRB assay after 3 days of treatment with the HDAC inhibitors, as described above. Dose-response curves were plotted to determine the half-maximal inhibitory concentrations (IC_{50}) for each compound using the GraphPad Prism software. Each dot on the curves represents mean \pm SD of six replicate wells.

2.4.2 Colony formation assays

The effect of histone deacetylase inhibitors on cell survival was determined by colony formation assays. 4T1Br4 cells (100 cells/well of 6-well plates) were seeded in three replicate wells per condition and incubated in 4 ml of growth medium containing either 1% DMSO, 1 μ M SAHA, 1 μ M SB939 or 1 μ M 1179.4b for 7 days at 37°C. After removing the medium, 3 ml of 0.1% crystal violet (dissolved in 1:1 methanol/Milli-Q water) was added to each well. Plates were incubated for 30 min at RT and then washed thoroughly with tap water and air-dried. Colonies with more than 50 cells were counted manually. Data show mean of colonies/culture condition \pm SD of triplicate wells.

To measure the radiosensitising effect of SB939 or 1179.4b on 4T1Br4 cells, 100 4T1Br4 cells were seeded in 2 ml of growth medium per well of 6-well plates (3 wells/test condition). Six hours after seeding, cells were pre-treated with 2 ml of medium containing either DMSO (control), 530 nM SB939 or 70 nM 1179.4b which correspond to the IC₅₀ of each drug determined by SRB assay (see Section 2.4.1). Eighteen hours later, the plates were irradiated and further incubated for 7 days at 37°C. Colonies were stained and counted as described above. Data show mean of colonies/culture condition ± SD of triplicate wells.

2.4.3 Tumour-endothelial cell adhesion assays

Adhesion assays on endothelial cells were performed in 96-well plates. Triplicate wells were coated overnight at 37°C with 1 X 10⁵ bEnd.3 cells in 200 µl of growth medium. Once bEnd.3 cells form a complete endothelial monolayer, they were washed twice with PBS before the addition of tumour cells. Tumour cells were labelled with 5 µl of calcein-AM (1 mg/ml) in SFM as per manufacturer's instructions and 4 X 10⁴ cells/100 µl of SFM were added to each well. The plates were incubated for 10 min at 4°C and further incubated for 30 min at 37°C. Non-adherent cells were removed by two gentle PBS washes and one wash with Tris-buffered saline (TBS, pH 7.4) supplemented with 2 mM CaCl₂ and 1 mM MgCl₂. Adherent cells were lysed with 1% sodium dodecyl sulfate (SDS) and cell adhesion was determined by measuring fluorescence at 530 nm emission with a Molecular imager FX reader (Biorad). Specific adhesion was expressed as the percentage of total cell input and calculated from a standard curve made up of 0, 12.5, 25, 50, 75 and 100 µl of calcein-labelled cell lysate derived from the initial cell suspension. The results represent the mean % of total cell input ± SD of triplicate wells. The statistical differences were analysed using a Student's t-test; p<0.05 was considered significant.

2.4.4 Migration and invasion assays

Chemotactic migration and invasion assays were performed in Transwell polycarbonate membrane inserts (8-µm pore size). For migration assays, tumour cells (2 X 10⁵ cells/200 µl of SFM) were seeded in the upper chamber of triplicate Transwells and allowed to migrate to the underside of the porous membrane. After 4 hours of incubation at 37°C, the Transwell membrane was fixed in 10% neutral buffered formalin at 4°C overnight. After a quick wash with PBS, the upper side of the membrane was wiped with a cotton swab. Cells on the underside of the membrane (migrated cells)

were permeabilised with 0.01% triton X-100 for 5 min at RT. Cells were washed with PBS once and were stained with 0.5 µg/mL of 4',6-diamidino-2-phenylindole (DAPI) for 30 min at RT in the dark. Three random fields per membrane were photographed on a BX61 fluorescence microscope (Olympus) at 20X magnification. The number of migrated cells was determined using Metamorph software.

For invasion assays, tumour cells (1×10^5 cells/100 µl of SFM) were mixed with 100 µl of Matrigel:medium (1:1 ratio) and seeded in the upper chamber of triplicate Transwells. The number of cells on the underside of the porous membrane was scored after 18 hours of incubation at 37°C, as described for migration assays.

The results show a representative experiment and were expressed as the mean number of migrated or invaded cells per field \pm SD of nine fields of view (3 replicates well \times 3 fields of view per test condition). The statistical differences were analysed using a Student's t-test; $p < 0.05$ was considered significant.

2.4.5 Trans-endothelial migration assays

Trans-endothelial migration assay was performed in triplicate Transwell polycarbonate membrane inserts (8-µm pore size). bEnd.3 cells (1×10^5 cells) were seeded in the upper chamber of the Transwells in DMEM medium supplemented with 10% FBS, 2 mM L-glutamine, 1 mM sodium pyruvate and 1% P/S. After 24 hrs in culture, endothelial cells were rinsed with PBS. Media from upper and bottom chambers were removed. Tumour cells (1×10^6) were labelled with 5 µl of calcein-AM (1 mg/ml) in 1 ml of SFM. Following the incubation, 2×10^5 cells/200 µl were added to the upper chamber. Six hundred µl of SFM supplemented with 5% FBS and LM-511 (1 µg/mL) were added to the lower chamber. After 48 hrs incubation at 37°C, migrated tumour cells (calcein-AM positive) on the underside of the porous membrane were fixed, processed for microscopy and counted as described for migration and invasion assays. The results represent the mean % of total cells \pm SD of triplicate wells. The statistical differences were analysed using a Student's t-test; $p < 0.05$ was considered significant.

2.5 In vivo assays

2.5.1 Mouse husbandry and animal ethics approval

Mice (5/box) were maintained in a specific pathogen-free environment with food and water freely available. Female BALB/C mice were obtained from either The Walter and Eliza Hall Institute (WEHI, Melbourne, Australia) or Animal Resources Centre (ARC, Perth, Australia), and female NOD scid gamma (NSG) mice from The Peter MacCallum Cancer Centre (Melbourne, Australia). Mice were monitored every day for signs of distress or ill health. All procedures involving mice were performed in accordance with the National Health and Medical Research Council animal ethics guidelines and were approved by the Peter MacCallum Cancer Centre Animal Experimentation and Ethics Committee (AEEC, approval numbers #E507 and E509).

2.5.2 Metastasis assays

2.5.2.1 Spontaneous metastasis

Female BALB/C mice (6-8 week old) were anaesthetised with isoflurane and injected with 2×10^4 viable mCherry expressing- 4T1 or 4T1Br4 cells in 20 μ l of PBS or saline into the fourth mammary fat pad. When tumours became palpable (approximately 10 days), tumour growth was monitored three times weekly using electronic callipers. Tumour volume was calculated using the formula $(\text{length} \times \text{width}^2)/2$.

For comparison of 4T1 and 4T1Br4 tumour growth rate, the tumour volume was recorded from day 10 after cell implantation (palpable tumours) until tumours reached 1.5 g (30 days). The effect of histone deacetylases inhibitors (SB939 and 1179.4b) on 4T1Br4 primary tumour growth was also investigated. Mice bearing palpable tumours were injected intraperitoneally once daily with either 100 μ l of vehicle (30% PEG in saline supplemented with 10% v/v DMSO), SB939 (50 mg/kg) or 1179.4b (20 mg/kg) for 20 days. Tumour volume was measured for the duration of the treatment. Tumours and organs including lung, femur, spine and brain were collected and either placed in 10% neutral buffered formalin to be processed for histology or snap-frozen in liquid nitrogen for metastatic burden analysis by genomic quantitative real-time PCR.

For comparison of 4T1 and 4T1Br4 spontaneous metastatic burden in each organ, tumours were resected when they reached 0.5 g (approximately 2 weeks after cell injection). Two weeks after tumour resection, organs were harvested and processed for histology or metastatic burden analysis, as described above. To gain further insight into

the effect of histone deacetylases inhibitors on the 4T1Br4 spontaneous brain metastatic burden, SB939 and 1179.4b treatments were started two days after tumour resection, when mice have recovered from surgery. Either 100 µl of vehicle (30% PEG in saline supplemented with 10% v/v DMSO), SB939 (50 mg/kg) or 1179.4b (10 mg/kg) were administered intraperitoneally once daily for 2 weeks. Brains were removed and metastases were visualised by Maestro fluorescence imaging. Other organs (lung, femur and spine) were collected for comparison of metastatic burden by genomic quantitative real-time PCR.

2.5.2.2 Experimental metastasis

To compare the brain-metastatic potential of limitrin expressing tumour cells with limitrin knocked down tumour cells, luciferase-expressing MDA-MB-231Br cells silenced for limitrin or control cells expressing a non-targeting shRNA (1 X 10⁵ cells/100 µl saline/mouse for the first experiment and 5 X 10⁴ cells/100 µl saline/mouse for the second experiment) were injected into the left ventricle of the heart of 6-8 week old NSG mice (15 mice/group). Mice were monitored every day after cell injection. Once a week from day 7, the brain metastatic burden was assessed by luminescence imaging. Mice were injected intraperitoneally with 200 µl of 15 mg/ml luciferin and imaged 10 min after injection using the IVIS *in vivo* imaging system, Lumina II (Xenogen). Kaplan Meier (KM) analysis was used to estimate the survival probability of mice injected with limitrin-shRNA cells compared to mice injected with control-shRNA cells. KM survival curves were generated using the GraphPad Prism software. Mice were humanely killed when showing signs of distress or ill health and this was used as the endpoint for the experiment. Organs were harvested and processed for histology or metastatic burden analysis, as described above.

2.6 Histology and immunostaining methods

2.6.1 Tissue fixation method

All tissues were fixed in 10% neutral buffered formalin (except brains that were fixed in 4% PFA) at 4°C overnight before being transferred in 70% ethanol and paraffin embedded by the Peter MacCallum Cancer Centre's histology staff.

2.6.2 Haematoxylin and eosin (H&E) staining

Four μm primary tumour tissue sections or six μm brain sections on poly-L-lysine coated slides were dewaxed in xylene for 10 min, followed by re-hydration in an ethanol series (100%, 90%, and 70% ethanol) for 4 min and deionised water for 1 min. Sections were then stained with Mayer's haematoxylin for 4 sec, washed in deionised water and in blue Scott's tap water. Tissues were counterstained with eosin, dehydrated in 70%, 90% and 100% ethanol followed by xylene, mounted in DPX and cover slipped. H&E staining and sectioning of tissue specimens were performed by the Microscopy and Imaging Core Facility (Peter MacCallum Cancer Centre, Melbourne, Australia).

2.6.3 Immunohistochemistry (IHC)

To confirm the epithelial origin of tumours and to assess the cell proliferation index of these tumours, pan-cytokeratin (pan-CK) and Ki-67 antibodies were used, respectively. Sections were dewaxed as previously described. For pan-CK staining, sections were incubated in antigen retrieval buffer (10 mM citrate buffer (pH 6.0)) for 3 min at 125°C and for an additional 10 sec at 90°C in a pressure cooker. For Ki-67 staining, sections were incubated in antigen retrieval buffer (10 mM citrate buffer (pH 6.0)) in the microwave at maximum power for 10 min. After antigen retrieval, sections were rinsed extensively in Milli-Q water and blocked for 30 min at RT in blocking buffer (3% BSA in PBS). Primary antibodies against pan-CK (1:400 dilution) and Ki-67 (1:250 dilution) were incubated overnight at 4°C under humidified atmosphere. The sections were washed three times with wash buffer (TBS containing 0.1% Tween-20) and incubated with an appropriate biotin-conjugated secondary antibody for 1 hr at RT. Unbound antibodies were washed as above and tissue endogenous peroxidases were inactivated in methanol containing 3% hydrogen peroxide for 10 min at RT. Specific primary-secondary antibody complexes were detected using the ABC reagent and visualised using a 3,3' Diaminobenzidine (DAB) substrate kit. All slides were developed in parallel and the reaction stopped before the detection of a non-specific staining in control isotype matched antibodies treated sections. Sections were counterstained with haematoxylin and mounted in DPX mounting medium.

To detect the presence of limitrin in breast cancer tissues, sections were dewaxed in xylene and rehydrated in graded ethanol solutions prior to antigen retrieval in 10 mM citrate buffer (pH 6.0) for 3 min at 125°C and for an additional 10 sec at 90°C in a

pressure cooker. Sections were blocked with 3% BSA in PBS for at least 30 min and incubated overnight at 4°C under a humidified atmosphere with a primary antibody against limitrin (1:1,000 dilution in blocking buffer). Washing steps, incubation with the secondary antibody and development with ABC reagent were performed as described above. A tissue microarray (TMA) slide obtained from tissue bank of Peter MacCallum Cancer Centre, Melbourne, Australia. Dr Siddhartha Deb (pathologist, Peter MacCallum Cancer Centre, Melbourne, Australia) generated TMA scoring data (intensity of limitrin (0-3) X proportion of cells that stain limitrin positive (0-4)).

2.6.4 Immunofluorescence (IF)

To measure the radiosensitising potential of SB939 or 1179.4b *in vitro*, MDA-MB-231Br cells (4×10^4 cells/500 μ l/well) were seeded in chamber slides in DMEM medium supplemented with 10% FBS and 1% P/S and incubated for 18 hrs at 37°C. The medium was removed and replaced with 500 μ l of growth medium containing either 1.7 μ M SAHA, 360 nM SB939 or 50 nM 1179.4b per well which correspond to the IC₅₀ of each drug determined by SRB assay (see Section 2.4.1). Following 24 hrs incubation at 37°C, cells were irradiated with 1 Gy. Either 1 or 24 hrs after irradiation, cells were rinsed in PBS and fixed with 4% PFA for 30 min, placed in 70% ice-cold ethanol and stored at 4°C for a maximum of 4 weeks. For γ -H2AX staining, cells were washed with PBS for 15 min at RT and blocked with 8% BSA in PBS containing 0.5% Tween-20 and 0.1% Triton X-100 (PBS-TT) for 30 min at RT. Slides were incubated with an anti- γ -H2AX antibody (rabbit polyclonal) (1:500 dilution in 1% BSA in PBS-TT) for 2 hrs at RT under a humidified atmosphere before washing three times with PBS for 5 min and incubated with a secondary antibody (Alexa fluor 488 conjugated goat anti-rabbit IgG, 1:500 dilution in 1% BSA in PBS-TT) for 1 hr at RT. Slides were washed three times as above and mounted with a Vectashield mounting medium containing DAPI.

The results are presented as a representative experiment from 3 independent experiments and were expressed as the mean number of cells positive for γ -H2AX per field \pm SD of nine fields of view (3 replicates X 3 fields of view per condition). Statistical differences were analysed using a Student's t-test; $p < 0.05$ was considered significant.

2.7 Molecular Techniques

2.7.1 Isolation of genomic DNA

Crushed frozen tissues were digested overnight at 55°C in 500 µl digestion buffer (50 mM Tris-HCl (pH 7.5), 1% SDS, 100 mM EDTA, 100 mM NaCl, 100 µg/ml proteinase K and 100 µg/ml RNase A). The next day, 350 µl of saturated NaCl solution was added and incubated on ice for 30 min. The solution was centrifuged at 13,000 x g for 10 min at 4°C and the supernatant was transferred to a fresh microcentrifuge tube. An equal volume of phenol/chloroform/isoamyl alcohol solution (25:24:1) was added to the tube and mixed thoroughly. The tube was centrifuged at 13,000 x g for 5 min at 4°C and the supernatant was collected into a fresh tube. To improve DNA purity, the “phenol/chloroform/isoamyl alcohol” step was performed twice. After adding an equal volume of chloroform/isoamyl alcohol solution (24:1) and centrifuged the tube (13,000 x g for 5 min at 4°C), the supernatant was transferred to a fresh tube and 1 ml of 5 M ammonium acetate/100% ethanol (1:4 ratio) was used to precipitate the DNA by gentle inversion and centrifugation at 13,000 x g for 30 min at 4°C. The supernatant was removed and the DNA pellet was washed twice with 70% ethanol by centrifugation at 13,000 x g for 5 min before being air-dried for 10 min at RT. The DNA was dissolved in 200 µl sterile water for injection. The genomic DNA was then quantified by NanoDrop technology (Biolab), diluted to 10 ng/µl in ultra clean water and stored at -20°C.

2.7.2 Quantitation of metastatic burden using a multiplex TaqMan® assay

Real-time quantitative PCR (qPCR) using TaqMan® chemistry was used to determine the relative metastatic burden in mouse organs. Genomic DNA isolated from tissues (Section 2.7.1) was subjected to multiplexed qPCR to detect the cycle threshold (Ct) for vimentin (total mouse and tumour cells) and mCherry (tumour cells only). By comparing the Ct values of vimentin and mCherry (ΔCt), a score for relative tumour burden was calculated using the following formula: Relative Tumour Burden (RTB) = $10,000/2^{\Delta Ct}$, where $\Delta Ct = Ct (mCherry) - Ct (vimentin)$. When comparing the metastatic burden from two cancer cell lines, the RTB values were adjusted to relative gene copy numbers calculated from the ratio of signals obtained from purified genomic DNA of each cell line in culture. Multiplex qPCR reactions consisted of (final concentrations shown): 40 ng genomic DNA (4 µl), 8 µl of 2X Taqman universal PCR master mix and 1 µM vimentin forward and reverse primer mixture (1 µl), 1 µM vimentin probe (1 µl), 1 µM mCherry forward and reverse primer mixture (1 µl) and 1 µM mCherry probe (1 µl). Total PCR reaction was 16 µl. The following PCR program was used: enzyme activation at 50°C for 2 min, 95°C for 15 min, 45 cycles of denaturation at 95°C for 15

sec and annealing/extension at 60°C for 1 min, followed by generation of melting curves (95°C for 1 min, 55°C for 1 min, and 55°C for 10 sec repeated for 40-50 cycles). All qPCR experiments were performed on a StepOne Real-Time PCR System (AB Applied Biosystems).

To determine the relative metastatic burden in organs of mice injected with shRNA-limitrin MDA-MB-231Br cells or control-shRNA MDA-MB-231Br cells, the Ct values of vimentin (host cells) and hTurboGFP (tumour cells) were used in the RTB formula above.

2.7.3 Isolation of total RNA

Cell pellets from confluent T75 cm² culture flasks were homogenised in 1 ml TRIzol reagent and incubated for 5 min at RT. Two hundred µl of chloroform were added and the samples were vortexed for 15 sec. The samples were incubated for 15 min at RT and then centrifuged at 12,000 x g at 4°C for 15 min. The aqueous phase containing RNA (upper phase) was transferred into a fresh microfuge tube and precipitated with 500 µl of iso-propanol. The samples were mixed by inversion, incubated for 10 min at RT and centrifuged at 12,000 x g at 4°C for 10 min. The supernatant was removed, and RNA pellets were washed twice with one volume of 70% ethanol and centrifuged at 7,500 x g for 5 min at 4°C. RNA was briefly air-dried before being re-suspended in 50 µl of ultra clean water. The concentration and purity of RNA was quantitated by NanoDrop technology. Samples were diluted to 1 µg/µl in ultra clean water and stored at -80°C.

2.7.4 Synthesis of cDNA

Reverse transcription was performed using M-MLV Reverse Transcriptase, RNase H Minus. Oligo (dT) primers (0.5 µl of a 0.5 µg/µl stock solution) were added to 1 µg of total RNA. Ultra clean water was added to bring the total reaction volume to 8 µl. The reaction mixture was incubated at 70°C for 5 min, and then placed on ice for 5 min before adding the following reagents: 2.5 µl of 5X M-MLV RT (H-) buffer, 2.5 µl of 10 mM dNTPs mixture (2.5 µl of each dATP, dTTP, dCTP and dGTP and 90 µl ultra clean water to bring the total volume to 100 µl) and 0.5 µl of M-MLV Reverse Transcriptase, RNase H Minus (200 units/µl). The mixture was incubated for 1 hr at 37°C and cDNA was kept at -20°C for long-term storage.

2.7.5 Assessment of limitrin mRNA expression levels utilising SYBR Green I technology

SYBR Green I was used to determine the relative level of limitrin mRNA expression compared to that of housekeeping genes mRPS27a (mouse) or hRPL37a (human). The PCR reaction solution (total volume of 10 µl/tube) consisted of 5 µl of 2X SYBR Green I master mix, 2 µl of 400 nM limitrin (mouse) or 2 µl of 100 nM limitrin (human) forward and reverse primer mixture, 1 µl of cDNA and 2 µl of ultra clean water. Standard cycling procedures were employed, i.e. enzyme activation at 50°C for 2 min, 95°C for 15 min, 40 cycles of denaturation at 95°C for 15 seconds and annealing/extension at 60°C for 1 min. Specific amplicon formation with each primer pair was confirmed by dissociation curve analysis (generation of melting curves: 95°C for 1 min, 55°C for 1 min, and 55°C for 10 sec repeated for 40 cycles). PCR experiments were performed on a StepOne Real-Time PCR System (AB Applied Biosystems). Gene expression was measured relative to the expression of mRPS27a or hRPL37a using the following formula: Relative transcript abundance (RTA) = $10,000/2^{\Delta CT}$, where $\Delta CT = CT(\text{limitrin}) - CT(\text{housekeeping gene})$; Ct being the cycle threshold value.

2.7.6 Transient knockdown of limitrin using small interfering RNA (siRNA)

MISSION® esiRNA (endoribonuclease-prepared siRNA) was used to generate limitrin small interfering RNA (siRNA). 4T1Br4 cells (1×10^5 cells/well of 6-well plates) were seeded in 4 ml of α -MEM supplemented with 5% FBS without P/S and incubated overnight. Lipofectamine 2000 (10 µl) was mixed with 490 µl of opti-mem and the mixture (total volume of 500 µl) was incubated for 5 min at RT. Twenty µM of limitrin or non-targeting (EGFP) esiRNA primers were diluted with opti-mem to a final volume of 500 µl which was added to the lipofectamine 2000/opti-mem mixture and incubated for a further 20 min at RT. The medium of each well was replaced with 1 ml of α -MEM supplemented with 5% FBS and 1 ml of the lipofectamine mixture. The cells were incubated for 24 hrs at 37°C before replacing the medium with α -MEM supplemented with 5% FBS and 1% P/S. Forty-eight hrs later, cells were washed with PBS, homogenised with 1 ml TRIzol reagent, frozen immediately and processed for total RNA isolation as described in Section 2.7.3.

2.7.7 Stable knockdown of limitrin using short hairpin RNA (shRNA)

2.7.7.1 Isolation of plasmid DNA containing human limitrin shRNA

Plasmid DNA containing a specific human limitrin shRNA sequence was extracted using the Qiagen-mini prep kit according to the manufacturer's instructions. The protocol is based on a modified alkaline lysis procedure followed by binding of plasmid DNA to QIAGEN resin. Plasmid DNA is then eluted in a high-salt buffer (Figure 2.2). Briefly, bacteria transfected with shRNA-containing plasmid were streaked on a 10-cm plate containing 10 ml of Luria broth-agar (LB-agar: 1% bacto-tryptone, 85 mM NaCl, 0.5% yeast extract, 1% casein hydrolysate and 1.5% bacto agar) supplemented with ampicillin (100 µg/ml) and incubated overnight at 37°C. Distinct single colonies of ampicillin resistant bacteria were picked and incubated for 18-24 hrs at 37°C with shaking (300 rpm) in glass tubes (1 colony/tube) containing 2 ml of LB medium supplemented with 100 µg/ml ampicillin. The bacterial cultures were then centrifuged at 10,000 x g for 10 min at 4°C and lysed in an alkaline lysis buffer. The lysate was applied to anion-exchanged-based QIAGEN tips, then wash with medium salt buffer before elution of plasmid DNA with high-salt buffer.

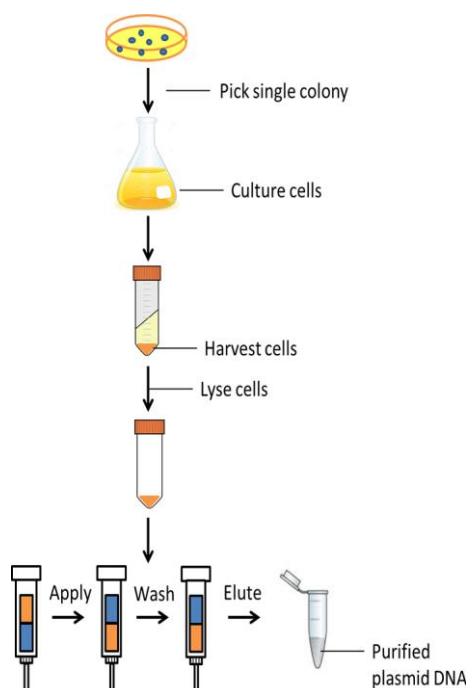


Figure 2.2 Schematic diagram of plasmid DNA extraction

2.7.7.2 Transduction of shRNA to limitrin in the human MDA-MB-231Br tumour

line

A monolayer of packaging HEK293T cells were seeded in T25 cm² flasks (~50% confluency) in DMEM with 10% FBS and 1% P/S and incubated for 24 hrs at 37°C with 5% CO₂. Two µg of each pGIPz vector plasmid or 2 µg of a negative transfer plasmid were mixed to 5 µg of pCMV R8.2 (packaging plasmid), 2.5 µg of pVSV-G (envelop plasmid) and DMEM to bring the total volume to 521 µl, vortexed for 10 sec at medium speed and incubated for 10 min at RT. Nine µl of the transfection reagent, polyethylenimine (PEI) (1 mg/ml) was added to HEK293T cells according to the manufacturer's instructions. Plasmids were briefly vortexed and added to the HEK293T cells by swirling the flasks. The cells were incubated for 18 hrs at 37°C with 5% CO₂, after which the transfection medium was replaced with fresh DMEM medium supplemented with 10% FBS. Twenty-four hrs later, the retroviral supernatant was harvested and filtered through a 0.45 µm filter to remove cell debris. Semi-confluent MDA-MB-231Br cells were incubated with 5 ml of retroviral supernatant containing polybrene (4 µg/ml) to aid the incorporation of viral particles. After 24 hrs incubation, stably infected cells were selected with puromycin (5 µg/ml) over a period of 7 days. Puromycin resistant cells were expanded in culture and utilised for *in vivo* experiments (Section 2.5.2.2).

2.8 Statistical analysis and digital imaging

2.8.1 Statistical methods

All statistical analyses were performed in GraphPad Prism 6 (GraphPad Software). P-values were calculated using a Student's t-test, one-way ANOVA with Bonferroni post-test, one-way ANOVA with Tukey post-test or a two-way ANOVA with Tukey post-test, as indicated in each figure legend. Values were considered significant when $p < 0.05$.

2.8.2 Digital imaging

Transmitted light images (H&E or immunohistochemistry staining) and fluorescent images were taken with a BX61 microscope (Olympus) and the images were captured using a Diagnostic Instruments SPOT camera. Microscopy images were analysed with MetaMorph (Molecular Devices). Western blots were quantitated using ImageJ (1.47v

version for Windows, The National Institutes of Health). *Ex-vivo* fluorescence imaging of mCherry expressing 4T1Br4 tumours and *in vivo* bioluminescence imaging of luciferase expressing MDA-MB-231Br tumours were performed using Maestro™ In-Vivo Imaging System (CRi) and IVIS Lumina II (Xenogen), respectively. Digital images were manipulated using Adobe Photoshop 13.0.1 software and collated using Corel Draw 12.

3. Development and characterisation of a novel syngeneic mouse model of spontaneous breast cancer brain metastasis

3.1 Introduction

As discussed in Chapter 1, brain metastasis is an increasing problem for which no curative therapies have been developed (Wadasadawala et al., 2007). Clinically relevant animal models of metastasis are essential to test the efficacy of anti-metastatic drugs and to investigate mechanisms controlling breast cancer brain metastasis (Eckhardt et al., 2012). Experimental models of breast cancer brain metastasis generally show high incidence of brain metastases but do not fully recapitulate the process of metastasis seen in breast cancer patients, as they bypass the early stages of the metastatic cascade (Palmieri et al., 2007b, Kodack et al., 2012). In addition, the majority of experimental models are xenograft models that require the use of immune deficient mice and therefore do not take into account the role of the immune system in regulating metastasis to the brain. Orthotopic tumour implantation models (in which breast cancer cells are injected into the anatomically relevant mammary fat pad) better recapitulate the spontaneous process of breast cancer metastasis (Eckhardt et al., 2012). However, few mouse models of spontaneous breast cancer brain metastasis have been developed so far. Bos and colleagues (Bos et al., 2009) generated a brain-seeking variant (CN34-BrM2) of the CN34 breast cancer cell line isolated from a breast cancer patient. The authors reported an impressive incidence (42%) of spontaneous brain metastasis in the CN34-BrM2 model. Surprisingly, despite such a remarkable finding, the study by Bos et al. and subsequent studies employing the same cell line (Valiente et al., 2014) only used the CN34-BrM2 model in experimental metastasis assays. Therefore, it is unclear how reproducible this model is in spontaneous metastasis assays. Moreover, since CN34-BrM2 is a xenograft model, it requires the use of immune compromised mice.

The syngeneic 4T1 mouse model is widely used to investigate metastasis (Miller et al., 1986, Lelekakis et al., 1999) and has been reported to give rise to spontaneous brain metastases (Pulaski and Ostrand-Rosenberg, 1998). However, spontaneous tumour spread to the brain is only occasionally observed, most likely reflecting the genetic/functional heterogeneity of 4T1 tumours. Nevertheless, brain-metastatic

variants of the 4T1 model have been described in the literature. Lockman and colleagues introduced the murine 4T1-Br5 brain seeking cell line but it is unclear from this study how the cell line was developed and how robust the model is in terms of incidence of mice developing spontaneous 4T1-Br5 brain metastases (Lockman et al., 2010). In addition, to the best of our knowledge, the 4T1-Br5 line has only been tested in immune compromised mice using experimental metastasis assays. More recently, Erin and colleagues (Erin et al., 2013) generated the murine 4TBM brain metastatic cell line derived from a 4T1 heart metastatic variant. While the 4TBM model has the advantage of being syngeneic, the authors did not report on the incidence of spontaneous brain metastasis in this model. Moreover, despite their advantages, the 4TBM and other syngeneic mouse models of breast cancer brain metastasis developed so far have not been thoroughly validated for relevance to the human disease. Reproducibility, high incidence of brain metastasis and phenotypic/genetic validation of mouse models are essential if these models are to be used for therapy testing and/or for functional characterisation of brain metastasis genes.

This chapter describes the development and characterisation of a new 4T1-derived syngeneic mouse model of spontaneous breast cancer brain metastasis (4T1Br4) and its phenotypic, functional and genetic validation.

3.2 Results

3.2.1 Isolation of a brain metastatic breast cancer cell line

Pulaski and Ostrand-Rosenberg were first to demonstrate that the murine 4T1 mammary carcinoma cells can spread spontaneously to the brain (Pulaski and Ostrand-Rosenberg, 1998). They injected the cells into the mammary glands of BALB/C mice and brains were harvested at 5-6 weeks after cell injection. To quantify the extent of metastasis, brains were minced, digested with collagenase and elastase, cultured in medium supplemented with 6-thioguanine to select 6-thioguanine resistant 4T1 cells and cell colonies were counted after 10-14 days. While a large number of colonies developed, due to the methodology used, it is difficult to determine whether these colonies originated from a single or multiple brain metastases and/or from circulating tumour cells in the brain vasculature. These observations have been independently verified by Dr Normand Pouliot in our laboratory (unpublished work and see results below).

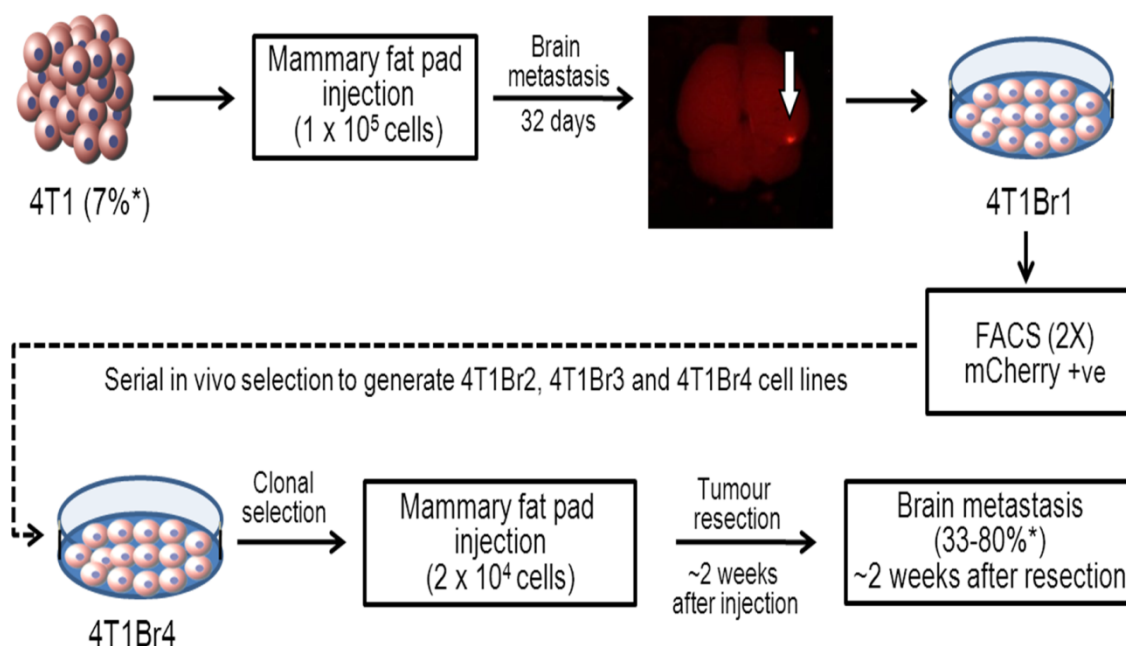
Therefore we chose parental 4T1 cells to derive more aggressive brain metastatic clonal variants. To facilitate the detection of brain metastases, 4T1 cells were first stably transduced with an mCherry fluorescent marker gene and then injected into the mammary fat pad of BALB/C mice. A single spontaneous brain metastasis was detected by fluorescence imaging in 1 out of 15 mice (7% incidence). The brain metastasis was microdissected and expanded in standard culture. mCherry-positive cells were then isolated by fluorescence activated cell sorting (FACS) and further expanded in culture (4T1Br1). This process was repeated four times to generate the 4T1Br2, 4T1Br3 and 4T1Br4 variants. At this stage, 4T1Br4 tumours gave rise to brain metastases in approximately 20% of mice compared to 7% in mice bearing parental 4T1 tumours (Table 3.1). Since brain metastasis is most commonly a late event during metastatic progression, to increase the incidence of mice developing brain metastases, we reduced the number of cells injected from 1×10^5 to 2×10^4 thereby allowing more time for cells to disseminate and form metastases in the brain. In addition, to prevent early termination of experiments due to excessive/unethical primary tumour size, tumours were resected when they reached approximately 0.4-0.5 g. This protocol also better reflects the clinical situation for breast cancer patients who typically undergo surgery to remove the primary tumour before they are diagnosed with brain metastases. Thus, after clonal selections by FACS, 2×10^4 cells of each clone of 4T1Br4 cells (12

in total) were injected into the mammary fat pad of 5 or 6 BALB/C mice. Approximately two weeks after primary tumour resection, mice were harvested and brains were imaged. This analysis revealed two clones (4T1Br4 clones 2 and 6) giving rise to high incidence of brain metastases (67-80% of mice) (Table 3-1). Although 4T1Br4 clone 2 showed the highest incidence of brain metastases, this cell line tended to form soft primary tumours in the mammary fat pad that were difficult to resect completely. Therefore this cell line was excluded from further experiments. For subsequent experiments we focused on 4T1Br4 clone 6 and refer to this variant as 4T1Br4 (Figure 3.1).

Table 3-1. Incidence of mice developing spontaneous brain metastases.

Variants	Incidence (%)
Parental 4T1 (Bulk)	1/15 (7)
4T1Br4 (Bulk)	1/5 (20)*
4T1Br4 clone 2	4/5 (80)
4T1Br4 clone 4	2/6 (33)
4T1Br4 clone 6	4/6 (67)

*The incidence of brain metastasis from other clonal populations (12 in total) was similar or lower than the 4T1Br4 bulk population.



* Incidence of mice developing spontaneous brain metastases

Figure 3.1 Schematic representation of the development of the 4T1Br4 brain metastatic model

mCherry-tagged 4T1 mammary carcinoma cells (1×10^5) were injected orthotopically into 15 mice. After 32 days, mice were sacrificed and the brains examined by Maestro fluorescence imaging for detection of mCherry (macrometastases). A single mouse showed a positive mCherry signal in the brain. The metastatic nodule was resected, minced and cultured. mCherry^{+ve} cells were isolated by FACS and expanded in culture twice (4T1Br1) before re-injecting (1×10^5 cells) into the mammary fat pad of mice. Following the fourth serial in vivo enrichments (4T1Br4), cells were single cell cloned and injected (2×10^4 cells) into the mammary fat pad of 5-6 mice per clone. Tumours were surgically removed when they reached 0.4-0.5 g and metastases were allowed to develop for an approximately 2 weeks. Two out of 12 clones gave rise to large brain metastases detectable by fluorescence imaging (macrometastases) and/or micrometastases detectable by H&E staining of brain tissue sections in up to 80% of animals.

3.2.2 In vivo functional characterisation of the 4T1Br4 model

To compare the growth of 4T1 parental and 4T1Br4 brain-metastatic tumours, 4T1 and 4T1Br4 cells were injected (2×10^4 cells) into the mammary fat pad and tumour growth was monitored over 30 days. There was no significant difference in the growth rate of 4T1 and 4T1Br4 tumours *in vivo* (Figure 3.2A). In a separate assay, 4T1 and 4T1Br4 cells were injected (2×10^4 cells) into the mammary fat pad of mice and primary tumours were resected about 2 weeks after cell injection when they reached approximately 0.4-0.5 g (Figure 3.2B). Organs including the brain, lung and spine were harvested and relative tumour burden (RTB) in each organ was compared between 4T1 and 4T1Br4 tumour-bearing mice. The 4T1Br4 group developed more extensive brain metastases than the 4T1 group (Figure 3.2C). However, there was no difference in lung (Figure 3.2D) or spine burden (Figure 3.2E) between groups. This indicates that the 4T1Br4 tumours are selectively more metastatic to the brain compared to parental 4T1 tumours.

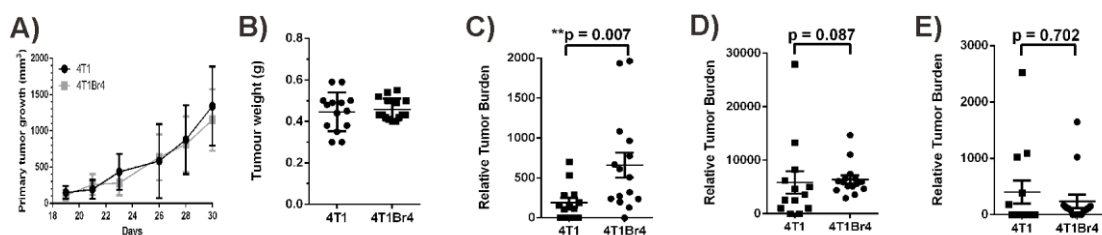


Figure 3.2 Comparison of 4T1 and 4T1Br4 tumour growth and metastatic burden in distant organs

(A) Tumour growth was measured between day 19 and day 30. Data show mean \pm SD from 15 mice per group. (B) For metastasis assays, 4T1 ($n = 13$) and 4T1Br4 ($n = 15$) primary tumours were resected when they reached approximately 0.5 g (~2 weeks after cell injection). RTB in (C) brain, (D) lung and (E) spine was measured 3 weeks after tumour resection. Each dot represents one mouse and the horizontal line represents mean \pm SD. p -values were calculated using a Student's t -test; $p < 0.05$ was considered significant.

Representative images of the brain and lung metastases visualized by fluorescence imaging are shown in Figure 3.3A. 4T1Br4 cells typically metastasise to the cerebrum. H&E staining of a large 4T1Br4 cerebral metastasis showed high level of vascularisation (Figure 3.3B, arrows) and proliferation as evidenced by high expression of the Ki-67 proliferation marker (Figure 3.3C). The epithelial nature of the metastatic lesion was confirmed by detection of cytokeratin (Figure 3.3D) absent in the normal brain except for the choroid plexus that produces the cerebrospinal fluid (Watanabe et al., 2012).

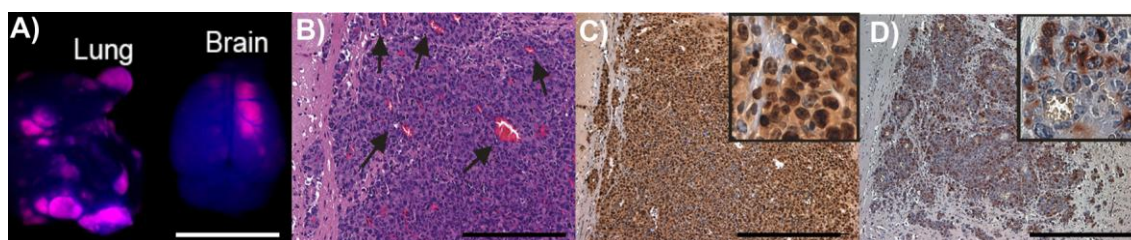


Figure 3.3 Fluorescence and histological examination of 4T1Br4 brain metastases

(A) Fluorescence imaging of mCherry^{+ve} (pink) in the lung and brain metastases. (B) H&E staining (arrows, blood vessels). (C) Ki-67 and (D) pan-cytokeratin were detected by standard immunohistochemistry. Scale bar = 1 cm in (A), 100 μ m in (B-D). High power images of (C) and (D) are shown in insets.

3.2.3 Phenotypic analysis of 4T1Br4 primary tumours and brain metastases

Tumours of the 4T1 model are basal-like and classified as TNBC (Johnstone et al., 2015). However, discordance in the expression of hormone receptors and HER2 between primary tumours and matched metastases has been reported in some breast cancer patients, a phenomenon termed “phenotypic conversion” (Eckhardt et al., 2012, de Duenas et al., 2014, Duchnowska et al., 2012).

Therefore, to determine the molecular phenotype of 4T1Br4, primary tumours and matched brain metastases were analysed for the expression of ER, PR and HER2 (Figure 3.4). As expected, 4T1Br4 primary tumours did not express nuclear ER or PR (Figure 3.4A-B). Similarly, membrane expression of HER2 was negligible (Figure 3.4C). Importantly, 4T1Br4 brain metastases lacked expression of nuclear ER (Figure 3.4D), PR (Figure 3.4E) or membrane HER2 (Figure 3.4F). Taken together, these results indicate that 4T1Br4 tumours are of the TNBC phenotype and that this phenotype is maintained in brain metastases.

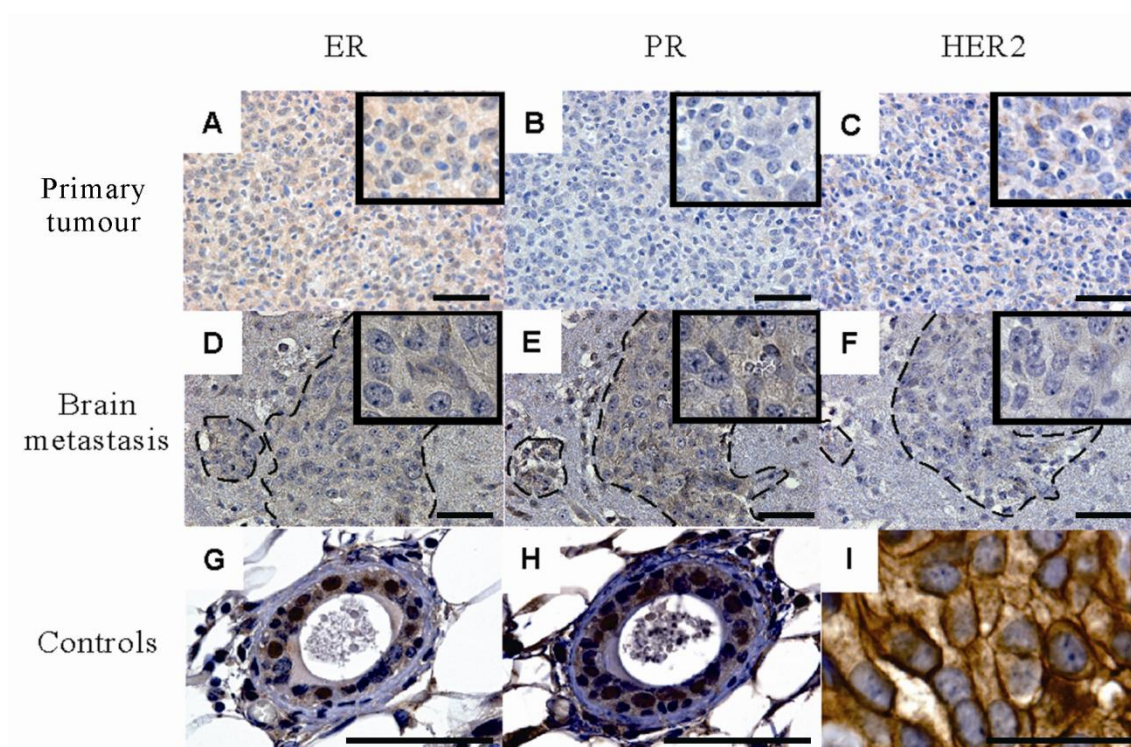


Figure 3.4 Confirmation of the TNBC phenotype in 4T1Br4 primary tumours and brain metastases

Standard immunohistochemistry was used for detection of ER, PR and HER2 in 4T1Br4 primary tumours (A-C) and brain metastases (D-F). High power images are shown in insets. Normal mammary glands were used as positive controls for nuclear expression of ER (G) and PR (H) (brown staining). Human SKBR3 primary tumour xenograft was used as a positive control for membrane expression of HER2 (I) (brown staining). Brain metastatic lesions are delineated by a dotted line. Hematoxylin was used for nuclear staining (blue). Scale bar = 50 μ m.

3.2.4 Functional characteristics of the 4T1 and 4T1Br4 cell lines in vitro

For successful development of spontaneous metastases, cancer cells need to survive and proliferate in the mammary gland, migrate through blood vessels (intravasation), survive in the circulation, adhere to endothelial cells in distant organs, migrate across the endothelium (extravasation), invade surrounding tissues and proliferate and survive to colonise a secondary organ (Francia et al., 2011, Nguyen et al., 2009).

To gain further understanding of the mechanisms by which 4T1Br4 tumours spontaneously spread to the brain, we compared the functional properties of 4T1 and 4T1Br4 cells in a series of *in vitro* functional assays that recapitulate specific aspects of the metastatic cascade. 4T1 and 4T1Br4 cells did not differ significantly in their proliferation rates (Figure 3.5A) or colony forming abilities (Figure 3.5B) in response to 5% serum. However, 4T1Br4 cells were significantly more migratory than 4T1 cells in Transwell chemotaxis assays (Figure 3.5C). Moreover, 4T1Br4 cells were significantly more adhesive to bEnd.3 brain microvascular endothelial cells (Figure 3.5D).

Laminins are important components of most epithelial and endothelial basement membranes (Timpl and Brown, 1996, Yurchenco, 2011, Hohenester and Yurchenco, 2013). In particular, laminin-511 is secreted by the endothelial cells of the BBB (Baeten and Akassoglou, 2011, Sorokin, 2010, Daneman and Prat, 2015) and contributes to the barrier function and to the attachment of tumour cells to the endothelial basement membrane through engagement of integrin receptors of laminin, e.g., $\alpha 3$ integrin (Tilling et al., 1998, Yoshimasu et al., 2004) and $\beta 4$ integrin (Fan et al., 2011). Thus, to better mimic the microenvironment of the brain vasculature in trans-endothelial migration assays (Figure 3.5E), laminin-511 was added to 5% FBS in the lower chamber wells as chemoattractant. Under these conditions, 4T1Br4 cells showed enhanced ability to migrate through a monolayer of brain microvascular endothelial cells compared to 4T1 cells (Figure 3.5E).

To test whether 4T1 and 4T1Br4 cells might respond differently to soluble factors secreted in the brain microenvironment, the effect of serum-free conditioned medium derived from whole brain primary cell cultures (BCM) was evaluated in invasion, proliferation and colony forming assays. 4T1Br4 cells were significantly more invasive than parental 4T1 cells in response to 50% BCM condition used as chemoattractant (Figure 3.5F). In contrast, 50% BCM alone was not sufficient to promote 4T1 or 4T1Br4 cell proliferation over 5 days (Figure 3.5G). Both cell lines proliferated in response to 1% serum and proliferation rate was further enhanced by combination of 1% FBS and 50% BCM. However, both lines responded equally well to this FBS/BCM combination (Figure 3.5G). Similarly, in colony forming assays, 4T1 and 4T1Br4 cell lines did not form colonies in 50% BCM alone after 10 days, but both cell lines formed similar number of colonies in 1% serum, irrespective of the presence or absence of 50% BCM (Figure 3.5H). These results indicate that BCM alone is not sufficient to promote survival or proliferation but enhances the proliferative effect of serum to the same extent in both 4T1 and 4T1Br4 cells.

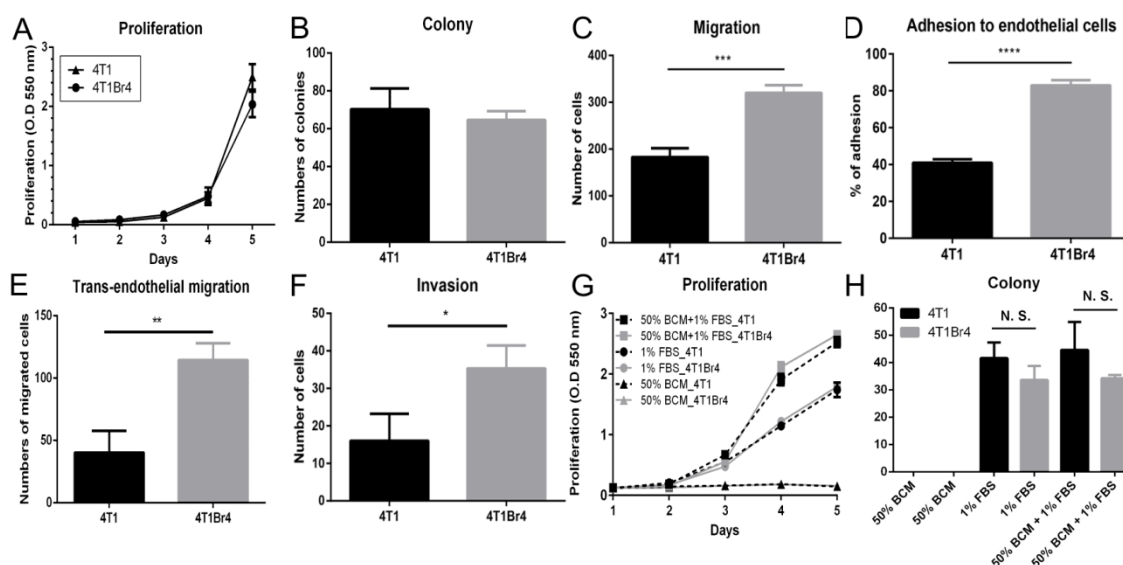


Figure 3.5 *In vitro* functional characterisation of the 4T1 and 4T1Br4 cell lines

(A) Proliferation assay. Cells were seeded at 500 cells/well in 96-well plates in the presence of 5% FBS and cultured for 5 days. (B) Colony forming assay. Cells were seeded at low density (100 cells/well in 6-well plates) in the presence of 5% FBS and colonies were counted after 10 days. (C) Migration assay. Cells were seeded in the upper well of Transwell chambers in serum-free medium and 5% FBS added to the lower well as chemoattractant. Cells that migrated to the underside of the porous membrane were counted after 4 hours at 37°C. (D) Adhesion assay. Calcein-labelled cells were seeded onto a monolayer of bEnd.3 brain microvascular endothelial cells and tumour cells attached to bEnd.3 cells were counted 10 min after cell seeding. (E) Trans-endothelial migration assay. Tumour cells were seeded onto a monolayer of bEnd.3 cells in the upper well of Transwell chambers and tumour cells that migrated to the underside of the membrane in response to 5% FBS + laminin-511 in the lower well were counted after 48 hr incubation at 37°C. (F) Invasion assay. Tumour cells were mixed with Matrigel (1:1 ratio) in upper well of Transwell chambers and cells that migrated to the underside of the membrane in response to 50% BCM in lower well were counted 18 hr after cell seeding. (G) Proliferation and (H) colony forming assays. Cells were seeded in the presence of 50% BCM, 1% FBS or both as indicated and cultured for 5 days (G) or 10 days (H). All experiments were conducted in triplicates and repeated three times ($n = 3$). p -values were calculated using a Student's t -test;

$p < 0.05$ was considered significant. N.S. not significant, * $p < 0.05$, ** $p < 0.01$, *** $p < 0.005$, **** $p < 0.001$.

3.2.5 Genetic validation of the 4T1Br4 model and relevance to human brain metastatic TNBC

The limited overlap in metastasis genes identified between various mouse models and human tissues has raised doubts about the relevance of mouse models for the identification of therapeutic targets. For example, a recent review of the literature (Daphu et al., 2013) identified only four brain metastasis genes whose expression was commonly increased in xenograft models and in tumour tissues from breast cancer patients (Bos et al., 2009, Hicks et al., 2006, Graesslin et al., 2010). A recent study by Bos and colleagues analysed clinical samples from breast cancer patients with known sites of recurrence and identified differentially expressed genes in brain metastatic versus non-metastatic human breast tumours (GEO dataset, GSE12276) (Bos et al., 2009). Thus, to validate the relevance of the 4T1Br4 model to human brain metastatic TNBC at the transcriptional level, in collaboration with Dr. Richard Redvers (Peter MacCallum Cancer Centre), we sought to determine whether the expression profile from 4T1Br4 tumours versus isogenic non-metastatic 67NR breast tumours (Figure 3.6) was enriched for gene signatures derived from differentially expressed genes of the brain metastatic versus non-metastatic samples in the Bos cohort. For these analyses, mCherry-positive tumour cells were freshly isolated from primary tumours by FACS and RNA subjected to array profiling using the GeneChip Mouse Exon 1.0 ST Array (Affymetrix Inc, California, US). Gene set enrichment analysis (Subramanian et al., 2005) was performed to investigate enrichment in our murine brain-metastatic tumours for the human brain-metastatic gene signatures derived from the Bos cohort (Table 3-2). This analysis revealed that up-regulated genes in 4T1Br4 tumours compared to 67NR tumours were significantly enriched in the top 100 up-regulated genes identified in human brain-metastatic TNBC by Bos and colleagues, as indicated by the normalised enrichment score (NES = 1.79) which provides a statistical measure of the degree to which a gene-set is over-expressed (Table 3-2). Moreover, down-regulated genes in 4T1Br4 tumours compared to 67NR tumours indicated significant enrichment for in the top 20 down-regulated genes in human brain-metastatic TNBC (NES = -1.71). From their analysis of human breast tumours, Bos and colleagues defined a 17-gene metastasis signature associated with brain relapse (Bos et al., 2009). Further adding to the relevance of the 4T1Br4 model to the human metastasis, we found that genes of the human breast cancer brain metastasis signature were over-

expressed in 4T1Br4 tumours, with seven genes in 4T1Br4 tumours contributing to the enrichment score, as compared to 67NR tumours (NES = 1.68). Collectively, these observations demonstrate that the 4T1Br4 model is genetically relevant to human brain-metastatic TNBC.

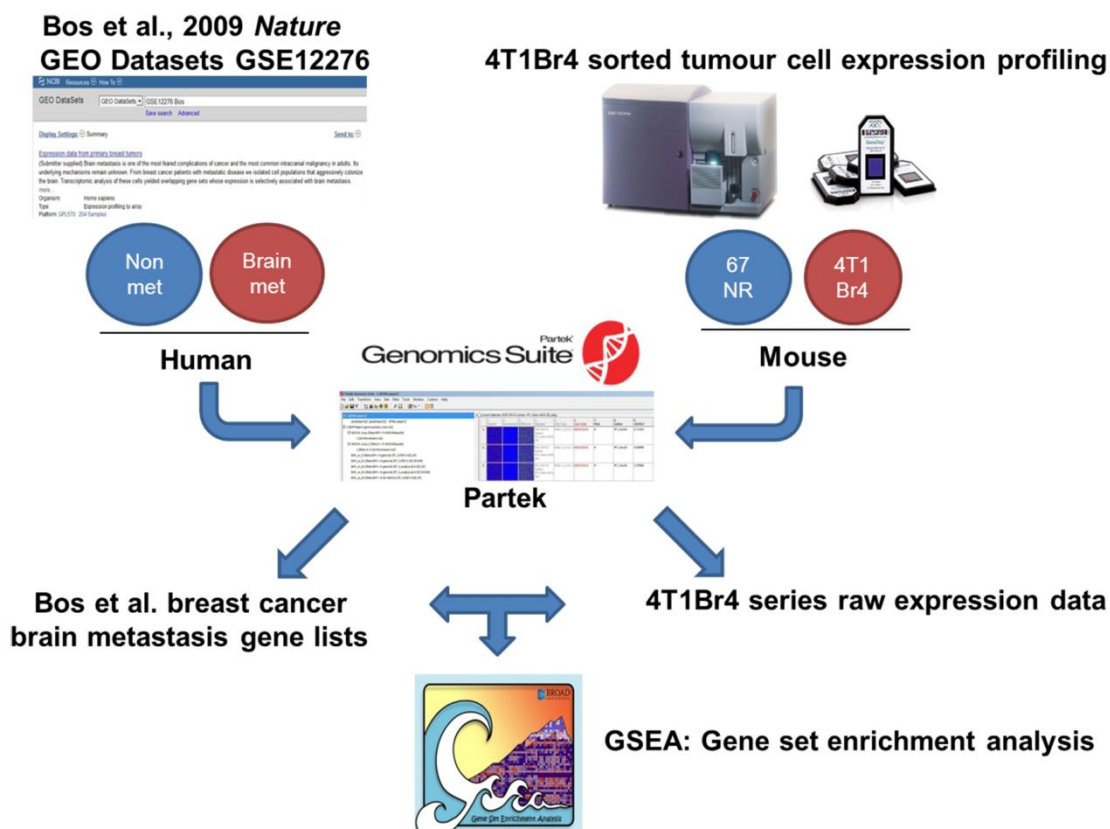


Figure 3.6 Genetic relevance of 4T1Br4 to breast cancer patients with brain metastases

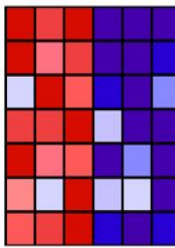
A schematic representation of gene array profiling and GSEA (gene set enrichment analysis) between primary 4T1Br4 tumours and breast cancer patients with brain metastases. The raw mRNA expression signal files from the Bos cohort (GSE12276) were obtained from GEO Datasets, uploaded into Partek Genomics Suite and samples annotated with their corresponding clinical data to identify TNBC, brain metastatic and non-metastatic samples for further analysis. Genes differentially expressed (fold-change ≤ -2 or ≥ 2 , p -value ≤ 0.05) between brain metastatic and non-metastatic TNBC samples were identified with a one-way ANOVA analysis. From these differentially expressed genes, subsets were used to define gene signatures as described in Table 3-2. In order to permit GSEA with our murine expression profile data, these human

genes were converted to functional mouse orthologs (NCBI Homologene; <http://www.ncbi.nlm.nih.gov/homologene/>) where they existed. Met, metastasis.

Table 3-2. Gene set enrichment analysis of 4T1Br4 versus brain-metastatic human breast tumours.

Bos et al. gene signatures (Bos et al., 2009)	NES	FDR
Top 100 up-regulated genes in TNBC patients with brain metastases	1.79	0.008
Top 20 down-regulated genes in TNBC patients with brain metastases	-1.71	0.041
17-gene breast cancer brain metastasis signature*	1.68	0.018

*4T1Br4 67NR



Csf3

Lama4

B4galt6

Angptl4

Peli1

Hbegf

Ltbp1

NES, normalised enrichment score, corrects for differences in enrichment score (ES) between gene-sets due to differences in gene-set sizes (>1.5 is significant). ES reflects the degree to which a gene-set is over-represented at the top or bottom of a ranked list of genes. FDR, false discovery rate, corrects for multiple hypothesis testing and enable a more correct comparison of the different tested gene-sets with each other (<0.05 is significant). Colony-stimulating factor 3, Csf3; laminin subunit alpha 4, Lama4; beta-1,4-galactosyltransferase 6, B4galt6; angiopoietin-like 4, Angptl4; pellino E3 ubiquitin protein ligase 1, Peli1; heparin-binding EGF-like growth factor, Hbegf; latent-transforming growth factor beta-binding protein 1, Ltbp1. Csf3 enhances lung metastasis of breast cancer cells (Kowanetz et al., 2010). Lama4 promotes breast cancer cell proliferation and metastasis (Ross et al., 2015). Angptl4 facilitates lung colonisation by breast cancer cells (Padua et al., 2008). Hbegf promoted breast cancer cell intravasation, metastasis and invasion (Zhou et al., 2014).

3.3 Discussion

The aim of this chapter was to develop and characterise a new clinically relevant model of breast cancer brain metastasis. Such a model is needed to investigate the mechanisms regulating breast cancer brain metastasis, to identify novel therapeutic/prognostic targets and to evaluate the efficacy of novel therapies. Current xenograft models of experimental breast cancer brain metastasis are useful to investigate late stages of metastasis but lack clinical relevance as they do not recapitulate the complete metastatic process observed in patients and require the use of immune deficient mice. Syngeneic mouse models typically metastasise more aggressive from the mammary gland than xenograft models and have the advantage of a fully functional immune system. However, few syngeneic mouse models of spontaneous breast cancer brain metastasis have been described and most have been derived from the 4T1 tumour line originally developed by Aslakson and Miller (Aslakson and Miller, 1992). Moreover, the incidence of spontaneous brain metastasis in these models was either not reported or was relatively low (Erin et al., 2013, Zhang et al., 2015b). Importantly, the phenotypic and genetic relevance of these syngeneic mouse models to human breast cancer brain metastasis has until now not been validated.

The 4T1Br4 model described herein possesses many of the desired attributes of a clinically relevant model of breast cancer brain metastasis. The 4T1Br4 model is robust and, to our knowledge, gives rise to a higher incidence of spontaneous brain metastasis than all models previously described. Since 4T1-derived tumours are aggressive and fast growing, reducing the number of cells inoculated in the mammary fat pad may have contributed in part to increasing the incidence of brain metastases by slightly extending the duration of the assay. Bailey-Downs et al. (Bailey-Downs et al., 2014) pointed out that optimisation of the number of cell implantation is key to obtain balance between inducing metastases and allowing time for drug testing in a 4T1 syngeneic mouse model.

Similarly, excision of the primary tumours prevented early termination of experiments due to excessive lung burden and/or primary tumour size, thereby allowing more time for the development of brain metastases. However, the dramatic increase in brain metastasis was observed following repeated *in vivo* selection of brain metastases and *in vitro* clonal selection of 4T1Br4 variants. Bulk 4T1Br4 cells isolated from brain lesions showed increased brain metastatic abilities (up to 20%) compared to parental 4T1 cells (7%). Clonal selection of 4T1Br4 variants drastically increased the incidence

of brain metastases by up to 80% (Table 3-1). This is consistent with the cellular and functional heterogeneity of 4T1 tumours (Wagenblast et al., 2015) and indicates that subsets of 4T1 cells have a greater ability to colonise the brain. Another important feature of the 4T1Br4 model is that the development of brain metastases in 4T1Br4 most resembles the majority of patients with brain metastases, with the late onset of brain metastases and extensive systemic disease (Zorrilla et al., 2001). Specifically, high incidence of lung metastases and moderate incidence of bone metastases observed in the 4T1Br4 model are consistent with observations in TNBC patients (Liedtke et al., 2008).

4T1Br4 tumour-bearing mice typically formed one or two brain lesions that preferentially developed in the cerebrum (Figure 3.3A). This is in agreement with observations in most advanced cancer patients with brain metastases (Delattre et al., 1988) but contrasts with the unusually large number (>100) and widespread distribution of brain metastases observed in some experimental models of breast cancer metastasis to the brain in which a large bolus of cells is inoculated directly into the heart or in the carotid artery (Fitzgerald et al., 2008, Gril et al., 2008). Spontaneous 4T1Br4 brain metastases were consistently highly vascularised (Figure 3.3B), a feature that is likely to contribute to their rapid growth in the brain parenchyma (Lorger and Felding-Habermann, 2010). High expression of the Ki-67 proliferation marker (Figure 3.3C), a feature of TNBC subsets associated with better response to chemotherapy in patients (Rhee et al., 2008, Keam et al., 2011), suggests that the 4T1Br4 brain metastases may be responsive to adjuvant chemotherapy such as docetaxel or doxorubicin. As such, the 4T1Br4 model may be particularly useful to test the efficacy of new approaches to deliver chemotherapeutic agents across the BBB.

Knowledge on the molecular phenotype of tumours can inform on the best therapy for advanced breast cancer patients (Brastianos et al., 2015). However, in some cases phenotypic discordance between primary tumour and matched metastases have been reported (Duchnowska et al., 2012, de Duenas et al., 2014, Shigematsu et al., 2011) suggesting that the efficacy of a given therapy based on the primary tumour phenotype may not always be the most appropriate for metastatic disease. It is not clear, however, whether phenotypic conversion is induced by the change of microenvironment in primary tumours versus brain metastases or whether it reflects clonal selection of a small subset of breast cancer cells with a different phenotype and greater affinity for the brain. In this context, we compared the expression of ER, PR and HER2 between 4T1Br4 primary tumours and brain metastases and observed no phenotypic

discordance, most likely reflecting the clonal nature of the 4T1Br4 model and therefore consistent with the clonal selection of a 4T1 variant with a TNBC phenotype but enhanced ability to spread to the brain.

Results from *in vivo* metastasis assays indicate that 4T1Br4 tumours are more metastatic to the brain but not to lung or bone compared to parental 4T1 tumours (Figure 3.2C-E). This suggested the acquisition of functional properties that “selectively” enhance brain metastasis in 4T1Br4 tumours. To address this, we performed a series of experiments comparing 4T1 and 4T1Br4 cells in *in vitro* functional assays. These assays revealed that proliferation or colony forming ability in the presence of serum did not differ significantly between 4T1 and 4T1Br4 cells (Figure 3.5A-B), a result in agreement with the similar tumour growth rates observed *in vivo* (Figure 3.2A). 4T1Br4 cells were more migratory than parental 4T1 cells in chemotaxis assays (Figure 3.5C). While increased migration may contribute to a more aggressive/metastatic phenotype, this property would be expected to enhance metastasis to multiple sites and is unlikely alone to explain the selectivity of 4T1Br4 tumours to metastasis to the brain.

Interestingly, 4T1Br4 cells showed enhanced adhesion to brain microvascular endothelial cells and enhanced trans-endothelial migration (Figure 3.5D-E). These properties are likely to facilitate homing of disseminating 4T1Br4 tumour cells to the brain by *in vivo* (Figure 3.2C). Consistent with our observations, Cruz-Munoz et al. developed a mouse model of spontaneous brain metastasis from melanoma (131/4-5B1 and 131/4-5B2) and found that brain-seeking properties are associated with increased adhesion to endothelial cells compared to the parental cell line (113/6-4L) (Cruz-Munoz et al., 2008). However, the authors also reported that brain conditioned medium induced a proliferative response in brain-metastatic variants. As this was not observed in 4T1Br4 cells, their study and ours suggest that melanoma and breast cancer cells respond differently to mitogenic factors produced in the brain. The Massagué group demonstrated that three genes (α 2,6-sialyltransferase ST6GALNAC5, cyclooxygenase COX2 and EGFR ligand HBEGF) are highly expressed in brain metastatic breast cancer cells isolated from a breast cancer patient (CN34) and in the brain-seeking MDA-MB-231Br breast cancer line (Bos et al., 2009). Their study revealed that inhibiting the expression of either of these three genes decreased trans-endothelial migration of breast cancer cells and increased survival of mice inoculated with human brain metastatic breast cancer cells. They concluded that the three genes facilitate trans-endothelial migration through the BBB. Consistent with this, the following

chapter describes the expression and function of a novel cell adhesion molecule (limitrin/DICAM) and investigates its potential role in regulating trans-endothelial migration and the spread of breast cancer to the brain.

4T1Br4 cells displayed another property that is likely to facilitate invasion of metastatic cells into the brain parenchyma. We found that stimulation with BCM enhanced invasion of 4T1Br4 by ~2-fold compared to parental 4T1 cells (Figure 3.5F). Consistent with our result, Wang et al. (Wang et al., 2013) reported that astrocyte conditioned media facilitates invasion of MDA-MB-231Br cells. The authors demonstrated the inhibition of MMP-2 and MMP-9 significantly decreased invasion of tumour cells induced by astrocyte conditioned media *in vitro* and reduced brain metastasis *in vivo*. Whether MMP-2 and MMP-9 are secreted in BCM produced from whole brain primary cell cultures has yet to be determined. However, in a separate study, we have found no evidence by immunohistochemistry that MMP-9 is expressed surrounding 4T1Br4 brain lesions (Dr Normand Pouliot, personal communication) suggesting that MMP-9 is not required or that other proteases may facilitate the invasive growth of 4T1Br4 brain metastases. Lastly, we found that BCM enhances serum-induced proliferation of brain metastatic 4T1Br4 cells but not cell survival (Figure 3.5G-H). Taken together, the results from *in vitro* assays indicate that enhanced adhesion to and migration through brain endothelial cells, together with increased invasive response to brain-derived soluble factors are likely to be key determinants of the selective brain metastatic ability of 4T1Br4 tumours.

Identifying differentially expressed genes that overlap between mouse 4T1Br4 tumours and patients' tumours would underpin the model's genetic relevance to human TNBC. Cell culture systems and/or mouse models used to identify genes associated with brain metastasis have been criticised for their lack of relevance at the transcriptomic level since they show minimal overlap with brain metastasis genes identified from patients' tissues (Daphu et al., 2013). For example, Vincent et al. (Vincent et al., 2015) recently reported significant differences in gene expression between breast cancer cell lines *in vitro* and tumours *in vivo*. These differences were attributed primarily to the lack of stromal cell populations and the absence of immune component in culture. However, a key difference between their study and ours is that we specifically isolated 4T1Br4 tumour cells by FACS from whole primary tumours and therefore tumour cells were subjected to the normal mammary tumour microenvironment of immune competent mice. To further address concerns about the relevance of syngeneic mouse models of metastasis to the human breast tumours, we compared differential gene expression at

the transcriptomic level between non-metastatic 67NR and 4T1Br4 mouse primary tumours and genes associated with brain recurrence in breast cancer patients identified from clinical samples with known sites of recurrence by Bos et al (Bos et al., 2009). These analyses showed significant overlap between breast cancer brain metastasis genes identified in human TNBC samples and those associated with 4T1Br4 brain metastasis and confirmed that the 4T1Br4 model is genetically relevant to TNBC patients with brain metastases.

In summary, we found that the 4T1Br4 syngeneic mouse model is phenotypically, functionally and genetically relevant to human brain metastatic TNBC. To our knowledge, the 4T1Br4 model shows the highest incidence of spontaneous brain metastasis among all spontaneous metastasis mouse models previously described. We propose that the 4T1Br4 model can serve as a clinically relevant platform to investigate the mechanisms regulating breast cancer metastasis to the brain, to identify prognostic factors and/or therapeutic targets relevant to human, and to test the efficacy of novel therapies against TNBC brain metastases. The following chapters investigate the prognostic significance and function of a new cell adhesion molecule, limitrin, in trans-endothelial migration assays and evaluate the anti-metastatic efficacy of novel HDAC inhibitors against brain-metastatic TNBC. These results are presented in Chapters 4 and 5, respectively.

4. Evaluation of limitrin as a prognostic marker and therapeutic target for breast cancer brain metastasis

4.1 Introduction

With assistance from Dr Normand Pouliot in the laboratory, differential gene expression between parental 4T1 cells and 4T1Br4 brain metastatic cells was assessed by gene array profiling (Affymetrix microarray technology), in either cultured cells or mCherry^{+ve} tumour cells isolated from primary tumours by FACS to exclude stromal cells. This analysis identified 17 genes up-regulated in 4T1Br4 cells compared to 4T1 cells, based on differential expression cut-off ≥ 3 -fold and statistical significance ($p \leq 0.05$).

Among these genes, limitrin, also known as Dual Immunoglobulin domain Containing Cell Adhesion Molecule (DICAM), Matrix-remodelling-associated protein 8 (MXRA8) or Adipocyte-specific protein 3 (Asp3), showed a 12-fold increased expression in 4T1Br4 cells compared to 4T1 cells (Dr Normand Pouliot, unpublished observations). Few studies have documented the expression and function of limitrin in normal tissues and to our knowledge, there is currently no reports on its role in cancer. Limitrin belongs to the immunoglobulin superfamily (IgSF), a group of molecules involved in cell adhesion (Jung et al., 2008). Many organs including brain, spleen, lung, colon, kidney, heart, small intestine, liver and stomach and cell lines (monocytes, epithelial cells and endothelial cells) express limitrin (Jung et al., 2008). In the normal brain, limitrin is localised at the end-feet of astrocytes of the BBB and was proposed to be involved in the formation and maintenance of the BBB integrity (Yonezawa et al., 2003). Limitrin shares structural homology with junctional adhesion molecule A (JAM-A), a protein also belonging to IgSF that is located in tight junctions (McSherry et al., 2011) and involved in the transmigration of leucocytes across the endothelium (Yonezawa et al., 2003). Interestingly, JAM-A has also been linked to poor prognosis in breast cancer patients (McSherry et al., 2009, Murakami et al., 2011). In addition, the expression of the JAM family proteins is increased in brain metastases compared to primary tumours in TNBC patients (Choi et al., 2013).

The structural similarity between limitrin and JAM-A led us to propose that limitrin may facilitate the adhesion and/or transmigration of tumour cells across the BBB and that its expression may have prognostic significance in breast cancer patients. Accordingly, Chapter 4 focuses on investigating the role of limitrin as a prognostic marker to identify

breast cancer patients at risk of developing brain metastasis. The contribution of limitrin to breast cancer metastasis to the brain is also examined in functional assays *in vitro* and in spontaneous and experimental metastasis assays in mice.

4.2 Results

4.2.1 *Prognostic significance of limitrin expression in brain-metastatic breast cancer*

4.2.1.1 **Analysis of the prognostic potential of limitrin in different subtypes of breast cancer**

To investigate the association between limitrin expression and disease outcome in various molecular subtypes of breast cancer, we used BreastMark prognostic analysis tool. BreastMark integrates gene expression and survival data from 26 datasets on 12 different microarray platforms allowing examination of the prognostic potential of approximately 17,000 genes in breast cancer (Madden et al., 2013). BreastMark analysis revealed a significant association between high expression of limitrin mRNA and poor clinical outcome in basal-like tumours but not in the other subtypes of breast cancer, i.e., luminal A, luminal B and HER2 positive tumours (Figure 4.1). Patients with basal-like breast tumour expressing high levels of limitrin are at higher risk of developing metastasis (distant disease free survival (DDFS)) and have a reduced overall survival (OS) time compared to those with low limitrin levels. Therefore, limitrin has the potential to be a prognostic marker of metastasis in basal-like breast cancers. In addition, it is important to note that these results are consistent with the basal-like/TNBC molecular subtype of the 4T1Br4 brain-metastatic mouse model described in Chapter 3.

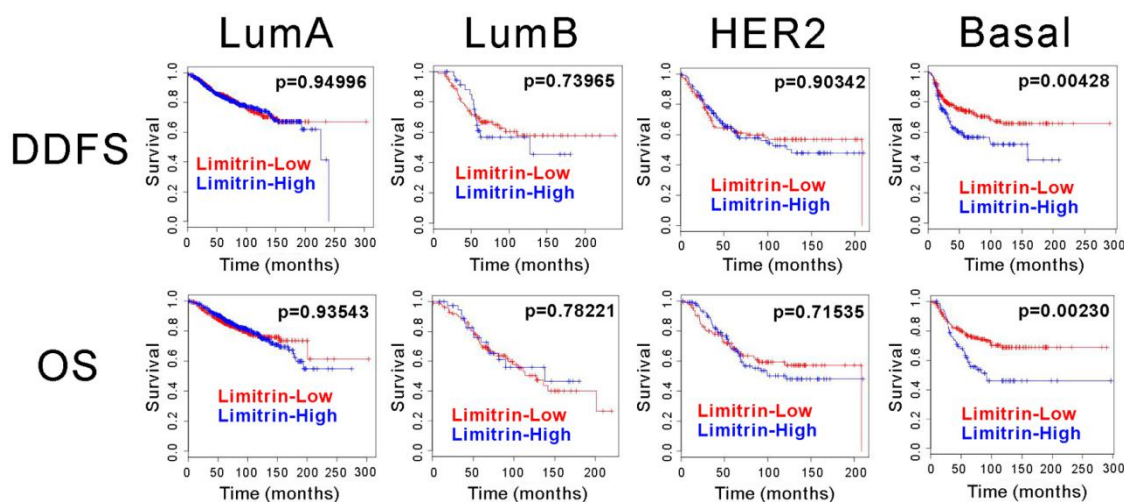


Figure 4.1 Association between limitrin expression in different subtypes of breast cancer and clinical outcomes

High expression of limitrin is associated with reduced distant disease free survival and overall survival in basal-like breast tumours. Data were analysed using BreastMark algorithm (<http://glados.ucd.ie/BreastMark/>). DDFS, distant disease free survival; OS, overall survival; LumA, luminal A; LumB, luminal B; Basal, basal-like breast tumour. $p < 0.05$ is considered significant.

4.2.1.2 Limitrin expression in various breast cancer cell lines and tumours

To further determine the prognostic potential of limitrin and, in particular, its association with brain metastasis, we examined limitrin mRNA and protein expression levels in a panel of mouse and human breast cancer cell lines of varying metastatic potential. The level of limitrin mRNA expression was measured by qRT-PCR and is shown in Figure 4.2. Consistent with our hypothesis, mouse non-metastatic 67NR cells (Aslakson and Miller, 1992) did not express detectable levels of limitrin mRNA. Intermediate levels were found in the weakly lung-metastatic 66cl4 cell line (Miller et al., 1986) and the lung- and bone-metastatic 4T1BM2 cell line (Kusuma et al., 2012). The highly lymph node-, lung- and bone-metastatic (but not brain-metastatic) 4T1.2 mouse cell line (Lelekakis et al., 1999) did not express detectable levels of limitrin. Importantly, the brain-metastatic 4T1Br4 variant expressed significantly higher levels of limitrin mRNA in both culture and whole tumours. Expression of limitrin in human cell lines was consistent with those observed in mouse cell lines. The human non-metastatic MCF-7 cell line (Moss et al., 1999) did not express detectable levels of limitrin mRNA. The lung-metastatic MDA-MB-231 cell line (Bos et al., 2009) expressed low levels of limitrin

mRNA. The highest levels of limitrin mRNA were detected in the brain-seeking MDA-MB-231Br variant of human MDA-MB-231 cells (Bos et al., 2009).

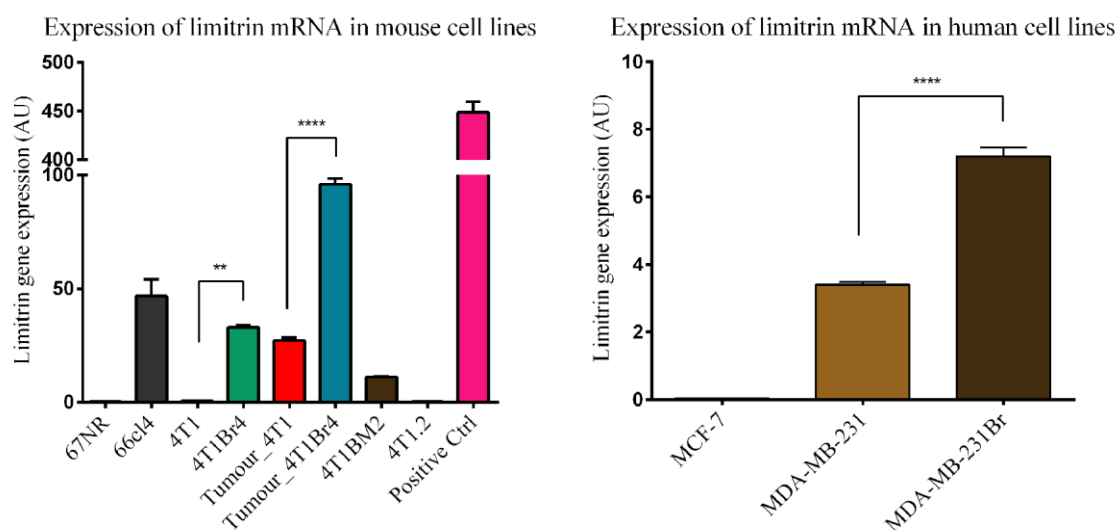


Figure 4.2 Limitrin mRNA expression in mouse and human breast cancer cell lines and mouse primary tumours

Cells or tissues were homogenised in TRIzol reagent to isolate RNA. RNAs were synthesised into cDNA and limitrin expression was measured using SYBR Green I assay. Limitrin expression was significantly higher in brain metastatic 4T1Br4 cells compared to parental 4T1 cells (in both cultured cells and tumours). Similarly, limitrin mRNA was expressed significantly more in human brain metastatic MDA-MB-231Br cells than parental MDA-MB-231 cells or non-metastatic MCF-7 cells. Mouse brain (pink bar) was used as a positive control since limitrin is abundantly expressed in astrocytes of the BBB. Data show fold-expression relative to housekeeping genes (mouse *RPS27a* or human *RPL37a*) ($n = 3$). It should be noted that the relative expression of mouse and human limitrin mRNA was determined using different housekeeping genes and therefore cannot be directly compared. p -values were calculated using a one-way ANOVA with a Bonferroni post-test; $p < 0.05$ was considered significant. ** $p < 0.01$, **** $p < 0.001$.

Next, we confirmed these observations at the protein level by western blotting. Since no commercial anti-limitrin antibodies were available, we generated anti-limitrin antibodies in-house in collaboration with Dr Bruce Kemp (St Vincent's Institute, Melbourne). Rabbit polyclonal limitrin antibodies were raised against a C-terminal

peptide sequence of human limitrin (ELAHSPLPAKYIDLKGFRENCK) as described by Yonezawa and colleagues (Yonezawa et al., 2003). The protein sequence of limitrin is highly conserved (78%) between human and mouse (Yonezawa et al., 2003, Jung et al., 2008). Table 4-1 and Table 4-2 show the protein coding sequences of mouse and human limitrin, respectively. A search for Express Sequence Tag (EST) transcript data in Ensemble.org revealed 8 mouse limitrin transcripts but only 2 protein coding sequences. The estimated molecular weight of these 2 forms of mouse limitrin are 49 kDa and 35 kDa. However, only the 49 kDa form possesses the sequence similar to the peptide sequence used for rabbit immunisation.

Table 4-1. Mouse limitrin protein coding sequences.

Two protein coding sequences in mouse
<p>ENSMUST0000030947: 442aa (estimated molecular weight: 49 kDa)</p> <p>MELLSRVLLWKLKLLQSSAVLSSGPSGTAAASSSLVSESVVSLAAGTQAVLRCQSPR MVWTQDRLHQRVHVWDLSSGGPGSQRRLVDMYSAGEQRVYEPDRDRLLLSF SAFHDGNFLLIRVDRGDEGVYTCNLHHHYCHLDESLAVRLEVTEDPLLSRAYWDGE KEVLVVAHGAPALMTCINRAHVWTDRLHLEEAQQVHVWDRQLPGVSHDRADRLLDLY ASGERRAYGPPFLRDRVSVNTNAFARGDFSLRIDELEERADEGIYSCHLHHHYCGLHE RRVFHLQVTEPAFEPPARASPGNGSGHSSAPSDPTLRGHSIINVIVPEDHTHFFQQ LGYVLATLLLFIILLITVVLATRYRHSGGCKTSDKKAGKSKGKDVNMVEFAVATRDQAP YRTEDIQLDYKNNILKERAELAHSPLPAKDVDLDKEFRKEYCK</p>
<p>ENSMUST00000141883: 321aa (estimated molecular weight: 35 kDa)</p> <p>MELLSRVLLWKLKLLQSSAVLSSGTAAASSSLVSESVVSLAAGTQAVLRCQSPRMVW TQDRLHQRVHVWDLSSGGPGSQRRLVDMYSAGEQRVYEPDRDRLLLSFSAFH DGNFLLIRAVDRGDEGVYTCNLHHHYCHLDESLAVRLEVTEDPLLSRAYWDGEKEV LVVAHGAPALMTCINRAHVWTDRLHLEEAQQVHVWDRQLPGVSHDRADRLLDLYASG ERRAYGPPFLRDRVSVNTNAFARGDFSLRIDELEERADEGIYSCHLHHHYCGLHERRV FHLQVTEPAFEPPARASPGNGSGHSSAPP</p>

RGD, potential integrin-binding site; **ELAHSPLPAKYIDLKGFRENCK**, immunogenic peptide used for the generation of anti-limitrin antibodies.

Regarding the human form of the protein, in EST data, we found limitrin has 10 transcripts but only 4 protein coding sequences with estimated molecular weights of 49 kDa, 48 kDa, 49.5 kDa and 37.5 kDa. All 4 proteins contain the peptide sequence used for rabbit immunisation and thus, we expect to detect these 4 forms by western blotting.

Table 4-2. Human limitrin protein coding sequences.**Four protein coding sequences in human****ENST00000309212: 442aa (estimated molecular weight: 49 kDa)**

MALPSRILLWKLVLLQSSAVLLHSGSSVPAAGSSVSESAVSWEAGARAVLRCQSP
 RMVWTQDRLHQRVLRVLDLHDLRGPGGGPARRLDLYSAGEQRVYEARDRGRLELSA
 SAFDDGNFSLIRAVEETDAGLYTCNLHHHYCHLYESLAVRLEVTDGPPATPAYWDG
 EKEVLAVARGAPALLTCVNRGHVWTDHRHVEEAQQVVHWDRQPPGVPHDRADRLD
 LYASGERRAYGPLFLRDRVAVGADAFE**RGD**FSLRIEPLVADEGTYSCHLHHHYCGL
 HERRVFHLTVAEPHAEPPIRGSPGNGSSHSGAPGPDPTLARGHNVINVIVPESRAHF
 FQQLGYVLATLLLFIILLVTVLLAARRRRGGYEYSDQKSGKSKGKDVNLAEFVAAGD
 QMLYRSEDIQLDYKNNILKERA**ELAHSPLPAKYIDLKGFRENCK**

ENST00000477278: 433aa (estimated molecular weight: 48 kDa)

MIRCAATGSVAVLLHSGSSVPAAGSSVSESAVSWEAGARAVLRCQSPRMVWTQDR
 LHQRVLRVLDLHDLRGPGGGPARRLDLYSAGEQRVYEARDRGRLELSASAFDDGNFS
 LLIRAVEETDAGLYTCNLHHHYCHLYESLAVRLEVTDGPPATPAYWDGEEKEVLAVARG
 APALLTCVNRGHVWTDHRHVEEAQQVVHWDRQPPGVPHDRADRLDLYASGERRAY
 GPLFLRDRVAVGADAFE**RGD**FSLRIEPLVADEGTYSCHLHHHYCGLHERRVFHLTV
 AEPHAEPPIRGSPGNGSSHSGAPGPDPTLARGHNVINVIVPESRAHFFQQLGYVLAT
 LLLFIILLVTVLLAARRRRGGYEYSDQKSGKSKGKDVNLAEFVAAGDQMLYRSEDIQ
 LDYKNNILKERA**ELAHSPLPAKYIDLKGFRENCK**

ENST00000342753: 341aa (estimated molecular weight: 37.5 kDa)

MIRCAATGSVAVLLHSGSSVPAAGSSVSESAVSWEAGARAVLRCQSPRMVWTQDR
 LHQRVLRVLDLHDLRGPGGGPARRLDLYSAGEQRVYEARDRGRLELSASAFDDGNFS
 LLIRAVEETDAGLYTCNLHHHYCHLYESLAVRLEVTDGPPATPAYWDGEEKEVLAVARG
 APALLTCVNRGHVWTDHRHVEEAQQVVHWDRQPPGVPHDRADRLDLYASGERRAY
 GPLFLRDRVAVGADAFE**RGD**FSLRIEPLVADEGTYSCHLHHHYCGLHERRVFHLTV
 AEPHAEPPIRGSPGNGSSHSGAPGPDPTLARGHNVINVIVPESRAHFFQQLGYVLAT
 LLLFIILLVTVLLAARRRRGGYEYSDQKSGKSKGKDVNLAEFVAAGDQMLYRSEDIQ
 LDYKNNILKERA**ELAHSPLPAKYIDLKGFRENCK**

ENST0000445648: 450aa (estimated molecular weight: 49.5 kDa)

MALPSRILLWKLVLLQSSAVLLHSGSSVPAAGSSVSESAVSWEAGARAVLRCQSP
 RMVWTQDRLHQRVLRVLDLHDLRGPGGGPARRLDLYSAGEQRVYEARDRGRLELSA

SAFDDGNFSLIRAVEETDAGLYTCNLHHHYCHLYESLAVRLEVTDGPPATPAYWDG
 EKEVLAVARGAPALLTCVNRGHVWTRHVEEAQQVVHWDRQPPGVPHDRADRLLD
 LYASGERRAYGPLFLRDRVAVGADAFERGFSLRIEPLVADEGTYSCHLHHHYCGL
 HERRVFHLTVAEPHAEPPIRGSPGNGSSSHSGAPGPDPTLARGHNVINVIVPESRAHF
 FQQLGYVLATLLLFIILLVTVLLAARRRRGGYEYSDQKSGKSKGKDVNLAEFAVAAGD
 QMLYRSEDIQLASSPPTYDYKNNILKERA**ELAHSP**PAKYIDLDK**DPSGLCPLGA**

RGD, potential integrin-binding site; **ELAHSP**PAKYIDLDK**GFRKENCK**, immunogenic peptide used for the generation of anti-limitrin antibodies.

The reactivity of limitrin antisera against the immunization peptide was confirmed by standard ELISA and reactive antibodies purified by affinity chromatography on protein G sepharose column. Four purified limitrin antibodies generated (R161, R184, R5553 and R6921) were further validated by western blotting. We found that R161 at 0.5 µg/ml and R6921 at 1 µg/ml from the 3rd bleed were best for detecting limitrin in mouse and human breast cancer cell lines, respectively (Figure 4.3). In mouse breast cancer cell lines, limitrin was not detected in 67NR cells but limitrin was strongly detected as a doublet in 4T1Br4 cells (Figure 4.3A). In human breast cancer cell lines, 2 bands corresponding to the estimated molecular weights of limitrin, i.e. 49 kDa and 37.5 kDa were detected in MDA-MB-231Br cells whereas only one band at 49 kDa with a slightly weaker signal was observed in MCF-7 cells (Figure 4.3B).

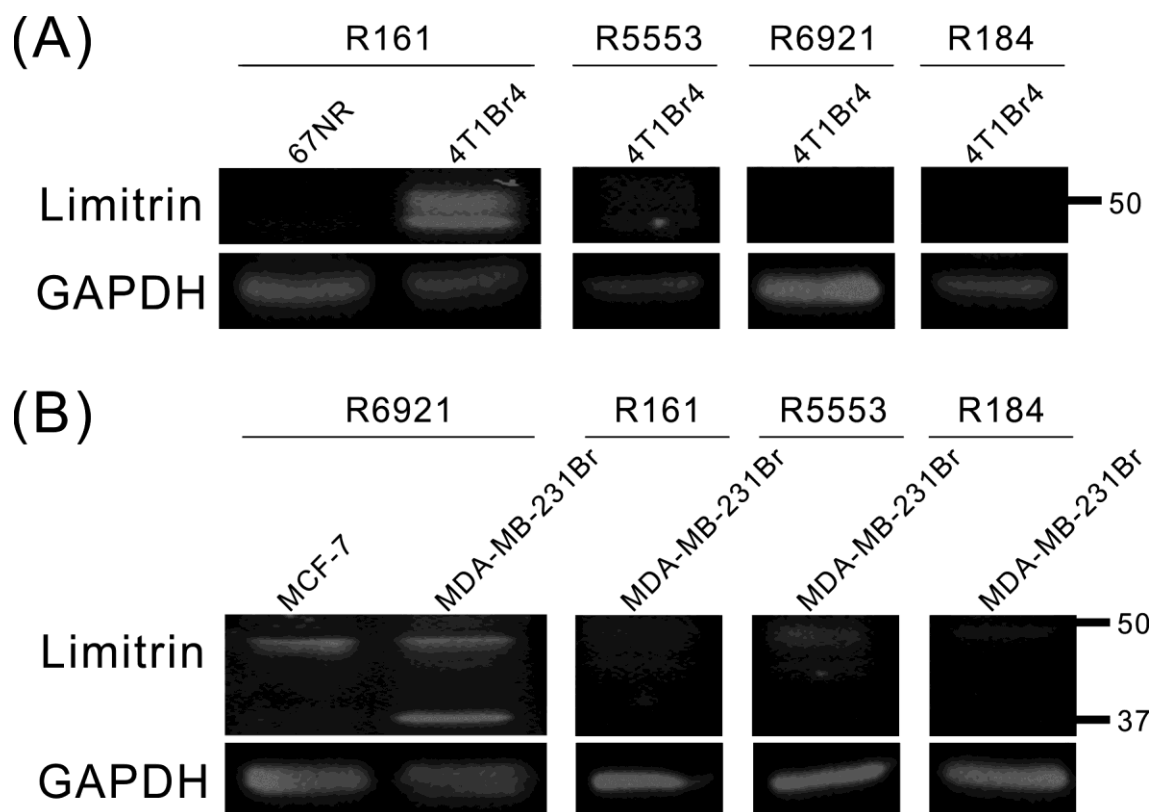


Figure 4.3 Anti-limitrin antibodies validation by western blotting in mouse and human breast cancer cell lines

Forty μg of protein was loaded into each lane. Immunoblot with R161, R184, R5553 and R6921 (0.5 $\mu\text{g}/\text{ml}$) in mouse cell lines (A). Immunoblot with R161, R184, R5553 and R6921 (1 $\mu\text{g}/\text{ml}$) in human cell lines (B). Based on limitrin mRNA expression determined in Figure 4.2, 67NR and MCF-7 cell lines were used as negative controls for mouse and human cell lines, respectively.

The levels of limitrin was further analysed with the selected anti-limitrin antibodies in the panel of mouse and human cell lines previously used for limitrin mRNA expression. The levels of limitrin in mouse cell lines corresponded well to the mRNA data shown in Figure 4.2. Non-metastatic 67NR and highly metastatic but non-brain-seeking 4T1.2 cells did not express limitrin protein (Figure 4.4). Brain-metastatic 4T1Br4 cells showed the highest level of limitrin of all mouse cell lines tested. On the blots (Figure 4.4, left panel), the band corresponding to limitrin appeared as a doublet that was differentially expressed in the different cell lines, most likely representing posttranslational modification. This is supported by the study of Jung and colleagues who demonstrated that limitrin has 8 glycosylation sites (Jung et al., 2008). Specifically, the authors detected a single limitrin mRNA transcript by northern blotting but two protein bands by

western blotting suggesting that limitrin could undergo active posttranslational processing (Jung et al., 2008).

Intriguingly, 66cl4 cells that are weakly metastatic to the lung but not to the brain from the mammary gland expressed intermediate levels of limitrin protein. The biological significance of this observation is currently unclear and is discussed in the Discussion section.

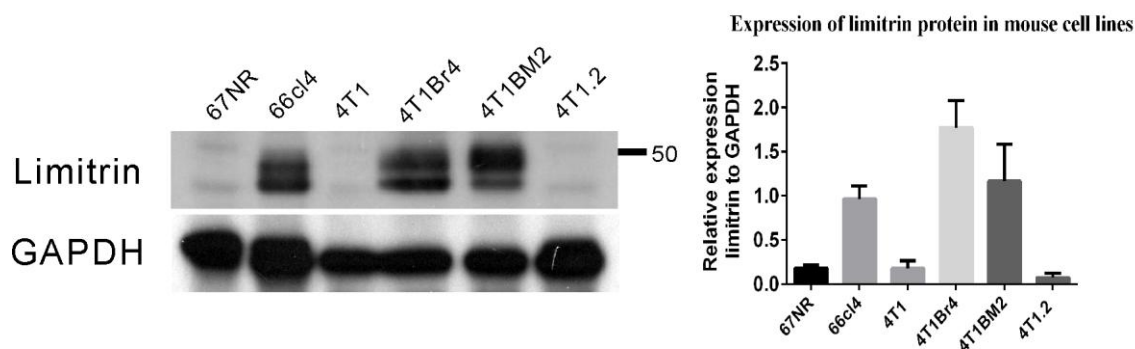


Figure 4.4 Limitrin expression by western blotting in mouse mammary cancer cell lines

Limitrin expression was significantly higher in mouse brain metastatic 4T1Br4 cells than in non-brain-seeking mouse breast cancer cell lines. Forty μg of protein were loaded into each lane. Left panel, representative immunoblot of limitrin ($n=3$) with R161 (0.5 $\mu\text{g}/\text{ml}$) from the 3rd bleed. Right panel, quantitation of limitrin levels relative to GAPDH by densitometry analysis of the bands on immunoblots. Results are expressed as mean \pm SD of 3 experiments.

In agreement with mRNA expression in human breast cancer cell lines, western blotting analyses confirmed that limitrin expression was higher in human brain-metastatic MDA-MB-231Br cells compared to non-brain metastatic MCF-7 and MDA-MB-231 cells (Figure 4.5). In MDA-MB-231Br cells, 2 bands were detected, one below the 50 kDa molecular marker and one near the 37 kDa marker (Figure 4.5, left panel). The upper band is likely to correspond to the 3 variants of limitrin that have a predicted molecular weight of 48, 49 and 49.5 kDa and the lower band to the 37.5 kDa form of limitrin. Similar to MDA-MB-231Br cells, MDA-MB-231 cells expressed both variants of limitrin. However, while the intensity for the lower molecular weight was similar in both cell lines, the signal for the higher molecular weight form was clearly stronger in MDA-

MB-231Br cells. The non-metastatic MCF-7 cells only weakly expressed the higher molecular form of limitrin.

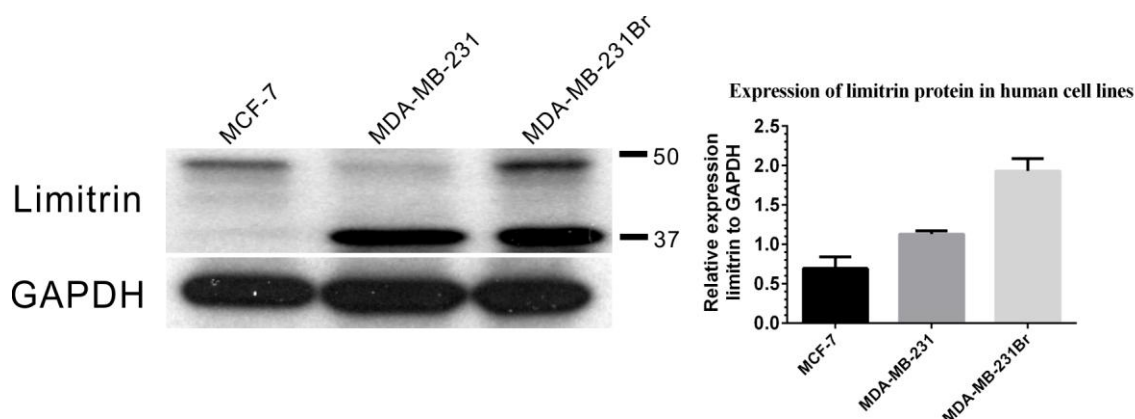


Figure 4.5 Limitrin expression by western blotting in human breast cancer cell lines

Limitrin expression was significantly higher in human brain metastatic MDA-MB-231Br cells than in other human breast cancer cell lines. Forty μg of total protein were loaded into each lane. Left panel, representative immunoblot of limitrin ($n=3$) with R6921 (1 $\mu\text{g}/\text{ml}$) from the 3rd bleed. Right panel, quantitation of limitrin levels (the signal from both bands was measured) relative to GAPDH by densitometry analysis of the bands on immunoblots. Results are expressed as mean \pm SD of 3 experiments.

4.2.1.3 Subcellular localisation of limitrin

Jung and colleagues reported previously that limitrin is expressed in the plasma membrane, cytoplasm and nucleus of normal epithelial cells (Jung et al., 2008). To gain further understanding of the subcellular localisation of limitrin in breast cancer cells, limitrin expression in the cytosol, membrane and nucleus of mouse cell lines was investigated. As shown in Figure 4.6, limitrin was expressed in all cellular fractions of both 66cl4 and 4T1Br4 cells. A doublet was detected in the cytoplasm and in the membrane of the cells. As mentioned in section 4.2.1.2, this doublet may correspond to different levels of glycosylation of limitrin. In the cytoplasm, both forms were present in equal amount. Interestingly, the lower molecular form of limitrin was most abundant in the membrane fraction of 66cl4 cells whereas 4T1Br4 expressed predominantly the higher molecular weight form. The higher molecular weight form was the main form

detected in the nucleus of both cell lines. These observations indicate that the relative abundance and the subcellular localisation of limitrin forms vary between cell lines.

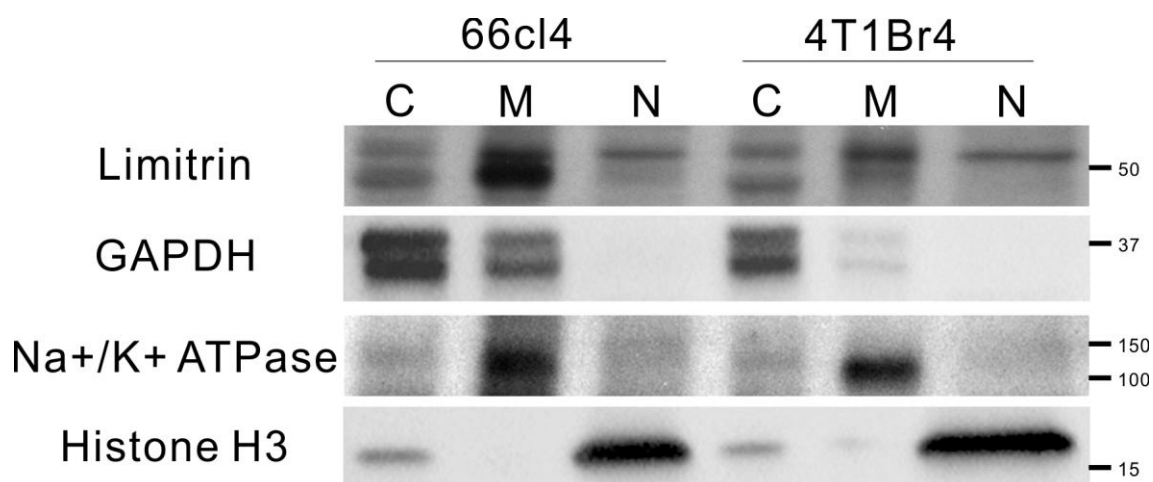


Figure 4.6 Differential subcellular localisation of limitrin in 66cl4 and 4T1Br4 cells

Limitrin is expressed in the cytosol, membrane and nuclear fractions (not including cytoskeletal proteins). Interestingly, 66cl4 cells showed more of the lower molecular weight form of limitrin and 4T1Br4 cells showed more of the higher molecular weight form of limitrin in the membrane. Forty μg of protein were loaded into each lane. Qproteome Cell Compartment Kit was used for this assay. C, M and N represent cytosol, membrane and nucleus, respectively. Limitrin (R161 (0.5 $\mu\text{g}/\text{ml}$) from the 3rd bleed), GAPDH, Na⁺/K⁺ ATPase and Histone H3 antibodies were used as markers for cytosol, membrane and nucleus, respectively.

4.2.1.4 Detection of limitrin by immunohistochemistry (IHC)

4.2.1.4.1 Optimisation of IHC protocol for anti-limitrin antibodies

In order to determine if limitrin is a prognostic marker for brain metastasis of breast cancer, it was essential to optimise the IHC protocol for limitrin antibodies. 4T1Br4 primary tumours were fixed either with 10% neutral buffered formalin (NBF) overnight at 4°C or with zinc-Tris buffer (2.8 mM calcium acetate, 22 mM zinc-acetate, 36.7 mM zinc chloride, and 0.1 M Tris-HCl, pH 7.4) for 48 hr at 4°C and processed for paraffin embedding. Sections (4 μm) were rehydrated, equilibrated in antigen retrieval buffer consisting of either citrate buffer (10 mM, pH 6.0) with pressure cooker at 125°C for 3 min and 90°C for 10 sec or trypsin buffer (1 mg/ml, pH 7.8) for 20 min at 37°C (Table 4-

3). Briefly, sections were blocked in 3% bovine serum albumin (BSA) for 30 min at room temperature (RT) and incubated with antisera against limitrin used at 5 µg/ml (R161 from the 3rd bleed that detected limitrin in western blots) or control poly rabbit antiserum (at 5 µg/ml) overnight at 4°C under humidified atmosphere. The sections were incubated with an appropriate biotin-conjugated secondary antibody for 1 hr at RT and a 3,3' Diaminobenzidine (DAB) substrate kit was used to develop the signal.

Table 4-3 IHC protocol optimisation for limitrin antibodies.

Tissue	Fixation	Antigen retrieval	Staining results
4T1Br4 primary tumour	10% NBF	Non	Good
		Trypsin 20 min	Non-specific
		Citrate buffer	Very good
	Zinc-Tris	Non	Non-specific
		Trypsin 5 min	Good
		Citrate buffer	Non-specific

10% NBF, 10% neutral buffered formalin.

The best signal was obtained on formalin-fixed paraffin embedded tissues (FFPE) with heat treatment in citrate buffer as antigen retrieval (Table 4-3). According to the Human Protein Atlas (www.proteinatlas.org), the normal mammary gland (as well as brain, kidney, pancreas and testis) expresses high levels of limitrin protein. Thus, for comparison, staining intensity in 4T1Br4 tumours and normal mammary gland was measured with the same protocol. As expected, limitrin was detected in epithelial cells of normal mammary glands and in 4T1Br4 tumours (Figure 4.7D, E and F). The intensity of the signal in the peripheral region corresponding to the highly proliferative and vascularised region of the tumours was higher than the central region (Figure 4.7E and F).

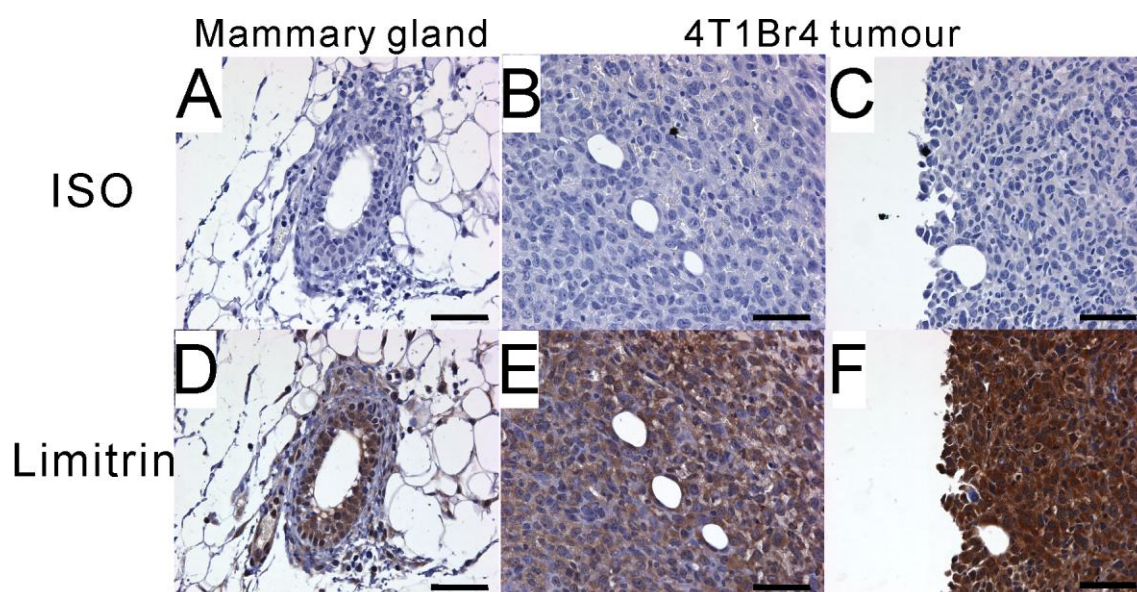


Figure 4.7 Detection of limitrin in normal mammary glands and in 4T1Br4 primary tumours by IHC

Tissue were fixed in 10% neutral buffered formalin (NBF) and embedded in paraffin. Antigen retrieval was performed by heat treatment with a pressure cooker in citrate buffer (pH 6.0). Normal mammary glands are shown in A and D. 4T1Br4 primary tumours are shown in B, C, E and F. Limitrin was strongly expressed in epithelial cells of normal mammary glands, consistent with the reported high expression in glandular structures of the human breast (<http://www.proteinatlas.org/ENSG00000162576-MXRA8/tissue/breast>) (D) and in 4T1Br4 tumours, especially in the peripheral regions (F). No staining was detected using a control isotype-matched antibody (ISO) (A-C). Nuclei were counterstained with hematoxylin (blue). Scale bar = 50 μ m.

Further optimisation was achieved by titrating the anti-limitrin antibodies on mouse (Figure 4.8) and xenograft tissues (Figure 4.9). The anti-limitrin antibodies, R161, R184, R5553 and R6921 were used at 0.5, 1 and 5 μ g/ml. Lower concentrations of antibodies (0.5 and 1 μ g/ml) were not sufficient to detect limitrin on 4T1Br4 and MDA-MB-231Br primary tissues. All anti-limitrin antibodies worked only at 5 μ g/ml concentration on both mouse and human tissues. Although all 4 anti-limitrin antibodies detected limitrin in 4T1Br4 primary tumours, R184, R5553 and R6921 (Figure 4.8F, 8G and 8H, respectively) also showed non-specific binding. Therefore, the R161 antibody (Figure 4.8E) at 5 μ g/ml was chosen for staining of limitrin on mouse tissues in subsequent experiments.

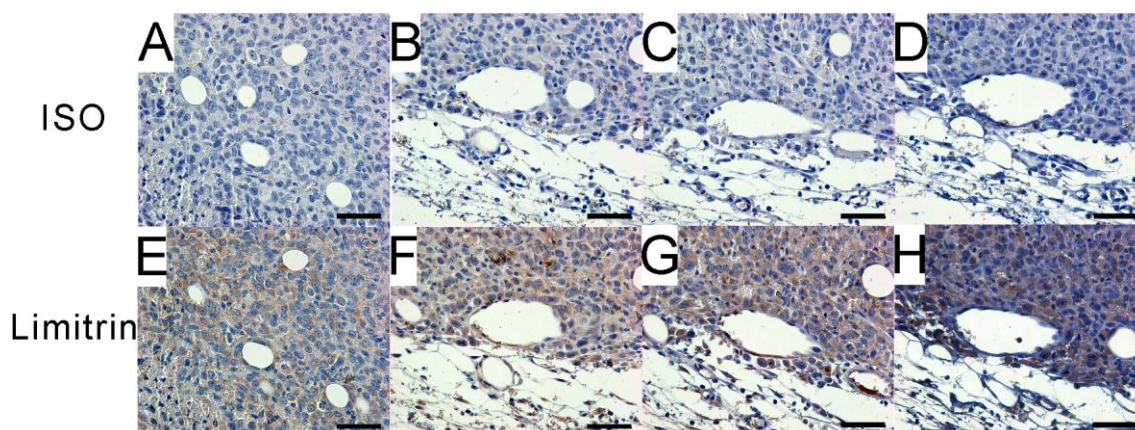


Figure 4.8 Limitrin IHC staining in 4T1Br4 primary tumour tissues with the four generated antibodies from 3rd bleed

Tissues were fixed in 10% neutral buffered formalin (NBF) and embedded in paraffin. Antigen retrieval was performed by heat treatment with a pressure cooker in citrate buffer (pH 6.0). Four anti-limitrin antibodies (R161 (E), R184 (F), R5553 (G) and R6921 (H) from the 3rd bleed) were used at 5 μ g/ml concentration and incubated overnight on 4T1Br4 primary tumour tissues. No staining was detected using a control isotype-matched antibody (ISO) (A-D). Nuclei were counterstained with hematoxylin (blue). Scale bar = 50 μ m.

All four antibodies also detected limitrin in FFPE MDA-MB-231Br xenograft tissues but R184, R5553 (Figure 4.9F and 9G) showed non-specific binding. Interestingly, R6921 (Figure 4.9H) showed stronger and more specific limitrin staining than R161 (Figure 4.9E) on human tissues. In addition, R6921 clearly detected limitrin in immunoblot (Figure 4.3). Therefore, the R6921 antibody at 5 μ g/ml was used to visualise limitrin in human tissues hereafter.

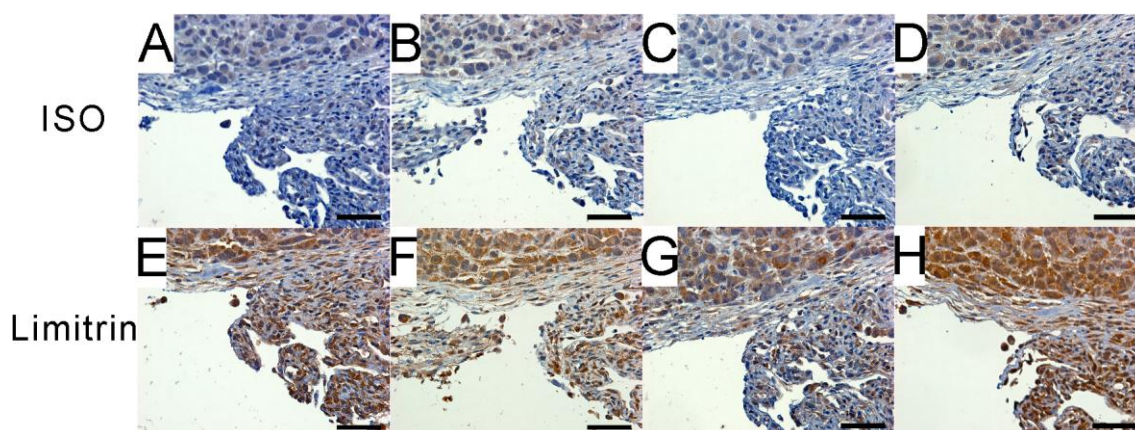


Figure 4.9 Limitrin IHC staining in MDA-MB-231Br xenograft tissues with the four generated antibodies from 3rd bleed

Tissues were fixed in 10% neutral buffered formalin (NBF) and embedded in paraffin. Antigen retrieval was performed by heat treatment with a pressure cooker in citrate buffer (pH 6.0). Four limitrin antibodies (R161 (E), R184 (F), R5553 (G) and R6921 (H) from the 3rd bleed) were used at 5 µg/ml concentration and incubated overnight on MDA-MB-231Br xenograft tissues. No staining was detected using a control isotype-matched antibody (ISO) (A-D). Nuclei were counterstained with hematoxylin (blue). Scale bar = 50 µm.

4.2.1.4.2 Limitrin expression by IHC in mouse and xenograft tissues

To confirm the reactivity of anti-limitrin antibodies against mouse and human tumours using the optimised protocol described above, a panel of mouse and human breast cancer cells was used to generate primary tumours and FFPE tissue sections were screened for limitrin expression (Figure 4.10 and 4.11). Consistent with mRNA and protein levels, only weak diffuse staining was observed in non-metastatic 67NR and highly metastatic but non-brain-seeking 4T1.2 tumours. The cytoplasm of the lung- and bone-metastatic 4T1BM2 stained moderately. Positive nuclear staining was observed in weakly metastatic 66cl4 cells and to a lesser extent in parental 4T1 tumours. A stronger limitrin signal was visualised in brain-metastatic 4T1Br4 tumours than in other mouse primary tumours. Specifically, limitrin staining was particularly high in the cytoplasm/membrane of 4T1Br4 tumours (Figure 4.10) compared to other tumour tissues.

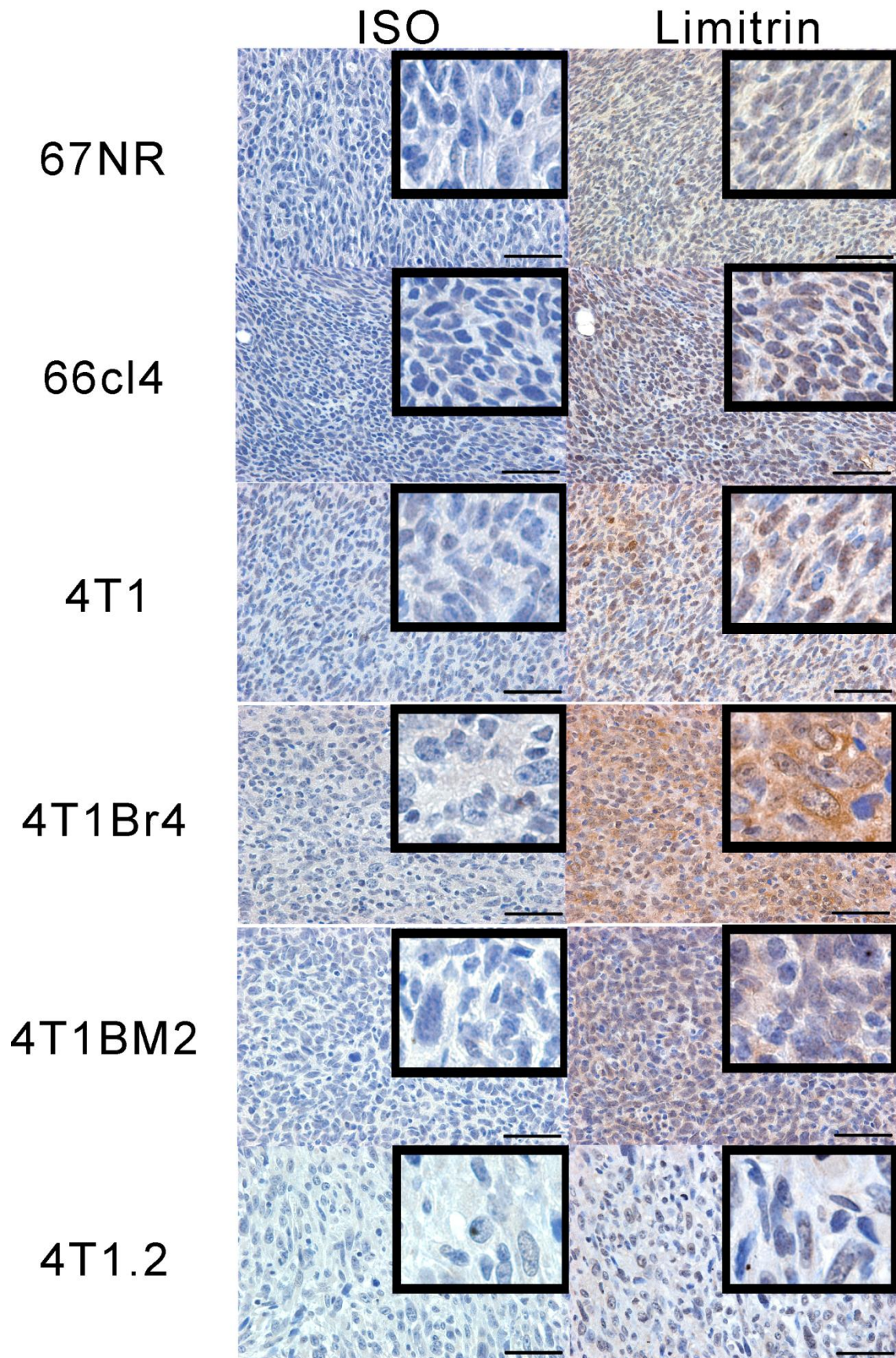


Figure 4.10 Immunohistochemical detection of limitrin in formalin-fixed paraffin embedded mouse tumours

Tissues were fixed in 10% neutral buffered formalin (NBF) and embedded in paraffin. Antigen retrieval was performed by heat treatment with a pressure cooker in citrate buffer (pH 6.0). Brain metastatic 4T1Br4 tumours showed the highest level of limitrin expression (brown staining) and notably in the cell membrane. None of the tumours stained positively using a control isotype-matched antibody (ISO). Nuclei were counterstained with hematoxylin (blue). Scale bar = 50 μ m. High magnification images are shown in insets.

Since archival material from patients is usually preserved as FFPE tissues, having antibodies that recognise limitrin in FFPE human tissues is essential for translation in the clinic. Hence, the same IHC protocol as for mouse tissues was used to detect limitrin in FFPE human xenograft tumours. As shown in Figure 4.11, non-metastatic MCF-7 tumours only expressed low levels of limitrin in the cytoplasm. Moderate expression of limitrin was detected in the cytoplasm of parental MDA-MB-231 tumours whereas the highest level of limitrin was observed in brain metastatic MDA-MB-231Br tumours. Similar to mouse 4T1Br4 tumours, limitrin localised primarily at the cell surface and cytoplasm in MDA-MB-231Br tumours.

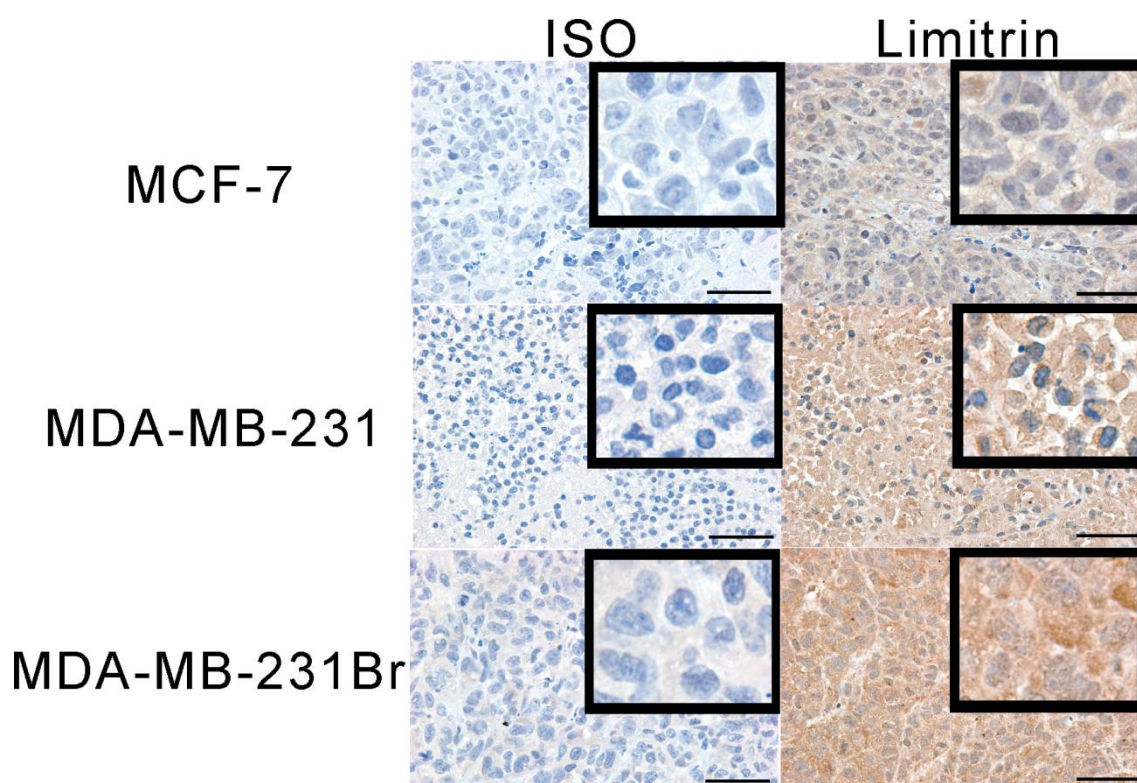


Figure 4.11 Immunohistochemical detection of limitrin in formalin-fixed paraffin embedded human xenograft tumours

Tissues were fixed in 10% neutral buffered formalin (NBF) and embedded in paraffin. Antigen retrieval was performed by heat treatment with a pressure cooker in citrate buffer (pH 6.0). Limitrin was strongly expressed in human brain metastatic MDA-MB-231Br tissues, especially in membranes (brown staining). Weaker staining of limitrin was detected in the cytoplasm of non-metastatic MCF-7 and parental MDA-MB-231 tumours. None of the tumours stained positively using a control isotype-matched antibody (ISO). Nuclei were counterstained with hematoxylin (blue). Scale bar = 50 μ m. High images are shown in insets.

Taken together, the data above demonstrate consistent results between limitrin mRNA and protein levels in both mouse and human breast cancer cell lines of varying metastatic potential. Brain metastatic 4T1Br4 and MDA-MB-231Br cell lines and tumours showed the highest levels of limitrin mRNA and protein. Moreover, consistent with its potential role in migration across the BBB, limitrin expression is particularly strong in the plasma membrane of both mouse and human brain metastatic tumours.

4.2.1.4.3 Prognostic marker analysis of limitrin in patient tissues

In Protein Atlas, limitrin expression is reported to be weak or negative in most breast cancer patient samples (high, 2; medium, 2; low, 1; not detected, 7 out of 12). Since we could not find any information on the molecular subtype, patient outcome or metastatic status, these data alone cannot be used to draw conclusions on the prognostic value of limitrin in each molecular subtype of breast cancer.

First, we used a tissue microarray (TMA) of FFPE samples of 33 human breast tumours including 14 luminal A, 5 luminal B, 3 HER2 positive and 11 TNBC. Limitrin was more strongly expressed in the cytoplasm/membrane of all subtypes of breast tumours compared to the nucleus (Figure 4.12). Notably, stronger limitrin expression was detected in the luminal A and B and TNBC subtypes. However, whether limitrin expression is associated with brain metastasis could not be determined in this small TMA due to the lack of long-term follow-up data on patient outcome and sites of recurrence.

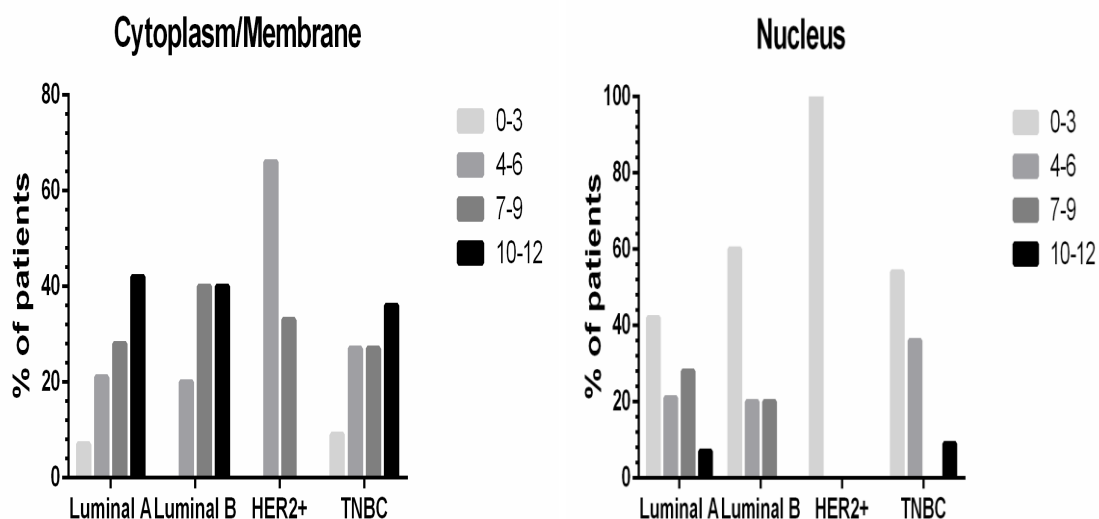


Figure 4.12 Quantification of limitrin IHC staining in a tissue microarray of 33 breast cancer patient samples

Tissues were fixed in 10% neutral buffered formalin (NBF) and embedded in paraffin. Antigen retrieval was performed by heat treatment with a pressure cooker in citrate buffer (pH 6.0). R6921 antibody from the 3rd bleed at 5 µg/ml was used for staining. TMA scoring was blindly performed by an independent pathologist based on intensity of limitrin (scored 0-3) X proportion of cells that stained positive for limitrin (scored 0-4). Limitrin was strongly expressed in cytoplasm/membrane of luminal A and B and TNBC primary tumours. None of the tumours stained positively using a control isotype-matched antibody (ISO). TNBC, triple negative breast cancer.

To more definitely address the prognostic/predictive value of limitrin for identifying patients at risk of developing brain metastases, a larger scale study in collaboration with Prof. Sunil Lakhani (University of Queensland) using human archival tissues is underway. For this analysis, we are using 39 matched pairs of primary breast cancers and brain metastases, 50% of which are TNBC and 25% are HER2 positive. In addition, 22 unmatched brain metastases and 40 TNBC cases with no reported metastases for at least 5 years after diagnosis are available. Limitrin expression will be correlated with the clinical outcome, breast cancer subtype and development of brain metastases in these patients. Due to time limitation, the data will be completed after the submission of this thesis.

4.2.2 Function of limitrin in brain-metastatic breast cancer

4.2.2.1 Function of limitrin *in vitro*

The precise function of limitrin is currently unknown. In Chapter 3 (Figure 3.5), we identified four functional features that may contribute to the enhanced brain metastatic abilities of 4T1Br4 tumours. Specifically, 4T1Br4 cells were more migratory, more adhesive to brain microvascular endothelial (bEnd.3) cells, more invasive in response to brain-derived soluble factors and showed increased abilities for trans-endothelial migration compared to parental 4T1 cells.

To further assess the role of limitrin in these functional responses, we generated transient limitrin knockdown in 4T1Br4 cells using limitrin-specific small inhibitory RNA (esiRNA from Sigma). Treating the cells with limitrin siRNA suppressed the expression of limitrin mRNA by up to 35% and the protein expression by up to 65% in 4T1Br4 cells compared to cells treated with a control non-targeting siRNA (Figure 4.13).

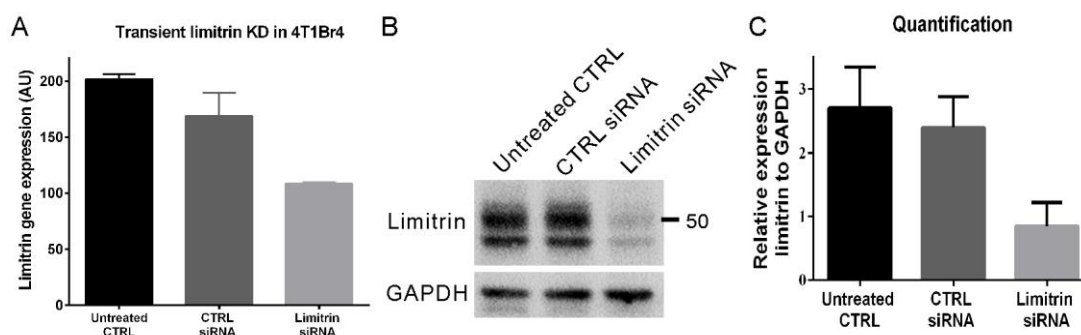


Figure 4.13 Suppression of limitrin expression by siRNA in 4T1Br4 cells

4T1Br4 cells were transfected with 20 nM of limitrin-specific or control non-targeting siRNAs for 24 hr and incubated with fresh medium for another 48 hr. Cells were washed with cold PBS and homogenised in TRIzol reagent to isolate RNA. Limitrin expression was suppressed at the mRNA level by up to 35% compared to control non-targeting siRNA (A). Data show a representative experiment ($n = 2$), mean \pm SD of triplicate wells. Limitrin expression was suppressed at the protein level by up to 65% compared to control non-targeting siRNA (B and C). Expression of limitrin protein was normalised to GAPDH. Results are expressed as mean \pm SD of 3 experiments (C).

As mentioned in the Introduction of Chapter 4, limitrin has a similar structure to JAM-A, a protein involved in the transmigration of leucocytes across the endothelium (Yonezawa et al., 2003). Conceivably, limitrin could have a role in trans-endothelial migration of tumour cells into the brain. To test this hypothesis, we compared the ability of 4T1Br4 cells (CTRL siRNA) to cross a monolayer of endothelial cells with that of 4T1Br4 limitrin knocked down cells (Limitrin siRNA) in a trans-endothelial migration assay. Downregulation of limitrin expression significantly reduced the ability of 4T1Br4 cells to migrate through a monolayer of bEnd.3 brain-derived endothelial cells (approximately 63% inhibition) (Figure 4.14A). In this assay, limitrin expression was downregulated by 55%, confirming the efficient knockdown of the gene (Figure 4.14B and 14C). These findings demonstrate that limitrin is essential for trans-endothelial migration, a response likely to be required for the crossing of the BBB.

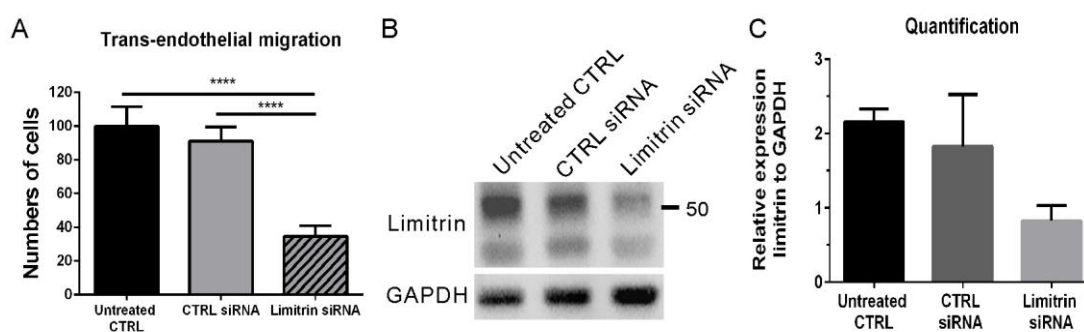


Figure 4.14 Downregulation of limitrin expression inhibits 4T1Br4 trans-endothelial migration

Migration of 4T1Br4 cells through a monolayer of bEnd.3 brain microvascular endothelial cells was measured in Transwell assays after 48 hr (A). Data show a representative experiment ($n = 3$) and are expressed as mean \pm SD of triplicate wells. p -values were calculated using a Student's t -test; $p < 0.05$ was considered significant. **** $p < 0.001$. Efficient knockdown (55%) of limitrin was confirmed by western blotting (B). Expression of limitrin was normalised to GAPDH. Data are expressed as mean \pm SD of triplicate experiments ($n = 3$) (C).

4.2.2.2 Function of limitrin *in vivo*

To assess whether limitrin plays a role in the crossing of the BBB *in vivo*, limitrin expression was stably knocked down by short hairpin RNA (shRNA). Five constructs

were generated and transfected in MDA-MB-231Br cells using lentiviruses that were produced by HEK293T cells. Infected MDA-MB-231Br cells were selected with puromycin over 7 days. Limitrin expression was reduced by up to 95% at the mRNA level and by 65-85% at the protein level with 3 out of 5 constructs (limitrin shRNA #1, #4 and #5) compared to control non-targeting shRNA (Figure 4.15). The most efficient knockdown of limitrin was obtained with limitrin-targeting shRNA construct #1. Cells expressing limitrin-targeting shRNA constructs #4 and #5 showed similar levels of limitrin knockdown. Therefore, limitrin-targeting shRNA #1 and #4 were used for *in vivo* studies.

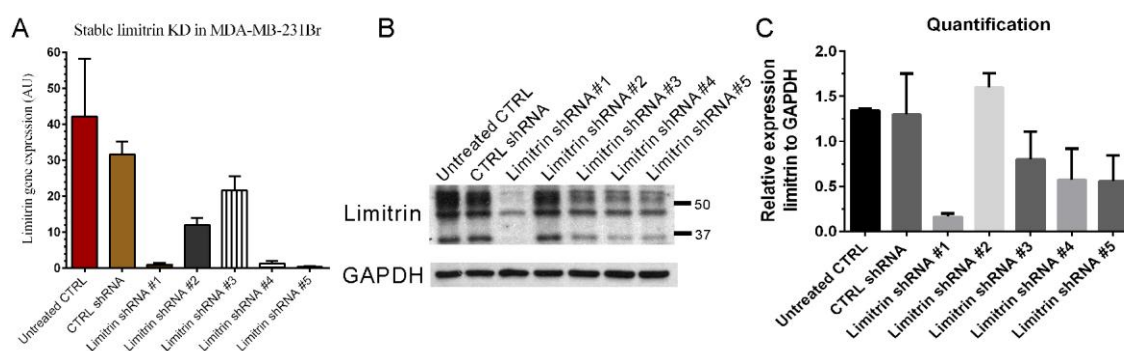


Figure 4.15 Suppression of limitrin expression by shRNA in MDA-MB-231Br cells

Limitrin mRNA expression by qRT-PCR in control cells and cells expressing limitrin shRNA constructs #1 to #5 (A). mRNA level of limitrin decreased by 95% in cells transfected with shRNA constructs #1, #4 and #5 compared to control non-targeting shRNA. Data show fold-expression relative to housekeeping genes (*RPL37a*) and are expressed as mean \pm SD of 3 experiments. Limitrin expression by western blotting with R6921 (1 μ g/ml) from 3rd bleed (B). Limitrin expression (normalised to GAPDH) was reduced by 65-85% with the selected limitrin-targeting shRNA (construct #1, #4 and #5) compared to control non-targeting shRNA (C). Data are expressed as mean \pm SD of triplicate experiments.

The loss of limitrin could affect proliferation of tumour cells and consequently metastatic burden *in vivo*. Thus, before performing *in vivo* experiments, we compared the proliferation rate of cells expressing the control non-targeting shRNA with that of cells expressing limitrin-targeting shRNAs (constructs #1 and #4). As shown in figure 4.16, knockdown of limitrin did not affect proliferation of the cells *in vitro*.

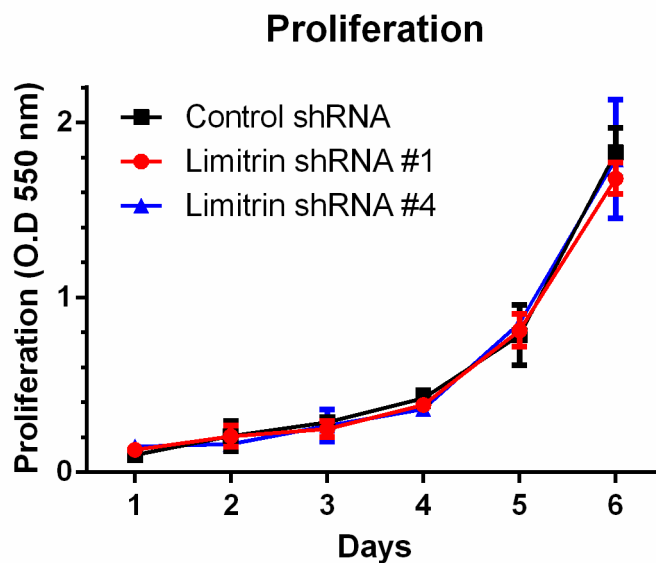


Figure 4.16 Growth curves of MDA-MB-231Br cells transfected with a control non-targeting shRNA and limitrin-targeting shRNA construct #1 or #4

MDA-MB-231Br cells (1×10^3 cells) transfected with control non-targeting shRNA (black) or limitrin-targeting shRNA construct #1 (red) or construct #4 (blue) were seeded in a well of 96-well plate and cultured for 6 days. Data show a representative experiment ($n = 2$) and are expressed as mean \pm SD of six replicate wells per time point.

For the first *in vivo* experiment, MDA-MB-231Br cells (1×10^5 cells per mouse) expressing control non-targeting shRNA or limitrin-targeting shRNA (constructs #1 or #4) were injected into NOD-SCID gamma (NSG) mice (16 mice for control shRNA, 10 mice for limitrin shRNA #1 and 17 mice for limitrin shRNA #4) via the left ventricle of the heart (experimental metastasis model) and the mice harvested when showing signs of distress. Under those conditions, 2 control mice had detectable brain metastases whereas a single mouse from each limitrin shRNA group developed brain metastases (Figure 4.17).

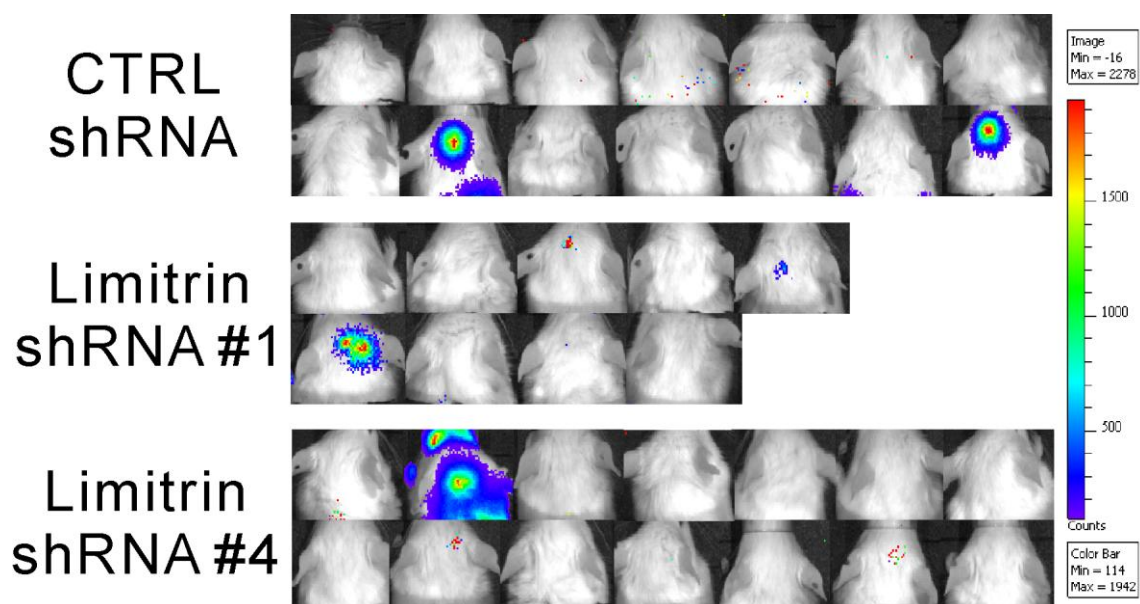


Figure 4.17 Bioluminescence images of brains of mice injected with limitrin knockdown MDA-MB-231Br cells

MDA-MB-231Br cells (1×10^5 cells) transfected with control non-targeting shRNA or limitrin-targeting shRNA construct #1 or #4 were injected in the heart of NSG mice. Mice were imaged before they were harvested when they displayed signs of distress or ill health. The luminescence images were obtained with IVIS Lumina II. In the control shRNA group, overt brain metastases were detected in 2 mice. In limitrin shRNA groups, brain metastases were found in one mouse each.

In this experiment, the majority of mice from the three groups likely died of extensive lung and liver metastases rather than overt brain metastases (Figure 4.18). As a result, no significant difference in survival was found (Figure 4.19).

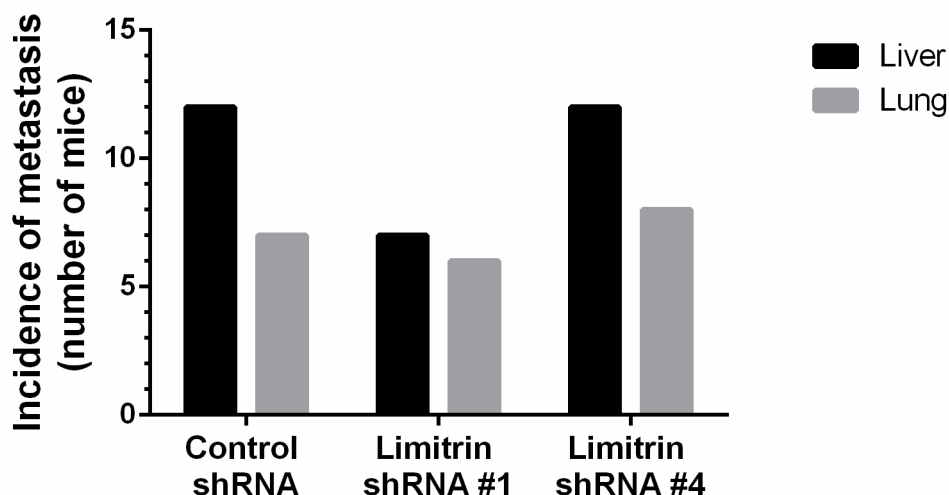


Figure 4.18 Incidence of mice with liver and lung metastases

MDA-MB-231Br cells (1×10^5 cells) transfected with control non-targeting shRNA or limitrin-targeting shRNA construct #1 or #4 were injected in the heart of NSG mice. Mice were harvested when they displayed signs of distress or ill health. The number of mice used to generate the graph were $n=14$ for control shRNA, $n=9$ for limitrin shRNA #1 and $n=14$ for limitrin shRNA #4. Mice developed extensive metastases either in the liver or lung, or in both.

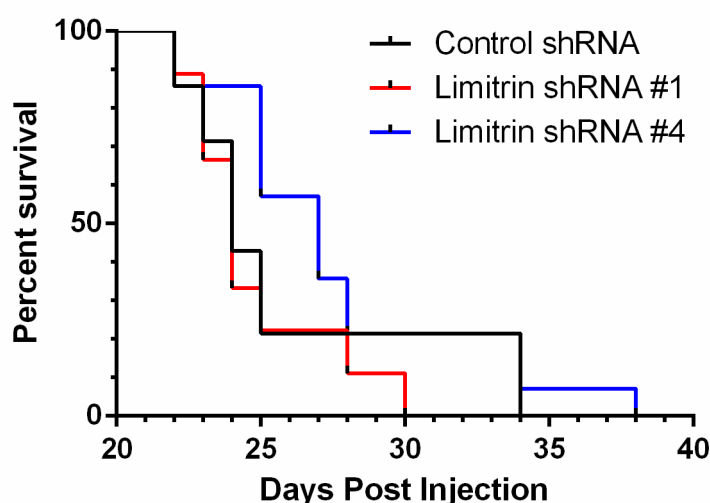


Figure 4.19 Overall survival curves of mice injected with limitrin knockdown MDA-MB-231Br cells

MDA-MB-231Br cells (1×10^5 cells) transfected with control non-targeting shRNA (black) or limitrin-targeting shRNA construct #1 (red) or #4 (blue) were injected in the heart of NSG mice at day 0. The endpoint of the study was reached when mice displayed signs of distress or ill health. Mice that died early (up to 5 days after cell injections) were excluded. Kaplan Meier survival curves were generated with GraphPad Prism software. The number of mice used to generate these survival curves were $n=14$ for control shRNA, $n=9$ for limitrin shRNA #1 and $n=14$ for limitrin shRNA #4.

Since brain metastasis is a relatively late event in the course of breast cancer, we performed another experiment where fewer cells (5×10^4 cells per mouse) were injected to delay the development of lung and liver metastasis, thereby allowing more time for the development of brain metastases. All mice were harvested 21 days after cell injection and organs including the liver, lung, spine and femur were collected and metastatic burden measured by genomic quantitative real-time PCR (qPCR). Unfortunately, we could not obtain the luminescence images of the mouse brains due to breakdown of the real-time *in vivo* imaging system (IVIS Lumina II) in our institute. For this reason, only metastatic burden in liver, lung, spine and femur could be analysed by qPCR. The majority of mice in the 3 groups had extensive liver and lung metastases, as noted in the previous experiment. There was no difference in the relative tumour burden (RTB) between groups for each organ analysed (Figure 4.20).

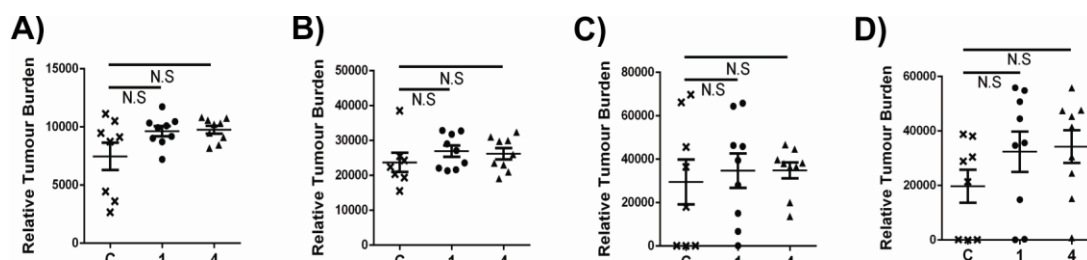


Figure 4.20 Comparison of metastatic burden in mice injected with control or limitrin knockdown MDA-MB-231Br cells

MDA-MB-231Br cells (5×10^4 cells) transfected with control non-targeting shRNA (C) or limitrin-targeting shRNA construct #1 (1) or #4 (4) were injected in the heart of NSG mice at day 0. On day 21, all mice were harvested and liver (A), lung (B), spine (C) and femur (D) were collected and metastatic burden measured by qPCR. Each dot represents one mouse and the horizontal line represents mean \pm SD. *p*-values were calculated using a Student's *t*-test. N.S. not significant. The number of mice used to

generate these graphs were n=8 for control shRNA, n=9 for limitrin shRNA #1 and n=9 for limitrin shRNA #4.

The severe immunodeficiency of NSG mice that we used may be too permissive and give rise to extensive visceral metastases in particular in the liver before development of brain metastases. As such, the use of SCID or nude mice as used by the Massagué group would be preferable in future experiments.

4.3 Discussion

The study of gene expression profiling of 4T1Br4 brain metastatic cells compared to 4T1 non-brain metastatic cells led to the identification of 17 up-regulated genes in 4T1Br4 cells and tissues. Among these genes, limitrin a protein belonging to the immunoglobulin superfamily and involved in cell adhesion was 12-fold overexpressed in the brain metastatic variant of 4T1 mouse mammary tumour. Until now, the role of limitrin in cancer and particularly in breast cancer metastasis has not been investigated. However, dysregulation of the expression of cell adhesion molecules including cadherins, integrins, selectins and members of the immunoglobulin superfamily have been shown to promote metastasis by mediating adhesive interactions between cancer cells and endothelial cells (Carter et al., 2015, Gassmann et al., 2010, Reymond et al., 2013). In addition, limitrin shares structural homology with JAM-A, another cell adhesion molecule that is involved in the transendothelial migration of leucocytes across the BBB (Yonezawa et al., 2003). On that basis, it was hypothesised that limitrin could play a similar role to promote breast cancer brain metastasis. Thus, the aim of this chapter was to investigate the prognostic value of limitrin in breast cancer and its function in brain metastasis.

BreastMark analysis revealed that limitrin mRNA is significantly associated with metastasis (DDFS) and poorer survival (OS) in basal-like breast cancer but not in other molecular subtypes. However, no data were available regarding the link with brain metastasis. Using qRT-PCR, we showed that the expression of limitrin mRNA is higher in brain metastatic mouse (4T1Br4) and human (MDA-MB-231Br) TNBC breast cancer cell lines than in non-brain metastatic breast cancer cell lines. To further analyse the prognostic significance of limitrin, we generated rabbit polyclonal anti-limitrin antibodies and tested them by Western blot analysis and IHC. By immunoblotting, limitrin antibody detected a doublet band at the expected molecular weight of limitrin (approximately 50 kDa) in mouse breast cancer cells. Results derived from EST data indicated that there is only 2 mouse limitrin variants (49 and 35 kDa). Since only the 49 kDa variant of mouse limitrin has the peptide sequence used for anti-limitrin antibody generation, it is likely that the different band sizes are due to post-translational modifications. This is supported by the study of Jung and collaborators who also observed 2 bands on immunoblots and who reported that limitrin has two putative *N*-glycosylation sites and six putative *O*-glycosylation sites (Jung et al., 2008). Therefore, the two bands detected on the blots are presumably two different glycosylation levels of the same core protein. The use of peptide-N-glycosylidase F for removal of N-linked glycosylation or a

combination of exoglycosidase (i.e. neuraminidase) and O-glycosidase for removal of O-linked glycosylation could clarify this possibility. Alternatively, the two limitrin bands observed could be due in part to excess salt present in extraction buffers that could interfere with protein mobility during electrophoresis. This possibility could easily be confirmed by addition of a desalting step to the sub-cellular fractionation protocol. In the human cell lines, the antibodies recognized one band at 49 kDa and one at 37 kDa corresponding to the expected molecular weight of human limitrin variants. Knockdown studies of limitrin also confirmed the identity of the bands detected by immunoblotting in both mouse and human breast cancer cells. Western blot analyses, like qTR-PCR data, indicated that human and mouse brain metastatic breast cancer cell lines expressed higher levels of limitrin.

Remarkably, the 66cl4 cell line that is weakly metastatic and that does not spontaneously spread to the brain also showed high limitrin expression. Previous studies in the laboratory established that the weak spontaneous metastatic ability of 66cl4 is attributable to the lack of $\beta 3$ integrin receptor expression, preventing the cells from escaping from the mammary gland and subsequently developing metastases (Sloan et al., 2006, Carter et al., 2015). In this context, expression of limitrin in the 66cl4 cell line suggests that these cells might form brain metastases in the experimental mouse model that uses direct cardiac injection and bypasses the primary tumour formation stage. Another unexpected finding was that the highly lung and bone metastatic 4T1BM2 tumours which do not spread spontaneously to the brain also express high levels of limitrin. We propose that the rapid development of visceral metastases (lung and bone) from 4T1BM2 tumours may not allow sufficient time for the development of brain metastases. Consistent with this possibility, parallel experiments in the laboratory showed that 4T1BM2 cells efficiently spread to the brain when inoculated directly into the left ventricle of the heart (unpublished data from Selda Onturk (PhD candidate, Peter MacCallum Cancer Centre, Melbourne, Australia). These observations are consistent with the contention that high limitrin expression contributes to brain metastasis but also suggest that other factors may be required for spontaneous brain metastasis to occur.

The final stage of the validation of limitrin as a prognostic marker for breast cancer brain metastasis, is to determine limitrin expression in patient samples. Since most archival material from breast cancer patients is usually available as FFPE, we optimised the IHC protocol on FFPE mouse and human tissue sections. Strong limitrin expression was also observed by IHC in brain metastatic tumours of both mouse and

human origin. Surprisingly, despite its structure and predicted membrane localisation (Yonezawa et al., 2003), we found that limitrin expression is not limited to membrane but is also abundant in the cytoplasm and nucleus of cells. These observations are consistent with the study of Jung et al. who showed a similar distribution in other cell types (Jung et al., 2008). Together their studies and ours suggest that limitrin distribution may be cell type specific and that its function in breast cancer may be regulated by its specific localisation. Clearly, the biology of limitrin is more complex than originally believed and further work will be required to address this. Changes in the sub-cellular distribution of limitrin is likely to indicate shuttling between the membrane, cytoplasm and the nucleus, as shown for many immunoglobulin-like proteins, such as EGFR (Li et al., 2009, Brand et al., 2011). Next, we stained a TMA of 33 human primary breast cancers for limitrin. Limitrin was strongly expressed in the cytoplasm/membrane of the luminal A and B and TNBC subtypes. Taken together, Breast Mark, qRT-PCR, Western blot and IHC findings indicate that high expression of limitrin may have prognostic value for predicting the development of brain metastases in TNBC patients. A larger scale study using several hundred samples using matched primary tumours and brain metastases with known clinical outcome as well as controls with no brain metastases (in collaboration with Prof. Sunil Lakhani, The University of Queensland) is underway to definitely confirm these results.

Next, we investigated whether limitrin has a role in the formation of breast cancer brain metastasis by assessing its function in *in vitro* and *in vivo* assays. To do so, we first downregulated limitrin in 4T1Br4 cells using siRNAs and performed trans-endothelial migration assays *in vitro*. 4T1Br4 cells with reduced limitrin levels were significantly less migratory through a monolayer of brain microvascular endothelial cells compared to control 4T1Br4 cells. This is the first report to demonstrate that limitrin contributes to trans-endothelial migration, a function likely to be critical for crossing of the BBB *in vivo*. Notably, as discussed in Chapter 1, three of the brain metastasis genes (COX2, HBEGF and ST6GALNAC5) that Bos and colleagues identified as being overexpressed in breast cancer brain metastases also enhanced BBB crossing (Bos et al., 2009). Indeed, molecular or pharmacological inhibition of the expression of these genes in a breast cancer brain metastatic cell line (CN-34-BrM2c) significantly decreased *in vitro* BBB transmigration activity of cancer cells (Bos et al., 2009). This is consistent with studies on lung cancer and melanoma that demonstrated that active extravasation across the vascular wall is an essential step in the formation of brain macrometastases (Kienast et al., 2010). It is also noteworthy that Bos and colleagues identified ST6GALNAC5 as a specific mediator of BBB extravasation (unlike COX2 and HBEGF

that are shared mediators of extravasation into the lung and brain) and that breast cancer cells expressing higher levels of ST6GALNAC5 were more adhesive to brain endothelial cells (Bos et al., 2009). ST6GALNAC5 is a sialyltransferase catalysing the addition of sialic acid to gangliosides and glycoproteins (Harduin-Lepers et al., 2001). Many studies highlighted a correlation between expression of heavily sialylated molecules at the surface of cancer cells and tumour cell invasion possibly due to increased cellular interactions with the microenvironment (Dall'Olio and Chiricolo, 2001, Harduin-Lepers et al., 2012). Considering that limitrin is a glycoprotein belonging to a family of cell adhesion molecules, it is conceivable that ST6GALNAC5 brain endothelial cell-specific adhesive properties are actually mediated through sialylation of limitrin. Altogether, these data indicate that inhibiting the formation of brain metastases by therapeutically targeting extravasation of tumour cells is clinically relevant and place limitrin as a potential therapeutic target.

The role of limitrin in the late stage of brain metastasis formation was further assessed *in vivo* by injecting either limitrin expressing or limitrin knockdown MDA-MB-231Br cells into the left ventricle of the heart of NSG mice to bypass the primary tumour formation. Unfortunately, in the 2 experiments we did, no significant difference was observed in terms of survival of mice likely because almost all mice from all groups developed extensive lung and liver metastases rather than brain metastases. Therefore, we could not conclude on the function of limitrin *in vivo* from these particular experiments. The severe immunodeficiency of NSG mice that we used may be too permissive and give rise to extensive visceral metastases in particular in the liver before development of brain metastases. As such, the use of SCID or nude mice as used by the Massagué group may be preferable in future experiments. Alternatively, the generation of conditional knockdown of limitrin could be used to study the role of limitrin in homing and colonisation of the brain.

Although the molecular mechanisms by which limitrin is involved in the brain metastatic cascade are currently unknown, Jung and colleagues demonstrated that limitrin facilitates cell-cell adhesion by interacting with $\alpha\beta3$ integrin (Jung et al., 2008). Our own group established that tumour expression of $\beta3$ integrin is essential for breast cancer cells to spontaneously escape the primary tumour but is not required to form bone or visceral metastases when tumour cells are injected via the left ventricle of the heart (Carter et al., 2015). In particular, tumour $\beta3$ integrin promotes trans-endothelial migration *in vitro* and vascular dissemination *in vivo* (Carter et al., 2015). Possibly, tumour limitrin and tumour $\beta3$ integrin interaction is necessary for the breast cancer

cells to disseminate to distant organs. This hypothesis implies that limitrin could be required early in the metastatic cascade and contribute to metastasis to multiple organs. Against this argument, 4T1.2 cells that do not express limitrin are highly metastatic but do not metastasise to the brain even when injected directly into the left cardiac ventricle (unpublished data from Dr. Normand Pouliot). This and the fact that limitrin promotes tumour cell migration through brain endothelial cells *in vitro*, is in favour of limitrin being a breast cancer brain metastasis protein. An interesting possibility is that tumour limitrin may interact with $\alpha\beta3$ integrin in brain endothelial cells and may act as a mediator of tumour cell extravasation into the brain. However, whether tumour limitrin interacts specifically with tumour and/or endothelial $\alpha\beta3$ integrin remains to be investigated. A simple way to demonstrate this would be to inhibit $\beta3$ integrin expressed on brain endothelial cells (either using a function blocking antibody, a pharmacological inhibitor or a molecular inhibitor) before seeding limitrin expressing breast tumour cells for the trans-endothelial migration assay *in vitro*. Inhibition of trans-endothelial migration of tumour cells through inhibition of $\beta3$ integrin on endothelial cells would support the interaction between tumour limitrin and endothelial $\beta3$ integrin. Previously, we showed that the use of $\beta3$ integrin knockout mice had no effect on the development of bone and visceral metastases but we have not looked at breast cancer brain metastasis (Carter et al., 2015). Future experiments may involve the injection of limitrin expressing 4T1Br4 cells either in the mammary fat pad or into the heart of $\beta3$ integrin knockout mice to clarify the contribution of limitrin/ $\beta3$ integrin interaction in the formation of brain metastasis.

Taken together, our data indicate that the ability of tumour cells to spread to the brain may be related to the expression and subcellular localisation of limitrin. In addition, other factors are likely to be important for the formation of brain metastases. For instance, tumour $\alpha\beta3$ integrin expression may be critical for breast cancer cells to escape the primary tumour and endothelial $\alpha\beta3$ integrin expression may facilitate tumour cell-BBB endothelial cell adhesion and extravasation into the brain. In conclusion, based on these findings we suggest that limitrin is not only a promising potential prognostic marker but also a potential molecular therapeutic target for breast cancer brain metastasis. Since there are currently no available pharmacological inhibitors of limitrin, blocking its interaction with $\alpha\beta3$ integrin using $\beta3$ inhibitors might be an efficient strategy to limit brain metastasis.

5. Novel histone deacetylase inhibitors (HDACi) to treat breast cancer brain metastasis

5.1 Introduction

The median survival for all cancer patients with brain metastasis is only 1-2 months if they are not treated (Wadasadawala et al., 2007). In particular, the TNBC subtype has been shown to have a high propensity to develop brain metastases and confer the poorest survival among all breast cancer subtypes (Adamo et al., 2011). While initially TNBC seems to be more sensitive to chemotherapy than other subtypes (Anders and Carey, 2009), resistance almost invariably develops, leading to high risk of disease recurrence that is unresponsive to chemotherapy (Carey et al., 2007, Andre and Zielinski, 2012). Moreover, the unique structure and physical properties of the BBB including tight cell-cell junctions and high levels of drug efflux pumps limit the entry of most chemotherapeutic drugs into the brain (Cheng and Hung, 2007, Steeg et al., 2011, Pardridge, 2007). Conventional endocrine or HER2-targeted therapies are not effective against TNBC brain metastases, due to the lack of hormone (ER or PR) and/or HER2 receptors (Allison, 2012). Therefore, it is urgent to develop more effective therapies against brain metastatic TNBC.

The aim of this chapter is to evaluate the efficacy of two novel histone deacetylase inhibitors (HDACi) namely SB939 and 1179.4b (Figure 5.1), in breast cancer brain metastasis models *in vitro* and *in vivo*. HDACi have been shown to have limited toxicity to normal tissues and to induce cell cycle arrest, differentiation, apoptosis and immune response in many tumour cell types *in vivo*, including leukemia, lung, prostate and breast cancers, by regulating acetylation of histone or non-histone proteins (Bolden et al., 2006, Johnstone, 2002, Falkenberg and Johnstone, 2014). Several of these HDACi are being tested in phase 1 and phase 2 clinical trials as potential treatment for various cancers such as leukaemia and advanced solid tumours (Johnstone, 2002, Mork et al., 2005, Minucci and Pelicci, 2006, Groselj et al., 2013). SAHA (Vorinostat) is known to have BBB permeability (Palmieri et al., 2009b, Steeg et al., 2011) and was shown to partially prevent the development of experimental MDA-MB-231Br breast cancer brain metastases (Palmieri et al., 2009b), to enhance radiosensitivity in the MDA-MB-231Br experimental model of brain metastasis and to prolong the survival of mice by 2-fold compared to SAHA alone or irradiation alone. However, this approach is not curative and only extends survival to 30 days (Baschnagel et al., 2009). More recently several

HDACi that are more potent than SAHA have been generated (Lu et al., 2007, Suzuki et al., 2004, Kulp et al., 2006, Fass et al., 2013). Among HDACi, SAHA, Panobinostat (LBH589) and valproic acid (VPA) are currently being evaluated in phase 1 clinical trials in combination with radiation therapy for the treatment of brain tumours or brain metastases (ClinicalTrials.gov identifier #NCT00838929, NCT01600742, NCT00946673, NCT01324635, NCT00437957 and NCT00513162). These HDACi are all pan-inhibitors of class I and class II histone deacetylases (HDACs) (Bolden et al., 2006). While pan-HDACi are less selective than class-specific HDACi, current evidence indicates that the activity of pan-HDACi on multiple protein targets may be necessary to achieve sufficient potency against solid tumours (Balasubramanian et al., 2009, Atadja, 2009).

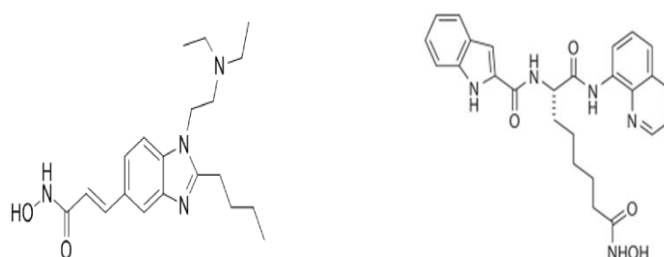


Figure 5.1 Chemical structure of SB939 and 1179.4b

Molecular weights of SB939 (left panel) and 1179.4b (right panel) are 358 and 473 Da, respectively.

Recently, Fairlie and colleagues have developed and tested the anti-tumour effects of several new hydroxamic acid based HDACi on cancer cell lines *in vitro* including breast, lung, prostate, colon, ovarian cancers and melanoma (Kahnberg et al., 2006). One of these compounds, 1179.4b (compound #52), demonstrated highly potent anti-tumour effects on breast cancer cell lines *in vitro* and selective cytotoxicity (>10-fold) against tumour cells compared to normal neonatal foreskin fibroblasts (NFF) (Kahnberg et al., 2006). However, the efficacy of this novel HDACi has yet to be evaluated *in vivo*. The BBB permeability of 1179.4b is expected to be limited based on preliminary assessment of its biochemical properties (i.e. 5-hydrogen bond donors and high surface polarity, personal communication, Prof Paul Stupple, Walter and Eliza Hall Institute of Medical Research, Melbourne). However, given its high potency demonstrated *in vitro* (Kahnberg et al., 2006), 1179.4b was included in our study as it may still be effective to “prevent” the development of brain metastases and/or against established brain metastases in which the BBB is disrupted, as reported for some

TNBCs (Yonemori et al., 2010).

SB939 (Pracinostat), an orally available HDACi, has excellent pharmacokinetic (Jayaraman et al., 2011) and pharmacodynamic properties (Razak et al., 2011) and is currently being evaluated in phase 2 clinical trials for the treatment of acute myeloid leukemia (AML) and myelodysplastic syndrome. SB939 showed higher potency than SAHA (average 3.5-fold) in various cancer cell lines *in vitro*, with low toxicity against normal human dermal fibroblasts (NHDF) (IC_{50} of $>100 \mu\text{M}$) and higher accumulation in tumour tissues than SAHA *in vivo* (Novotny-Diermayr et al., 2010). SB939 is expected to cross the BBB, as it meets several requirements for the BBB penetration including low molecular weight (≤ 500 Da) and oil/water distribution coefficient ($(\text{LogP}) \leq 5$) and absence of efflux ratio indicating that it is unlikely to be a p-gp transporter substrate. SB939 has not been evaluated in pre-clinical models of breast cancer or brain metastasis. Here, we document for the first time the effect of SB939 and 1179.4b in two brain metastatic TNBC models (4T1Br4 and MDA-MB-231Br) *in vitro* and *in vivo*. Further, we present preliminary data on the radiosensitising properties of these novel HDACi *in vitro*.

5.2 Results

5.2.1 Evaluation of the efficacy of SB939 and 1179.4b *in vitro*

The relative potency of SB939 and 1179.4b against 4T1Br4 and MDA-MB-231Br cells was first assessed in colony formation assays *in vitro* using a set concentration of 1 μ M. SAHA was used as a positive control based on a report that this HDACi effectively reduced MDA-MB-231Br colony formation by approximately 60% at 1 μ M (Palmieri et al., 2009b). For these assays, 4T1Br4 cells (1×10^2 /well) were seeded in 6 well plates, allowed to attach for 6 hr and then treated with either DMSO (vehicle control) or 1 μ M of SAHA or SB939 or 1179.4b. The number and average size of colonies were measured after 7 days. In the presence of DMSO alone, 4T1Br4 cells formed approximately 80 colonies (80% plating efficiency) (Figure 5.2). Treatment with SAHA did not reduce the number of 4T1Br4 colonies compared to control DMSO but reduced the average size of colonies by about 20% (right panel, $p < 0.01$) indicating that SAHA is cytostatic rather than cytotoxic at this concentration. By comparison, SB939 significantly inhibited colony formation (~45% inhibition, $p < 0.01$) and reduced colony size by more than 50% ($p < 0.001$) whereas 1179.4b completely inhibited 4T1Br4 colony formation ($p < 0.001$).

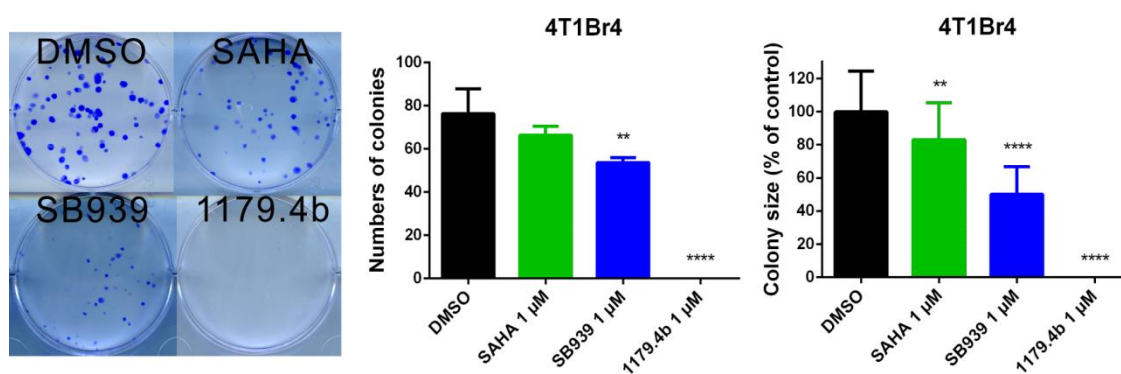


Figure 5.2 SB939 and 1179.4b inhibit survival of 4T1Br4 cells

4T1Br4 cells (1×10^2 /well) were seeded in 6 well plates, allowed to attach for 6 hr at 37°C and adherent cells treated with 1 μ M of SB939 or 1179.4b or SAHA or DMSO (vehicle control) as indicated. The number and size of colonies (>50 cells) were measured after 7 days. Representative images of colonies are shown on the left and a quantitation of triplicate wells/condition shown on the middle and right ($n=3$). Data show average number of colonies/culture condition \pm SD of triplicate wells (middle panel) and

average size of colonies/culture condition \pm SD of triplicate wells (right panel) (** $p < 0.01$, **** $p < 0.001$ compared to DMSO control). p -values were calculated using a one-way ANOVA with a Bonferroni post-test; $p < 0.05$ was considered significant.

In parallel experiments, we investigated the effect of SB939 and 1179.4b on MDA-MB-231Br colony formation. However colonies did not form well with this cell line due to the high motility of the cells and scattering of the colonies in culture.

The effect of SB939 and 1179.4b on cell proliferation was investigated in a standard sulforhodamine B colorimetric assay (Figure 5.3). For this assay, 4T1Br4 or MDA-MB-231Br cells were treated with increasing concentrations of SB939 or 1179.4b and cell proliferation was measured after 3 days and IC_{50} values were calculated for each inhibitor in each cell line (Table 5-1). 1179.4b and SB939 showed significantly greater potency than SAHA in this assays, with IC_{50} values of 71 nM and 527 nM respectively in 4T1Br4 cells or 50 nM and 364 nM respectively in MDA-MB-231Br cells. By comparison, IC_{50} values for SAHA were greater than 1 μ M in both cell lines (Table 5-1).

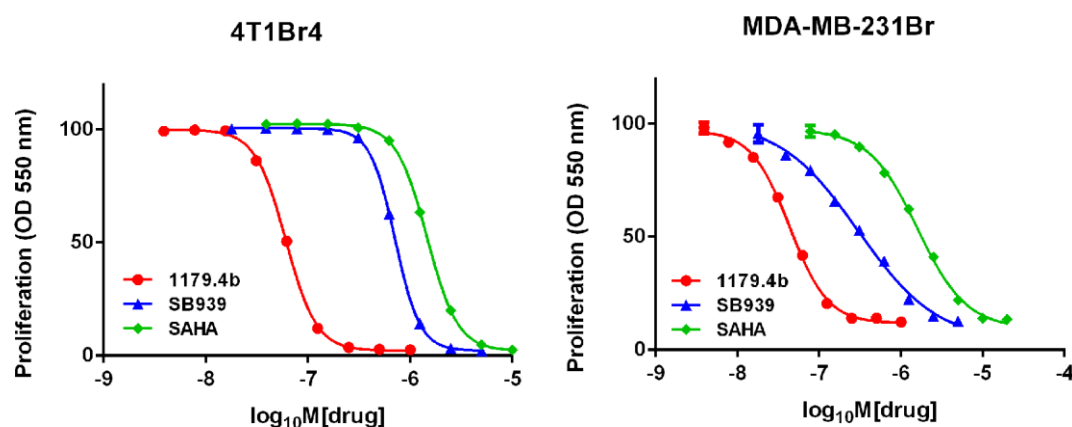


Figure 5.3 SB939 and 1179.4b inhibit proliferation of 4T1Br4 and MDA-MB-231Br cells

4T1Br4 (1×10^3 /well) and MDA-MB-231Br cells (2×10^3 /well) were seeded in 96-well plates and treated with SB939 (blue), 1179.4b (red) or SAHA (green) for 72 hr at 37°C. Proliferation was measured by colorimetric sulforhodamine B (SBR) assay. Data show a representative experiment ($n=3$) and expressed as means \pm SD of six replicate wells per time point.

Table 5-1. IC₅₀ of SB939, 1179.4b and SAHA in 4T1Br4 and MDA-MB-231Br cells.

HDACi	4T1Br4	MDA-MB-231Br
SAHA	1.28 μ M	1.71 μ M
SB939	527 nM	364 nM
1179.4b	71 nM	50 nM

IC₅₀, HDACi concentration required for 50% inhibition of cell proliferation.

The cytostatic and cytotoxic effects of SAHA, SB939 and 1179.4b were further evaluated in colony assays using their respective IC₅₀ concentration (see Table 5-1). This experiment proceeded as described in Figure 5.2. 4T1Br4 cells formed approximately 65 colonies (65% plating efficiency) in DMSO alone (control) (Figure 5.4). SAHA (1.3 μ M) and SB939 (530nM) did not reduce the number of colonies compared to control. However, 1179.4b, even at concentration as low as 70 nM, was sufficient to significantly reduce the number of 4T1Br4 colonies (Figure 5.4, middle panel). As expected, all three HDACi decreased the size of 4T1Br4 colonies compared to control (Figure 5.4, right panel). Taken together, these results indicate that SB939 and 1179.4b are more potent inhibitors than SAHA and that SAHA and SB939 are primarily cytostatic whereas 1179.4b exert both cytostatic and cytotoxic activities against 4T1Br4 cells at the concentrations tested.

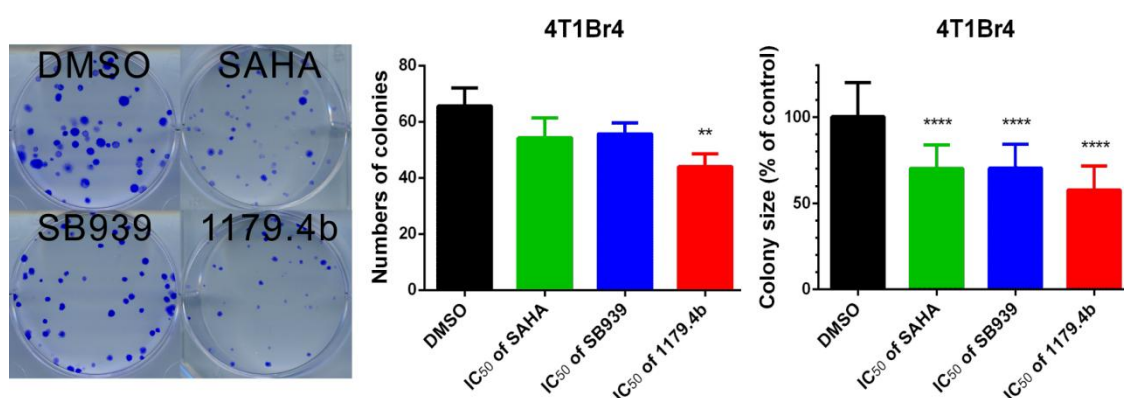


Figure 5.4 IC₅₀ of SAHA, SB939 and 1179.4b inhibits size of colonies of 4T1Br4 cells

4T1Br4 cells (1×10^2 /well) were seeded in 6 well plates, allowed to attach for 6 hours at 37°C and then treated with IC₅₀ of SB939 (530 nM) or 1179.4b (70 nM) or SAHA (1.3 μ M) or DMSO (control) as shown in Table 5-1. Colonies (>50 cells) were counted and

the sizes of colonies were measured after 7 days. Representative images of colonies are shown on the left and a quantitation of triplicate wells/condition shown on the middle and right ($n=3$). Data show average number of colonies/culture condition \pm SD of triplicate wells (middle panel) and average size of colonies/culture condition \pm SD of triplicate wells (right panel) (** $p<0.01$, **** $p<0.001$ compared to control. p -values were calculated using a one-way ANOVA with a Bonferroni post-test; $p<0.05$ was considered significant).

5.2.2 Identification of biomarker for the efficacy of HDACi in vitro

Acetylation of histones is commonly used as a marker of the inhibitory activity of the HDACis (Marks et al., 2000, Gottlicher et al., 2001, Somech et al., 2004). Increased acetylation of histones H3 and H4 has been associated with transcriptional activation of several genes involved in the suppression of tumour growth such as p21 and p53 (Hadnagy et al., 2008, Gui et al., 2004, Butler et al., 2001). Novotny-Deirmayr et al. suggested that acetylation of histone H3 might predict favourable outcome in cancer patients (Novotny-Diermayr et al., 2011). Similarly, Toh et al. reported that acetylation of histone H4 is associated with good prognosis in patients with esophageal squamous cell cancer (Toh et al., 2004).

SB939 has been shown to induce hyperacetylation of histone H3 in HCT116 (human colon cancer) and HL-60 (human promyelocytic leukaemia) cell lines and peripheral blood mononuclear cells from patients with various malignant tumours (Novotny-Diermayr et al., 2010, Novotny-Diermayr et al., 2011, Yong et al., 2011). To our knowledge, the effect of 1179.4b on acetylation of histone H3 or H4 has not been reported.

To determine if SB939 and 1179.4b induce a similar response in 4T1Br4 and MDA-MB-231Br cells, changes in acetylation of histone H3 were examined by immunoblotting following exposure of the cells to SB939 or 1179.4b for 24 hr. As shown in Figure 5.5A (4T1Br4) and Figure 5.5B (MDA-MB-231Br), while acetylation of histone H3 increased in a dose-dependent manner following treatment with SB939, histone H3 hyperacetylation in response to 1179.4b was evident even at concentrations as low as 312 nM in both cell lines. These observations were consistent with their respective potency demonstrated in colony formation and proliferation assays.

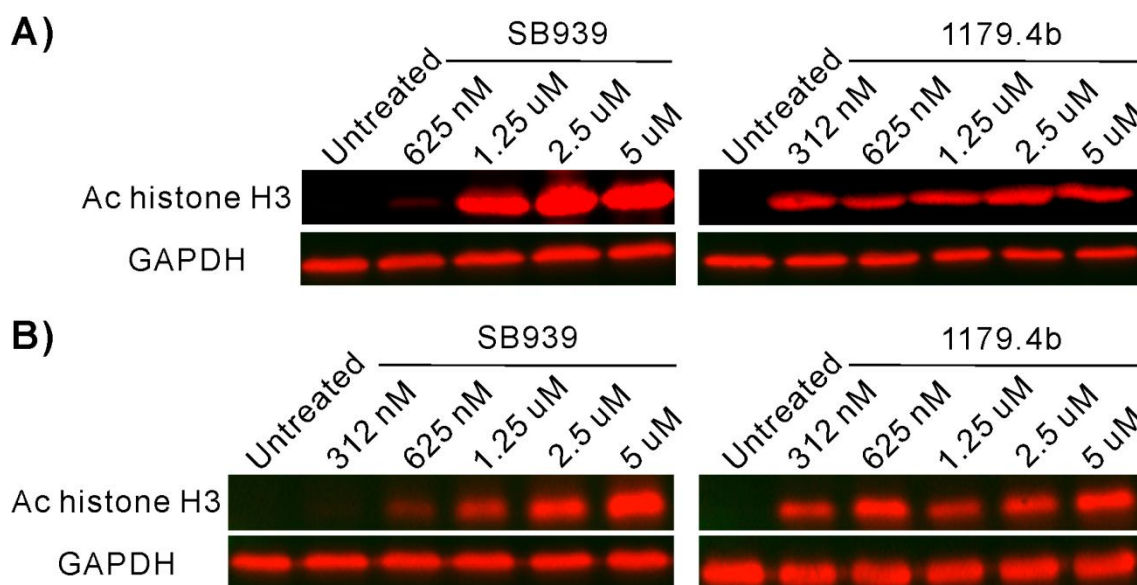


Figure 5.5 SB939 and 1179.4b induce dose-dependent hyperacetylation of histone H3 in 4T1Br4 and MDA-MB-231Br cells

4T1Br4 (A) and MDA-MB-231Br (B) cells were treated with SB939 or 1179.4b at the concentrations indicated for 24 hr and cell lysates processed for western blotting. GAPDH was used as a protein loading control. Ac histone H3, acetylated histone H3. Data show a representative experiment ($n=2$).

Next, to guide the dosing regimen for *in vivo* experiments, we performed time-course experiments using a single dose of SB939 (2 μ M) or 1179.4b (1 μ M) at which acetylation of histone H3 was clearly evident as shown in Figure 5.5. While SB939 or 1179.4b did not induce significant acetylation of histone H3 at 1 or 6 hr in 4T1Br4 cells, hyperacetylation was strongly induced by either inhibitor 24 hr post-treatment (Figure 5.6A). By comparison, histone H3 acetylation increased gradually from 1 hr to 24 hr in response to SB939 in MDA-MB-231Br cells or from 6 hr to 24 hr in response to 1179.4b (Figure 5.6B). Thus, histone H3 hyperacetylation was maximal at 24 hr for both compounds in both cell lines, albeit with a slower kinetic in 4T1Br4 cells than in MDA-MB-231Br cells.

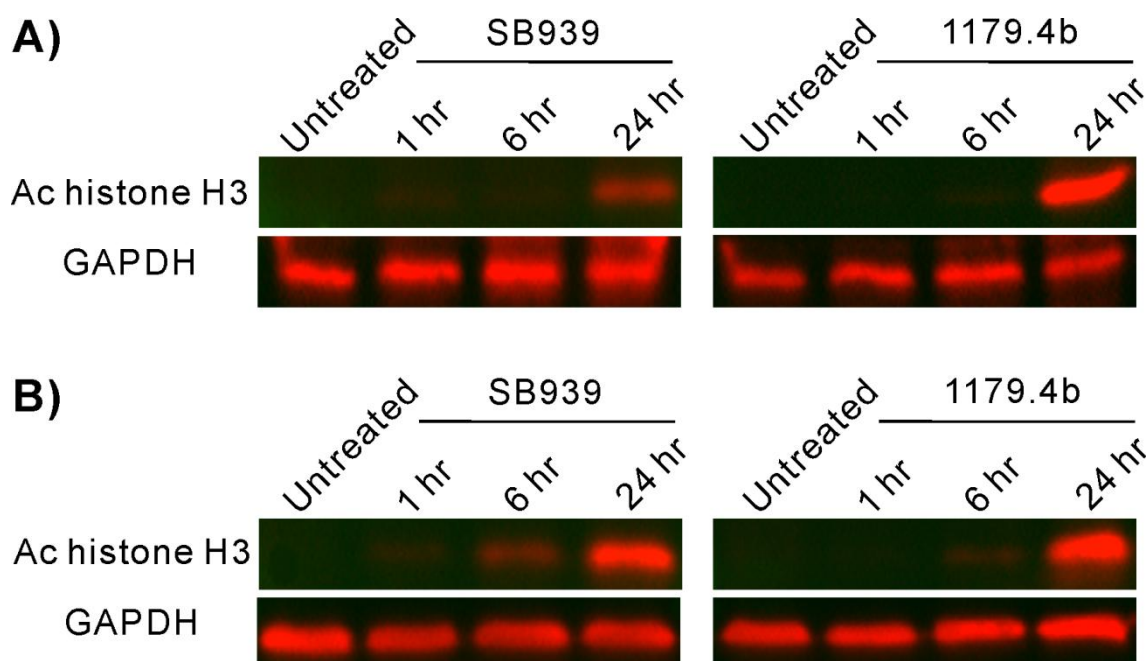


Figure 5.6 SB939 and 1179.4b induce time-dependent hyperacetylation of histone H3 in 4T1Br4 and MDA-MB-231Br cells

4T1Br4 (A) and MDA-MB-231Br (B) cells were treated with SB939 (2 μ M) and 1179.4b (1 μ M) for up to 24 hr and cell lysates processed for western blotting at the indicated times. GAPDH was used as a protein loading control. Ac histone H3, acetylated histone H3. Data show a representative experiment ($n=2$).

To determine whether hyperacetylation of histone H3 in response to SB939 or 1179.4b is reversible, cells were treated with each HDACi for 24 hr and changes in the level of histone H3 acetylation in 4T1Br4 (Figure 5.7A) and MDA-MB-231Br (Figure 5.7B) cells were measured over 24 hr after removal of the inhibitors. Cells treated with SB939 (2 μ M) showed a rapid decrease in the level of histone H3 acetylation following drug removal in 4T1Br4 cells but it remained detectable for up to 8 hr in MDA-MB-231Br. Cells treated with 1179.4b (1 μ M) retained higher levels of histone H3 acetylation for up to 4 hr in 4T1Br4 cells and up to 24 hr in MDA-MB-231Br cells compared to both of SB939 treated cell lines. Collectively, these data indicate that 1179.4b sustains acetylation of histone H3 longer in both cell lines compared to SB939 and that both SB939 and 1179.4b induce higher acetylation of histone H3 in MDA-MB-231Br than in 4T1Br4 cells. These results are again consistent with the greater potency of SB939 and 1179.4b in MDA-MB-231Br than in 4T1Br4 cells demonstrated in proliferation inhibition assays (Table 5-1).

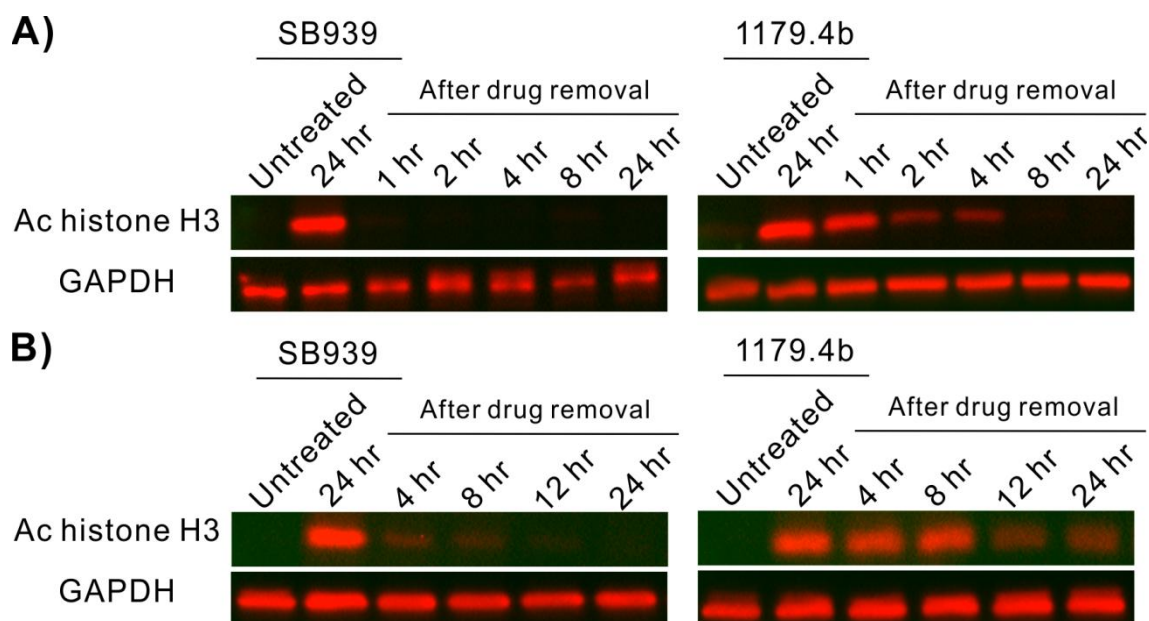


Figure 5.7 SB939 and 1179.4b-induced hyperacetylation of histone H3 is reversible

4T1Br4 (A) and MDA-MB-231Br (B) cells treated with SB939 (2 μ M) or 1179.4b (1 μ M) for 24 hr. The cells were washed with PBS gently twice to remove excess HDACi and changes in histone H3 acetylation were determined by immunoblotting after 1-24 hr as indicated. GAPDH was used as a protein loading control. Ac histone H3, acetylated histone H3. Data show a representative experiment ($n=2$).

5.2.3 Impacts of HDACi on 4T1Br4 primary tumour growth and brain metastasis *in vivo*

Since neither SB939 nor 1179.4b has been evaluated in breast cancer metastasis models, we first assessed the tolerability of these inhibitors in BALB/C mice. SB939 (10, 20 or 40 mg/kg) or 1179.4b (10, 20 or 40 mg/kg) was administered intraperitoneally once daily for 8 days. There was no significant decrease in body weight of mice ($\pm 10\%$ of changes) treated with either inhibitor at all doses tested (vehicle, SB939 or 1179.4b) (Figure 5.8). Daily monitoring of mice for signs of distress (lethargy, hunched back, scruffiness, rapid breathing) also indicated no overt toxicity and that both inhibitors are well tolerated. However, 1179.4b (40 mg/kg) had poor solubility in 30% poly(ethylene glycol) 300, and therefore this concentration was excluded from further *in vivo* experiments.

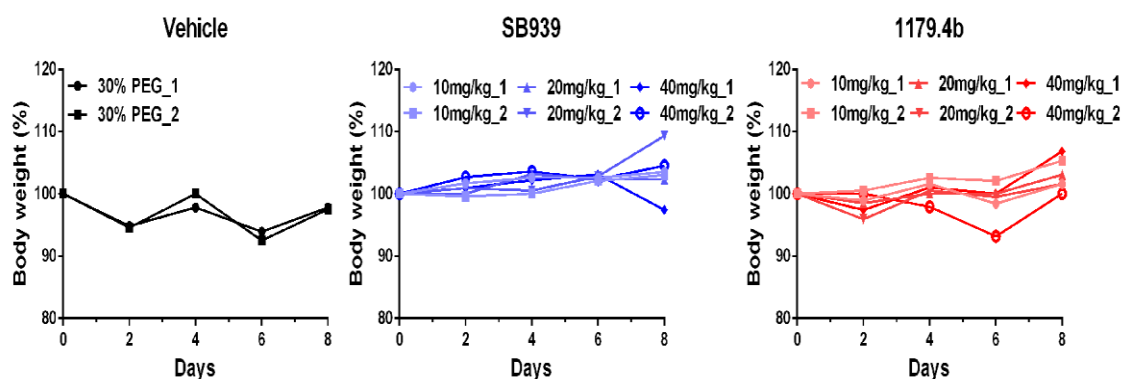


Figure 5.8 Effect of SB939 or 1179.4b on BALB/C mouse weight

Vehicle (30% PEG with 10% v/v DMSO, left panel) or SB939 (10, 20 or 40 mg/kg, middle panel) or 1179.4b (10, 20 or 40 mg/kg, right panel) was administered intraperitoneally once daily for 8 days. Body weight was recorded every 2 days. Two mice were used for each condition. PEG, poly(ethylene glycol) 300.

Based on the limited solubility of 1179.4b at 40 mg/kg, a dose of 20 mg/kg was chosen for subsequent *in vivo* experiments. For SB939, the dose was increased to 50 mg/kg since it retained good solubility at this concentration and was well tolerated at the highest dose tested (40 mg/kg). To investigate the effect of SB939 and 1179.4b *in vivo*, 4T1Br4 (2×10^4) cells were injected into the mammary fat pad of 6-8 weeks old BALB/C mice and drug treatment initiated on day 9, when primary tumours were palpable. SB939 (50 mg/kg) or 1179.4b (20 mg/kg) was injected intraperitoneally once daily until completion of the experiment on day 28. Both SB939 and 1179.4b significantly reduced 4T1Br4 primary tumour growth (Figure 5.9, left panel). Reduced tumour growth was confirmed by a lower tumour weight in HDACi-treated mice at endpoint compared to control mice (Figure 5.9, middle panel). While the primary objective of this experiment was to evaluate the impact of SB939 and 1179.4b on primary tumour growth, spines were also collected and relative tumour burden was measured by genomic quantitative real-time PCR (qPCR) detection of the mCherry marker gene. Interestingly, metastatic burden in spines was significantly reduced by either SB939 or 1179.4b treatment *in vivo* (Figure 5.9, right panel). Brain metastasis was not evaluated in this experiment since fewer mice/group (8-10) were used, tumours were not resected, and the experiment had to be terminated earlier (day 28) due to the large primary tumours size/weight in the control group.

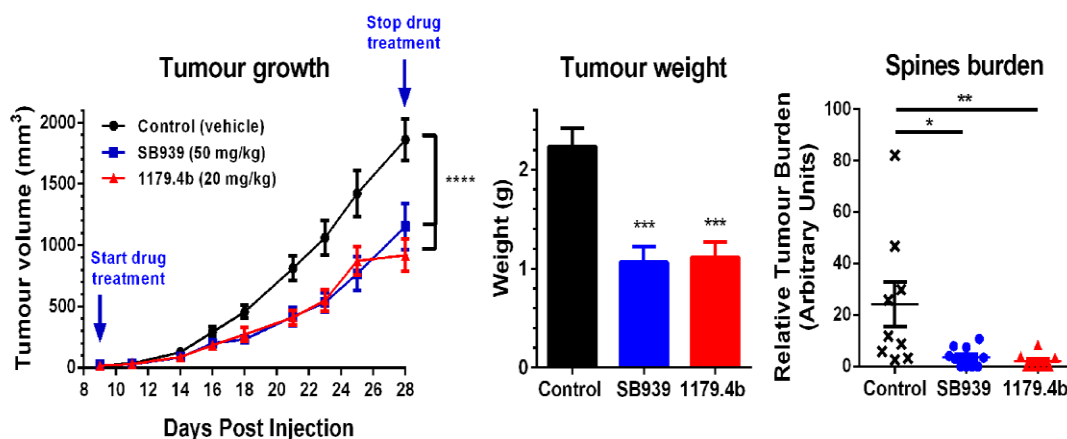


Figure 5.9 SB939 and 1179.4b inhibit 4T1Br4 primary tumour growth and metastatic burden in spines

4T1Br4 (2×10^4) cells were injected into the mammary fat pad of mice and tumour growth measured 3 times a week with electronic calipers (left panel). Tumour growth/volume was calculated using the formula $(\text{length} \times \text{width}^2)/2$. SB939 (50 mg/kg, blue) or 1179.4b (20 mg/kg, red) was administered intraperitoneally once daily from day 9 to day 28. Mice were harvested 1 hr after the last drug treatment. *4T1Br4* primary tumours were collected and weighed (middle panel). Metastatic burden in spines was analysed by qPCR (right panel). Data from one experiment ($n=1$) are expressed as means \pm SEM of tumour volume/tumour weight/metastatic burden in spines. Control ($n=9$), SB939 ($n=10$) and 1179.4b ($n=8$) mice were used. p -values were calculated using a two-way ANOVA with a Tukey post-test for tumour growth, one-way ANOVA with a Tukey post-test for tumour weight and a Student t -test for metastatic burden in spines. * $p < 0.05$, ** $p < 0.01$, *** $p < 0.005$, **** $p < 0.001$ compared to control (vehicle).

To confirm that effective doses of HDACi reached the primary tumours under the conditions used, primary tumours were analysed for changes in histone H3 acetylation by immunoblotting (Figure 5.10). As expected, SB939- or 1179.4b-treated mice showed a strong increase in acetylation of histone H3 in primary tumours compared to tumours from control mice confirming that both SB939 and 1179.4b effectively blocked HDAC activity *in vivo* and resulted in reduced primary tumour growth.

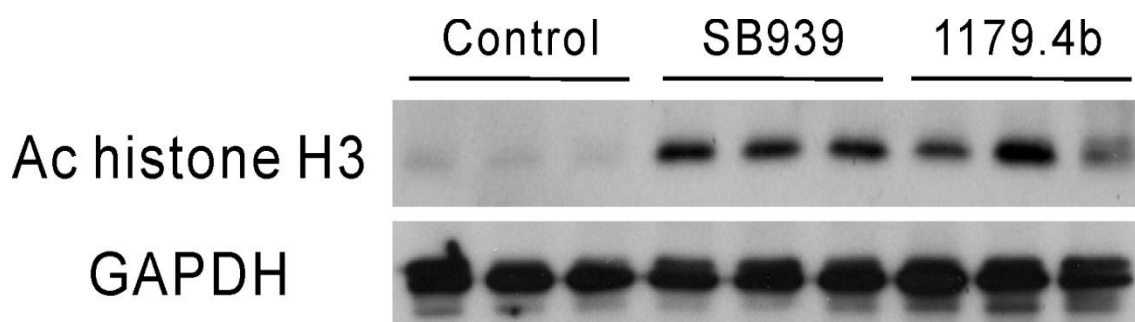


Figure 5.10 SB939 and 1179.4b increase acetylation of histone H3 in 4T1Br4 primary tumours

4T1Br4 primary tumours were collected 1 hr after the last treatment on day 28. Tumours (n=3/group) were homogenised and analysed for acetylation of histone H3 by western blotting. GAPDH was used as a protein loading control.

To investigate the effects of SB939 and 1179.4b specifically on spontaneous breast cancer brain metastases, 4T1Br4 (2×10^4) cells were injected into the mammary fat pad of 6-8 weeks old BALB/C mice. Tumours were resected when they reached approximately 0.5 g. As shown in Figure 5.11, tumour weights were not significantly different between groups.

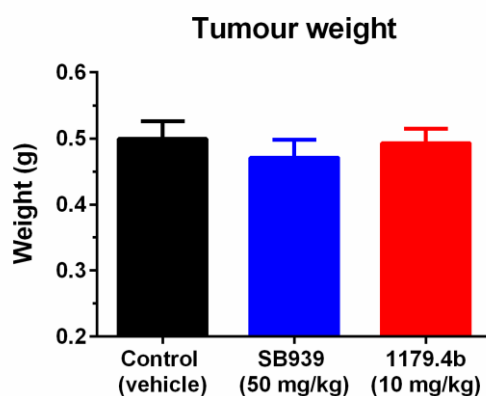


Figure 5.11 Tumour weight after resection

4T1Br4 (2×10^4) cells were injected into the mammary fat pad of mice and tumours were resected when they reached ~0.5 g (~2 weeks after cell injection). Drug treatment was initiated two days after primary tumour resection and continued until completion of

the experiment. Control ($n=11$), SB939 ($n=11$) and 1179.4b ($n=12$) mice were used for this experiment ($n=1$).

SB939 (50 mg/kg) or 1179.4b (10 mg/kg) was injected into mice intraperitoneally once daily for 2 weeks starting two days after tumour resection. One hour after the last HDACi treatment, mice were harvested (day 33). Brains were collected for fluorescence imaging and the incidence of mice with detectable mCherry^{+ve} lesions was scored (Figure 5.12). Under these conditions, spontaneous brain macrometastases were detected in 45% (5/11) of control mice. In contrast, the number of mice with brain metastases was dramatically reduced in the SB939 (2/11, 18%) and 1179.4b (1/12, 8%) treated groups.

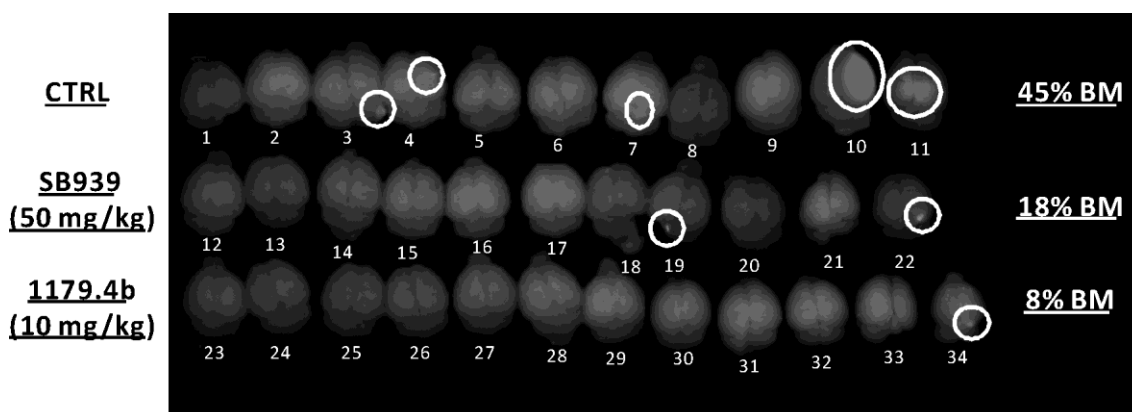


Figure 5.12 SB939 and 1179.4b inhibit 4T1Br4 spontaneous brain metastases

Two days after tumour resection, mice were treated once daily with SB939 (50 mg/kg) or 1179.4b (10 mg/kg) by intraperitoneal injection for 2 weeks. Mice were harvested and the brains were imaged by fluorescence for detection of mCherry^{+ve} lesions. Control ($n=11$), SB939 ($n=11$) and 1179.4b ($n=12$) mice were used for this experiment ($n=1$).

5.2.4 Analysis of the radiosensitising properties of HDACi in vitro

Whole brain radiation therapy (WBRT) is the mainstay of treatment for patients with brain cancer or brain metastases and is commonly combined with chemotherapy (Eichler and Loeffler, 2007). However, toxicity to the normal tissue and impairment of cognitive functions limit the dose that can be administered in patients (Chargari et al., 2010, Welzel et al., 2008). Therapeutic agents with radiosensitising properties could

therefore provide an effective strategy to increase the efficacy of radiation therapy while minimising the side effects of WBRT (Chung et al., 2009, Russo et al., 2009, Morgan et al., 2010, Gerster et al., 2010). The radiosensitising properties of SB939 and 1179.4b were evaluated first in 4T1Br4 cells using *in vitro* colony forming assays. Each HDACi was used at their IC₅₀ concentration (see Table 5-1) either alone or in combination with increasing radiation doses. As shown in Figure 5.13, both SB939 and 1179.4b significantly enhanced radiation-induced cell death, resulting in fewer cell colonies compared to radiation alone (Figure 5.13). Dose enhancement factor (DEF) at 50% cell survival was 1.45 for both SB939 and 1179.4b.

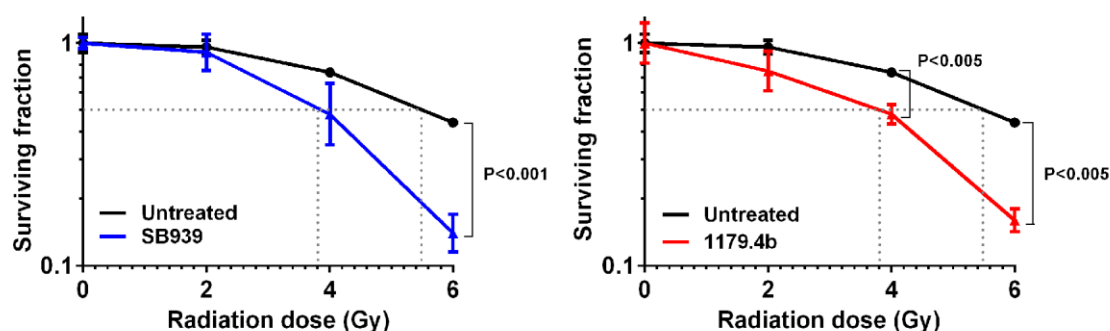


Figure 5.13 SB939 and 1179.4b radiosensitise 4T1Br4 cells

Adherent 4T1Br4 cells were treated with SB939 or 1179.4b for 24 hr followed by irradiation at the indicated doses. The plates were incubated for 7 days and colonies (>50 cells) were counted. The effect of SB939 (530 nM, blue) and 1179.4b (70 nM, red) is shown in the left and right panels respectively. Radiation alone is shown in black in both panels. 4T1Br4 colonies were significantly decreased by combination of either SB939 or 1179.4b with radiation compared to radiation alone. Data show a representative experiment ($n=3$) and expressed as means \pm SD of triplicate wells. p -values were calculated using a Student t -test.

SB939 and 1179.4b also decreased the size of 4T1Br4 colonies. As shown in Figure 5.14 (SB939) and Figure 5.15 (1179.4b), combination treatments reduced the size of colonies compared to radiation alone at all radiation doses used (e.g., 2 Gy vs 2 Gy + either HDACi, 4 Gy vs 4 Gy + either HDACi and 6 Gy vs 6 Gy + either HDACi). Taken together, these results indicate that SB939 and 1179.4b increase not only radiation-induced cell death (Figure 5.13) but also radiation-induced anti-proliferative effect

(Figure 5.14 and Figure 5.15).

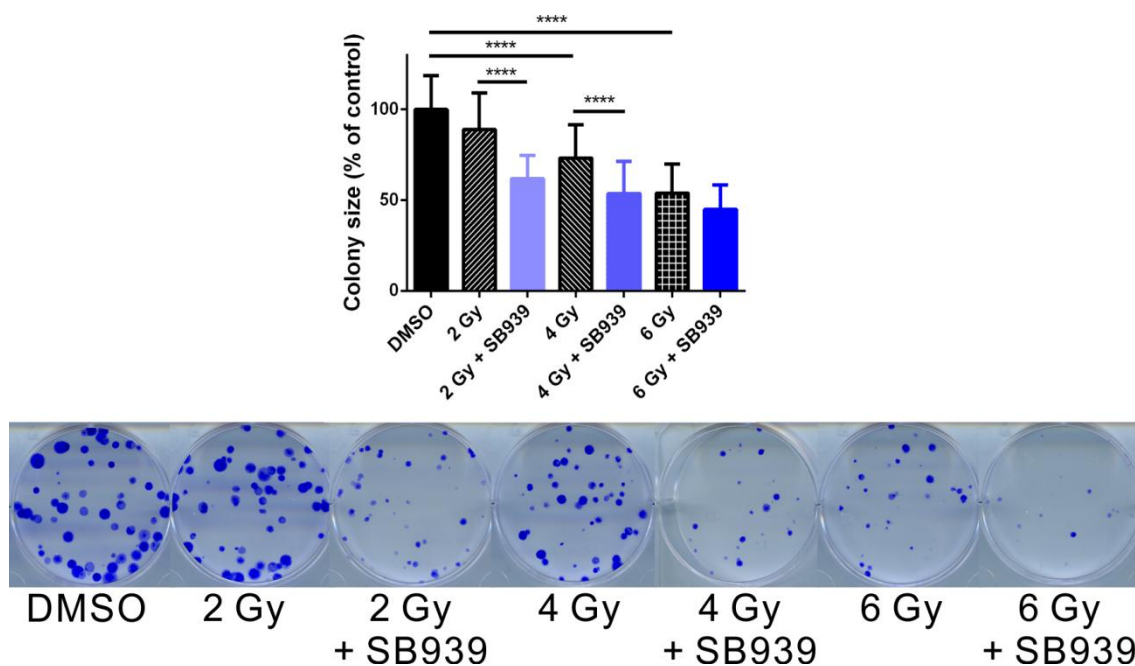


Figure 5.14 Radiosensitising effect of SB939 (colony size)

Adherent 4T1Br4 cells were treated with SB939 (530 nM) for 24 hr followed by irradiation at the indicated doses. The plates were incubated for 7 days and the size of surviving colonies measured. The size of 4T1Br4 colonies was significantly decreased by combination of SB939 + radiation compared to radiation alone. Data show a representative experiment (n=3) and expressed as means \pm SD of triplicate wells (top panel). p-values were calculated using a one-way ANOVA with a Bonferroni post-test; $p < 0.05$ was considered significant. Representative images of colonies are shown in the bottom panel.

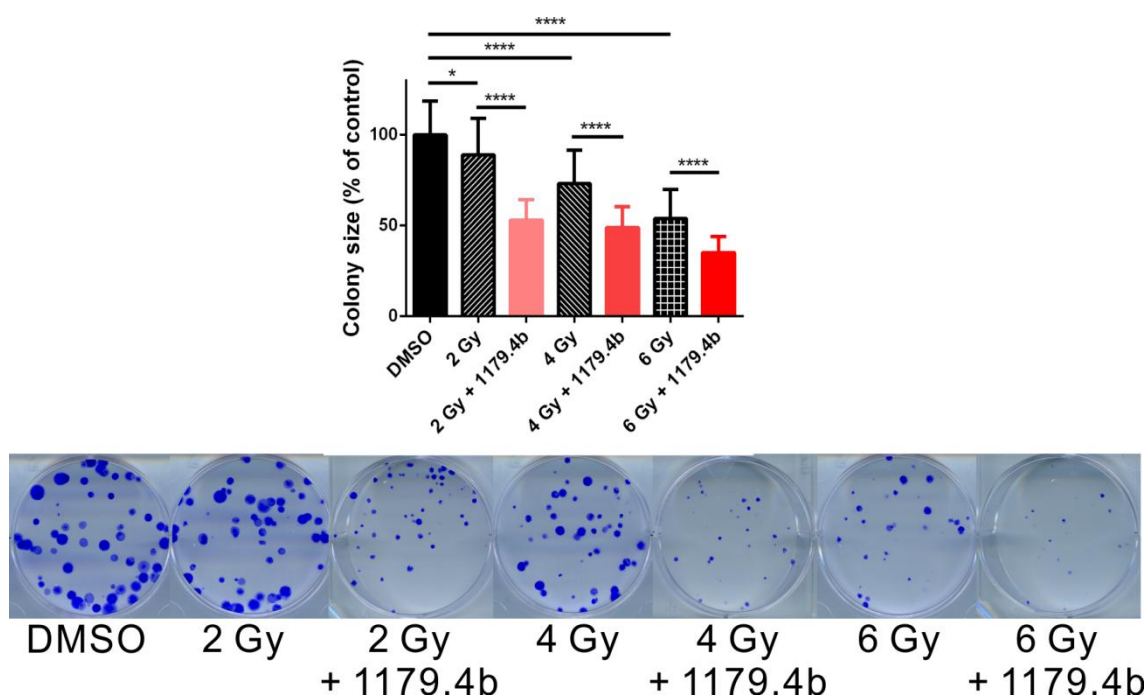


Figure 5.15 Radiosensitising effect of 1179.4b (colony size)

Adherent 4T1Br4 cells were treated with 1179.4b (70 nM) for 24 hr followed by irradiation at the indicated doses. The plates were incubated for 7 days and the size of colonies measured. The size of 4T1Br4 colonies was significantly decreased by combination of 1179.4b + radiation compared to radiation alone. Data show a representative experiment (n=3) and expressed as means \pm SD of triplicate wells (top panel). p-values were calculated using a one-way ANOVA with a Bonferroni post-test; $p < 0.05$ was considered significant. Representative images of colonies are shown in the bottom panel.

Since MDA-MB-231Br cells tend to scatter in colony assays, we used an alternative method to quantitate the radiosensitising effects of SB939 and 1179.4b by measuring the induction of γ -H2AX nuclear foci. γ -H2AX is recruited to DNA double strand breaks induced by ionising radiation and is commonly used as a marker for DNA damage (Kuo and Yang, 2008, Mah et al., 2010, Sharma et al., 2012). Sustained γ -H2AX induction (>24 hr) usually indicates inability to repair extensive DNA damage induced by ionising agents and was suggested to be a predictor of tumour radiosensitivity (Taneja et al., 2004) and cytotoxicity (Denoyer et al., 2015).

For this assay, SB939 and 1179.4b were used at their respective IC_{50} (see Table 5-1)

either alone or in combination with a low dose of radiation (1 Gy) (Figure 5.16 and 5.17). As expected, untreated control groups showed only low levels of γ -H2AX-positive cells (~15%) at both 1 hr and 24 hr time points. Irradiation alone induced a strong γ -H2AX response in approximately 60% of the cells 1 hr after treatment which returned close to baseline after 24 hr (~25%) indicating a near complete recovery of the cells after low dose irradiation alone. Treatment with SB939 alone was sufficient to induce γ -H2AX in 20-25% of the cells at 1 hr and increased γ -H2AX further (40-45%) at 24 hr. The combination of SB939 and irradiation significantly increased γ -H2AX (80%) at 1 hr compared to SB939 or irradiation alone. Importantly, activation of γ -H2AX in response to the combination of SB939 and irradiation was sustained for at least 24 hr in 70% of the cells, suggesting that cells were unable to recover from extensive DNA damage induced by the combination of SB939 and irradiation (Figure 5.16).

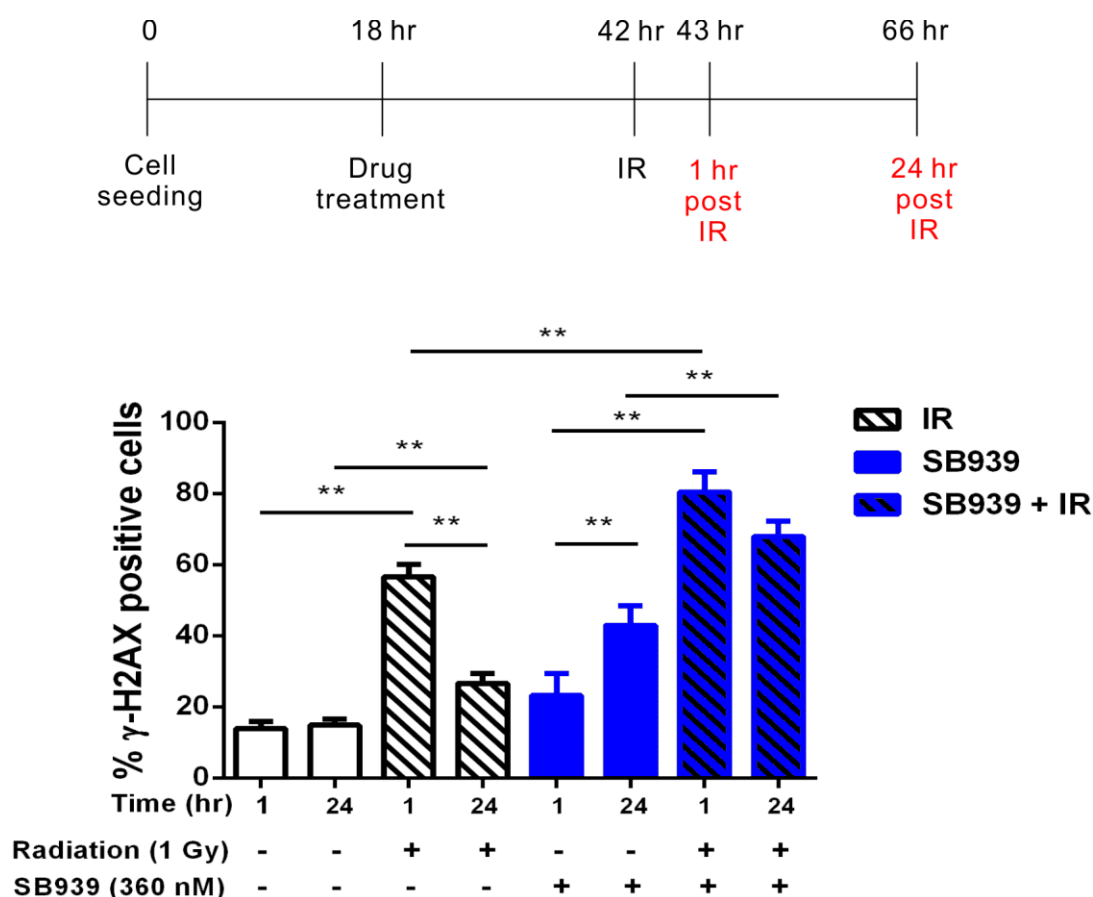


Figure 5.16 SB939 radiosensitises MDA-MB-231Br cells

MDA-MB-231Br cells (4×10^4 /well) were seeded in chamber slides, allowed to adhere for 18 hr at 37°C and treated with SB939 (360 nM) for 24 hr. Cells were irradiated with

1 Gy and incubated for an additional 1 hr or 24 hr at 37°C before analysis of γ -H2AX foci formation by immunofluorescence (top panel). SB939 increased γ -H2AX (a marker for DNA double strands breaks) in MDA-MB-231Br cells when combined with radiation compared to untreated control, radiation alone or SB939 alone at 1 hr and 24 hr. SB939 induced sustained expression of γ -H2AX for up to 24 hr when used alone or in combination with radiation (bottom panel). Data show a representative experiment ($n=3$) and expressed as means \pm SEM of six fields of view (2 replicates well X 3 fields of view per condition). p -values were calculated using a Student t -test. $**p<0.01$. IR, irradiation.

Treatment with 1179.4b alone or in combination with irradiation showed a very similar pattern of DNA damage as SB939 shown in Figure 5.16. 1179.4b alone was also sufficient to induce γ -H2AX in 25% of the cells at 1 hr and increased γ -H2AX further (50%) at 24 hr (Figure 5.17). The combination of 1179.4b and irradiation significantly increased γ -H2AX (90%) at 1 hr compared to 1179.4b or irradiation alone. Importantly, activation of γ -H2AX in response to the combination of 1179.4b and irradiation was sustained for at least 24 hr in 75-80% of the cells, suggesting that the majority of cells treated with 1179.4b + IR were unable to recover from extensive DNA damage, as observed with the SB939 + IR combination.

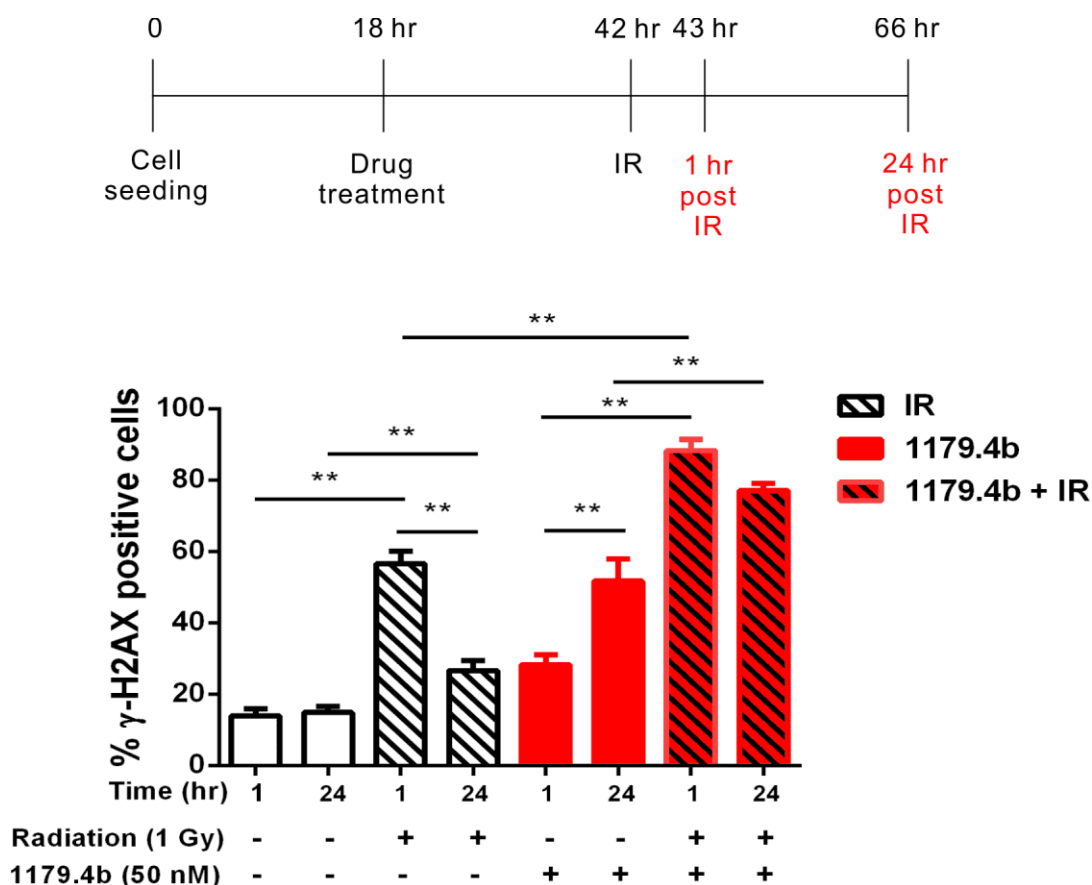


Figure 5.17 1179.4b radiosensitises MDA-MB-231Br cells

MDA-MB-231Br cells (4×10^4 /well) were seeded in chamber slides, allowed to adhere for 18 hr at 37°C and treated with 1179.4b (50 nM) for 24 hr. Cells were irradiated with 1 Gy and incubated for an additional 1 hr or 24 hr at 37°C before analysis of γ -H2AX foci formation by immunofluorescence (top panel). 1179.4b increased γ -H2AX (a marker for DNA double strands breaks) in MDA-MB-231Br cells when combined with radiation compared to untreated control, radiation alone or 1179.4b alone at 1 hr and 24 hr. 1179.4b induced sustained expression of γ -H2AX for up to 24 hr when used alone or in combination with radiation (bottom panel). Data show a representative experiment ($n=3$) and expressed as means \pm SEM of six fields of view (2 replicates well X 3 fields of view per condition). p -values were calculated using a Student t -test. ** $p < 0.01$. IR, irradiation.

5.3 Discussion

The median survival of patients with brain metastases is 1-2 months if untreated. Despite advances in therapies for breast cancer patients, the incidence of patients developing brain metastases remains high and is increasing. This has been attributed to the fact that current therapies extend life primarily by controlling visceral metastases but have limited efficacy against late-stage brain metastases. In addition, most chemotherapeutic agents used for the treatment of brain metastases have limited BBB permeability. Moreover, whereas hormone (ER or PR) and/or HER2 receptor-positive breast cancer patients can benefit from targeted therapies, radiation alone or in combination with chemotherapy are the only option for TNBC patients with brain metastases.

Here, we evaluated the efficacy of two novel HDACi, SB939 and 1179.4b, in clinically relevant models of breast cancer brain metastasis *in vitro* and *in vivo*. Until now, neither compound had been tested for the treatment of breast cancer or brain metastasis *in vivo*. We firstly investigated the potency of SB939 and 1179.4b *in vitro* using colony forming and proliferation assays in both mouse (4T1Br4) and human (MDA-MB-231Br) TNBC lines (Figure 5.2 and 5.3). Both SB939 and 1179.4b showed greater cytotoxic and cytostatic effects in these mouse and human breast cancer brain metastatic cell lines compared to SAHA, a HDACi currently being tested in phase 1 clinical trials for the treatment of breast cancer patients with brain metastases. Our results in brain-metastatic breast tumour lines are in agreement with the study by Novotny-Diermayr et al. (Novotny-Diermayr et al., 2010) showing that SB939 was more potent than SAHA in various cancer cell lines including colon, ovarian, prostate and breast cancers *in vitro*.

Our study is the first to show that SB939 (50 mg/kg) or 1179.4b (20 mg/kg) significantly inhibits the orthotopic growth of brain-metastatic breast tumours (Figure 5.9). Whilst we have yet to investigate the specific mechanisms and signalling pathways by which SB939 and 1179.4b exert their inhibitory effects *in vivo*, our data suggest that the significant reduction in tumour growth observed *in vivo* may be mediated in part by inhibition of histone H3 deacetylation as seen *in vitro* (Figure 5.5-5.7) and *in vivo* (Figure 5.10). SB939 inhibits multiple classes of HDACs (classes I, II and IV) (Novotny-Diermayr et al., 2010) whereas 1179.4b strongly inhibits HDAC class I (HDAC 1) and class II (HDAC 6) (Gupta et al., 2010). Park et al. reported that HDAC class I (HDAC 1 and 8) and class II (HDAC 6) have an important role in invasion in breast cancer (Park et al., 2011). In light of these studies, it is reasonable to propose that the potency of

SB939 and 1179.4b in 4T1Br4 and MDA-MB-231Br cells may be explained by their abilities to inhibit both class I and class II HDACs.

Moreover, SB939 and 1179.4b have been reported also to increase the activity of p21 protein and induce cell cycle arrest in colon and lung cancer cells *in vitro*, respectively (Novotny-Diermayr et al., 2010, Kahnberg et al., 2006). This observation is consistent with the potent cytostatic (and cytotoxic) effect of SB939 and 1179.4b observed in colony forming assays (Figure 5.4) and suggests that SB939 and 1179.4b may also increase p21 function in 4T1Br4 cells. This possibility remains to be investigated.

Interestingly, strong acetylation of histone H3 *in vitro* was detected only 24 hr after single treatment of 4T1Br4 cells with SB939 or 1179.4b (Figure 5.6). Moreover, the effect of SB939 and 1179.4b was reversible and histone H3 was rapidly deacetylated upon removal of SB939 (<1 hr) or 1179.4b (<8 hr) *in vitro* (Figure 5.7). This contrasts the high acetylation level seen in primary tumours analysed 1 hr after the last treatment (Figure 5.10). These observations suggest that SB939 and 1179.4b may accumulate and induce sustained acetylation of histone H3 in primary tumours following daily treatment and that this dosage regimen is sufficient to achieve potent inhibition of 4T1Br4 tumour growth. This is consistent with the greater potency of SB939 shown in HCT116 (human colon cancer) xenograft tumours (Novotny-Diermayr et al., 2010) and the reports on the drug's excellent pharmacokinetic (Jayaraman et al., 2011) and pharmacodynamic (Razak et al., 2011) properties. Additional studies are warranted to evaluate the complete pharmacokinetic/pharmacodynamic properties of 1179.4b *in vivo*.

To our knowledge, our study is also the first to demonstrate that SB939 and 1179.4b significantly inhibit spontaneous metastasis to bone (Figure 5.9). Given that SB939 and 1179.4b also inhibited primary tumour growth in this experiment, it is unclear whether reduced bone metastasis is attributable to reduced metastatic spread from smaller tumours or a direct effect of these inhibitors on the growth of metastases in bone or both. Interestingly, a recent study showed that 1179.4b potentially inhibits osteoclast bone resorption activity *in vitro* (Cantley et al., 2011). Osteoclasts are important mediators of osteolytic activity and bone loss associated with the development of breast cancer bone metastases (Yin et al., 2005). Together, these studies and ours suggest that, in addition to their direct inhibitory effect on tumour cells, inhibition of osteoclast function by pan-HDACi such as 1179.4b may further contribute to the potent inhibition of bone metastasis observed in the 4T1Br4 model. Future studies should confirm these observations in mouse and human xenograft models *in vivo*.

In the subsequent series of *in vivo* experiments investigating the effect of SB939 and 1179.4b on the development of brain metastases, primary tumours were resected when they reached ~0.5 g, to allow more time for the development of brain lesions (33 days) (Fig 5.11). To specifically test the impact of SB939 and 1179.4b on the ability to home and colonise the brain, treatment with SB939 (50 mg/kg) and 1179.4b (10 mg/kg) was initiated after tumour resection. Two weeks after drug treatment commenced, spontaneous 4T1Br4 brain macrometastases of 4T1Br4 decreased from 45% of control mice to 18% (SB939) and 8% (1179.4b) (Figure 5.12). These results demonstrate conclusively that SB939 and 1179.4b potentially inhibit brain metastases even when treatment is initiated after surgical removal of the primary tumour and dissemination of 4T1Br4 cells. It was not possible to determine whether spontaneous brain micrometastases were already present prior to the beginning of HDACi treatment started due to the limited mCherry fluorescence signal in micro-lesions. Thus, further investigations are warranted to confirm whether these HDACi effectively kill circulating breast cancer cells in the vasculature before they home to and colonise the brain (preventive effect) or directly inhibit established brain metastases. The predicted limited permeability of 1179.4b across the BBB, suggests that its effect is likely to be primarily preventive although a direct effect on brain metastases in which the BBB is disrupted, as seen in some patients with TNBC brain metastases (Steeg et al., 2011, Yonemori et al., 2010) cannot be completely ruled out. Further studies using intracardiac injection of luciferase-transduced MDA-MB-231Br cells (experimental metastasis model) would be ideally suited to answer this question. A third possibility is that HDACi could reduce the trans-endothelial migration ability of tumour cells by directly affecting the tightness or viability of endothelial cells of the BBB. This could be tested in *in vitro* transmigration assays by measuring the effect of HDACi pre-treatment on cultured brain endothelial cells prior to addition of tumour cells. To our knowledge, the work presented in this chapter provides the first direct demonstration of the potent anti-tumour and anti-metastatic effects of SB939 and 1179.4b in clinically relevant models of spontaneous TNBC brain metastasis.

Our preliminary evaluation of SB939 and 1179.4b radiosensitising properties indicates that both inhibitors can sensitise 4T1Br4 and MDA-MB-231Br cells to radiation *in vitro* (Figure 5.13-17). To our knowledge, this is the first report demonstrating the radiosensitising properties of SB939 and 1179.4b in brain-metastatic TNBC models. SB939 or 1179.4b alone increased the expression of γ -H2AX at both 1 and 24 hr time points (Figure 5.16-17). The precise mechanisms by which SB939 and 1179.4b directly

induce DNA damage are not fully understood. DNA damage could arise from suppression of DNA repair proteins, such as Rad50 and MRE11, in cancer cells (Lee et al., 2010) or through the generation of reactive oxygen species (Robert and Rassool, 2012). These events would be expected to lead to recruitment and sustained γ -H2AX induction at sites of DNA damage in cancer cells. Sustained induction of γ -H2AX by the combination of either SB939 or 1179.4b and low dose radiation (1 Gy) (Figure 5.16-17) indicates that extensive DNA damage occurs under those conditions and contribute to the anti-tumour effect of SB939 and 1179.4b. Based on these promising results, *in vivo* mouse studies should be initiated to assess whether the same combination could improve the response of established brain metastases to WBRT in mouse and, if successful, in patients.

In conclusion, we confirmed that HDACi SB939 and 1179.4b showed potent cytotoxic and cytostatic effects in the brain metastatic breast cancer 4T1Br4 and MDA-MB-231Br cell lines *in vitro*. They also significantly reduced not only 4T1Br4 primary tumour growth but also spontaneous bone and brain metastasis *in vivo*. In addition, we observed both HDACi enhance radiosensitivity in both 4T1Br4 and MDA-MB-231br cell lines *in vitro*. These findings provide a strong rationale for further studies exploring the mechanisms of action of SB939 and 1179.4b in metastatic breast cancers and the efficacy of therapies combining WBRT with either of these HDACi for the treatment of brain metastasis from breast cancer or other tumour types.

6. Summary and Conclusion

The increasing incidence of brain metastases in breast cancer patients and their dismal prognosis justifies the need for a more thorough understanding of this incurable disease (Steeg et al., 2011, Eichler et al., 2011, Wadasadawala et al., 2007). However, the lack of clinically relevant models of brain metastasis from breast cancer has limited our ability to investigate its etiology and regulation by intrinsic and extrinsic factors. Clinically relevant models of breast cancer brain metastasis are also urgently needed to test and develop more effective therapies for patients. Current therapies for brain metastases are only palliative and patients' survival remains bleak (Wadasadawala et al., 2007).

In this PhD thesis, we aimed firstly these needs by developing and characterising a syngeneic mouse model of spontaneous breast cancer brain metastasis. For this purpose, we chose the murine 4T1 TNBC mammary carcinoma cell line, known to spontaneously spread to the brain but with a low incidence (Pulaski and Ostrand-Rosenberg, 1998). The resulting 4T1Br4 variant was developed through repeated *in vivo* selection followed by clonal selection *in vitro*. To our knowledge, the 4T1Br4 model gives rise to the highest incidence of spontaneous brain metastasis among all spontaneous metastasis mouse models reported to date. An important attribute of the 4T1Br4 model is that it retains a fully functional immune system known to have an important regulatory role in metastasis (Kitamura et al., 2015, Fitzgerald et al., 2008, He et al., 2006, Loriger and Felding-Habermann, 2010). Immune-competent animal models provide a more clinically relevant setting to investigate metastatic processes and its regulation by the stromal microenvironment. Notably, the results presented in chapter 3 showed that the 4T1Br4 variant line are more adhesive to and more migratory through brain microvascular endothelial cells and more invasive than its 4T1 parental cell line in response to brain derived factors. These properties are likely to contribute to the remarkably high incidence of 4T1Br4 brain metastasis. We also demonstrated, by analysing differential gene expressions, that the 4T1Br4 syngeneic model is genetically relevant to brain metastatic human TNBC. In this context, future studies should focus on investigating the role of genes whose expression was found to be commonly altered in both human breast cancer brain metastasis tissues and 4T1Br4 tumours. In addition, at least seventeen candidate target genes were identified by differential expression analysis between parental 4T1 and 4T1Br4 tumours.

Among these genes, we investigated the prognostic significance of limitrin and found that its expression (mRNA and protein) is elevated in brain metastatic mouse (4T1Br4) and human (MDA-MB-231Br) TNBC cell lines compared to non-brain metastatic breast cancer cell lines and tumours. While consistent with our initial hypothesis, further validation of limitrin's prognostic significance and association with TNBC brain metastasis will be required. Analysis of limitrin expression in large cohorts of patients with known clinical outcome is currently underway. However, due to time limitation, completion of this analysis will extend beyond my PhD project. If our study confirms the association between limitrin and TNBC brain metastasis, our work could pave the way towards identifying patients at higher risk of developing brain metastases, before the disease progresses to the brain when therapeutic options are limited.

Another aspect of our study was to investigate the function of limitrin in brain metastasis of breast cancer. Importantly, we demonstrated for the first time that limitrin plays a significant role in promoting trans-endothelial migration of brain metastatic cells *in vitro*. While these *in vitro* findings are consistent with the proposed role of limitrin in promoting tumour cell migration through the BBB, data from *in vivo* experiments were inconclusive due to the unexpectedly high level of liver and lung metastasis from MDA-MB-231Br cells. We propose that this may be due to the use of NSG mice in our study providing a permissive environment for metastasis to these organs before the development of overt brain metastases. Optimisation of this model, including reducing the number of cells injected or the use of less severely compromised mice (SCID or nude) is needed. If the function of limitrin *in vivo* can be successfully demonstrated, this may open new possibilities to develop potential limitrin-targeting inhibitors for TNBC patients with brain metastases. One potential caveat, however, could be that systemic delivery of limitrin inhibitors may also disrupt the BBB since limitrin is expressed in the endfeet of astrocytes in the brain (Yonezawa et al., 2003). In this regard, a good strategy could be to deliver inhibitors that specifically target tumour limitrin or as discussed in chapter 4 integrin β 3. Alternatively therapies could aim to target limitrin in primary tumours or in circulating tumour cells before they reach the brain.

Lastly, we made use of the 4T1Br4 and MDA-MB-231Br models as platforms to test two novel HDACi (SB939 and 1179.4b) for their effects on brain metastasis of breast cancer cells *in vitro* and *in vivo*. Neither SB939 nor 1179.4b had been used for the study of breast cancer or brain metastasis *in vivo*. From our results, both HDACi showed potent cytotoxic and cytostatic effects in both 4T1Br4 and MDA-MB-231Br cells *in vitro* and significantly reduced primary tumour growth and spontaneous brain

metastases of 4T1Br4 *in vivo*. Further studies are warranted to clarify whether these inhibitors kill brain metastatic cells in the vasculature before they colonise the brain or decrease actual brain metastases. To answer this question, drug treatments should start after confirmation of the presence of brain metastases by luciferase imaging of using spontaneous or experimental models.

While patients with brain cancer or brain metastases are commonly treated with WBRT (Eichler and Loeffler, 2007), radiation is typically accompanied by toxicity to the normal tissue and impairment of cognitive functions in patients (Chargari et al., 2010, Welzel et al., 2008). In this context, developing therapeutic agents with radiosensitising properties is an effective strategy to increase the efficacy of radiation therapy while minimising the side effects of WBRT (Chung et al., 2009, Russo et al., 2009, Morgan et al., 2010, Gerster et al., 2010). Our study is the first to report that SB939 and 1179.4b radiosensitised both 4T1Br4 and MDA-MB-231Br cell lines *in vitro*. Further studies on the combination of either of these two HDACi and radiation in primary tumour and brain metastases of TNBC are strongly warranted.

In conclusion, we have developed and characterised a robust mouse model of spontaneous breast cancer brain metastasis. The 4T1Br4 model closely recapitulates the metastatic process and the contribution of the immune system. The model also gives rise to high incidence of brain metastases enabling testing of experimental therapies targeting novel molecular targets. The 4T1Br4 is therefore an ideal platform to investigate mechanisms regulating brain metastasis from breast cancer, to investigate potential prognostic/therapeutic target including limitrin, and to test novel therapies against TNBC brain metastases such as novel HDACi (SB939 and 1179.4b) as presented in chapter 5.

Bibliography

- ABBOTT, N. J., PATABENDIGE, A. A., DOLMAN, D. E., YUSOF, S. R. & BEGLEY, D. J. 2010. Structure and function of the blood-brain barrier. *Neurobiol Dis*, 37, 13-25.
- ABBRUSCATO, T. J. & DAVIS, T. P. 1999. Protein expression of brain endothelial cell E-cadherin after hypoxia/aglycemia: influence of astrocyte contact. *Brain Res*, 842, 277-86.
- ABREY, L. E., OLSON, J. D., RAIZER, J. J., MACK, M., RODAVITCH, A., BOUTROS, D. Y. & MALKIN, M. G. 2001. A phase II trial of temozolomide for patients with recurrent or progressive brain metastases. *J Neurooncol*, 53, 259-65.
- ADAMO, B., DEAL, A. M., BURROWS, E., GERADTS, J., HAMILTON, E., BLACKWELL, K. L., LIVASY, C., FRITCHIE, K., PRAT, A., HARRELL, J. C., EWEND, M. G., CAREY, L. A., MILLER, C. R. & ANDERS, C. K. 2011. Phosphatidylinositol 3-kinase pathway activation in breast cancer brain metastases. *Breast Cancer Res*, 13, R125.
- AGRAWAL, S., ANDERSON, P., DURBEEJ, M., VAN ROOIJEN, N., IVARS, F., OPDENAKKER, G. & SOROKIN, L. M. 2006. Dystroglycan is selectively cleaved at the parenchymal basement membrane at sites of leukocyte extravasation in experimental autoimmune encephalomyelitis. *J Exp Med*, 203, 1007-19.
- ALKINS, R. D., BRODERSEN, P. M., SODHI, R. N. & HYNYNEN, K. 2013. Enhancing drug delivery for boron neutron capture therapy of brain tumors with focused ultrasound. *Neuro Oncol*, 15, 1225-35.
- ALLISON, K. H. 2012. Molecular pathology of breast cancer: what a pathologist needs to know. *Am J Clin Pathol*, 138, 770-80.
- ALSIDAWI, S., MALEK, E. & DRISCOLL, J. J. 2014. MicroRNAs in brain metastases: potential role as diagnostics and therapeutics. *Int J Mol Sci*, 15, 10508-26.
- ANDERS, C. K. & CAREY, L. A. 2009. Biology, metastatic patterns, and treatment of patients with triple-negative breast cancer. *Clin Breast Cancer*, 9 Suppl 2, S73-81.
- ANDRE, F. & ZIELINSKI, C. C. 2012. Optimal strategies for the treatment of metastatic triple-negative breast cancer with currently approved agents. *Ann Oncol*, 23 Suppl 6, vi46-51.
- ANDREWS, D. W., SCOTT, C. B., SPERDUTO, P. W., FLANDERS, A. E., GASPAR, L. E., SCHELL, M. C., WERNER-WASIK, M., DEMAS, W., RYU, J., BAHARY, J. P., SOUHAMI, L., ROTMAN, M., MEHTA, M. P. & CURRAN, W. J., JR. 2004. Whole brain radiation therapy with or without stereotactic radiosurgery boost for patients with one to three brain metastases: phase III results of the RTOG 9508 randomised trial. *Lancet*, 363, 1665-72.
- AOYAMA, H., SHIRATO, H., TAGO, M., NAKAGAWA, K., TOYODA, T., HATANO, K., KENJYO, M., OYA, N., HIROTA, S., SHIOURA, H., KUNIEDA, E., INOMATA, T., HAYAKAWA, K., KATOH, N. & KOBASHI, G. 2006. Stereotactic radiosurgery plus whole-brain radiation therapy vs stereotactic radiosurgery alone for treatment of brain metastases: a randomized controlled trial. *JAMA*, 295, 2483-91.
- ASLAKSON, C. J. & MILLER, F. R. 1992. Selective events in the metastatic process defined by analysis of the sequential dissemination of subpopulations of a mouse mammary tumor. *Cancer Res*, 52, 1399-405.
- ATADJA, P. 2009. Development of the pan-DAC inhibitor panobinostat (LBH589): successes and challenges. *Cancer Lett*, 280, 233-41.
- AUSTRALIAN INSTITUTE OF HEALTH AND WELFARE 2014. Cancer in Australia: an overview 2014. CAN 75.
- BACHELOT, T., ROMIEU, G., CAMPONE, M., DIERAS, V., CROPET, C., DALENC, F., JIMENEZ, M., LE RHUN, E., PIERGA, J. Y., GONCALVES, A., LEHEURTEUR, M., DOMONT, J., GUTIERREZ, M., CURE, H., FERRERO, J. M. & LABBE-DEVILLIERS, C. 2013. Lapatinib plus capecitabine in

patients with previously untreated brain metastases from HER2-positive metastatic breast cancer (LANDSCAPE): a single-group phase 2 study. *Lancet Oncol*, 14, 64-71.

- BAETEN, K. M. & AKASSOGLU, K. 2011. Extracellular matrix and matrix receptors in blood-brain barrier formation and stroke. *Dev Neurobiol*, 71, 1018-39.
- BAILEY-DOWNS, L. C., THORPE, J. E., DISCH, B. C., BASTIAN, A., HAUSER, P. J., FARASYN, T., BERRY, W. L., HURST, R. E. & IHNAT, M. A. 2014. Development and characterization of a preclinical model of breast cancer lung micrometastatic to macrometastatic progression. *PLoS One*, 9, e98624.
- BALASUBRAMANIAN, S., VERNER, E. & BUGGY, J. J. 2009. Isoform-specific histone deacetylase inhibitors: the next step? *Cancer Lett*, 280, 211-21.
- BALLABH, P., BRAUN, A. & NEDERGAARD, M. 2004. The blood-brain barrier: an overview: structure, regulation, and clinical implications. *Neurobiol Dis*, 16, 1-13.
- BARLESI, F., GERVAIS, R., LENA, H., HUREAUX, J., BERARD, H., PAILLOTIN, D., BOTA, S., MONNET, I., CHAJARA, A. & ROBINET, G. 2011. Pemetrexed and cisplatin as first-line chemotherapy for advanced non-small-cell lung cancer (NSCLC) with asymptomatic inoperable brain metastases: a multicenter phase II trial (GFPC 07-01). *Ann Oncol*, 22, 2466-70.
- BARTELT, S., MOMM, F., WEISSENBERGER, C. & LUTTERBACH, J. 2004. Patients with brain metastases from gastrointestinal tract cancer treated with whole brain radiation therapy: prognostic factors and survival. *World J Gastroenterol*, 10, 3345-8.
- BARTSCH, R., ROTTENFUSSER, A., WENZEL, C., DIECKMANN, K., PLUSCHNIG, U., ALTORJAI, G., RUDAS, M., MADER, R. M., POETTER, R., ZIELINSKI, C. C. & STEGER, G. G. 2007. Trastuzumab prolongs overall survival in patients with brain metastases from Her2 positive breast cancer. *J Neurooncol*, 85, 311-7.
- BASCHNAGEL, A., RUSSO, A., BURGAN, W. E., CARTER, D., BEAM, K., PALMIERI, D., STEEG, P. S., TOFILON, P. & CAMPHAUSEN, K. 2009. Vorinostat enhances the radiosensitivity of a breast cancer brain metastatic cell line grown in vitro and as intracranial xenografts. *Mol Cancer Ther*, 8, 1589-95.
- BASELGA, J., BRADBURY, I., EIDTMANN, H., DI COSIMO, S., DE AZAMBUJA, E., AURA, C., GOMEZ, H., DINH, P., FAURIA, K., VAN DOOREN, V., AKTAN, G., GOLDBIRSCHE, A., CHANG, T. W., HORVATH, Z., COCCIA-PORTUGAL, M., DOMONT, J., TSENG, L. M., KUNZ, G., SOHN, J. H., SEMIGLAZOV, V., LERZO, G., PALACOVA, M., PROBACHAI, V., PUSZTAI, L., UNTCH, M., GELBER, R. D., PICCART-GEBHART, M. & NEO, A. S. T. 2012. Lapatinib with trastuzumab for HER2-positive early breast cancer (NeoALTTO): a randomised, open-label, multicentre, phase 3 trial. *Lancet*, 379, 633-40.
- BASHIR, A., HODGE, C. J., JR., DABABNEH, H., HUSSAIN, M., HAHN, S. & CANUTE, G. W. 2014. Impact of the number of metastatic brain lesions on survival after Gamma Knife radiosurgery. *J Clin Neurosci*, 21, 1928-33.
- BATOVA, A., SHAO, L. E., DICCIANNI, M. B., YU, A. L., TANAKA, T., REPHAELI, A., NUDELMAN, A. & YU, J. 2002. The histone deacetylase inhibitor AN-9 has selective toxicity to acute leukemia and drug-resistant primary leukemia and cancer cell lines. *Blood*, 100, 3319-24.
- BAZZONI, G., MARTINEZ-ESTRADA, O. M., MUELLER, F., NELBOECK, P., SCHMID, G., BARTFAI, T., DEJANA, E. & BROCKHAUS, M. 2000. Homophilic interaction of junctional adhesion molecule. *J Biol Chem*, 275, 30970-6.
- BEAVON, I. R. 2000. The E-cadherin-catenin complex in tumour metastasis: structure, function and regulation. *Eur J Cancer*, 36, 1607-20.
- BERNARDI, R. & GIANNI, L. 2014. Hallmarks of triple negative breast cancer emerging at last? *Cell Res*, 24, 904-5.
- BERTUCCI, F., FINETTI, P., CERVERA, N., ESTERNI, B., HERMITTE, F., VIENS, P. & BIRNBAUM, D. 2008. How basal are triple-negative breast cancers? *Int J Cancer*, 123, 236-40.

- BLACKWELL, K. L., BURSTEIN, H. J., STORNILO, A. M., RUGO, H. S., SLEDGE, G., AKTAN, G., ELLIS, C., FLORANCE, A., VUKELJA, S., BISCHOFF, J., BASELGA, J. & O'SHAUGHNESSY, J. 2012. Overall survival benefit with lapatinib in combination with trastuzumab for patients with human epidermal growth factor receptor 2-positive metastatic breast cancer: final results from the EGF104900 Study. *J Clin Oncol*, 30, 2585-92.
- BLANCHARD, D. K., SHETTY, P. B., HILSENBECK, S. G. & ELLEDGE, R. M. 2008. Association of surgery with improved survival in stage IV breast cancer patients. *Ann Surg*, 247, 732-8.
- BLECHARZ, K. G., COLLA, R., ROHDE, V. & VAJKOCZY, P. 2015. Control of the blood-brain barrier function in cancer cell metastasis. *Biol Cell*, 107, 342-71.
- BOLDEN, J. E., PEART, M. J. & JOHNSTONE, R. W. 2006. Anticancer activities of histone deacetylase inhibitors. *Nat Rev Drug Discov*, 5, 769-84.
- BOOGERD, W., DALESIO, O., BAIS, E. M. & VAN DER SANDE, J. J. 1992. Response of brain metastases from breast cancer to systemic chemotherapy. *Cancer*, 69, 972-80.
- BORST, P., EVERS, R., KOOL, M. & WIJNHOLDS, J. 2000. A family of drug transporters: the multidrug resistance-associated proteins. *J Natl Cancer Inst*, 92, 1295-302.
- BOS, P. D., ZHANG, X. H., NADAL, C., SHU, W., GOMIS, R. R., NGUYEN, D. X., MINN, A. J., VAN DE VIJVER, M. J., GERALD, W. L., FOEKENS, J. A. & MASSAGUE, J. 2009. Genes that mediate breast cancer metastasis to the brain. *Nature*, 459, 1005-9.
- BOURIS, P., SKANDALIS, S. S., PIPERIGKOU, Z., AFRATIS, N., KARAMANOU, K., ALETRAS, A. J., MOUSTAKAS, A., THEOCHARIS, A. D. & KARAMANOS, N. K. 2015. Estrogen receptor alpha mediates epithelial to mesenchymal transition, expression of specific matrix effectors and functional properties of breast cancer cells. *Matrix Biol*, 43, 42-60.
- BRAND, T. M., IIDA, M., LI, C. & WHEELER, D. L. 2011. The nuclear epidermal growth factor receptor signaling network and its role in cancer. *Discov Med*, 12, 419-32.
- BRASTIANOS, P. K., CARTER, S. L., SANTAGATA, S., CAHILL, D. P., TAYLOR-WEINER, A., JONES, R. T., VAN ALLEN, E. M., LAWRENCE, M. S., HOROWITZ, P. M., CIBULSKIS, K., LIGON, K. L., TABERNERO, J., SEOANE, J., MARTINEZ-SAEZ, E., CURRY, W. T., DUNN, I. F., PAEK, S. H., PARK, S. H., MCKENNA, A., CHEVALIER, A., ROSENBERG, M., BARKER, F. G., 2ND, GILL, C. M., VAN HUMMELEN, P., THORNER, A. R., JOHNSON, B. E., HOANG, M. P., CHOUAIRI, T. K., SIGNORETTI, S., SOUGNEZ, C., RABIN, M. S., LIN, N. U., WINER, E. P., STEMMER-RACHAMIMOV, A., MEYERSON, M., GARRAWAY, L., GABRIEL, S., LANDER, E. S., BEROUKHIM, R., BATCHELOR, T. T., BASELGA, J., LOUIS, D. N., GETZ, G. & HAHN, W. C. 2015. Genomic Characterization of Brain Metastases Reveals Branched Evolution and Potential Therapeutic Targets. *Cancer Discov*, 5, 1164-77.
- BREEDVELD, P., PLUIM, D., CIPRIANI, G., WIELINGA, P., VAN TELLINGEN, O., SCHINKEL, A. H. & SCHELLENS, J. H. 2005. The effect of Bcrp1 (Abcg2) on the in vivo pharmacokinetics and brain penetration of imatinib mesylate (Gleevec): implications for the use of breast cancer resistance protein and P-glycoprotein inhibitors to enable the brain penetration of imatinib in patients. *Cancer Res*, 65, 2577-82.
- BRENNAN, K., MCSHERRY, E. A., HUDSON, L., KAY, E. W., HILL, A. D., YOUNG, L. S. & HOPKINS, A. M. 2013. Junctional adhesion molecule-A is co-expressed with HER2 in breast tumors and acts as a novel regulator of HER2 protein degradation and signaling. *Oncogene*, 32, 2799-804.
- BRIA, E., CUPPONE, F., FORNIER, M., NISTICO, C., CARLINI, P., MILELLA, M., SPERDUTI, I., TERZOLI, E., COGNETTI, F. & GIANNARELLI, D. 2008. Cardiotoxicity and incidence of brain metastases after adjuvant trastuzumab for early breast cancer: the dark side of the moon? A meta-analysis of the randomized trials. *Breast Cancer Res Treat*, 109, 231-9.
- BROWN, R. C. & DAVIS, T. P. 2002. Calcium modulation of adherens and tight junction function: a potential mechanism for blood-brain barrier disruption after stroke. *Stroke*, 33, 1706-11.
- BRUFISKY, A. M., MAYER, M., RUGO, H. S., KAUFMAN, P. A., TAN-CHIU, E., TRIPATHY, D., TUDOR, I. C., WANG, L. I., BRAMMER, M. G., SHING, M., YOOD, M. U. & YARDLEY, D. A. 2011. Central nervous system metastases in patients with HER2-positive metastatic breast cancer: incidence,

- treatment, and survival in patients from registHER. *Clin Cancer Res*, 17, 4834-43.
- BUNDRED, N. 2005. Preclinical and clinical experience with fulvestrant (Faslodex) in postmenopausal women with hormone receptor-positive advanced breast cancer. *Cancer Invest*, 23, 173-81.
- BUTLER, K. V. & KOZIKOWSKI, A. P. 2008. Chemical origins of isoform selectivity in histone deacetylase inhibitors. *Curr Pharm Des*, 14, 505-28.
- BUTLER, L. M., WEBB, Y., AGUS, D. B., HIGGINS, B., TOLENTINO, T. R., KUTKO, M. C., LAQUAGLIA, M. P., DROBNJAK, M., CORDON-CARDO, C., SCHER, H. I., BRESLOW, R., RICHON, V. M., RIFKIND, R. A. & MARKS, P. A. 2001. Inhibition of transformed cell growth and induction of cellular differentiation by pyroxamide, an inhibitor of histone deacetylase. *Clin Cancer Res*, 7, 962-70.
- BUTT, A. M., JONES, H. C. & ABBOTT, N. J. 1990. Electrical resistance across the blood-brain barrier in anaesthetized rats: a developmental study. *J Physiol*, 429, 47-62.
- CAMERON, M. D., SCHMIDT, E. E., KERKVIET, N., NADKARNI, K. V., MORRIS, V. L., GROOM, A. C., CHAMBERS, A. F. & MACDONALD, I. C. 2000. Temporal progression of metastasis in lung: cell survival, dormancy, and location dependence of metastatic inefficiency. *Cancer Res*, 60, 2541-6.
- CANTLEY, M. D., BARTOLD, P. M., MARINO, V., FAIRLIE, D. P., LE, G. T., LUCKE, A. J. & HAYNES, D. R. 2011. Histone deacetylase inhibitors and periodontal bone loss. *J Periodontal Res*, 46, 697-703.
- CARBONELL, W. S., ANSORGE, O., SIBSON, N. & MUSCHEL, R. 2009. The vascular basement membrane as "soil" in brain metastasis. *PLoS One*, 4, e5857.
- CARDAMONE, M. D., BARDELLA, C., GUTIERREZ, A., DI CROCE, L., ROSENFELD, M. G., DI RENZO, M. F. & DE BORTOLI, M. 2009. ERalpha as ligand-independent activator of CDH-1 regulates determination and maintenance of epithelial morphology in breast cancer cells. *Proc Natl Acad Sci U S A*, 106, 7420-5.
- CAREY, L. A., DEES, E. C., SAWYER, L., GATTI, L., MOORE, D. T., COLLICHIO, F., OLLILA, D. W., SARTOR, C. I., GRAHAM, M. L. & PEROU, C. M. 2007. The triple negative paradox: primary tumor chemosensitivity of breast cancer subtypes. *Clin Cancer Res*, 13, 2329-34.
- CAREY, L. A., RUGO, H. S., MARCOM, P. K., MAYER, E. L., ESTEVA, F. J., MA, C. X., LIU, M. C., STORNILOLO, A. M., RIMAWI, M. F., FORERO-TORRES, A., WOLFF, A. C., HOBDDAY, T. J., IVANOVA, A., CHIU, W. K., FERRARO, M., BURROWS, E., BERNARD, P. S., HOADLEY, K. A., PEROU, C. M. & WINER, E. P. 2012. TBCRC 001: randomized phase II study of cetuximab in combination with carboplatin in stage IV triple-negative breast cancer. *J Clin Oncol*, 30, 2615-23.
- CARTER, R. Z., MICOCCI, K. C., NATOLI, A., REDVERS, R. P., PAQUET-FIFIELD, S., MARTIN, A. C., DENOYER, D., LING, X., KIM, S. H., TOMASIN, R., SELISTRE-DE-ARAUJO, H., ANDERSON, R. L. & POULIOT, N. 2015. Tumour but not stromal expression of beta3 integrin is essential, and is required early, for spontaneous dissemination of bone-metastatic breast cancer. *J Pathol*, 235, 760-72.
- CHAMBERS, A. F., GROOM, A. C. & MACDONALD, I. C. 2002. Dissemination and growth of cancer cells in metastatic sites. *Nat Rev Cancer*, 2, 563-72.
- CHANG, E. L. & LO, S. 2003. Diagnosis and management of central nervous system metastases from breast cancer. *Oncologist*, 8, 398-410.
- CHANG, E. L., WEFEL, J. S., HESS, K. R., ALLEN, P. K., LANG, F. F., KORNGUTH, D. G., ARBUCKLE, R. B., SWINT, J. M., SHIU, A. S., MAOR, M. H. & MEYERS, C. A. 2009. Neurocognition in patients with brain metastases treated with radiosurgery or radiosurgery plus whole-brain irradiation: a randomised controlled trial. *Lancet Oncol*, 10, 1037-44.
- CHARGARI, C., CAMPANA, F., PIERGA, J. Y., VEDRINE, L., RICARD, D., LE MOULEC, S., FOURQUET, A. & KIROVA, Y. M. 2010. Whole-brain radiation therapy in breast cancer patients with brain metastases. *Nat Rev Clin Oncol*, 7, 632-40.
- CHAVAKIS, T., KEIPER, T., MATZ-WESTPHAL, R., HERSEMAYER, K., SACHS, U. J., NAWROTH, P. P.,

- PREISSNER, K. T. & SANTOSO, S. 2004. The junctional adhesion molecule-C promotes neutrophil transendothelial migration in vitro and in vivo. *J Biol Chem*, 279, 55602-8.
- CHEANG, M. C., VODUC, D., BAJDIK, C., LEUNG, S., MCKINNEY, S., CHIA, S. K., PEROU, C. M. & NIELSEN, T. O. 2008. Basal-like breast cancer defined by five biomarkers has superior prognostic value than triple-negative phenotype. *Clin Cancer Res*, 14, 1368-76.
- CHEN, C. S., WANG, Y. C., YANG, H. C., HUANG, P. H., KULP, S. K., YANG, C. C., LU, Y. S., MATSUYAMA, S., CHEN, C. Y. & CHEN, C. S. 2007. Histone deacetylase inhibitors sensitize prostate cancer cells to agents that produce DNA double-strand breaks by targeting Ku70 acetylation. *Cancer Res*, 67, 5318-27.
- CHEN, X., LI, J., GRAY, W. H., LEHMANN, B. D., BAUER, J. A., SHYR, Y. & PIETENPOL, J. A. 2012. TNBCtype: A Subtyping Tool for Triple-Negative Breast Cancer. *Cancer Inform*, 11, 147-56.
- CHEN, Y. L., CHENG, W. F., HSIEH, C. Y. & CHEN, C. A. 2011. Brain metastasis as a late manifestation of ovarian carcinoma. *Eur J Cancer Care (Engl)*, 20, 44-9.
- CHENG, X. & HUNG, M. C. 2007. Breast cancer brain metastases. *Cancer Metastasis Rev*, 26, 635-43.
- CHIU, H. W., YEH, Y. L., WANG, Y. C., HUANG, W. J., CHEN, Y. A., CHIOU, Y. S., HO, S. Y., LIN, P. & WANG, Y. J. 2013. Suberoylanilide hydroxamic acid, an inhibitor of histone deacetylase, enhances radiosensitivity and suppresses lung metastasis in breast cancer in vitro and in vivo. *PLoS One*, 8, e76340.
- CHIU, P. S. & LAI, S. C. 2013. Matrix metalloproteinase-9 leads to claudin-5 degradation via the NF-kappaB pathway in BALB/c mice with eosinophilic meningoencephalitis caused by *Angiostrongylus cantonensis*. *PLoS One*, 8, e53370.
- CHOI, Y. K., WOO, S. M., CHO, S. G., MOON, H. E., YUN, Y. J., KIM, J. W., NOH, D. Y., JANG, B. H., SHIN, Y. C., KIM, J. H., SHIN, H. D., PAEK, S. H. & KO, S. G. 2013. Brain-metastatic triple-negative breast cancer cells regain growth ability by altering gene expression patterns. *Cancer Genomics Proteomics*, 10, 265-75.
- CHUNG, E. J., BROWN, A. P., ASANO, H., MANDLER, M., BURGAN, W. E., CARTER, D., CAMPHAUSEN, K. & CITRIN, D. 2009. In vitro and in vivo radiosensitization with AZD6244 (ARRY-142886), an inhibitor of mitogen-activated protein kinase/extracellular signal-regulated kinase 1/2 kinase. *Clin Cancer Res*, 15, 3050-7.
- CHURCH, D. N., MODGIL, R., GUGLANI, S., BAHL, A., HOPKINS, K., BRAYBROOKE, J. P., BLAIR, P. & PRICE, C. G. 2008. Extended survival in women with brain metastases from HER2 overexpressing breast cancer. *Am J Clin Oncol*, 31, 250-4.
- CISTERNINO, S., ROUSSELLE, C., DAGENAIS, C. & SCHERRMANN, J. M. 2001. Screening of multidrug-resistance sensitive drugs by in situ brain perfusion in P-glycoprotein-deficient mice. *Pharm Res*, 18, 183-90.
- COSOLO, W. C., MARTINELLO, P., LOUIS, W. J. & CHRISTOPHIDIS, N. 1989. Blood-brain barrier disruption using mannitol: time course and electron microscopy studies. *Am J Physiol*, 256, R443-7.
- COUTINHO, E., SILVA, A. M., FREITAS, C. & SANTOS, E. 2011. Graves' disease presenting as pseudotumor cerebri: a case report. *J Med Case Rep*, 5, 68.
- CRESSEY, D. 2010. Translational research: Talking up translation. *Nature*, 463, 422-3.
- CRISCITIELLO, C., AZIM, H. A., JR., SCHOUTEN, P. C., LINN, S. C. & SOTIRIOU, C. 2012. Understanding the biology of triple-negative breast cancer. *Ann Oncol*, 23 Suppl 6, vi13-8.
- CRISCITIELLO, C., FUMAGALLI, D., SAINI, K. S. & LOI, S. 2011. Tamoxifen in early-stage estrogen receptor-positive breast cancer: overview of clinical use and molecular biomarkers for patient selection. *Onco Targets Ther*, 4, 1-11.
- CROXTALL, J. D. & MCKEAGE, K. 2011. Fulvestrant: a review of its use in the management of hormone

- receptor-positive metastatic breast cancer in postmenopausal women. *Drugs*, 71, 363-80.
- CRUZ-MUNOZ, W., MAN, S., XU, P. & KERBEL, R. S. 2008. Development of a preclinical model of spontaneous human melanoma central nervous system metastasis. *Cancer Res*, 68, 4500-5.
- D'ANTONIO, C., PASSARO, A., GORI, B., DEL SIGNORE, E., MIGLIORINO, M. R., RICCIARDI, S., FULVI, A. & DE MARINIS, F. 2014. Bone and brain metastasis in lung cancer: recent advances in therapeutic strategies. *Ther Adv Med Oncol*, 6, 101-14.
- DA SILVA, L., SIMPSON, P. T., SMART, C. E., COCCIARDI, S., WADDELL, N., LANE, A., MORRISON, B. J., VARGAS, A. C., HEALEY, S., BEESLEY, J., PAKKIRI, P., PARRY, S., KURNIAWAN, N., REID, L., KEITH, P., FARIA, P., PEREIRA, E., SKALOVA, A., BILOUS, M., BALLEINE, R. L., DO, H., DOBROVIC, A., FOX, S., FRANCO, M., REYNOLDS, B., KHANNA, K. K., CUMMINGS, M., CHENEVIX-TRENCH, G. & LAKHANI, S. R. 2010. HER3 and downstream pathways are involved in colonization of brain metastases from breast cancer. *Breast Cancer Res*, 12, R46.
- DALL'OLIO, F. & CHIRICOLO, M. 2001. Sialyltransferases in cancer. *Glycoconj J*, 18, 841-50.
- DANEMAN, R. & PRAT, A. 2015. The blood-brain barrier. *Cold Spring Harb Perspect Biol*, 7, a020412.
- DAPHU, I., SUNDSTROM, T., HORN, S., HUSZTHY, P. C., NICLOU, S. P., SAKARIASSEN, P. O., IMMERVOLL, H., MILETIC, H., BJERKVIG, R. & THORSEN, F. 2013. In vivo animal models for studying brain metastasis: value and limitations. *Clin Exp Metastasis*, 30, 695-710.
- DAWOOD, S., BROGLIO, K., ESTEVA, F. J., IBRAHIM, N. K., KAU, S. W., ISLAM, R., ALDAPE, K. D., YU, T. K., HORTOBAGYI, G. N. & GONZALEZ-ANGULO, A. M. 2008. Defining prognosis for women with breast cancer and CNS metastases by HER2 status. *Ann Oncol*, 19, 1242-8.
- DE DUENAS, E. M., HERNANDEZ, A. L., ZOTANO, A. G., CARRION, R. M., LOPEZ-MUNIZ, J. I., NOVOA, S. A., RODRIGUEZ, A. L., FIDALGO, J. A., LOZANO, J. F., GASION, O. B., CARRASCAL, E. C., CAPILLA, A. H., LOPEZ-BARAJAS, I. B., MATEU, M. M., DE CEBALLOS REYNA, M. H., FERRANDO, A. O., JANEZ, N. M., BALLERINI, V. C., TORRES, A. A., CATALAN, G., SAENZ, J. A., MENJON, S. & GONZALEZ-ANGULO, A. M. 2014. Prospective evaluation of the conversion rate in the receptor status between primary breast cancer and metastasis: results from the GEICAM 2009-03 ConvertHER study. *Breast Cancer Res Treat*, 143, 507-15.
- DE VOS, M., SCHREIBER, V. & DANTZER, F. 2012. The diverse roles and clinical relevance of PARPs in DNA damage repair: current state of the art. *Biochem Pharmacol*, 84, 137-46.
- DEEKEN, J. F. & LOSCHER, W. 2007. The blood-brain barrier and cancer: transporters, treatment, and Trojan horses. *Clin Cancer Res*, 13, 1663-74.
- DEJANA, E. 2006. The transcellular railway: insights into leukocyte diapedesis. *Nat Cell Biol*, 8, 105-7.
- DEL MASCHIO, A., DE LUIGI, A., MARTIN-PADURA, I., BROCKHAUS, M., BARTFAI, T., FRUSCELLA, P., ADORINI, L., MARTINO, G., FURLAN, R., DE SIMONI, M. G. & DEJANA, E. 1999. Leukocyte recruitment in the cerebrospinal fluid of mice with experimental meningitis is inhibited by an antibody to junctional adhesion molecule (JAM). *J Exp Med*, 190, 1351-6.
- DELATTRE, J. Y., KROL, G., THALER, H. T. & POSNER, J. B. 1988. Distribution of brain metastases. *Arch Neurol*, 45, 741-4.
- DENOYER, D., LOBACHEVSKY, P., JACKSON, P., THOMPSON, M., MARTIN, O. A. & HICKS, R. J. 2015. Analysis of ¹⁷⁷Lu-DOTA-octreotate therapy-induced DNA damage in peripheral blood lymphocytes of patients with neuroendocrine tumors. *J Nucl Med*, 56, 505-11.
- DENT, R., HANNA, W. M., TRUDEAU, M., RAWLINSON, E., SUN, P. & NAROD, S. A. 2009. Pattern of metastatic spread in triple-negative breast cancer. *Breast Cancer Res Treat*, 115, 423-8.
- DENT, R., TRUDEAU, M., PRITCHARD, K. I., HANNA, W. M., KAHN, H. K., SAWKA, C. A., LICKLEY, L. A., RAWLINSON, E., SUN, P. & NAROD, S. A. 2007. Triple-negative breast cancer: clinical features and patterns of recurrence. *Clin Cancer Res*, 13, 4429-34.
- DEROANNE, C. F., BONJEAN, K., SERVOTTE, S., DEVY, L., COLIGE, A., CLAUSSE, N., BLACHER, S.,

- VERDIN, E., FOIDART, J. M., NUSGENS, B. V. & CASTRONOVO, V. 2002. Histone deacetylases inhibitors as anti-angiogenic agents altering vascular endothelial growth factor signaling. *Oncogene*, 21, 427-36.
- DEXTER, D. L., KOWALSKI, H. M., BLAZAR, B. A., FLIGIEL, Z., VOGEL, R. & HEPNER, G. H. 1978. Heterogeneity of tumor cells from a single mouse mammary tumor. *Cancer Res*, 38, 3174-81.
- DI TOMASO, E., SNUDERL, M., KAMOUN, W. S., DUDA, D. G., AULUCK, P. K., FAZLOLLAHI, L., ANDRONESI, O. C., FROSCHE, M. P., WEN, P. Y., PLOTKIN, S. R., HEDLEY-WHYTE, E. T., SORENSEN, A. G., BATCHELOR, T. T. & JAIN, R. K. 2011. Glioblastoma recurrence after cediranib therapy in patients: lack of "rebound" revascularization as mode of escape. *Cancer Res*, 71, 19-28.
- DIGNAM, J. J., WIEAND, K., JOHNSON, K. A., FISHER, B., XU, L. & MAMOUNAS, E. P. 2003. Obesity, tamoxifen use, and outcomes in women with estrogen receptor-positive early-stage breast cancer. *J Natl Cancer Inst*, 95, 1467-76.
- DIJKERS, E. C., OUDE MUNNINK, T. H., KOSTERINK, J. G., BROUWERS, A. H., JAGER, P. L., DE JONG, J. R., VAN DONGEN, G. A., SCHRODER, C. P., LUB-DE HOOGE, M. N. & DE VRIES, E. G. 2010. Biodistribution of 89Zr-trastuzumab and PET imaging of HER2-positive lesions in patients with metastatic breast cancer. *Clin Pharmacol Ther*, 87, 586-92.
- DOI, M., THYBOLL, J., KORTESMAA, J., JANSSON, K., IIVANAINEN, A., PARVARDEH, M., TIMPL, R., HEDIN, U., SWEDENBORG, J. & TRYGGVASON, K. 2002. Recombinant human laminin-10 (alpha5beta1gamma1). Production, purification, and migration-promoting activity on vascular endothelial cells. *J Biol Chem*, 277, 12741-8.
- DOYLE, L. A., YANG, W., ABRUZZO, L. V., KROGMANN, T., GAO, Y., RISHI, A. K. & ROSS, D. D. 1998. A multidrug resistance transporter from human MCF-7 breast cancer cells. *Proc Natl Acad Sci U S A*, 95, 15665-70.
- DRION, N., LEMAIRE, M., LEFAUCONNIER, J. M. & SCHERRMANN, J. M. 1996. Role of P-glycoprotein in the blood-brain transport of colchicine and vinblastine. *J Neurochem*, 67, 1688-93.
- DU, L., RISINGER, A. L., KING, J. B., POWELL, D. R. & CICHEWICZ, R. H. 2014. A potent HDAC inhibitor, 1-alaninechlamydocin, from a *Tolypocladium* sp. induces G2/M cell cycle arrest and apoptosis in MIA PaCa-2 cells. *J Nat Prod*, 77, 1753-7.
- DUCHNOWSKA, R., DZIADZIUSZKO, R., TROJANOWSKI, T., MANDAT, T., OCH, W., CZARTORYSKA-ARLUKOWICZ, B., RADECKA, B., OLSZEWSKI, W., SZUBSTARSKI, F., KOZLOWSKI, W., JAROSZ, B., ROGOWSKI, W., KOWALCZYK, A., LIMON, J., BIERNAT, W., JASSEM, J. & POLISH BRAIN METASTASIS, C. 2012. Conversion of epidermal growth factor receptor 2 and hormone receptor expression in breast cancer metastases to the brain. *Breast Cancer Res*, 14, R119.
- DUFFY, K. R. & PARDRIDGE, W. M. 1987. Blood-brain barrier transcytosis of insulin in developing rabbits. *Brain Res*, 420, 32-8.
- EARLY BREAST CANCER TRIALISTS' COLLABORATIVE, G. 2005. Effects of chemotherapy and hormonal therapy for early breast cancer on recurrence and 15-year survival: an overview of the randomised trials. *Lancet*, 365, 1687-717.
- ECKHARDT, B. L., FRANCIS, P. A., PARKER, B. S. & ANDERSON, R. L. 2012. Strategies for the discovery and development of therapies for metastatic breast cancer. *Nat Rev Drug Discov*, 11, 479-97.
- ECKHARDT, B. L., PARKER, B. S., VAN LAAR, R. K., RESTALL, C. M., NATOLI, A. L., TAVARIA, M. D., STANLEY, K. L., SLOAN, E. K., MOSELEY, J. M. & ANDERSON, R. L. 2005. Genomic analysis of a spontaneous model of breast cancer metastasis to bone reveals a role for the extracellular matrix. *Mol Cancer Res*, 3, 1-13.
- EICHLER, A. F., CHUNG, E., KODACK, D. P., LOEFFLER, J. S., FUKUMURA, D. & JAIN, R. K. 2011. The biology of brain metastases-translation to new therapies. *Nat Rev Clin Oncol*, 8, 344-56.
- EICHLER, A. F. & LOEFFLER, J. S. 2007. Multidisciplinary management of brain metastases. *Oncologist*,

- EISENBLATTER, T., HUWEL, S. & GALLA, H. J. 2003. Characterisation of the brain multidrug resistance protein (BMDP/ABCG2/BCRP) expressed at the blood-brain barrier. *Brain Res*, 971, 221-31.
- EMERICH, D. F., SNODGRASS, P., DEAN, R., AGOSTINO, M., HASLER, B., PINK, M., XIONG, H., KIM, B. S. & BARTUS, R. T. 1999. Enhanced delivery of carboplatin into brain tumours with intravenous Cereport (RMP-7): dramatic differences and insight gained from dosing parameters. *Br J Cancer*, 80, 964-70.
- ENGELHARDT, B. & WOLBURG, H. 2004. Mini-review: Transendothelial migration of leukocytes: through the front door or around the side of the house? *Eur J Immunol*, 34, 2955-63.
- ERIN, N., KALE, S., TANRIOVER, G., KOKSOY, S., DUYMUS, O. & KORCUM, A. F. 2013. Differential characteristics of heart, liver, and brain metastatic subsets of murine breast carcinoma. *Breast Cancer Res Treat*, 139, 677-89.
- EWING, J. 1922. Neoplastic diseases; a treatise on tumors.
- FALKENBERG, K. J. & JOHNSTONE, R. W. 2014. Histone deacetylases and their inhibitors in cancer, neurological diseases and immune disorders. *Nat Rev Drug Discov*, 13, 673-91.
- FAN, J., CAI, B., ZENG, M., HAO, Y., GIANCOTTI, F. G. & FU, B. M. 2011. Integrin beta4 signaling promotes mammary tumor cell adhesion to brain microvascular endothelium by inducing ErbB2-mediated secretion of VEGF. *Ann Biomed Eng*, 39, 2223-41.
- FAN, J., YIN, W. J., LU, J. S., WANG, L., WU, J., WU, F. Y., DI, G. H., SHEN, Z. Z. & SHAO, Z. M. 2008. ER alpha negative breast cancer cells restore response to endocrine therapy by combination treatment with both HDAC inhibitor and DNMT inhibitor. *J Cancer Res Clin Oncol*, 134, 883-90.
- FARACO, G., PANCANI, T., FORMENTINI, L., MASCAGNI, P., FOSSATI, G., LEONI, F., MORONI, F. & CHIARUGI, A. 2006. Pharmacological inhibition of histone deacetylases by suberoylanilide hydroxamic acid specifically alters gene expression and reduces ischemic injury in the mouse brain. *Mol Pharmacol*, 70, 1876-84.
- FASS, D. M., REIS, S. A., GHOSH, B., HENNIG, K. M., JOSEPH, N. F., ZHAO, W. N., NIELAND, T. J., GUAN, J. S., KUHNLE, C. E., TANG, W., BARKER, D. D., MAZITSCHEK, R., SCHREIBER, S. L., TSAI, L. H. & HAGGARTY, S. J. 2013. Crebinostat: a novel cognitive enhancer that inhibits histone deacetylase activity and modulates chromatin-mediated neuroplasticity. *Neuropharmacology*, 64, 81-96.
- FAZAKAS, C., WILHELM, I., NAGYOSZI, P., FARKAS, A. E., HASKO, J., MOLNAR, J., BAUER, H., BAUER, H. C., AYAYDIN, F., DUNG, N. T., SIKLOS, L. & KRIZBAI, I. A. 2011. Transmigration of melanoma cells through the blood-brain barrier: role of endothelial tight junctions and melanoma-released serine proteases. *PLoS One*, 6, e20758.
- FELDING-HABERMANN, B., O'TOOLE, T. E., SMITH, J. W., FRANSVEA, E., RUGGERI, Z. M., GINSBERG, M. H., HUGHES, P. E., PAMPORI, N., SHATTIL, S. J., SAVEN, A. & MUELLER, B. M. 2001. Integrin activation controls metastasis in human breast cancer. *Proc Natl Acad Sci U S A*, 98, 1853-8.
- FIDLER, I. J. 2011. The role of the organ microenvironment in brain metastasis. *Semin Cancer Biol*, 21, 107-12.
- FIDLER, I. J. & NICOLSON, G. L. 1976. Organ selectivity for implantation survival and growth of B16 melanoma variant tumor lines. *J Natl Cancer Inst*, 57, 1199-202.
- FIDLER, I. J. & NICOLSON, G. L. 1977. Fate of recirculating B16 melanoma metastatic variant cells in parabiotic syngeneic recipients. *J Natl Cancer Inst*, 58, 1867-72.
- FISHER, B., BRYANT, J., DIGNAM, J. J., WICKERHAM, D. L., MAMOUNAS, E. P., FISHER, E. R., MARGOLESE, R. G., NESBITT, L., PAIK, S., PISANSKY, T. M., WOLMARK, N., NATIONAL SURGICAL ADJUVANT, B. & BOWEL, P. 2002. Tamoxifen, radiation therapy, or both for prevention of ipsilateral breast tumor recurrence after lumpectomy in women with invasive breast cancers of one centimeter or less. *J Clin Oncol*, 20, 4141-9.

- FITZGERALD, D. P., PALMIERI, D., HUA, E., HARGRAVE, E., HERRING, J. M., QIAN, Y., VEGA-VALLE, E., WEIL, R. J., STARK, A. M., VORTMEYER, A. O. & STEEG, P. S. 2008. Reactive glia are recruited by highly proliferative brain metastases of breast cancer and promote tumor cell colonization. *Clin Exp Metastasis*, 25, 799-810.
- FOLKMAN, J. & KLAGSBRUN, M. 1987. Angiogenic factors. *Science*, 235, 442-7.
- FRANCIA, G., CRUZ-MUNOZ, W., MAN, S., XU, P. & KERBEL, R. S. 2011. Mouse models of advanced spontaneous metastasis for experimental therapeutics. *Nat Rev Cancer*, 11, 135-41.
- FURUSE, M., HIRASE, T., ITOH, M., NAGAFUCHI, A., YONEMURA, S., TSUKITA, S. & TSUKITA, S. 1993. Occludin: a novel integral membrane protein localizing at tight junctions. *J Cell Biol*, 123, 1777-88.
- GAEDCKE, J., TRAUB, F., MILDE, S., WILKENS, L., STAN, A., OSTERTAG, H., CHRISTGEN, M., VON WASIELEWSKI, R. & KREIPE, H. H. 2007. Predominance of the basal type and HER-2/neu type in brain metastasis from breast cancer. *Mod Pathol*, 20, 864-70.
- GARCIA-BECERRA, R., SANTOS, N., DIAZ, L. & CAMACHO, J. 2012. Mechanisms of resistance to endocrine therapy in breast cancer: focus on signaling pathways, miRNAs and genetically based resistance. *Int J Mol Sci*, 14, 108-45.
- GASSMANN, P., KANG, M. L., MEES, S. T. & HAIER, J. 2010. In vivo tumor cell adhesion in the pulmonary microvasculature is exclusively mediated by tumor cell-endothelial cell interaction. *BMC Cancer*, 10, 177.
- GAZINSKA, P., GRIGORIADIS, A., BROWN, J. P., MILLIS, R. R., MERA, A., GILLET, C. E., HOLMBERG, L. H., TUTT, A. N. & PINDER, S. E. 2013. Comparison of basal-like triple-negative breast cancer defined by morphology, immunohistochemistry and transcriptional profiles. *Mod Pathol*, 26, 955-66.
- GEMICI, C. & YAPRAK, G. 2015. Whole-brain radiation therapy for brain metastases: detrimental or beneficial? *Radiat Oncol*, 10, 153.
- GERSTER, K., SHI, W., NG, B., YUE, S., ITO, E., WALDRON, J., GILBERT, R. & LIU, F. F. 2010. Targeting polo-like kinase 1 enhances radiation efficacy for head-and-neck squamous cell carcinoma. *Int J Radiat Oncol Biol Phys*, 77, 253-60.
- GHOLAM, D., CHEBIB, A., HAUTEVILLE, D., BRALET, M. P. & JASMIN, C. 2007. Combined paclitaxel and cetuximab achieved a major response on the skin metastases of a patient with epidermal growth factor receptor-positive, estrogen receptor-negative, progesterone receptor-negative and human epidermal growth factor receptor-2-negative (triple-negative) breast cancer. *Anticancer Drugs*, 18, 835-7.
- GIBSON, B. A. & KRAUS, W. L. 2012. New insights into the molecular and cellular functions of poly(ADP-ribose) and PARPs. *Nat Rev Mol Cell Biol*, 13, 411-24.
- GOTTLICHER, M., MINUCCI, S., ZHU, P., KRAMER, O. H., SCHIMPF, A., GIAVARA, S., SLEEMAN, J. P., LO COCO, F., NERVI, C., PELICCI, P. G. & HEINZEL, T. 2001. Valproic acid defines a novel class of HDAC inhibitors inducing differentiation of transformed cells. *EMBO J*, 20, 6969-78.
- GRAESSLIN, O., ABDULKARIM, B. S., COUTANT, C., HUGUET, F., GABOS, Z., HSU, L., MARPEAU, O., UZAN, S., PUSZTAI, L., STROM, E. A., HORTOBAGYI, G. N., ROUZIER, R. & IBRAHIM, N. K. 2010. Nomogram to predict subsequent brain metastasis in patients with metastatic breast cancer. *J Clin Oncol*, 28, 2032-7.
- GREENUP, R., BUCHANAN, A., LORIZIO, W., RHOADS, K., CHAN, S., LEEDOM, T., KING, R., MCLENNAN, J., CRAWFORD, B., KELLY MARCOM, P. & SHELLEY HWANG, E. 2013. Prevalence of BRCA mutations among women with triple-negative breast cancer (TNBC) in a genetic counseling cohort. *Ann Surg Oncol*, 20, 3254-8.
- GREGOR, A., LIND, M., NEWMAN, H., GRANT, R., HADLEY, D. M., BARTON, T. & OSBORN, C. 1999. Phase II studies of RMP-7 and carboplatin in the treatment of recurrent high grade glioma. RMP-7 European Study Group. *J Neurooncol*, 44, 137-45.

- GREGORETTI, I. V., LEE, Y. M. & GOODSON, H. V. 2004. Molecular evolution of the histone deacetylase family: functional implications of phylogenetic analysis. *J Mol Biol*, 338, 17-31.
- GRIL, B., PALMIERI, D., BRONDER, J. L., HERRING, J. M., VEGA-VALLE, E., FEIGENBAUM, L., LIEWEHR, D. J., STEINBERG, S. M., MERINO, M. J., RUBIN, S. D. & STEEG, P. S. 2008. Effect of lapatinib on the outgrowth of metastatic breast cancer cells to the brain. *J Natl Cancer Inst*, 100, 1092-103.
- GROSELJ, B., SHARMA, N. L., HAMDY, F. C., KERR, M. & KILTIE, A. E. 2013. Histone deacetylase inhibitors as radiosensitisers: effects on DNA damage signalling and repair. *Br J Cancer*, 108, 748-54.
- GRYDER, B. E., SODJI, Q. H. & OYELERE, A. K. 2012. Targeted cancer therapy: giving histone deacetylase inhibitors all they need to succeed. *Future Med Chem*, 4, 505-24.
- GUARINO, M., RUBINO, B. & BALLABIO, G. 2007. The role of epithelial-mesenchymal transition in cancer pathology. *Pathology*, 39, 305-18.
- GUI, C. Y., NGO, L., XU, W. S., RICHON, V. M. & MARKS, P. A. 2004. Histone deacetylase (HDAC) inhibitor activation of p21WAF1 involves changes in promoter-associated proteins, including HDAC1. *Proc Natl Acad Sci U S A*, 101, 1241-6.
- GUPTA, P., ADKINS, C., LOCKMAN, P. & SRIVASTAVA, S. K. 2013. Metastasis of Breast Tumor Cells to Brain Is Suppressed by Phenethyl Isothiocyanate in a Novel Metastasis Model. *PLoS One*, 8, e67278.
- GUPTA, P. K., REID, R. C., LIU, L., LUCKE, A. J., BROOMFIELD, S. A., ANDREWS, M. R., SWEET, M. J. & FAIRLIE, D. P. 2010. Inhibitors selective for HDAC6 in enzymes and cells. *Bioorg Med Chem Lett*, 20, 7067-70.
- GUSTERSON, B. A., ROSS, D. T., HEATH, V. J. & STEIN, T. 2005. Basal cytokeratins and their relationship to the cellular origin and functional classification of breast cancer. *Breast Cancer Res*, 7, 143-8.
- HADNAGY, A., BEAULIEU, R. & BALICKI, D. 2008. Histone tail modifications and noncanonical functions of histones: perspectives in cancer epigenetics. *Mol Cancer Ther*, 7, 740-8.
- HARDUIN-LEPERS, A., KRZEWINSKI-RECCHI, M. A., COLOMB, F., FOULQUIER, F., GROUX-DEGROOTE, S. & DELANNOY, P. 2012. Sialyltransferases functions in cancers. *Front Biosci (Elite Ed)*, 4, 499-515.
- HARDUIN-LEPERS, A., VALLEJO-RUIZ, V., KRZEWINSKI-RECCHI, M. A., SAMYN-PETIT, B., JULIEN, S. & DELANNOY, P. 2001. The human sialyltransferase family. *Biochimie*, 83, 727-37.
- HART, I. R. & FIDLER, I. J. 1980. Role of organ selectivity in the determination of metastatic patterns of B16 melanoma. *Cancer Res*, 40, 2281-7.
- HE, B. P., WANG, J. J., ZHANG, X., WU, Y., WANG, M., BAY, B. H. & CHANG, A. Y. 2006. Differential reactions of microglia to brain metastasis of lung cancer. *Mol Med*, 12, 161-70.
- HEITZ, F., HARTER, P., LUECK, H. J., FISSLER-ECKHOFF, A., LORENZ-SALEHI, F., SCHEIL-BERTRAM, S., TRAUT, A. & DU BOIS, A. 2009. Triple-negative and HER2-overexpressing breast cancers exhibit an elevated risk and an earlier occurrence of cerebral metastases. *Eur J Cancer*, 45, 2792-8.
- HERSCHKOWITZ, J. I., SIMIN, K., WEIGMAN, V. J., MIKAELIAN, I., USARY, J., HU, Z., RASMUSSEN, K. E., JONES, L. P., ASSEFNIA, S., CHANDRASEKHARAN, S., BACKLUND, M. G., YIN, Y., KHRAMTSOV, A. I., BASTEIN, R., QUACKENBUSH, J., GLAZER, R. I., BROWN, P. H., GREEN, J. E., KOPELOVICH, L., FURTH, P. A., PALAZZO, J. P., OLOPADE, O. I., BERNARD, P. S., CHURCHILL, G. A., VAN DYKE, T. & PEROU, C. M. 2007. Identification of conserved gene expression features between murine mammary carcinoma models and human breast tumors. *Genome Biol*, 8, R76.
- HESS-STUMPP, H., BRACKER, T. U., HENDERSON, D. & POLITZ, O. 2007. MS-275, a potent orally available inhibitor of histone deacetylases--the development of an anticancer agent. *Int J*

- HESS, K. R., VARADHACHARY, G. R., TAYLOR, S. H., WEI, W., RABER, M. N., LENZI, R. & ABBRUZZESE, J. L. 2006. Metastatic patterns in adenocarcinoma. *Cancer*, 106, 1624-33.
- HEWITT, K. J., AGARWAL, R. & MORIN, P. J. 2006. The claudin gene family: expression in normal and neoplastic tissues. *BMC Cancer*, 6, 186.
- HICKS, D. G., SHORT, S. M., PRESCOTT, N. L., TARR, S. M., COLEMAN, K. A., YODER, B. J., CROWE, J. P., CHOUEIRI, T. K., DAWSON, A. E., BUDD, G. T., TUBBS, R. R., CASEY, G. & WEIL, R. J. 2006. Breast cancers with brain metastases are more likely to be estrogen receptor negative, express the basal cytokeratin CK5/6, and overexpress HER2 or EGFR. *Am J Surg Pathol*, 30, 1097-104.
- HICKS, M., MACRAE, E. R., ABDEL-RASOUL, M., LAYMAN, R., FRIEDMAN, S., QUERRY, J., LUSTBERG, M., RAMASWAMY, B., MROZEK, E., SHAPIRO, C. & WESOLOWSKI, R. 2015. Neoadjuvant Dual HER2-Targeted Therapy With Lapatinib and Trastuzumab Improves Pathologic Complete Response in Patients With Early Stage HER2-Positive Breast Cancer: A Meta-Analysis of Randomized Prospective Clinical Trials. *Oncologist*, 20, 337-43.
- HO-TIN-NOE, B., GOERGE, T. & WAGNER, D. D. 2009. Platelets: guardians of tumor vasculature. *Cancer Res*, 69, 5623-6.
- HOCKLY, E., RICHON, V. M., WOODMAN, B., SMITH, D. L., ZHOU, X., ROSA, E., SATHASIVAM, K., GHAZI-NOORI, S., MAHAL, A., LOWDEN, P. A., STEFFAN, J. S., MARSH, J. L., THOMPSON, L. M., LEWIS, C. M., MARKS, P. A. & BATES, G. P. 2003. Suberoylanilide hydroxamic acid, a histone deacetylase inhibitor, ameliorates motor deficits in a mouse model of Huntington's disease. *Proc Natl Acad Sci U S A*, 100, 2041-6.
- HOHENESTER, E. & YURCHENCO, P. D. 2013. Laminins in basement membrane assembly. *Cell Adh Migr*, 7, 56-63.
- HOLLY, J. & PERKS, C. 2006. The role of insulin-like growth factor binding proteins. *Neuroendocrinology*, 83, 154-60.
- HOLMGREN, L., O'REILLY, M. S. & FOLKMAN, J. 1995. Dormancy of micrometastases: balanced proliferation and apoptosis in the presence of angiogenesis suppression. *Nat Med*, 1, 149-53.
- HOWELL, S. J., JOHNSTON, S. R. & HOWELL, A. 2004. The use of selective estrogen receptor modulators and selective estrogen receptor down-regulators in breast cancer. *Best Pract Res Clin Endocrinol Metab*, 18, 47-66.
- HOWLADER N, N. A., KRAPCHO M, GARSHELL J, NEYMAN N, ALTEKRUSE SF, KOSARY CL, YU M, RUHL J, TATALOVICH Z, CHO H, MARIOTTO A, LEWIS DR, CHEN HS, FEUER EJ, CRONIN KA 2013. SEER Cancer Statistics Review, 1975-2010.
- HUANG, Q., ZHAO, M. & ZHAO, K. 2014. Alteration of vascular permeability in burn injury. *MedicalExpress*, 1, 62-76.
- INCORVATI, J. A., SHAH, S., MU, Y. & LU, J. 2013. Targeted therapy for HER2 positive breast cancer. *J Hematol Oncol*, 6, 38.
- INSINGA, A., MONESTIROLI, S., RONZONI, S., GELMETTI, V., MARCHESI, F., VIALE, A., ALTUCCI, L., NERVI, C., MINUCCI, S. & PELICCI, P. G. 2005. Inhibitors of histone deacetylases induce tumor-selective apoptosis through activation of the death receptor pathway. *Nat Med*, 11, 71-6.
- IRVIN, W. J., JR. & CAREY, L. A. 2008. What is triple-negative breast cancer? *Eur J Cancer*, 44, 2799-805.
- JABOIN, J. J., FERRARO, D. J., DEWEES, T. A., RICH, K. M., CHICOINE, M. R., DOWLING, J. L., MANSUR, D. B., DRZYMALA, R. E., SIMPSON, J. R., MAGNUSON, W. J., PATEL, A. H. & ZOBBERI, I. 2013. Survival following gamma knife radiosurgery for brain metastasis from breast cancer. *Radiat Oncol*, 8, 131.
- JAIN, R. K., DI TOMASO, E., DUDA, D. G., LOEFFLER, J. S., SORENSEN, A. G. & BATCHELOR, T. T.

2007. Angiogenesis in brain tumours. *Nat Rev Neurosci*, 8, 610-22.
- JAYARAMAN, R., PILLA REDDY, V., PASHA, M. K., WANG, H., SANGTHONGPITAG, K., YEO, P., HU, C. Y., WU, X., XIN, L., GOH, E., NEW, L. S. & ETHIRAJULU, K. 2011. Preclinical metabolism and disposition of SB939 (Pracinostat), an orally active histone deacetylase inhibitor, and prediction of human pharmacokinetics. *Drug Metab Dispos*, 39, 2219-32.
- JOENSUU, H., KELLOKUMPU-LEHTINEN, P. L., BONO, P., ALANKO, T., KATAJA, V., ASOLA, R., UTRIAINEN, T., KOKKO, R., HEMMINKI, A., TARKKANEN, M., TURPEENNIEMI-HUJANEN, T., JYRKKIO, S., FLANDER, M., HELLE, L., INGALSUO, S., JOHANSSON, K., JAASKELAINEN, A. S., PAJUNEN, M., RAUHALA, M., KALEVA-KEROLA, J., SALMINEN, T., LEINONEN, M., ELOMAA, I., ISOLA, J. & FINHER STUDY, I. 2006. Adjuvant docetaxel or vinorelbine with or without trastuzumab for breast cancer. *N Engl J Med*, 354, 809-20.
- JOHNSON-LEGER, C. A., AURRAND-LIONS, M., BELTRAMINELLI, N., FASEL, N. & IMHOF, B. A. 2002. Junctional adhesion molecule-2 (JAM-2) promotes lymphocyte transendothelial migration. *Blood*, 100, 2479-86.
- JOHNSTON, S. J. & CHEUNG, K. L. 2010. Fulvestrant - a novel endocrine therapy for breast cancer. *Curr Med Chem*, 17, 902-14.
- JOHNSTONE, C. N., SMITH, Y. E., CAO, Y., BURROWS, A. D., CROSS, R. S., LING, X., REDVERS, R. P., DOHERTY, J. P., ECKHARDT, B. L., NATOLI, A. L., RESTALL, C. M., LUCAS, E., PEARSON, H. B., DEB, S., BRITT, K. L., RIZZITELLI, A., LI, J., HARMEY, J. H., POULIOT, N. & ANDERSON, R. L. 2015. Functional and molecular characterisation of EO771.LMB tumours, a new C57BL/6-mouse-derived model of spontaneously metastatic mammary cancer. *Dis Model Mech*, 8, 237-51.
- JOHNSTONE, R. W. 2002. Histone-deacetylase inhibitors: novel drugs for the treatment of cancer. *Nat Rev Drug Discov*, 1, 287-99.
- JONES, A. R. & SHUSTA, E. V. 2007. Blood-brain barrier transport of therapeutics via receptor-mediation. *Pharm Res*, 24, 1759-71.
- JONES, S. E. 2003. Fulvestrant: an estrogen receptor antagonist that downregulates the estrogen receptor. *Semin Oncol*, 30, 14-20.
- JORDAN, V. C. 1993. Fourteenth Gaddum Memorial Lecture. A current view of tamoxifen for the treatment and prevention of breast cancer. *Br J Pharmacol*, 110, 507-17.
- JUNG, Y. K., JIN, J. S., JEONG, J. H., KIM, H. N., PARK, N. R. & CHOI, J. Y. 2008. DICAM, a novel dual immunoglobulin domain containing cell adhesion molecule interacts with alphavbeta3 integrin. *J Cell Physiol*, 216, 603-14.
- KAHNBERG, P., LUCKE, A. J., GLENN, M. P., BOYLE, G. M., TYNDALL, J. D., PARSONS, P. G. & FAIRLIE, D. P. 2006. Design, synthesis, potency, and cytoselectivity of anticancer agents derived by parallel synthesis from alpha-aminosuberic acid. *J Med Chem*, 49, 7611-22.
- KANAPATHY PILLAI, S. K., TAY, A., NAIR, S. & LEONG, C. O. 2012. Triple-negative breast cancer is associated with EGFR, CK5/6 and c-KIT expression in Malaysian women. *BMC Clin Pathol*, 12, 18.
- KANG, Y. S. & PARDRIDGE, W. M. 1994. Brain delivery of biotin bound to a conjugate of neutral avidin and cationized human albumin. *Pharm Res*, 11, 1257-64.
- KARRISON, T. G., FERGUSON, D. J. & MEIER, P. 1999. Dormancy of mammary carcinoma after mastectomy. *J Natl Cancer Inst*, 91, 80-5.
- KAST, R. E., RAMIRO, S., LLADO, S., TORO, S., COVENAS, R. & MUNOZ, M. 2015. Antitumor action of temozolomide, ritonavir and aprepitant against human glioma cells. *J Neurooncol*.
- KEAM, B., IM, S. A., KIM, H. J., OH, D. Y., KIM, J. H., LEE, S. H., CHIE, E. K., HAN, W., KIM, D. W., MOON, W. K., KIM, T. Y., PARK, I. A., NOH, D. Y., HEO, D. S., HA, S. W. & BANG, Y. J. 2007. Prognostic impact of clinicopathologic parameters in stage II/III breast cancer treated with neoadjuvant docetaxel and doxorubicin chemotherapy: paradoxical features of the triple negative breast cancer. *BMC Cancer*, 7, 203.

- KEAM, B., IM, S. A., LEE, K. H., HAN, S. W., OH, D. Y., KIM, J. H., LEE, S. H., HAN, W., KIM, D. W., KIM, T. Y., PARK, I. A., NOH, D. Y., HEO, D. S. & BANG, Y. J. 2011. Ki-67 can be used for further classification of triple negative breast cancer into two subtypes with different response and prognosis. *Breast Cancer Res*, 13, R22.
- KEEN, J. C., YAN, L., MACK, K. M., PETTIT, C., SMITH, D., SHARMA, D. & DAVIDSON, N. E. 2003. A novel histone deacetylase inhibitor, scriptaid, enhances expression of functional estrogen receptor alpha (ER) in ER negative human breast cancer cells in combination with 5-aza 2'-deoxycytidine. *Breast Cancer Res Treat*, 81, 177-86.
- KEMPER, E. M., VAN ZANDBERGEN, A. E., CLEYPPOOL, C., MOS, H. A., BOOGERD, W., BEIJNEN, J. H. & VAN TELLINGEN, O. 2003. Increased penetration of paclitaxel into the brain by inhibition of P-Glycoprotein. *Clin Cancer Res*, 9, 2849-55.
- KHAN, N., JEFFERS, M., KUMAR, S., HACKETT, C., BOLDOG, F., KHRAMTSOV, N., QIAN, X., MILLS, E., BERGHS, S. C., CAREY, N., FINN, P. W., COLLINS, L. S., TUMBER, A., RITCHIE, J. W., JENSEN, P. B., LICHENSTEIN, H. S. & SEHESTED, M. 2008. Determination of the class and isoform selectivity of small-molecule histone deacetylase inhibitors. *Biochem J*, 409, 581-9.
- KHUON, S., LIANG, L., DETTMAN, R. W., SPORN, P. H., WYSOLMERSKI, R. B. & CHEW, T. L. 2010. Myosin light chain kinase mediates transcellular intravasation of breast cancer cells through the underlying endothelial cells: a three-dimensional FRET study. *J Cell Sci*, 123, 431-40.
- KIENAST, Y., VON BAUMGARTEN, L., FUHRMANN, M., KLINKERT, W. E., GOLDBRUNNER, R., HERMS, J. & WINKLER, F. 2010. Real-time imaging reveals the single steps of brain metastasis formation. *Nat Med*, 16, 116-22.
- KIM, H. J. & BAE, S. C. 2011. Histone deacetylase inhibitors: molecular mechanisms of action and clinical trials as anti-cancer drugs. *Am J Transl Res*, 3, 166-79.
- KIM, H. J., IM, S. A., KEAM, B., KIM, Y. J., HAN, S. W., KIM, T. M., OH, D. Y., KIM, J. H., LEE, S. H., CHIE, E. K., HAN, W., KIM, D. W., KIM, T. Y., NOH, D. Y., HEO, D. S., PARK, I. A., BANG, Y. J. & HA, S. W. 2012. Clinical outcome of central nervous system metastases from breast cancer: differences in survival depending on systemic treatment. *J Neurooncol*, 106, 303-13.
- KIM, H. P., YOON, Y. K., KIM, J. W., HAN, S. W., HUR, H. S., PARK, J., LEE, J. H., OH, D. Y., IM, S. A., BANG, Y. J. & KIM, T. Y. 2009. Lapatinib, a dual EGFR and HER2 tyrosine kinase inhibitor, downregulates thymidylate synthase by inhibiting the nuclear translocation of EGFR and HER2. *PLoS One*, 4, e5933.
- KIM, L. S., HUANG, S., LU, W., LEV, D. C. & PRICE, J. E. 2004. Vascular endothelial growth factor expression promotes the growth of breast cancer brain metastases in nude mice. *Clin Exp Metastasis*, 21, 107-18.
- KIM, S. J., KIM, J. S., PARK, E. S., LEE, J. S., LIN, Q., LANGLEY, R. R., MAYA, M., HE, J., KIM, S. W., WEIHUA, Z., BALASUBRAMANIAN, K., FAN, D., MILLS, G. B., HUNG, M. C. & FIDLER, I. J. 2011. Astrocytes upregulate survival genes in tumor cells and induce protection from chemotherapy. *Neoplasia*, 13, 286-98.
- KIM, S. W., CHOI, H. J., LEE, H. J., HE, J., WU, Q., LANGLEY, R. R., FIDLER, I. J. & KIM, S. J. 2014. Role of the endothelin axis in astrocyte- and endothelial cell-mediated chemoprotection of cancer cells. *Neuro Oncol*, 16, 1585-98.
- KIRSCH, D. G., LEDEZMA, C. J., MATHEWS, C. S., BHAN, A. K., ANCUKIEWICZ, M., HOCHBERG, F. H. & LOEFFLER, J. S. 2005. Survival after brain metastases from breast cancer in the trastuzumab era. *J Clin Oncol*, 23, 2114-6; author reply 2116-7.
- KITAMURA, T., QIAN, B. Z. & POLLARD, J. W. 2015. Immune cell promotion of metastasis. *Nat Rev Immunol*, 15, 73-86.
- KLEIN, A., OLENDROWITZ, C., SCHMUTZLER, R., HAMPL, J., SCHLAG, P. M., MAASS, N., ARNOLD, N., WESSEL, R., RAMSER, J., MEINDL, A., SCHERNECK, S. & SEITZ, S. 2009. Identification of brain- and bone-specific breast cancer metastasis genes. *Cancer Lett*, 276, 212-20.
- KOCHER, M., SOFFIETTI, R., ABACIOGLU, U., VILLA, S., FAUCHON, F., BAUMERT, B. G., FARISELLI,

- L., TZUK-SHINA, T., KORTMANN, R. D., CARRIE, C., BEN HASSEL, M., KOURI, M., VALEINIS, E., VAN DEN BERGE, D., COLLETTE, S., COLLETTE, L. & MUELLER, R. P. 2011. Adjuvant whole-brain radiotherapy versus observation after radiosurgery or surgical resection of one to three cerebral metastases: results of the EORTC 22952-26001 study. *J Clin Oncol*, 29, 134-41.
- KODACK, D. P., CHUNG, E., YAMASHITA, H., INCIO, J., DUYVERMAN, A. M., SONG, Y., FARRAR, C. T., HUANG, Y., AGER, E., KAMOUN, W., GOEL, S., SNUDERL, M., LUSSIEZ, A., HIDDINGH, L., MAHMOOD, S., TANNOUS, B. A., EICHLER, A. F., FUKUMURA, D., ENGELMAN, J. A. & JAIN, R. K. 2012. Combined targeting of HER2 and VEGFR2 for effective treatment of HER2-amplified breast cancer brain metastases. *Proc Natl Acad Sci U S A*, 109, E3119-27.
- KONDZIOLKA, D., PATEL, A., LUNSFORD, L. D., KASSAM, A. & FLICKINGER, J. C. 1999. Stereotactic radiosurgery plus whole brain radiotherapy versus radiotherapy alone for patients with multiple brain metastases. *Int J Radiat Oncol Biol Phys*, 45, 427-34.
- KOOP, S., SCHMIDT, E. E., MACDONALD, I. C., MORRIS, V. L., KHOKHA, R., GRATTAN, M., LEONE, J., CHAMBERS, A. F. & GROOM, A. C. 1996. Independence of metastatic ability and extravasation: metastatic ras-transformed and control fibroblasts extravasate equally well. *Proc Natl Acad Sci U S A*, 93, 11080-4.
- KOWANETZ, M., WU, X., LEE, J., TAN, M., HAGENBEEK, T., QU, X., YU, L., ROSS, J., KORSISAARI, N., CAO, T., BOU-RESLAN, H., KALLOP, D., WEIMER, R., LUDLAM, M. J., KAMINKER, J. S., MODRUSAN, Z., VAN BRUGGEN, N., PEALE, F. V., CARANO, R., MENG, Y. G. & FERRARA, N. 2010. Granulocyte-colony stimulating factor promotes lung metastasis through mobilization of Ly6G+Ly6C+ granulocytes. *Proc Natl Acad Sci U S A*, 107, 21248-55.
- KRUSCHE, C. A., WULFING, P., KERSTING, C., VLOET, A., BOCKER, W., KIESEL, L., BEIER, H. M. & ALFER, J. 2005. Histone deacetylase-1 and -3 protein expression in human breast cancer: a tissue microarray analysis. *Breast Cancer Res Treat*, 90, 15-23.
- KULP, S. K., CHEN, C. S., WANG, D. S., CHEN, C. Y. & CHEN, C. S. 2006. Antitumor effects of a novel phenylbutyrate-based histone deacetylase inhibitor, (S)-HDAC-42, in prostate cancer. *Clin Cancer Res*, 12, 5199-206.
- KUMLER, I., TUXEN, M. K. & NIELSEN, D. L. 2014. A systematic review of dual targeting in HER2-positive breast cancer. *Cancer Treat Rev*, 40, 259-70.
- KUO, L. J. & YANG, L. X. 2008. Gamma-H2AX - a novel biomarker for DNA double-strand breaks. *In Vivo*, 22, 305-9.
- KUSUMA, N., DENOYER, D., EBLE, J. A., REDVERS, R. P., PARKER, B. S., PELZER, R., ANDERSON, R. L. & POULIOT, N. 2012. Integrin-dependent response to laminin-511 regulates breast tumor cell invasion and metastasis. *Int J Cancer*, 130, 555-66.
- LANGLEY, R. R. & FIDLER, I. J. 2011. The seed and soil hypothesis revisited--the role of tumor-stroma interactions in metastasis to different organs. *Int J Cancer*, 128, 2527-35.
- LAVAUD, P. & ANDRE, F. 2014. Strategies to overcome trastuzumab resistance in HER2-overexpressing breast cancers: focus on new data from clinical trials. *BMC Med*, 12, 132.
- LE RHUN, E., TAILLIBERT, S. & CHAMBERLAIN, M. C. 2013. Carcinomatous meningitis: Leptomeningeal metastases in solid tumors. *Surg Neurol Int*, 4, S265-88.
- LEE, J. H., CHOY, M. L., NGO, L., FOSTER, S. S. & MARKS, P. A. 2010. Histone deacetylase inhibitor induces DNA damage, which normal but not transformed cells can repair. *Proc Natl Acad Sci U S A*, 107, 14639-44.
- LEE, K. Y., KIM, Y. J., YOO, H., LEE, S. H., PARK, J. B. & KIM, H. J. 2011. Human brain endothelial cell-derived COX-2 facilitates extravasation of breast cancer cells across the blood-brain barrier. *Anticancer Res*, 31, 4307-13.
- LEE, T. H., AVRAHAM, H. K., JIANG, S. & AVRAHAM, S. 2003. Vascular endothelial growth factor modulates the transendothelial migration of MDA-MB-231 breast cancer cells through regulation of brain microvascular endothelial cell permeability. *J Biol Chem*, 278, 5277-84.

- LEHMANN, B. D., BAUER, J. A., CHEN, X., SANDERS, M. E., CHAKRAVARTHY, A. B., SHYR, Y. & PIETENPOL, J. A. 2011. Identification of human triple-negative breast cancer subtypes and preclinical models for selection of targeted therapies. *J Clin Invest*, 121, 2750-67.
- LEHMANN, B. D., PIETENPOL, J. A. & TAN, A. R. 2015. Triple-negative breast cancer: molecular subtypes and new targets for therapy. *Am Soc Clin Oncol Educ Book*, 35, e31-9.
- LELEKAKIS, M., MOSELEY, J. M., MARTIN, T. J., HARDS, D., WILLIAMS, E., HO, P., LOWEN, D., JAVNI, J., MILLER, F. R., SLAVIN, J. & ANDERSON, R. L. 1999. A novel orthotopic model of breast cancer metastasis to bone. *Clin Exp Metastasis*, 17, 163-70.
- LI, C., IIDA, M., DUNN, E. F., GHIA, A. J. & WHEELER, D. L. 2009. Nuclear EGFR contributes to acquired resistance to cetuximab. *Oncogene*, 28, 3801-13.
- LIEBNER, S., FISCHMANN, A., RASCHER, G., DUFFNER, F., GROTE, E. H., KALBACHER, H. & WOLBURG, H. 2000. Claudin-1 and claudin-5 expression and tight junction morphology are altered in blood vessels of human glioblastoma multiforme. *Acta Neuropathol*, 100, 323-31.
- LIEDTKE, C., MAZOUNI, C., HESS, K. R., ANDRE, F., TORDAI, A., MEJIA, J. A., SYMMANS, W. F., GONZALEZ-ANGULO, A. M., HENNESSY, B., GREEN, M., CRISTOFANILLI, M., HORTOBAGYI, G. N. & PUSZTAI, L. 2008. Response to neoadjuvant therapy and long-term survival in patients with triple-negative breast cancer. *J Clin Oncol*, 26, 1275-81.
- LIN, E. Y., JONES, J. G., LI, P., ZHU, L., WHITNEY, K. D., MULLER, W. J. & POLLARD, J. W. 2003. Progression to malignancy in the polyoma middle T oncoprotein mouse breast cancer model provides a reliable model for human diseases. *Am J Pathol*, 163, 2113-26.
- LIN, N. U., DIERAS, V., PAUL, D., LOSSIGNOL, D., CHRISTODOULOU, C., STEMMLER, H. J., ROCHE, H., LIU, M. C., GREIL, R., CIRUELOS, E., LOIBL, S., GORI, S., WARDLEY, A., YARDLEY, D., BRUFISKY, A., BLUM, J. L., RUBIN, S. D., DHARAN, B., STEPLEWSKI, K., ZEMBRYKI, D., OLIVA, C., ROYCHOWDHURY, D., PAOLETTI, P. & WINER, E. P. 2009. Multicenter phase II study of lapatinib in patients with brain metastases from HER2-positive breast cancer. *Clin Cancer Res*, 15, 1452-9.
- LIN, N. U., FREEDMAN, R. A., RAMAKRISHNA, N., YOUNGER, J., STORNILOLO, A. M., BELLON, J. R., COME, S. E., GELMAN, R. S., HARRIS, G. J., HENDERSON, M. A., MACDONALD, S. M., MAHADEVAN, A., EISENBERG, E., LIGIBEL, J. A., MAYER, E. L., MOY, B., EICHLER, A. F. & WINER, E. P. 2013. A phase I study of lapatinib with whole brain radiotherapy in patients with Human Epidermal Growth Factor Receptor 2 (HER2)-positive breast cancer brain metastases. *Breast Cancer Res Treat*, 142, 405-14.
- LINDEMANN, R. K., GABRIELLI, B. & JOHNSTONE, R. W. 2004. Histone-deacetylase inhibitors for the treatment of cancer. *Cell Cycle*, 3, 779-88.
- LINDNER, R., SULLIVAN, C., OFFOR, O., LEZON-GEYDA, K., HALLIGAN, K., FISCHBACH, N., SHAH, M., BOSSUYT, V., SCHULZ, V., TUCK, D. P. & HARRIS, L. N. 2013. Molecular phenotypes in triple negative breast cancer from African American patients suggest targets for therapy. *PLoS One*, 8, e71915.
- LIU, Y., KOMOHARA, Y., DOMENICK, N., OHNO, M., IKEURA, M., HAMILTON, R. L., HORBINSKI, C., WANG, X., FERRONE, S. & OKADA, H. 2012. Expression of antigen processing and presenting molecules in brain metastasis of breast cancer. *Cancer Immunol Immunother*, 61, 789-801.
- LOCKMAN, P. R., MITTAPALLI, R. K., TASKAR, K. S., RUDRARAJU, V., GRIL, B., BOHN, K. A., ADKINS, C. E., ROBERTS, A., THORSHEIM, H. R., GAASCH, J. A., HUANG, S., PALMIERI, D., STEEG, P. S. & SMITH, Q. R. 2010. Heterogeneous blood-tumor barrier permeability determines drug efficacy in experimental brain metastases of breast cancer. *Clin Cancer Res*, 16, 5664-78.
- LORGER, M. & FELDING-HABERMANN, B. 2010. Capturing changes in the brain microenvironment during initial steps of breast cancer brain metastasis. *Am J Pathol*, 176, 2958-71.
- LORGER, M., KRUEGER, J. S., O'NEAL, M., STAFLIN, K. & FELDING-HABERMANN, B. 2009. Activation of tumor cell integrin $\alpha v \beta 3$ controls angiogenesis and metastatic growth in the brain. *Proc Natl Acad Sci U S A*, 106, 10666-71.

- LOSCHER, W. & POTSCHKA, H. 2005. Role of drug efflux transporters in the brain for drug disposition and treatment of brain diseases. *Prog Neurobiol*, 76, 22-76.
- LOUIE, E., CHEN, X. F., COOMES, A., JI, K., TSIRKA, S. & CHEN, E. I. 2013. Neurotrophin-3 modulates breast cancer cells and the microenvironment to promote the growth of breast cancer brain metastasis. *Oncogene*, 32, 4064-77.
- LU, X. & KANG, Y. 2007. Organotropism of breast cancer metastasis. *J Mammary Gland Biol Neoplasia*, 12, 153-62.
- LU, Y. S., KASHIDA, Y., KULP, S. K., WANG, Y. C., WANG, D., HUNG, J. H., TANG, M., LIN, Z. Z., CHEN, T. J., CHENG, A. L. & CHEN, C. S. 2007. Efficacy of a novel histone deacetylase inhibitor in murine models of hepatocellular carcinoma. *Hepatology*, 46, 1119-30.
- LUDWIG, R. J., HARDT, K., HATTING, M., BISTRAN, R., DIEHL, S., RADEKE, H. H., PODDA, M., SCHON, M. P., KAUFMANN, R., HENSCHLER, R., PFEILSCHIFTER, J. M., SANTOSO, S. & BOEHNCKE, W. H. 2009. Junctional adhesion molecule (JAM)-B supports lymphocyte rolling and adhesion through interaction with alpha4beta1 integrin. *Immunology*, 128, 196-205.
- LUDWIG, R. J., ZOLLNER, T. M., SANTOSO, S., HARDT, K., GILLE, J., BAATZ, H., JOHANN, P. S., PFEFFER, J., RADEKE, H. H., SCHON, M. P., KAUFMANN, R., BOEHNCKE, W. H. & PODDA, M. 2005. Junctional adhesion molecules (JAM)-B and -C contribute to leukocyte extravasation to the skin and mediate cutaneous inflammation. *J Invest Dermatol*, 125, 969-76.
- LUZZI, K. J., MACDONALD, I. C., SCHMIDT, E. E., KERKVLIT, N., MORRIS, V. L., CHAMBERS, A. F. & GROOM, A. C. 1998. Multistep nature of metastatic inefficiency: dormancy of solitary cells after successful extravasation and limited survival of early micrometastases. *Am J Pathol*, 153, 865-73.
- MADDEN, S. F., CLARKE, C., GAULE, P., AHERNE, S. T., O'DONOVAN, N., CLYNES, M., CROWN, J. & GALLAGHER, W. M. 2013. BreastMark: an integrated approach to mining publicly available transcriptomic datasets relating to breast cancer outcome. *Breast Cancer Res*, 15, R52.
- MAH, L. J., EL-OSTA, A. & KARAGIANNIS, T. C. 2010. gammaH2AX: a sensitive molecular marker of DNA damage and repair. *Leukemia*, 24, 679-86.
- MAMDOUH, Z., MIKHAILOV, A. & MULLER, W. A. 2009. Transcellular migration of leukocytes is mediated by the endothelial lateral border recycling compartment. *J Exp Med*, 206, 2795-808.
- MARKS, P., RIFKIND, R. A., RICHON, V. M., BRESLOW, R., MILLER, T. & KELLY, W. K. 2001. Histone deacetylases and cancer: causes and therapies. *Nat Rev Cancer*, 1, 194-202.
- MARKS, P. A., RICHON, V. M. & RIFKIND, R. A. 2000. Histone deacetylase inhibitors: inducers of differentiation or apoptosis of transformed cells. *J Natl Cancer Inst*, 92, 1210-6.
- MARTIN-PADURA, I., LOSTAGLIO, S., SCHNEEMANN, M., WILLIAMS, L., ROMANO, M., FRUSCELLA, P., PANZERI, C., STOPPACCIARO, A., RUCO, L., VILLA, A., SIMMONS, D. & DEJANA, E. 1998. Junctional adhesion molecule, a novel member of the immunoglobulin superfamily that distributes at intercellular junctions and modulates monocyte transmigration. *J Cell Biol*, 142, 117-27.
- MATSUKADO, K., INAMURA, T., NAKANO, S., FUKUI, M., BARTUS, R. T. & BLACK, K. L. 1996. Enhanced tumor uptake of carboplatin and survival in glioma-bearing rats by intracarotid infusion of bradykinin analog, RMP-7. *Neurosurgery*, 39, 125-33; discussion 133-4.
- MCDANNOLD, N., VYKHODTSEVA, N. & HYNENEN, K. 2006. Targeted disruption of the blood-brain barrier with focused ultrasound: association with cavitation activity. *Phys Med Biol*, 51, 793-807.
- MCNEIL, C. 2006. Two targets, one drug for new EGFR inhibitors. *J Natl Cancer Inst*, 98, 1102-3.
- MCSHERRY, E. A., BRENNAN, K., HUDSON, L., HILL, A. D. & HOPKINS, A. M. 2011. Breast cancer cell migration is regulated through junctional adhesion molecule-A-mediated activation of Rap1 GTPase. *Breast Cancer Res*, 13, R31.
- MCSHERRY, E. A., MCGEE, S. F., JIRSTROM, K., DOYLE, E. M., BRENNAN, D. J., LANDBERG, G., DERVAN, P. A., HOPKINS, A. M. & GALLAGHER, W. M. 2009. JAM-A expression positively

- correlates with poor prognosis in breast cancer patients. *Int J Cancer*, 125, 1343-51.
- MEHROTRA, J., VALI, M., MCVEIGH, M., KOMINSKY, S. L., FACKLER, M. J., LAHTI-DOMENICI, J., POLYAK, K., SACCHI, N., GARRETT-MAYER, E., ARGANI, P. & SUKUMAR, S. 2004. Very high frequency of hypermethylated genes in breast cancer metastasis to the bone, brain, and lung. *Clin Cancer Res*, 10, 3104-9.
- MELTZER, A. 1990. Dormancy and breast cancer. *J Surg Oncol*, 43, 181-8.
- MENDES, O., KIM, H. T. & STOICA, G. 2005. Expression of MMP2, MMP9 and MMP3 in breast cancer brain metastasis in a rat model. *Clin Exp Metastasis*, 22, 237-46.
- METZGER-FILHO, O., TUTT, A., DE AZAMBUJA, E., SAINI, K. S., VIALE, G., LOI, S., BRADBURY, I., BLISS, J. M., AZIM, H. A., JR., ELLIS, P., DI LEO, A., BASELGA, J., SOTIRIOU, C. & PICCART-GEHART, M. 2012. Dissecting the heterogeneity of triple-negative breast cancer. *J Clin Oncol*, 30, 1879-87.
- MILLER, B. E., MCINERNEY, D., JACKSON, D. & MILLER, F. R. 1986. Metabolic cooperation between mouse mammary tumor subpopulations in three-dimensional collagen gel cultures. *Cancer Res*, 46, 89-93.
- MILLIS, S. Z., GATALICA, Z., WINKLER, J., VRANIC, S., KIMBROUGH, J., REDDY, S. & O'SHAUGHNESSY, J. A. 2015. Predictive Biomarker Profiling of > 6000 Breast Cancer Patients Shows Heterogeneity in TNBC, With Treatment Implications. *Clin Breast Cancer*, 15, 473-481 e3.
- MINUCCI, S. & PELICCI, P. G. 2006. Histone deacetylase inhibitors and the promise of epigenetic (and more) treatments for cancer. *Nat Rev Cancer*, 6, 38-51.
- MISRA, A., GANESH, S., SHAHIWALA, A. & SHAH, S. P. 2003. Drug delivery to the central nervous system: a review. *J Pharm Pharm Sci*, 6, 252-73.
- MITTAPALLI, R. K., LIU, X., ADKINS, C. E., NOUNOU, M. I., BOHN, K. A., TERRELL, T. B., QHATTAL, H. S., GELDENHUYS, W. J., PALMIERI, D., STEEG, P. S., SMITH, Q. R. & LOCKMAN, P. R. 2013. Paclitaxel-hyaluronic nanoconjugates prolong overall survival in a preclinical brain metastases of breast cancer model. *Mol Cancer Ther*, 12, 2389-99.
- MORGAN, M. A., PARSELS, L. A., ZHAO, L., PARSELS, J. D., DAVIS, M. A., HASSAN, M. C., ARUMUGARAJAH, S., HYLANDER-GANS, L., MOROSINI, D., SIMEONE, D. M., CANMAN, C. E., NORMOLLE, D. P., ZABLUDOFF, S. D., MAYBAUM, J. & LAWRENCE, T. S. 2010. Mechanism of radiosensitization by the Chk1/2 inhibitor AZD7762 involves abrogation of the G2 checkpoint and inhibition of homologous recombinational DNA repair. *Cancer Res*, 70, 4972-81.
- MORITA, K., SASAKI, H., FURUSE, M. & TSUKITA, S. 1999. Endothelial claudin: claudin-5/TMVCF constitutes tight junction strands in endothelial cells. *J Cell Biol*, 147, 185-94.
- MORK, C. N., FALLER, D. V. & SPANJAARD, R. A. 2005. A mechanistic approach to anticancer therapy: targeting the cell cycle with histone deacetylase inhibitors. *Curr Pharm Des*, 11, 1091-104.
- MOSS, M. S., SISKEN, B., ZIMMER, S. & ANDERSON, K. W. 1999. Adhesion of nonmetastatic and highly metastatic breast cancer cells to endothelial cells exposed to shear stress. *Biorheology*, 36, 359-71.
- MURAKAMI, M., GIAMPIETRO, C., GIANNOTTA, M., CORADA, M., TORSSELLI, I., ORSENIGO, F., COCITO, A., D'ARIO, G., MAZZAROL, G., CONFALONIERI, S., DI FIORE, P. P. & DEJANA, E. 2011. Abrogation of junctional adhesion molecule-A expression induces cell apoptosis and reduces breast cancer progression. *PLoS One*, 6, e21242.
- MURAKAMI, T., SATO, A., CHUN, N. A., HARA, M., NAITO, Y., KOBAYASHI, Y., KANO, Y., OHTSUKI, M., FURUKAWA, Y. & KOBAYASHI, E. 2008. Transcriptional modulation using HDACi depsipeptide promotes immune cell-mediated tumor destruction of murine B16 melanoma. *J Invest Dermatol*, 128, 1506-16.
- NAIK, M. U., NAIK, T. U., SUCKOW, A. T., DUNCAN, M. K. & NAIK, U. P. 2008. Attenuation of junctional adhesion molecule-A is a contributing factor for breast cancer cell invasion. *Cancer Res*, 68, 2194-203.

- NAKAGAWA, M., ODA, Y., EGUCHI, T., AISHIMA, S., YAO, T., HOSOI, F., BASAKI, Y., ONO, M., KUWANO, M., TANAKA, M. & TSUNEYOSHI, M. 2007. Expression profile of class I histone deacetylases in human cancer tissues. *Oncol Rep*, 18, 769-74.
- NAM, B. H., KIM, S. Y., HAN, H. S., KWON, Y., LEE, K. S., KIM, T. H. & RO, J. 2008. Breast cancer subtypes and survival in patients with brain metastases. *Breast Cancer Res*, 10, R20.
- NEBBIOSO, A., CLARKE, N., VOLTZ, E., GERMAIN, E., AMBROSINO, C., BONTEMPO, P., ALVAREZ, R., SCHIAVONE, E. M., FERRARA, F., BRESCIANI, F., WEISZ, A., DE LERA, A. R., GRONEMEYER, H. & ALTUCCI, L. 2005. Tumor-selective action of HDAC inhibitors involves TRAIL induction in acute myeloid leukemia cells. *Nat Med*, 11, 77-84.
- NEMAN, J., CHOY, C., KOWOLIK, C. M., ANDERSON, A., DUENAS, V. J., WALIANY, S., CHEN, B. T., CHEN, M. Y. & JANDIAL, R. 2013. Co-evolution of breast-to-brain metastasis and neural progenitor cells. *Clin Exp Metastasis*, 30, 753-68.
- NEW, M., OLZSCHA, H. & LA THANGUE, N. B. 2012. HDAC inhibitor-based therapies: can we interpret the code? *Mol Oncol*, 6, 637-56.
- NGUYEN, D. X., BOS, P. D. & MASSAGUE, J. 2009. Metastasis: from dissemination to organ-specific colonization. *Nat Rev Cancer*, 9, 274-84.
- NICOLSON, G. L., BRUNSON, K. W. & FIDLER, I. J. 1978. Specificity of arrest, survival, and growth of selected metastatic variant cell lines. *Cancer Res*, 38, 4105-11.
- NING, Z. Q., LI, Z. B., NEWMAN, M. J., SHAN, S., WANG, X. H., PAN, D. S., ZHANG, J., DONG, M., DU, X. & LU, X. P. 2012. Chidamide (CS055/HBI-8000): a new histone deacetylase inhibitor of the benzamide class with antitumor activity and the ability to enhance immune cell-mediated tumor cell cytotoxicity. *Cancer Chemother Pharmacol*, 69, 901-9.
- NITTA, T., HATA, M., GOTOH, S., SEO, Y., SASAKI, H., HASHIMOTO, N., FURUSE, M. & TSUKITA, S. 2003. Size-selective loosening of the blood-brain barrier in claudin-5-deficient mice. *J Cell Biol*, 161, 653-60.
- NOH, J. H., JUNG, K. H., KIM, J. K., EUN, J. W., BAE, H. J., XIE, H. J., CHANG, Y. G., KIM, M. G., PARK, W. S., LEE, J. Y. & NAM, S. W. 2011. Aberrant regulation of HDAC2 mediates proliferation of hepatocellular carcinoma cells by deregulating expression of G1/S cell cycle proteins. *PLoS One*, 6, e28103.
- NOVOTNY-DIERMAYR, V., SANGTHONGPITAG, K., HU, C. Y., WU, X., SAUSGRUBER, N., YEO, P., GREICIUS, G., PETTERSSON, S., LIANG, A. L., LOH, Y. K., BONDAY, Z., GOH, K. C., HENTZE, H., HART, S., WANG, H., ETHIRAJULU, K. & WOOD, J. M. 2010. SB939, a novel potent and orally active histone deacetylase inhibitor with high tumor exposure and efficacy in mouse models of colorectal cancer. *Mol Cancer Ther*, 9, 642-52.
- NOVOTNY-DIERMAYR, V., SAUSGRUBER, N., LOH, Y. K., PASHA, M. K., JAYARAMAN, R., HENTZE, H., YONG, W. P., GOH, B. C., TOH, H. C., ETHIRAJULU, K., ZHU, J. & WOOD, J. M. 2011. Pharmacodynamic evaluation of the target efficacy of SB939, an oral HDAC inhibitor with selectivity for tumor tissue. *Mol Cancer Ther*, 10, 1207-17.
- OLSON, J. A., JR. & MARCOM, P. K. 2008. Benefit or bias? The role of surgery to remove the primary tumor in patients with metastatic breast cancer. *Ann Surg*, 247, 739-40.
- ON, N. H., KIPTOO, P., SIAHAAN, T. J. & MILLER, D. W. 2014. Modulation of blood-brain barrier permeability in mice using synthetic E-cadherin peptide. *Mol Pharm*, 11, 974-81.
- ONITILLO, A. A., ENGEL, J. M., GREENLEE, R. T. & MUKESH, B. N. 2009. Breast cancer subtypes based on ER/PR and Her2 expression: comparison of clinicopathologic features and survival. *Clin Med Res*, 7, 4-13.
- OSCAR-BERMAN, M., SHAGRIN, B., EVERT, D. L. & EPSTEIN, C. 1997. Impairments of brain and behavior: the neurological effects of alcohol. *Alcohol Health Res World*, 21, 65-75.
- OSTERMANN, G., WEBER, K. S., ZERNECKE, A., SCHRODER, A. & WEBER, C. 2002. JAM-1 is a ligand of the beta(2) integrin LFA-1 involved in transendothelial migration of leukocytes. *Nat*

- Immunol*, 3, 151-8.
- OUBAN, A. & AHMED, A. A. 2010. Claudins in human cancer: a review. *Histol Histopathol*, 25, 83-90.
- PADUA, D., ZHANG, X. H., WANG, Q., NADAL, C., GERALD, W. L., GOMIS, R. R. & MASSAGUE, J. 2008. TGFbeta primes breast tumors for lung metastasis seeding through angiopoietin-like 4. *Cell*, 133, 66-77.
- PAGET, S. 1989. The distribution of secondary growths in cancer of the breast. 1889. *Cancer Metastasis Rev*, 8, 98-101.
- PAJOUHESH, H. & LENZ, G. R. 2005. Medicinal chemical properties of successful central nervous system drugs. *NeuroRx*, 2, 541-53.
- PAL, D., AUDUS, K. L. & SIAHAAN, T. J. 1997. Modulation of cellular adhesion in bovine brain microvessel endothelial cells by a decapeptide. *Brain Res*, 747, 103-13.
- PALMIERI, D., BRONDER, J. L., HERRING, J. M., YONEDA, T., WEIL, R. J., STARK, A. M., KUREK, R., VEGA-VALLE, E., FEIGENBAUM, L., HALVERSON, D., VORTMEYER, A. O., STEINBERG, S. M., ALDAPE, K. & STEEG, P. S. 2007a. Her-2 overexpression increases the metastatic outgrowth of breast cancer cells in the brain. *Cancer Res*, 67, 4190-8.
- PALMIERI, D., CHAMBERS, A. F., FELDING-HABERMANN, B., HUANG, S. & STEEG, P. S. 2007b. The biology of metastasis to a sanctuary site. *Clin Cancer Res*, 13, 1656-62.
- PALMIERI, D., FITZGERALD, D., SHREEVE, S. M., HUA, E., BRONDER, J. L., WEIL, R. J., DAVIS, S., STARK, A. M., MERINO, M. J., KUREK, R., MEHDORN, H. M., DAVIS, G., STEINBERG, S. M., MELTZER, P. S., ALDAPE, K. & STEEG, P. S. 2009a. Analyses of resected human brain metastases of breast cancer reveal the association between up-regulation of hexokinase 2 and poor prognosis. *Mol Cancer Res*, 7, 1438-45.
- PALMIERI, D., LOCKMAN, P. R., THOMAS, F. C., HUA, E., HERRING, J., HARGRAVE, E., JOHNSON, M., FLORES, N., QIAN, Y., VEGA-VALLE, E., TASKAR, K. S., RUDRARAJU, V., MITTAPALLI, R. K., GAASCH, J. A., BOHN, K. A., THORSHEIM, H. R., LIEWEHR, D. J., DAVIS, S., REILLY, J. F., WALKER, R., BRONDER, J. L., FEIGENBAUM, L., STEINBERG, S. M., CAMPHAUSEN, K., MELTZER, P. S., RICHON, V. M., SMITH, Q. R. & STEEG, P. S. 2009b. Vorinostat inhibits brain metastatic colonization in a model of triple-negative breast cancer and induces DNA double-strand breaks. *Clin Cancer Res*, 15, 6148-57.
- PARDRIDGE, W. M. 1994. New approaches to drug delivery through the blood-brain barrier. *Trends Biotechnol*, 12, 239-45.
- PARDRIDGE, W. M. 2007. Blood-brain barrier delivery. *Drug Discov Today*, 12, 54-61.
- PARK, I. H., RO, J., LEE, K. S., NAM, B. H., KWON, Y. & SHIN, K. H. 2009a. Trastuzumab treatment beyond brain progression in HER2-positive metastatic breast cancer. *Ann Oncol*, 20, 56-62.
- PARK, S. Y., JUN, J. A., JEONG, K. J., HEO, H. J., SOHN, J. S., LEE, H. Y., PARK, C. G. & KANG, J. 2011. Histone deacetylases 1, 6 and 8 are critical for invasion in breast cancer. *Oncol Rep*, 25, 1677-81.
- PARK, Y. H., PARK, M. J., JI, S. H., YI, S. Y., LIM, D. H., NAM, D. H., LEE, J. I., PARK, W., CHOI, D. H., HUH, S. J., AHN, J. S., KANG, W. K., PARK, K. & IM, Y. H. 2009b. Trastuzumab treatment improves brain metastasis outcomes through control and durable prolongation of systemic extracranial disease in HER2-overexpressing breast cancer patients. *Br J Cancer*, 100, 894-900.
- PATCHELL, R. A., TIBBS, P. A., WALSH, J. W., DEMPSEY, R. J., MARUYAMA, Y., KRYSZCIO, R. J., MARKESBERY, W. R., MACDONALD, J. S. & YOUNG, B. 1990. A randomized trial of surgery in the treatment of single metastases to the brain. *N Engl J Med*, 322, 494-500.
- PATNAYAK, R., JENA, A., VIJAYLAXMI, B., LAKSHMI, A. Y., PRASAD, B., CHOWHAN, A. K., RUKMANGADHA, N., PHANEENDRA, B. V. & REDDY, M. K. 2013. Metastasis in central nervous system: Clinicopathological study with review of literature in a tertiary care center in South India. *South Asian J Cancer*, 2, 245-9.

- PEROU, C. M., SORLIE, T., EISEN, M. B., VAN DE RIJN, M., JEFFREY, S. S., REES, C. A., POLLACK, J. R., ROSS, D. T., JOHNSEN, H., AKSLEN, L. A., FLUGE, O., PERGAMENSHIKOV, A., WILLIAMS, C., ZHU, S. X., LONNING, P. E., BORRESEN-DALE, A. L., BROWN, P. O. & BOTSTEIN, D. 2000. Molecular portraits of human breast tumours. *Nature*, 406, 747-52.
- PETRI, B. & BIXEL, M. G. 2006. Molecular events during leukocyte diapedesis. *FEBS J*, 273, 4399-407.
- PICCART-GEBHART, M. J., PROCTER, M., LEYLAND-JONES, B., GOLDBIRSCHE, A., UNTCH, M., SMITH, I., GIANNI, L., BASELGA, J., BELL, R., JACKISCH, C., CAMERON, D., DOWSETT, M., BARRIOS, C. H., STEGER, G., HUANG, C. S., ANDERSSON, M., INBAR, M., LICHINITSER, M., LANG, I., NITZ, U., IWATA, H., THOMSEN, C., LOHRISCH, C., SUTER, T. M., RUSCHOFF, J., SUTO, T., GREATOR, V., WARD, C., STRAEHLE, C., MCFADDEN, E., DOLCI, M. S., GELBER, R. D. & HERCEPTIN ADJUVANT TRIAL STUDY, T. 2005. Trastuzumab after adjuvant chemotherapy in HER2-positive breast cancer. *N Engl J Med*, 353, 1659-72.
- PIENKOWSKI, T. & ZIELINSKI, C. C. 2010. Trastuzumab treatment in patients with breast cancer and metastatic CNS disease. *Ann Oncol*, 21, 917-24.
- PIEPER, D. R., HESS, K. R. & SAWAYA, R. E. 1997. Role of surgery in the treatment of brain metastases in patients with breast cancer. *Ann Surg Oncol*, 4, 481-90.
- POHLMANN, P. R., MAYER, I. A. & MERNAUGH, R. 2009. Resistance to Trastuzumab in Breast Cancer. *Clin Cancer Res*, 15, 7479-7491.
- POLYAK, K. 2011. Heterogeneity in breast cancer. *J Clin Invest*, 121, 3786-8.
- POLYAK, K. & GARBER, J. 2011. Targeting the missing links for cancer therapy. *Nat Med*, 17, 283-4.
- POSTMUS, P. E. & SMIT, E. F. 1999. Chemotherapy for brain metastases of lung cancer: a review. *Ann Oncol*, 10, 753-9.
- PRIES, A. R. & KUEBLER, W. M. 2006. Normal endothelium. *Handb Exp Pharmacol*, 1-40.
- PRINTZ, C. 2014. I-SPY2 trial yields first results on combination therapy for triple-negative breast cancer. *Cancer*, 120, 773.
- PULASKI, B. A. & OSTRAND-ROSENBERG, S. 1998. Reduction of established spontaneous mammary carcinoma metastases following immunotherapy with major histocompatibility complex class II and B7.1 cell-based tumor vaccines. *Cancer Res*, 58, 1486-93.
- QI, J., CHEN, N., WANG, J. & SIU, C. H. 2005. Transendothelial migration of melanoma cells involves N-cadherin-mediated adhesion and activation of the beta-catenin signaling pathway. *Mol Biol Cell*, 16, 4386-97.
- QI, J., WANG, J., ROMANYUK, O. & SIU, C. H. 2006. Involvement of Src family kinases in N-cadherin phosphorylation and beta-catenin dissociation during transendothelial migration of melanoma cells. *Mol Biol Cell*, 17, 1261-72.
- RADES, D., HUTTENLOCHER, S., HORNUNG, D., BLANCK, O., SCHILD, S. E. & FISCHER, D. 2014. Do patients with very few brain metastases from breast cancer benefit from whole-brain radiotherapy in addition to radiosurgery? *Radiat Oncol*, 9, 267.
- RAMIS-CONDE, I., CHAPLAIN, M. A., ANDERSON, A. R. & DRASDO, D. 2009. Multi-scale modelling of cancer cell intravasation: the role of cadherins in metastasis. *Phys Biol*, 6, 016008.
- RAPITI, E., VERKOOIJEN, H. M., VLASTOS, G., FIORETTA, G., NEYROUD-CASPAR, I., SAPPINO, A. P., CHAPPUIS, P. O. & BOUCHARDY, C. 2006. Complete excision of primary breast tumor improves survival of patients with metastatic breast cancer at diagnosis. *J Clin Oncol*, 24, 2743-9.
- RAY, P. S., WANG, J., QU, Y., SIM, M. S., SHAMONKI, J., BAGARIA, S. P., YE, X., LIU, B., ELASHOFF, D., HOON, D. S., WALTER, M. A., MARTENS, J. W., RICHARDSON, A. L., GIULIANO, A. E. & CUI, X. 2010. FOXC1 is a potential prognostic biomarker with functional significance in basal-like breast cancer. *Cancer Res*, 70, 3870-6.

- RAZAK, A. R., HOTTE, S. J., SIU, L. L., CHEN, E. X., HIRTE, H. W., POWERS, J., WALSH, W., STAYNER, L. A., LAUGHLIN, A., NOVOTNY-DIERMAYR, V., ZHU, J. & EISENHAEUER, E. A. 2011. Phase I clinical, pharmacokinetic and pharmacodynamic study of SB939, an oral histone deacetylase (HDAC) inhibitor, in patients with advanced solid tumours. *Br J Cancer*, 104, 756-62.
- REN, M., LENG, Y., JEONG, M., LEEDS, P. R. & CHUANG, D. M. 2004. Valproic acid reduces brain damage induced by transient focal cerebral ischemia in rats: potential roles of histone deacetylase inhibition and heat shock protein induction. *J Neurochem*, 89, 1358-67.
- REYMOND, N., D'AGUA, B. B. & RIDLEY, A. J. 2013. Crossing the endothelial barrier during metastasis. *Nat Rev Cancer*, 13, 858-70.
- RHEE, J., HAN, S. W., OH, D. Y., KIM, J. H., IM, S. A., HAN, W., PARK, I. A., NOH, D. Y., BANG, Y. J. & KIM, T. Y. 2008. The clinicopathologic characteristics and prognostic significance of triple-negativity in node-negative breast cancer. *BMC Cancer*, 8, 307.
- RHODES, L. V., TATE, C. R., SEGAR, H. C., BURKS, H. E., PHAMDUY, T. B., HOANG, V., ELLIOTT, S., GILLIAM, D., POUNDER, F. N., ANBALAGAN, M., CHRISEY, D. B., ROWAN, B. G., BUROW, M. E. & COLLINS-BUROW, B. M. 2014. Suppression of triple-negative breast cancer metastasis by pan-DAC inhibitor panobinostat via inhibition of ZEB family of EMT master regulators. *Breast Cancer Res Treat*, 145, 593-604.
- RICCI-VITIANI, L., PALLINI, R., BIFFONI, M., TODARO, M., INVERNICI, G., CENCI, T., MAIRA, G., PARATI, E. A., STASSI, G., LAROCCA, L. M. & DE MARIA, R. 2010. Tumour vascularization via endothelial differentiation of glioblastoma stem-like cells. *Nature*, 468, 824-8.
- RIFFELL, J. L., LORD, C. J. & ASHWORTH, A. 2012. Tankyrase-targeted therapeutics: expanding opportunities in the PARP family. *Nat Rev Drug Discov*, 11, 923-36.
- RIVENBARK, A. G., O'CONNOR, S. M. & COLEMAN, W. B. 2013. Molecular and cellular heterogeneity in breast cancer: challenges for personalized medicine. *Am J Pathol*, 183, 1113-24.
- ROBERT, C. & RASSOOL, F. V. 2012. HDAC inhibitors: roles of DNA damage and repair. *Adv Cancer Res*, 116, 87-129.
- RODRIGUEZ, P. L., JIANG, S., FU, Y., AVRAHAM, S. & AVRAHAM, H. K. 2014. The proinflammatory peptide substance P promotes blood-brain barrier breaching by breast cancer cells through changes in microvascular endothelial cell tight junctions. *Int J Cancer*, 134, 1034-44.
- ROMOND, E. H., PEREZ, E. A., BRYANT, J., SUMAN, V. J., GEYER, C. E., JR., DAVIDSON, N. E., TANCHIU, E., MARTINO, S., PAIK, S., KAUFMAN, P. A., SWAIN, S. M., PISANSKY, T. M., FEHRENBACHER, L., KUTTEH, L. A., VOGEL, V. G., VISSCHER, D. W., YOTHERS, G., JENKINS, R. B., BROWN, A. M., DAKHIL, S. R., MAMOUNAS, E. P., LINGLE, W. L., KLEIN, P. M., INGLE, J. N. & WOLMARK, N. 2005. Trastuzumab plus adjuvant chemotherapy for operable HER2-positive breast cancer. *N Engl J Med*, 353, 1673-84.
- ROSS, J. B., HUH, D., NOBLE, L. B. & TAVAZOIE, S. F. 2015. Identification of molecular determinants of primary and metastatic tumour re-initiation in breast cancer. *Nat Cell Biol*, 17, 651-64.
- ROTH, E. S., FETZER, D. T., BARRON, B. J., JOSEPH, U. A., GAYED, I. W. & WAN, D. Q. 2009. Does colon cancer ever metastasize to bone first? a temporal analysis of colorectal cancer progression. *BMC Cancer*, 9, 274.
- RUBIN, P., GASH, D. M., HANSEN, J. T., NELSON, D. F. & WILLIAMS, J. P. 1994. Disruption of the blood-brain barrier as the primary effect of CNS irradiation. *Radiother Oncol*, 31, 51-60.
- RUEFLI, A. A., AUSSERLECHNER, M. J., BERNHARD, D., SUTTON, V. R., TANTON, K. M., KOFLER, R., SMYTH, M. J. & JOHNSTONE, R. W. 2001. The histone deacetylase inhibitor and chemotherapeutic agent suberoylanilide hydroxamic acid (SAHA) induces a cell-death pathway characterized by cleavage of Bid and production of reactive oxygen species. *Proc Natl Acad Sci U S A*, 98, 10833-8.
- RUFFER, C. & GERKE, V. 2004. The C-terminal cytoplasmic tail of claudins 1 and 5 but not its PDZ-binding motif is required for apical localization at epithelial and endothelial tight junctions. *Eur J Cell Biol*, 83, 135-44.

- RUSSO, A. L., KWON, H. C., BURGAN, W. E., CARTER, D., BEAM, K., WEIZHENG, X., ZHANG, J., SLUSHER, B. S., CHAKRAVARTI, A., TOFILON, P. J. & CAMPHAUSEN, K. 2009. In vitro and in vivo radiosensitization of glioblastoma cells by the poly (ADP-ribose) polymerase inhibitor E7016. *Clin Cancer Res*, 15, 607-12.
- RYKEN, T. C., MCDERMOTT, M., ROBINSON, P. D., AMMIRATI, M., ANDREWS, D. W., ASHER, A. L., BURRI, S. H., COBBS, C. S., GASPAR, L. E., KONDZIOLKA, D., LINSKEY, M. E., LOEFFLER, J. S., MEHTA, M. P., MIKKELSEN, T., OLSON, J. J., PALEOLOGOS, N. A., PATCHELL, R. A. & KALKANIS, S. N. 2010. The role of steroids in the management of brain metastases: a systematic review and evidence-based clinical practice guideline. *J Neurooncol*, 96, 103-14.
- SABNIS, G. J., GOLOUBEVA, O., CHUMSRI, S., NGUYEN, N., SUKUMAR, S. & BRODIE, A. M. 2011. Functional activation of the estrogen receptor-alpha and aromatase by the HDAC inhibitor entinostat sensitizes ER-negative tumors to letrozole. *Cancer Res*, 71, 1893-903.
- SAMBROOK, J., FRITSCH, E. & MANIATIS, T. 1989. *Molecular cloning: A laboratory Manual*, USA, Cold springs Harbor Laboratory Press.
- SANOVICH, E., BARTUS, R. T., FRIDEN, P. M., DEAN, R. L., LE, H. Q. & BRIGHTMAN, M. W. 1995. Pathway across blood-brain barrier opened by the bradykinin agonist, RMP-7. *Brain Res*, 705, 125-35.
- SANTOSO, S., SACHS, U. J., KROLL, H., LINDER, M., RUF, A., PREISSNER, K. T. & CHAVAKIS, T. 2002. The junctional adhesion molecule 3 (JAM-3) on human platelets is a counterreceptor for the leukocyte integrin Mac-1. *J Exp Med*, 196, 679-91.
- SCHRADE, A., SADE, H., COURAUD, P. O., ROMERO, I. A., WEKSLER, B. B. & NIEWOEHNER, J. 2012. Expression and localization of claudins-3 and -12 in transformed human brain endothelium. *Fluids Barriers CNS*, 9, 6.
- SCOTT, C., SUH, J., STEA, B., NABID, A. & HACKMAN, J. 2007. Improved survival, quality of life, and quality-adjusted survival in breast cancer patients treated with efaproxiral (Efaproxyn) plus whole-brain radiation therapy for brain metastases. *Am J Clin Oncol*, 30, 580-7.
- SEAMAN, E. K., ROSS, S. & SAWCZUK, I. S. 1995. High incidence of asymptomatic brain lesions in metastatic renal cell carcinoma. *J Neurooncol*, 23, 253-6.
- SENKUS, E., KYRIAKIDES, S., OHNO, S., PENALT-LLORCA, F., POORTMANS, P., RUTGERS, E., ZACKRISSON, S., CARDOSO, F. & COMMITTEE, E. G. 2015. Primary breast cancer: ESMO Clinical Practice Guidelines for diagnosis, treatment and follow-up. *Ann Oncol*, 26 Suppl 5, v8-30.
- SEONG, M. W., KIM, K. H., CHUNG, I. Y., KANG, E., LEE, J. W., PARK, S. K., LEE, M. H., LEE, J. E., NOH, D. Y., SON, B. H., PARK, H. L., CHO, S. I., PARK, S. S., KOREAN HEREDITARY BREAST CANCER STUDY, G. & KIM, S. W. 2014. A multi-institutional study on the association between BRCA1/BRCA2 mutational status and triple-negative breast cancer in familial breast cancer patients. *Breast Cancer Res Treat*, 146, 63-9.
- SEVENICH, L., BOWMAN, R. L., MASON, S. D., QUAIL, D. F., RAPAPORT, F., ELIE, B. T., BROGI, E., BRASTIANOS, P. K., HAHN, W. C., HOLSINGER, L. J., MASSAGUE, J., LESLIE, C. S. & JOYCE, J. A. 2014. Analysis of tumour- and stroma-supplied proteolytic networks reveals a brain-metastasis-promoting role for cathepsin S. *Nat Cell Biol*, 16, 876-88.
- SHARMA, A., SINGH, K. & ALMASAN, A. 2012. Histone H2AX phosphorylation: a marker for DNA damage. *Methods Mol Biol*, 920, 613-26.
- SHIEN, T., KINOSHITA, T., SHIMIZU, C., HOJO, T., TAIRA, N., DOIHARA, H. & AKASHI-TANAKA, S. 2009. Primary tumor resection improves the survival of younger patients with metastatic breast cancer. *Oncol Rep*, 21, 827-32.
- SHIGEMATSU, H., KADOYA, T., KOBAYASHI, Y., KAJITANI, K., SASADA, T., EMI, A., MASUMOTO, N., HARUTA, R., KATAOKA, T., ODA, M., ARIHIRO, K. & OKADA, M. 2011. A case of HER-2-positive recurrent breast cancer showing a clinically complete response to trastuzumab-containing chemotherapy after primary treatment of triple-negative breast cancer. *World J Surg Oncol*, 9, 146.

- SHIMOYAMA, Y., HIROHASHI, S., HIRANO, S., NOGUCHI, M., SHIMOSATO, Y., TAKEICHI, M. & ABE, O. 1989. Cadherin cell-adhesion molecules in human epithelial tissues and carcinomas. *Cancer Res*, 49, 2128-33.
- SHULTZ, M. D., CAO, X., CHEN, C. H., CHO, Y. S., DAVIS, N. R., ECKMAN, J., FAN, J., FEKETE, A., FIRESTONE, B., FLYNN, J., GREEN, J., GROWNEY, J. D., HOLMQVIST, M., HSU, M., JANSSON, D., JIANG, L., KWON, P., LIU, G., LOMBARDO, F., LU, Q., MAJUMDAR, D., META, C., PEREZ, L., PU, M., RAMSEY, T., REMISZEWSKI, S., SKOLNIK, S., TRAEBERT, M., URBAN, L., UTTAMSINGH, V., WANG, P., WHITEBREAD, S., WHITEHEAD, L., YAN-NEALE, Y., YAO, Y. M., ZHOU, L. & ATADJA, P. 2011. Optimization of the in vitro cardiac safety of hydroxamate-based histone deacetylase inhibitors. *J Med Chem*, 54, 4752-72.
- SIEGEL, R. L., MILLER, K. D. & JEMAL, A. 2015. Cancer statistics, 2015. *CA Cancer J Clin*, 65, 5-29.
- SLAMON, D., EIERMANN, W., ROBERT, N., PIENKOWSKI, T., MARTIN, M., PRESS, M., MACKEY, J., GLASPY, J., CHAN, A., PAWLICKI, M., PINTER, T., VALERO, V., LIU, M. C., SAUTER, G., VON MINCKWITZ, G., VISCO, F., BEE, V., BUYSE, M., BENDAHMANE, B., TABAH-FISCH, I., LINDSAY, M. A., RIVA, A., CROWN, J. & BREAST CANCER INTERNATIONAL RESEARCH, G. 2011. Adjuvant trastuzumab in HER2-positive breast cancer. *N Engl J Med*, 365, 1273-83.
- SLOAN, E. K., POULIOT, N., STANLEY, K. L., CHIA, J., MOSELEY, J. M., HARDS, D. K. & ANDERSON, R. L. 2006. Tumor-specific expression of alphavbeta3 integrin promotes spontaneous metastasis of breast cancer to bone. *Breast Cancer Res*, 8, R20.
- SMITH, T. R., LALL, R. R., LALL, R. R., ABECASSIS, I. J., ARNAOUT, O. M., MARYMONT, M. H., SWANSON, K. R. & CHANDLER, J. P. 2014. Survival after surgery and stereotactic radiosurgery for patients with multiple intracranial metastases: results of a single-center retrospective study. *J Neurosurg*, 121, 839-45.
- SODA, Y., MARUMOTO, T., FRIEDMANN-MORVINSKI, D., SODA, M., LIU, F., MICHIEUE, H., PASTORINO, S., YANG, M., HOFFMAN, R. M., KESARI, S. & VERMA, I. M. 2011. Transdifferentiation of glioblastoma cells into vascular endothelial cells. *Proc Natl Acad Sci U S A*, 108, 4274-80.
- SOFFIETTI, R., CORNU, P., DELATTRE, J. Y., GRANT, R., GRAUS, F., GRISOLD, W., HEIMANS, J., HILDEBRAND, J., HOSKIN, P., KALLJO, M., KRAUSENECK, P., MAROSI, C., SIEGAL, T. & VECHT, C. 2006. EFNS Guidelines on diagnosis and treatment of brain metastases: report of an EFNS Task Force. *Eur J Neurol*, 13, 674-81.
- SOMECH, R., IZRAELI, S. & A, J. S. 2004. Histone deacetylase inhibitors--a new tool to treat cancer. *Cancer Treat Rev*, 30, 461-72.
- SORLIE, T., PEROU, C. M., TIBSHIRANI, R., AAS, T., GEISLER, S., JOHNSEN, H., HASTIE, T., EISEN, M. B., VAN DE RIJN, M., JEFFREY, S. S., THORSEN, T., QUIST, H., MATESE, J. C., BROWN, P. O., BOTSTEIN, D., LONNING, P. E. & BORRESEN-DALE, A. L. 2001. Gene expression patterns of breast carcinomas distinguish tumor subclasses with clinical implications. *Proc Natl Acad Sci U S A*, 98, 10869-74.
- SOROKIN, L. 2010. The impact of the extracellular matrix on inflammation. *Nat Rev Immunol*, 10, 712-23.
- SOSA, M. S., AVIVAR-VALDERAS, A., BRAGADO, P., WEN, H. C. & AGUIRRE-GHISO, J. A. 2011. ERK1/2 and p38alpha/beta signaling in tumor cell quiescence: opportunities to control dormant residual disease. *Clin Cancer Res*, 17, 5850-7.
- SPERDUTO, P. W., KASED, N., ROBERGE, D., XU, Z., SHANLEY, R., LUO, X., SNEED, P. K., CHAO, S. T., WEIL, R. J., SUH, J., BHATT, A., JENSEN, A. W., BROWN, P. D., SHIH, H. A., KIRKPATRICK, J., GASPAR, L. E., FIVEASH, J. B., CHIANG, V., KNISELY, J. P., SPERDUTO, C. M., LIN, N. & MEHTA, M. 2012. Effect of tumor subtype on survival and the graded prognostic assessment for patients with breast cancer and brain metastases. *Int J Radiat Oncol Biol Phys*, 82, 2111-7.
- STEEG, P. S., CAMPHAUSEN, K. A. & SMITH, Q. R. 2011. Brain metastases as preventive and therapeutic targets. *Nat Rev Cancer*, 11, 352-63.
- STEFFAN, J. S., BODAI, L., PALLOS, J., POELMAN, M., MCCAMPBELL, A., APOSTOL, B. L.,

- KAZANTSEV, A., SCHMIDT, E., ZHU, Y. Z., GREENWALD, M., KUROKAWA, R., HOUSMAN, D. E., JACKSON, G. R., MARSH, J. L. & THOMPSON, L. M. 2001. Histone deacetylase inhibitors arrest polyglutamine-dependent neurodegeneration in *Drosophila*. *Nature*, 413, 739-43.
- STEWART, D. J., LEAVENS, M., MAOR, M., FEUN, L., LUNA, M., BONURA, J., CAPRIOLI, R., LOO, T. L. & BENJAMIN, R. S. 1982. Human central nervous system distribution of cis-diamminedichloroplatinum and use as a radiosensitizer in malignant brain tumors. *Cancer Res*, 42, 2474-9.
- STEWART, D. J., LU, K., BENJAMIN, R. S., LEAVENS, M. E., LUNA, M., YAP, H. Y. & LOO, T. L. 1983. Concentration of vinblastine in human intracerebral tumor and other tissues. *J Neurooncol*, 1, 139-44.
- STEWART, D. J., RICHARD, M. T., HUGENHOLTZ, H., DENNERY, J. M., BELANGER, R., GERIN-LAJOIE, J., MONTPETIT, V., NUNDY, D., PRIOR, J. & HOPKINS, H. S. 1984. Penetration of VP-16 (etoposide) into human intracerebral and extracerebral tumors. *J Neurooncol*, 2, 133-9.
- STOLETOV, K., BOND, D., HEBRON, K., RAHA, S., ZIJLSTRA, A. & LEWIS, J. D. 2014. Metastasis as a therapeutic target in prostate cancer: a conceptual framework. *Am J Clin Exp Urol*, 2, 45-56.
- SUBRAMANIAN, A., TAMAYO, P., MOOTHA, V. K., MUKHERJEE, S., EBERT, B. L., GILLETTE, M. A., PAULOVICH, A., POMEROY, S. L., GOLUB, T. R., LANDER, E. S. & MESIROV, J. P. 2005. Gene set enrichment analysis: a knowledge-based approach for interpreting genome-wide expression profiles. *Proc Natl Acad Sci U S A*, 102, 15545-50.
- SUH, J. H. 2004. Efavoxiral: a novel radiation sensitizer. *Expert Opin Investig Drugs*, 13, 543-50.
- SUH, J. H., STEA, B., NABID, A., KRESL, J. J., FORTIN, A., MERCIER, J. P., SENZER, N., CHANG, E. L., BOYD, A. P., CAGNONI, P. J. & SHAW, E. 2006. Phase III study of efavoxiral as an adjunct to whole-brain radiation therapy for brain metastases. *J Clin Oncol*, 24, 106-14.
- SUZUKI, T., KOUKETSU, A., MATSUURA, A., KOHARA, A., NINOMIYA, S., KOHDA, K. & MIYATA, N. 2004. Thiol-based SAHA analogues as potent histone deacetylase inhibitors. *Bioorg Med Chem Lett*, 14, 3313-7.
- TAMAI, I. & TSUJI, A. 2000. Transporter-mediated permeation of drugs across the blood-brain barrier. *J Pharm Sci*, 89, 1371-88.
- TANEJA, N., DAVIS, M., CHOY, J. S., BECKETT, M. A., SINGH, R., KRON, S. J. & WEICHSELBAUM, R. R. 2004. Histone H2AX phosphorylation as a predictor of radiosensitivity and target for radiotherapy. *J Biol Chem*, 279, 2273-80.
- TARIN, D., PRICE, J. E., KETTLEWELL, M. G., SOUTER, R. G., VASS, A. C. & CROSSLEY, B. 1984. Mechanisms of human tumor metastasis studied in patients with peritoneovenous shunts. *Cancer Res*, 44, 3584-92.
- TASKAR, K. S., RUDRARAJU, V., MITTAPALLI, R. K., SAMALA, R., THORSHEIM, H. R., LOCKMAN, J., GRIL, B., HUA, E., PALMIERI, D., POLLI, J. W., CASTELLINO, S., RUBIN, S. D., LOCKMAN, P. R., STEEG, P. S. & SMITH, Q. R. 2012. Lapatinib distribution in HER2 overexpressing experimental brain metastases of breast cancer. *Pharm Res*, 29, 770-81.
- TATE, C. R., RHODES, L. V., SEGAR, H. C., DRIVER, J. L., POUNDER, F. N., BUROW, M. E. & COLLINS-BUROW, B. M. 2012. Targeting triple-negative breast cancer cells with the histone deacetylase inhibitor panobinostat. *Breast Cancer Res*, 14, R79.
- TELLI, M. 2014. Optimizing chemotherapy in triple-negative breast cancer: the role of platinum. *Am Soc Clin Oncol Educ Book*, e37-42.
- TEPASS, U., TRUONG, K., GODT, D., IKURA, M. & PEIFER, M. 2000. Cadherins in embryonic and neural morphogenesis. *Nat Rev Mol Cell Biol*, 1, 91-100.
- THIAGALINGAM, S., CHENG, K. H., LEE, H. J., MINEVA, N., THIAGALINGAM, A. & PONTE, J. F. 2003. Histone deacetylases: unique players in shaping the epigenetic histone code. *Ann N Y Acad Sci*, 983, 84-100.

- THIERY, J. P. 2002. Epithelial-mesenchymal transitions in tumour progression. *Nat Rev Cancer*, 2, 442-54.
- THOMAS, D. W., GOULD, C. M., HANDOKO, Y. & SIMPSON, K. J. 2014. Functional genomics down under: RNAi screening in the Victorian Centre for Functional Genomics. *Comb Chem High Throughput Screen*, 17, 343-55.
- THOMAS, F. C., TASKAR, K., RUDRARAJU, V., GODA, S., THORSHEIM, H. R., GAASCH, J. A., MITTAPALLI, R. K., PALMIERI, D., STEEG, P. S., LOCKMAN, P. R. & SMITH, Q. R. 2009. Uptake of ANG1005, a novel paclitaxel derivative, through the blood-brain barrier into brain and experimental brain metastases of breast cancer. *Pharm Res*, 26, 2486-94.
- TILLING, T., KORTE, D., HOHEISEL, D. & GALLA, H. J. 1998. Basement membrane proteins influence brain capillary endothelial barrier function in vitro. *J Neurochem*, 71, 1151-7.
- TIMPL, R. & BROWN, J. C. 1996. Supramolecular assembly of basement membranes. *Bioessays*, 18, 123-32.
- TIRABY, C., HAZEN, B. C., GANTNER, M. L. & KRALLI, A. 2011. Estrogen-related receptor gamma promotes mesenchymal-to-epithelial transition and suppresses breast tumor growth. *Cancer Res*, 71, 2518-28.
- TOH, Y., OHGA, T., ENDO, K., ADACHI, E., KUSUMOTO, H., HARAGUCHI, M., OKAMURA, T. & NICOLSON, G. L. 2004. Expression of the metastasis-associated MTA1 protein and its relationship to deacetylation of the histone H4 in esophageal squamous cell carcinomas. *Int J Cancer*, 110, 362-7.
- TSAO, M. N. 2015. Brain metastases: advances over the decades. *Ann Palliat Med*, 4, 225-32.
- TSAO, M. N., LLOYD, N., WONG, R. K., CHOW, E., RAKOVITCH, E., LAPERRIERE, N., XU, W. & SAHGAL, A. 2012. Whole brain radiotherapy for the treatment of newly diagnosed multiple brain metastases. *Cochrane Database Syst Rev*, 4, CD003869.
- TSUTSUI, S., OHNO, S., MURAKAMI, S., HACHITANDA, Y. & ODA, S. 2002. Prognostic value of epidermal growth factor receptor (EGFR) and its relationship to the estrogen receptor status in 1029 patients with breast cancer. *Breast Cancer Res Treat*, 71, 67-75.
- TUNG, N., GARBER, J. E., LINCOLN, A. & DOMCHEK, S. M. 2012. Frequency of triple-negative breast cancer in BRCA1 mutation carriers: comparison between common Ashkenazi Jewish and other mutations. *J Clin Oncol*, 30, 4447-8.
- TURNER, N., TUTT, A. & ASHWORTH, A. 2004. Hallmarks of 'BRCAness' in sporadic cancers. *Nat Rev Cancer*, 4, 814-9.
- VALIENTE, M., OBENAU, A. C., JIN, X., CHEN, Q., ZHANG, X. H., LEE, D. J., CHAFT, J. E., KRIS, M. G., HUSE, J. T., BROGI, E. & MASSAGUE, J. 2014. Serpins promote cancer cell survival and vascular co-option in brain metastasis. *Cell*, 156, 1002-16.
- VALLOW, L. A. 2009. Stereotactic radiosurgery alone to treat brain metastases. *Nat Rev Clin Oncol*, 6, 377-8.
- VAN 'T VEER, L. J., DAI, H., VAN DE VIJVER, M. J., HE, Y. D., HART, A. A., MAO, M., PETERSE, H. L., VAN DER KOOY, K., MARTON, M. J., WITTEVEEN, A. T., SCHREIBER, G. J., KERKHOVEN, R. M., ROBERTS, C., LINSLEY, P. S., BERNARDS, R. & FRIEND, S. H. 2002. Gene expression profiling predicts clinical outcome of breast cancer. *Nature*, 415, 530-6.
- VARGHESE, H. J., DAVIDSON, M. T., MACDONALD, I. C., WILSON, S. M., NADKARNI, K. V., GROOM, A. C. & CHAMBERS, A. F. 2002. Activated ras regulates the proliferation/apoptosis balance and early survival of developing micrometastases. *Cancer Res*, 62, 887-91.
- VERGER, E., GIL, M., YAYA, R., VINOLAS, N., VILLA, S., PUJOL, T., QUINTO, L. & GRAUS, F. 2005. Temozolomide and concomitant whole brain radiotherapy in patients with brain metastases: a phase II randomized trial. *Int J Radiat Oncol Biol Phys*, 61, 185-91.
- VERMA, S., MILES, D., GIANNI, L., KROP, I. E., WELSLAU, M., BASELGA, J., PEGRAM, M., OH, D. Y.,

- DIERAS, V., GUARDINO, E., FANG, L., LU, M. W., OLSEN, S., BLACKWELL, K. & GROUP, E. S. 2012. Trastuzumab emtansine for HER2-positive advanced breast cancer. *N Engl J Med*, 367, 1783-91.
- VIANI, G. A., AFONSO, S. L., STEFANO, E. J., DE FENDI, L. I. & SOARES, F. V. 2007. Adjuvant trastuzumab in the treatment of her-2-positive early breast cancer: a meta-analysis of published randomized trials. *BMC Cancer*, 7, 153.
- VIANI, G. A., MANTA, G. B., FONSECA, E. C., DE FENDI, L. I., AFONSO, S. L. & STEFANO, E. J. 2009. Whole brain radiotherapy with radiosensitizer for brain metastases. *J Exp Clin Cancer Res*, 28, 1.
- VINCENT, K. M., FINDLAY, S. D. & POSTOVIT, L. M. 2015. Assessing breast cancer cell lines as tumour models by comparison of mRNA expression profiles. *Breast Cancer Res*, 17, 114.
- VODUC, K. D., CHEANG, M. C., TYLDESLEY, S., GELMON, K., NIELSEN, T. O. & KENNECKE, H. 2010. Breast cancer subtypes and the risk of local and regional relapse. *J Clin Oncol*, 28, 1684-91.
- WADASADAWALA, T., GUPTA, S., BAGUL, V. & PATIL, N. 2007. Brain metastases from breast cancer: management approach. *J Cancer Res Ther*, 3, 157-65.
- WAGENBLAST, E., SOTO, M., GUTIERREZ-ANGEL, S., HARTL, C. A., GABLE, A. L., MACELI, A. R., ERARD, N., WILLIAMS, A. M., KIM, S. Y., DICKOPF, S., HARRELL, J. C., SMITH, A. D., PEROU, C. M., WILKINSON, J. E., HANNON, G. J. & KNOTT, S. R. 2015. A model of breast cancer heterogeneity reveals vascular mimicry as a driver of metastasis. *Nature*, 520, 358-62.
- WANG, L., COSSETTE, S. M., RARICK, K. R., GERSHAN, J., DWINELL, M. B., HARDER, D. R. & RAMCHANDRAN, R. 2013. Astrocytes directly influence tumor cell invasion and metastasis in vivo. *PLoS One*, 8, e80933.
- WANG, R., CHADALAVADA, K., WILSHIRE, J., KOWALIK, U., HOVINGA, K. E., GEBER, A., FLIGELMAN, B., LEVERSHA, M., BRENNAN, C. & TABAR, V. 2010. Glioblastoma stem-like cells give rise to tumour endothelium. *Nature*, 468, 829-33.
- WATANABE, M., KANG, Y. J., DAVIES, L. M., MEGHPARA, S., LAU, K., CHUNG, C. Y., KATHIRIYA, J., HADJANTONAKIS, A. K. & MONUKI, E. S. 2012. BMP4 sufficiency to induce choroid plexus epithelial fate from embryonic stem cell-derived neuroepithelial progenitors. *J Neurosci*, 32, 15934-45.
- WEICHERT, W. 2009. HDAC expression and clinical prognosis in human malignancies. *Cancer Lett*, 280, 168-76.
- WELLS, A., YATES, C. & SHEPARD, C. R. 2008. E-cadherin as an indicator of mesenchymal to epithelial reverting transitions during the metastatic seeding of disseminated carcinomas. *Clin Exp Metastasis*, 25, 621-8.
- WELZEL, G., FLECKENSTEIN, K., SCHAEFER, J., HERMANN, B., KRAUS-TIEFENBACHER, U., MAI, S. K. & WENZ, F. 2008. Memory function before and after whole brain radiotherapy in patients with and without brain metastases. *Int J Radiat Oncol Biol Phys*, 72, 1311-8.
- WEST, A. C. & JOHNSTONE, R. W. 2014. New and emerging HDAC inhibitors for cancer treatment. *J Clin Invest*, 124, 30-9.
- WIJNHOLDS, J., DELANGE, E. C., SCHEFFER, G. L., VAN DEN BERG, D. J., MOL, C. A., VAN DER VALK, M., SCHINKEL, A. H., SCHEPER, R. J., BREIMER, D. D. & BORST, P. 2000. Multidrug resistance protein 1 protects the choroid plexus epithelium and contributes to the blood-cerebrospinal fluid barrier. *J Clin Invest*, 105, 279-85.
- WIK, E., RAEDER, M. B., KRAKSTAD, C., TROVIK, J., BIRKELAND, E., HOVIK, E. A., MJOS, S., WERNER, H. M., MANNELQVIST, M., STEFANSSON, I. M., OYAN, A. M., KALLAND, K. H., AKSLEN, L. A. & SALVESEN, H. B. 2013. Lack of estrogen receptor-alpha is associated with epithelial-mesenchymal transition and PI3K alterations in endometrial carcinoma. *Clin Cancer Res*, 19, 1094-105.
- WILHELM, I., MOLNAR, J., FAZAKAS, C., HASKO, J. & KRIZBAI, I. A. 2013. Role of the blood-brain barrier in the formation of brain metastases. *Int J Mol Sci*, 14, 1383-411.

- WILLIAMS, M. J., LOWRIE, M. B., BENNETT, J. P., FIRTH, J. A. & CLARK, P. 2005. Cadherin-10 is a novel blood-brain barrier adhesion molecule in human and mouse. *Brain Res*, 1058, 62-72.
- WODITSCHKA, S., EVANS, L., DUCHNOWSKA, R., REED, L. T., PALMIERI, D., QIAN, Y., BADVE, S., SLEDGE, G., JR., GRIL, B., ALADJEM, M. I., FU, H., FLORES, N. M., GOKMEN-POLAR, Y., BIERNAT, W., SZUTOWICZ-ZIELINSKA, E., MANDAT, T., TROJANOWSKI, T., OCH, W., CZARTORYSKA-ARLUKOWICZ, B., JASSEM, J., MITCHELL, J. B. & STEEG, P. S. 2014. DNA double-strand break repair genes and oxidative damage in brain metastasis of breast cancer. *J Natl Cancer Inst*, 106.
- WOLBURG, H., WOLBURG-BUCHHOLZ, K., KRAUS, J., RASCHER-EGGSTEIN, G., LIEBNER, S., HAMM, S., DUFFNER, F., GROTE, E. H., RISAU, W. & ENGELHARDT, B. 2003. Localization of claudin-3 in tight junctions of the blood-brain barrier is selectively lost during experimental autoimmune encephalomyelitis and human glioblastoma multiforme. *Acta Neuropathol*, 105, 586-92.
- WRONSKI, M., ARBIT, E. & MCCORMICK, B. 1997. Surgical treatment of 70 patients with brain metastases from breast carcinoma. *Cancer*, 80, 1746-54.
- YANG, J. & WEINBERG, R. A. 2008. Epithelial-mesenchymal transition: at the crossroads of development and tumor metastasis. *Dev Cell*, 14, 818-29.
- YAO, Y., TU, Z., LIAO, C., WANG, Z., LI, S., YAO, H., LI, Z. & JIANG, S. 2015. Discovery of Novel Class I Histone Deacetylase Inhibitors with Promising in Vitro and in Vivo Antitumor Activities. *J Med Chem*, 58, 7672-80.
- YAP, Y. S., CORNELIO, G. H., DEVI, B. C., KHORPRASERT, C., KIM, S. B., KIM, T. Y., LEE, S. C., PARK, Y. H., SOHN, J. H., SUTANDYO, N., WONG, D. W., KOBAYASHI, M., LANDIS, S. H., YEOH, E. M., MOON, H. & RO, J. 2012. Brain metastases in Asian HER2-positive breast cancer patients: anti-HER2 treatments and their impact on survival. *Br J Cancer*, 107, 1075-82.
- YE, J., WU, D., SHEN, J., WU, P., NI, C., CHEN, J., ZHAO, J., ZHANG, T., WANG, X. & HUANG, J. 2012. Enrichment of colorectal cancer stem cells through epithelial-mesenchymal transition via CDH1 knockdown. *Mol Med Rep*, 6, 507-12.
- YE, Y., XIAO, Y., WANG, W., YEARSLEY, K., GAO, J. X., SHETUNI, B. & BARSKY, S. H. 2010. ERalpha signaling through slug regulates E-cadherin and EMT. *Oncogene*, 29, 1451-62.
- YIN, J. J., POLLOCK, C. B. & KELLY, K. 2005. Mechanisms of cancer metastasis to the bone. *Cell Res*, 15, 57-62.
- YONEMORI, K., TSUTA, K., ONO, M., SHIMIZU, C., HIRAKAWA, A., HASEGAWA, T., HATANAKA, Y., NARITA, Y., SHIBUI, S. & FUJIWARA, Y. 2010. Disruption of the blood brain barrier by brain metastases of triple-negative and basal-type breast cancer but not HER2/neu-positive breast cancer. *Cancer*, 116, 302-8.
- YONEZAWA, T., OHTSUKA, A., YOSHITAKA, T., HIRANO, S., NOMOTO, H., YAMAMOTO, K. & NINOMIYA, Y. 2003. Limitrin, a novel immunoglobulin superfamily protein localized to glia limitans formed by astrocyte endfeet. *Glia*, 44, 190-204.
- YONG, W. P., GOH, B. C., SOO, R. A., TOH, H. C., ETHIRAJULU, K., WOOD, J., NOVOTNY-DIERMAYR, V., LEE, S. C., YEO, W. L., CHAN, D., LIM, D., SEAH, E., LIM, R. & ZHU, J. 2011. Phase I and pharmacodynamic study of an orally administered novel inhibitor of histone deacetylases, SB939, in patients with refractory solid malignancies. *Ann Oncol*, 22, 2516-22.
- YOO, J. Y., YANG, S. H., LEE, J. E., CHO, D. G., KIM, H. K., KIM, S. H., KIM, I. S., HONG, J. T., SUNG, J. H., SON, B. C. & LEE, S. W. 2012. E-cadherin as a predictive marker of brain metastasis in non-small-cell lung cancer, and its regulation by pioglitazone in a preclinical model. *J Neurooncol*, 109, 219-27.
- YOSHIMASU, T., SAKURAI, T., OURA, S., HIRAI, I., TANINO, H., KOKAWA, Y., NAITO, Y., OKAMURA, Y., OTA, I., TANI, N. & MATSUURA, N. 2004. Increased expression of integrin alpha3beta1 in highly brain metastatic subclone of a human non-small cell lung cancer cell line. *Cancer Sci*, 95, 142-8.

- YU, X. Y., LIN, S. G., CHEN, X., ZHOU, Z. W., LIANG, J., DUAN, W., CHOWBAY, B., WEN, J. Y., CHAN, E., CAO, J., LI, C. G. & ZHOU, S. F. 2007. Transport of cryptotanshinone, a major active triterpenoid in *Salvia miltiorrhiza* Bunge widely used in the treatment of stroke and Alzheimer's disease, across the blood-brain barrier. *Curr Drug Metab*, 8, 365-78.
- YURCHENCO, P. D. 2011. Basement membranes: cell scaffoldings and signaling platforms. *Cold Spring Harb Perspect Biol*, 3.
- ZHANG, J., PIONTEK, J., WOLBURG, H., PIEHL, C., LISS, M., OTTEN, C., CHRIST, A., WILLNOW, T. E., BLASIG, I. E. & ABDELILAH-SEYFRIED, S. 2010. Establishment of a neuroepithelial barrier by Claudin5a is essential for zebrafish brain ventricular lumen expansion. *Proc Natl Acad Sci U S A*, 107, 1425-30.
- ZHANG, L., SULLIVAN, P. S., GOODMAN, J. C., GUNARATNE, P. H. & MARCHETTI, D. 2011. MicroRNA-1258 suppresses breast cancer brain metastasis by targeting heparanase. *Cancer Res*, 71, 645-54.
- ZHANG, L., ZHOU, Z., MEI, X., YANG, Z., MA, J., CHEN, X., WANG, J., LIU, G., YU, X. & GUO, X. 2015a. Intraoperative Radiotherapy Versus Whole-Breast External Beam Radiotherapy in Early-Stage Breast Cancer: A Systematic Review and Meta-Analysis. *Medicine (Baltimore)*, 94, e1143.
- ZHANG, Y., ZHANG, N., HOFFMAN, R. M. & ZHAO, M. 2015b. Surgically-Induced Multi-organ Metastasis in an Orthotopic Syngeneic Imageable Model of 4T1 Murine Breast Cancer. *Anticancer Res*, 35, 4641-6.
- ZHENG, L., ZHOU, B., MENG, X., ZHU, W., ZUO, A., WANG, X., JIANG, R. & YU, S. 2014. A model of spontaneous mouse mammary tumor for human estrogen receptor- and progesterone receptor-negative breast cancer. *Int J Oncol*, 45, 2241-9.
- ZHOU, J., ZAMDBORG, L. & SEBASTIAN, E. 2015. Review of advanced catheter technologies in radiation oncology brachytherapy procedures. *Cancer Manag Res*, 7, 199-211.
- ZHOU, Z. N., SHARMA, V. P., BEATY, B. T., ROH-JOHNSON, M., PETERSON, E. A., VAN ROOIJEN, N., KENNY, P. A., WILEY, H. S., CONDEELIS, J. S. & SEGALL, J. E. 2014. Autocrine HBEGF expression promotes breast cancer intravasation, metastasis and macrophage-independent invasion in vivo. *Oncogene*, 33, 3784-93.
- ZORRILLA, M., ALONSO, V., HERRERO, A., CORRAL, M., PUERTOLAS, T., TRUFERO, J. M., ARTAL, A. & ANTON, A. 2001. Brain metastases from colorectal carcinoma. *Tumori*, 87, 332-4.



Minerva Access is the Institutional Repository of The University of Melbourne

Author/s:

Kim, Soo-Hyun

Title:

Investigating breast cancer metastasis to brain in pre-clinical mouse models of metastasis

Date:

2015

Persistent Link:

<http://hdl.handle.net/11343/91433>

File Description:

INVESTIGATING BREAST CANCER METASTASIS TO BRAIN IN PRE-CLINICAL MOUSE MODELS OF METASTASIS